# Steric and Electronic Control of Low-Coordinate Pnictogen Bonding

by

Charles L.B. Macdonald

Submitted in partial fulfilment of the requirements
for the degree of Doctor of Philosophy

at

Dalhousie University
Halifax, Nova Scotia
May 1998

For Mom and Dad

## Table of Contents

## List of Figures

## List of Tables

## Abstract

This work examines the concepts of steric and electronic stabilization and provides a rationale for their application to the structure and bonding of group 15 (Pnictogen) elements.

Synthetic and *ab initio* studies demonstrate that electronic factors determine the bonding of pnictogenium cations (group 15 carbenoids) and suggest that the dimerization of arsenium cations is a solid-state packing phenomenon. The contrasting cycloaddition reactivity of phosphenium and arsenium cations is explained. The 2,4,6-tris(trifluoromethyl)phenyl (Fmes) substituent is not suitable for the stabilization of pnictogenium cations.

Identical reactions involving the bulky 2,4,6-tri-$^t$butylphenyl (Mes*) and slightly smaller 2,6-diisopropylphenyl (Dip) ligands yield either trisaminopnictines, pnictazanes or iminoaminopnictines depending on the pnictogen atom. A steric scale of relative thermodynamic stability for the structure and bonding of compounds containing the N-Pn-N (Pn = P, As, Sb, Bi) moiety is formulated.

Study of the unprecedented dimerization of Mes*N=P-$OSO_2CF_3$ yields a qualitative assessment of kinetic and thermodynamic effects of bulky substituents. Reagents that allow for the synthesis of compounds containing the [Mes*N=As] fragment are described. These will allow for the development of a new chapter of main group inorganic chemistry.

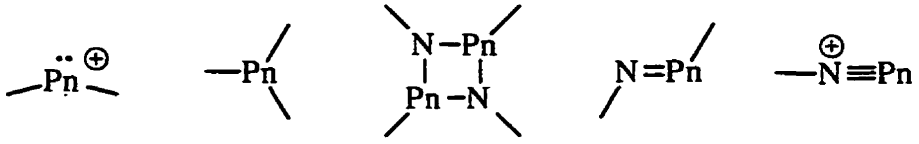


Pn = P, As, Sb, Bi

## List of Abbreviations and Symbols

| | |
|---|---|
| μs | microsecond |
| μ | bridging |
| 2D | two-dimensional |
| Å | ångstrom |
| Abbreviations for substituents are listed in Figure 1.1 | |
| Ar | aryl |
| BD | butadiene |
| $\beta_{NMR}$ | angle between $\delta_{33}$ and internuclear vector |
| br | broad (vibrational spec.) |
| Bu | butyl |
| C | celsius |
| Ch | Chalcogen |
| cm | centimeter |
| $cm^{-1}$ | wavenumber |
| COSY | correlated spectroscopy |
| CP | cross polarization |
| CSD | Cambridge Structural Database |
| CST | chemical shift tensor |
| δ | chemical shift |
| d | doublet singlet (NMR spec.) |
| Δ | change in |
| Δ | heat |
| DA | Diels-Alder |
| DBU | 1,8-diazabicyclo[5.4.0]undec-7-ene |
| $D_{calc}$ | calculated density |
| $\delta_{ii}$ | principal component of CST |
| $\delta_{iso}$ | isotropic chemical shift |
| DME | 1,2-dimethoxyethane |
| E | energy |
| E | element (in structural drawings) |
| $E_a$ | activation energy |
| $E_{el}$ | electronic energy |
| EIMS | electron ionization mass spectrometry |
| $E_{prep}$ | preparation energy |
| $E_{s \rightarrow t}$ | singlet triplet energy difference |
| Et | ethyl |
| eV | electron Volt |
| $E^p$ | electrostatic energy |

| | |
|---|---|
| FT | Fourrier transform |
| g | gram |
| G | Gibbs' energy |
| h | hour |
| H | enthalpy |
| HETCOR | heteronuclear correlated spectroscopy |
| HF | Hartree-Fock |
| hν | radiation |
| HOMO | highest occupied molecular orbital |
| Hz | hertz |
| I | nuclear spin quantum number |
| IR | infrared |
| J | joule |
| J | spin-spin coupling (constant) |
| κ | skew of spectrum |
| k | kilo |
| K | kelvin |
| $K_{eq}$ | equilibrium constant |
| LUMO | lowest unoccupied molecular orbital |
| m | multiplet singlet (NMR spec.) |
| m/z | mass to charge ratio |
| m | medium (vibrational spec.) |
| M | metal |
| m.p. | melting point |
| MAS | magic angle spinning |
| Me | methyl |
| mm | millimeter |
| MO | molecular orbital |
| MP | Møller-Plesset |
| ms | millisecond |
| MS | mass spectrometry |
| n | principal quantum number |
| n/d | not determined |
| N | number of atoms |
| N imag | number of imaginary freqencies |
| NBO | natural bond orbital |
| NMR | nuclear magnetic resonance |
| Ph | phenyl |
| Pn | Pnictogen |
| ppm | parts per million |
| Pr | propyl |
| pyr | pyridine |
| q | quartet singlet (NMR spec.) |
| Q | reaction quotient |
| R | restricted (*ab initio* calculations) |
| $R_1$ | unweighted agreement factor |
| s | second |

| | |
|---|---|
| s | strong (vibrational spec.) |
| s | singlet (NMR spec.) |
| sh | shoulder (vibrational spec.) |
| t | triplet singlet (NMR spec.) |
| THF | tetrahydrofuran |
| TMS | trimethylsilyl |
| U | unrestricted (*ab initio* calculations) |
| v | very (vibrational spec.) |
| V | volume |
| VDW | van der Waals |
| VT | variable-temperature |
| w | weak (vibrational spec.) |
| $\Omega$ | span of spectrum |
| $w_{1/2}$ | width at half-height |
| X | Halogen |
| Z | atomic number |
| ZPVE | zero-point vibrational energy |
| ° | degrees |

**Acknowledgements**

Many people have helped and supported me over the years and have thus contributed, either directly or indirectly, in the realization of this thesis.

I thank my parents for everything they have given me. Their support for me has been unwavering. I would also like to thank my mother for proof reading this thesis - you are obviously an avid reader, Mom.

I thank my supervisor, Neil Burford, for his patience and persistence over the years. He has offered me invaluable advice and commentary on matters scientific and otherwise. My decision to become an academic was strongly influenced by Neil and for that I am grateful.

I would also like to thank the past members of our research group from whom I have learned much. Dr. T. Parks, Dr. P. Losier, Dr. A. Whitla and particularly Dr. J. Clyburne taught me how to be a scientist, and G.B. Yhard and L. Agocs were always interesting to have around. I would like to also acknowledge my current lab mates, some of whom have contributed directly to this thesis. D. Walsh, A. Phillips and Dr. D. Leblanc have been most helpful and I appreciate the comments of G. Briand and H. Maguire. I thank all the honours students I have worked with for having given me the opportunity to learn how to supervise others. I also thank Donna Silvert for the final proofreading of this work.

I am deeply indebted to Dr. T.S. Cameron. He has gone to great lengths to help me throughout my stay at Dalhousie and he has managed to find crystal structures for even the least promising samples I have given him. I thank the other past and present members of DALX for the work they have performed for this thesis. These include B. Borecka, Dr. S. Sereda, Dr. P. Bakshi, K. Robertson, Dr. W. Kwiatkowski and S. Lantos.

I must also thank the Atlantic Regional Magnetic Resonance Center and Drs. D. Hooper, M. Lumsden and G. Wu for their help with solution-state NMR experiments.

I thank Rob Schurko for everything he has done for me. He has influenced me in ways too numerous to list. I also thank him and the members of Dr. R. Wasylishen's group for their solid-state NMR work.

I thank Dr. R. Boyd and his research group for allowing me to use their computers for *ab initio* calculations. I have inconvenienced them and I thank them for their patience.

J. Müller is thanked for all the glassware he has made for me - without him, the work in this thesis would not have been possible.

I must thank the office staff for all of the support they have given me. In particular Giselle and Deanna have helped me above and beyond the call of duty, particularly in the final days before the submission of this work.

I am indebted to my supervisory committee and the Office of Graduate Studies for their patience and understanding during the submission of this thesis.

I thank NSERC, the Killam Trust and Dalhousie University for their generous financial support.

Finally I thank all of my friends, both past and present, who have made my stay at Dalhousie a genuinely enjoyable experience.

# Chapter 1. Introduction to the Thesis.

## 1.1 General Introduction

The Pnictogens (group 15 elements) are a family of elements that occupy an interesting part of the main group (p-block) of the periodic table.[1] The lighter elements (N and P) are non-metals that are mainstays of organic and biological chemistry; the heaviest member of the group, bismuth, is a heavy metal, while the remaining elements, arsenic and antimony, are two of the six metalloids in the periodic table. The importance of the pnictogens is reflected in the immense variety of compounds in which they are found including the ubiquitous (e.g. $N_{2(g)}$), the essential (e.g. amino acids), the exotic (e.g. GaAs) and the deadly (e.g. Sarin).

The goals of this thesis, in a general sense, are to obtain a better understanding of the bonding properties of group 15 elements and to document and rationalize the similarities and differences in the behaviour of analogous pnictogen compounds. Specifically, the bonding and reactivity of compounds containing pnictogen atoms in low-coordinate and electron deficient bonding environments (*vide infra*) are examined synthetically and theoretically. Additionally, the effects of some commonly used sterically demanding substituents (*vide infra*) on the structure and bonding of such compounds is examined and such substituents are used to control the bonding in the pnictogen species.

Because of the variety of projects examined in this thesis, each chapter contains an introductory section to acquaint the reader with the appropriate background information for the material that immediately follows. In addition, the conclusion section of each chapter contains suggestions for work to be done in the future for each project. The general introduction below consists of information pertaining to the pnictogens and their bonding, a brief introduction to low-coordinate compounds and an examination of the use

of sterically demanding substituents in the isolation of low-coordinate species. The nomenclature of compounds used throughout this thesis conforms to that commonly found in the literature of this field (which is often derived from the nomenclature of organic chemistry) and does not necessarily follow the conventions of IUPAC. Important compounds are numbered in each chapter (these are cross referenced when necessary) and *ab initio* model compounds are indicated with an apostrophe.

## 1.2 Group 15 Elements - "Pnictogens"

### 1.2.1 General Properties

Some general information about each pnictogen element and other selected elements relevant to the thesis is listed in Table 1.1 and Table 1.2, respectively.[2,3,4,5,6]

**Table 1.1.** Properties of group 15 elements.

| Element | Z | Atomic mass (g/mol) | Electronegativity Pauling (Allen) | VDW, Covalent radii (Å) | Isotopes (%), I |
|---|---|---|---|---|---|
| N | 7 | 14.00674(7) | 3.04 (3.066) | 1.55, 0.73 | $^{14}$N (99.634), 1<br>$^{15}$N (0.366), 1/2 |
| P | 15 | 30.973762(4) | 2.19 (2.253) | 1.85, 1.10 | $^{31}$P (100), 1/2 |
| As | 33 | 74.92159(2) | 2.18 (2.211) | 2.0, 1.21 | $^{75}$As (100), 3/2 |
| Sb | 51 | 121.760(1) | 2.05 (1.984) | 2.2, 1.41 | $^{121}$Sb (57.36), 5/2<br>$^{123}$Sb (42.64), 7/2 |
| Bi | 83 | 208.98037(3) | 2.02 (n/d) | 2.3, 1.52 | $^{209}$Bi (100), 9/2 |

**Table 1.2.** Electronegativity and radii for elements bonded to pnictogen atoms in this thesis.

| Element | Electronegativity Pauling (Allen) | VDW, covalent radii (Å) |
|---|---|---|
| O | 3.44 (3.610) | 1.40, 0.70 |
| Cl | 3.16 (2.869) | 1.80, 0.97 |
| C | 2.55 (2.544) | 1.70, 0.77 |
| Si | 1.90 (1.916) | 2.10, 1.17 |
| H | 2.20 (2.300) | 1.30, 0.37 |
| F | 3.98 (4.193) | 1.35, 0.54 |

Examples of typical Pn-element bond lengths will be given throughout the thesis; however, various crystallographically determined main group element bond lengths have been assembled in a review.[7]

### 1.2.2 Characterization of Compounds

Because only the spin 1/2 nuclei $^{31}P$ and $^{15}N$ can be studied conveniently through the use of solution state nuclear magnetic resonance spectroscopy, there is a much more complete understanding of the chemistry of these elements than the chemistry of the heavier pnictogens. The bonding at the heavier pnictogen atoms can only be inferred by NMR through the examination of the spectra of other appropriate spin 1/2 nuclei such as $^{1}H$, $^{13}C$ or $^{19}F$.

The other characterization techniques used in this thesis include vibrational spectroscopy (FT-IR and FT-Raman) which yields information about bonding environments and functional groups present in the molecules and is used to characterize analogous compounds. Elemental analysis and mass spectrometry are used to obtain

molecular composition and molecular weight information (and fragment weight information for MS). The most important characterization technique for the examination of structure and bonding is X-ray crystallography as crystal structures are still often considered to be necessary proof of the synthetic results in main group inorganic chemistry.

### 1.2.3 Oxidation States [8]

Although nitrogen can readily adopt formal oxidation states between -3 ($NH_3$) and +5 ($HNO_3$) the preferred oxidation states of the heavier (n > 2) pnictogens depends on their position in the periodic table. Phosphorus and antimony tend to adopt the +3 or the +5 oxidation state (as would be predicted by the five valence electrons in group 15) while arsenic and bismuth usually adopt only the +3 oxidation state. Arsenic tends to adopt the +3 oxidation state instead of the +5 oxidation state because of the "d-block contraction". This term describes the incomplete screening of the nuclear charge by the first shell of d-electrons resulting in a higher effective nuclear charge on the 4s electrons, which have a finite probability of being found at the nucleus and a smaller radial distribution than do the 4p electrons, making them less likely to be removed. For bismuth, the heaviest stable element, relativistic effects favour the +3 state over the +5 state. The term "relativistic effect" indicates that the inner core electrons (particularly 1s which have the highest probability of being close to the nucleus) are moving at relativistic speed because of the high nuclear charge. For bismuth the 1s electrons are calculated to move at *ca.* 60% of the speed of light; thus from Einstein's special theory of relativity, the mass of these electrons increases and the Bohr radius of the 1s orbital decreases. To retain the orthogonality of all orbitals, the contraction of the 1s orbital causes a contraction of all spherically symmetric orbitals which lowers the energy of the 6s electrons and makes them less likely to be removed, thus favouring the +3 oxidation state.

### 1.2.4 Bonding in Group 15

Nitrogen, the pnictogen in the second row of the periodic table, is the only group 15 element for which multiple bonding is inherently favourable (groups 13, 14 and 16 exhibit similar behaviour). There are many different rationalizations for this behaviour including the size of atoms, the size of orbitals (and their relative overlap), the energy required to form a planar bonding environment (not always important) and others. For various explanations of the factors governing the favourability of multiple bonding, the interested reader may consult a variety of sources.[3,8,9,10,11,12,13,14]

## 1.3 Low-Coordinate and Electron Deficient Bonding Environments

The term "low-coordinate" denotes that the atom in question is bonded to fewer atoms than its formal oxidation state; the term "subvalent" is often used interchangeably with "low-coordinate". This definition implies that all compounds containing pπ-pπ multiple bonds are to be considered low-coordinate. Electron deficient, on the other hand, implies that an atom does not have the number of valence electrons required to fill all its valence orbitals (or an octet of electrons for second row elements).

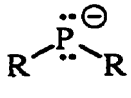

**1.1**

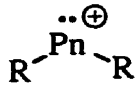

**1.2**

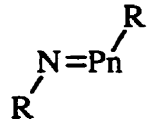

**1.3**

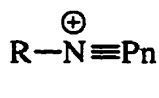

**1.4**

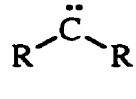

**1.5**

Pn = N, P, As, Sb, Bi

The terms "low-coordinate" and "electron deficient" are not mutually inclusive as demonstrated by compounds such as phosphides **1.1** which are low-coordinate (P(+3) with only two ligands) but electron precise (8 valence electrons in the 8 available orbitals for P: $3s\alpha,3s\beta,3p_x\alpha,3p_x\beta,3p_y\alpha,3p_y\beta,3p_z\alpha,3p_z\beta$).[6] An alternative electron counting

formalism would would lead to phosphides being termed "electron rich" (6 valence electrons, where P requires only 5).

Low-coordinate and electron deficient species are of interest for several reasons including: their sometimes novel structure and bonding; their potential to undergo addition reactions, making them useful synthons; and their potential for reactivity that is significantly different than that observed for electron precise or electron rich compounds. Additionally, some types of electron deficient species are thought to be intermediate products in chemical reactions and thus an understanding of the chemistry of such compounds can confirm or refute previous beliefs about chemical reactivity.

The types of low-coordinate and electron deficient bonding environments that are examined in this thesis include pnictogenium cations **1.2**, iminopnictines **1.3** and pnictazonium cations **1.4** (Pn = P, As, Sb or Bi). Pnictogenium cations are low-coordinate electron deficient species that are isovalent to carbenes **1.5** whereas iminopnictines and pnictazonium cations (formally) are low-coordinate compounds. Bonding environments of the type **1.3** and **1.4** are not unusual when Pn is N — these are the azo compounds and diazonium cations of organic chemistry — and are known for Pn = P, however these bonding arrangements are rare or unknown for the heavier pnictogen atoms (Pn = As, Sb, Bi).

## 1.4 Sterically Demanding Substituents

The use of sterically demanding substituents has been critical in the development of low-coordinate and electron deficient chemistry of heavier main group elements (particularly for $n > 3$). The term "sterically demanding" refers to a ligand with a large spatial requirement and typically implies that a ligand consists of a relatively large number of atoms which are fixed in close proximity to an atom or moiety of interest.[15,16]

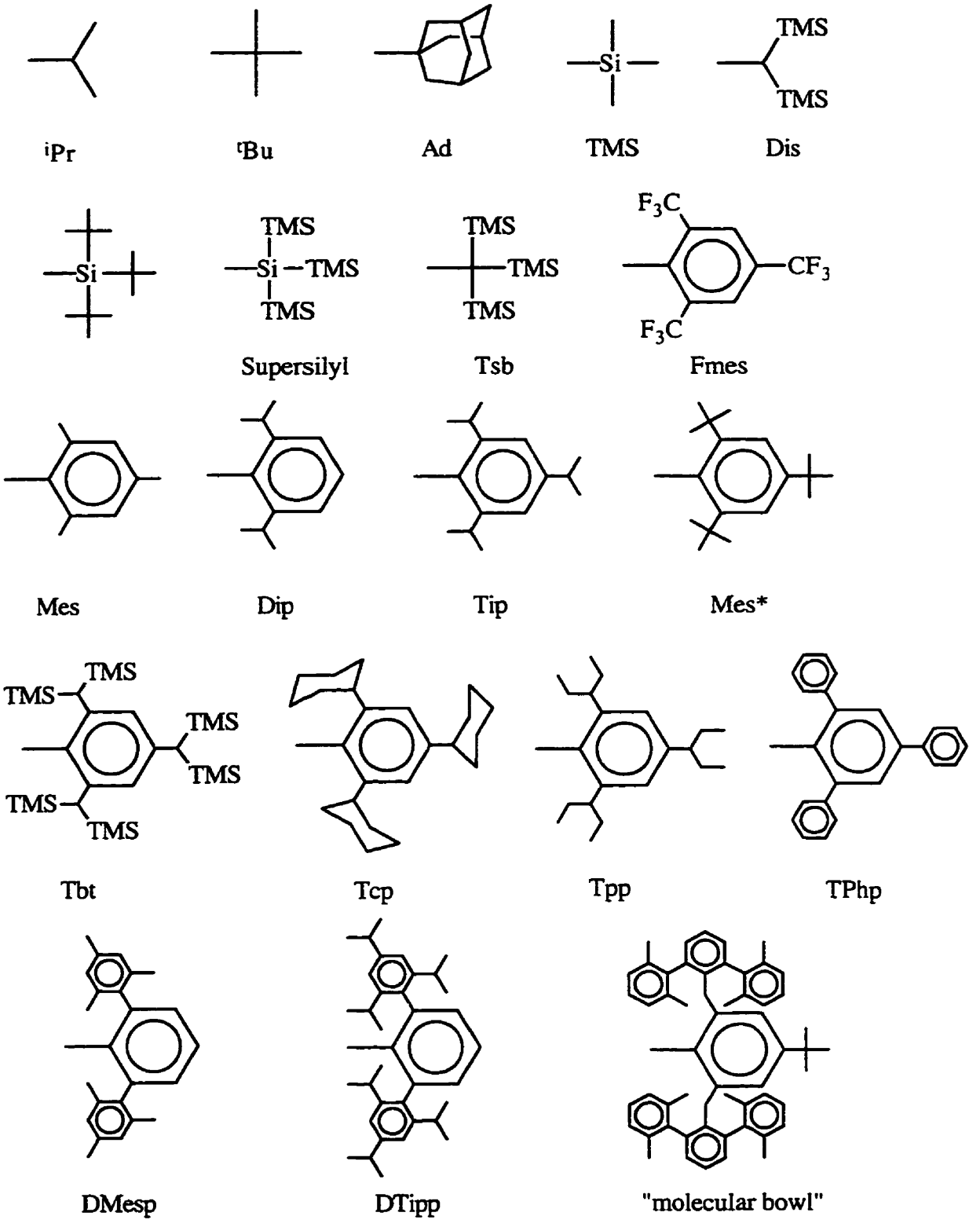


**Figure 1.1.** Sterically demanding substituents.

Examples of such ligands are shown in Figure 1.1 and include alkyl, silyl and aryl based substituents.[17] The most commonly used bulky substituent in main group synthesis is the 2,4,6-tri$^t$butylphenyl (supermesityl, Mes*) ligand which is examined in detail in this thesis along with the slightly less bulky 2,6-diisopropylphenyl (Dip) substituent (*vide infra*).

An immense variety of low-coordinate compounds and interesting reactivity has been achieved through the use of bulky substituents and the interested reader is directed to several reviews[18] and books.[19] Some recent highlights in main group chemistry include the isolation of compounds containing: Sb=Sb[20] and Bi=Bi[21] **1.6** double bonds, the very controversial Ga-Ga **1.7**[22,23,24] and Ga-M **1.8** "triple-bonds"[25,26], inorganic aldehyde **1.9**[27] and ketone **1.10**[28] fragments[29], the As≡C triple bond **1.11**[30], isolable group 13 multiple-bonded radical anions **1.12**[31], stable thioaminyl radicals **1.13**[32], persistent triplet carbene units **1.14**[33], a mono-coordinate indium(I) moiety **1.15**[34] and main group aromatic rings **1.16**,[35] **1.17**[36]and **1.18**.[37]

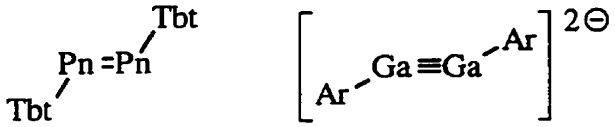


**1.6**

Pn = Sb, Bi




**1.7**


**1.8**

Ar = DTipp

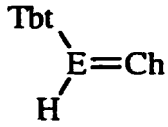

**1.9**

E = C, Si, Ge, Sn
Ch = S, Se, Te

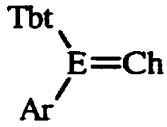

**1.10**

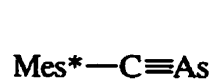

**1.11**

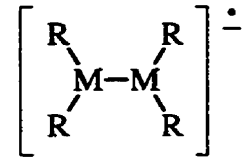

**1.12**

M = Al, Ga
R = Dis

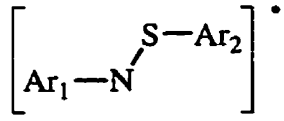

**1.13**

$Ar_1$ = 6-cyano-2,4-diphenylphenyl
$Ar_2$ = 2,4-dichlorophenyl

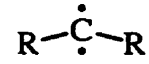

**1.14**

R = 2,4,6-trihalophenyl, fluorenyl, tripticyl(aryl)

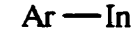

**1.15**

Ar = DTipp

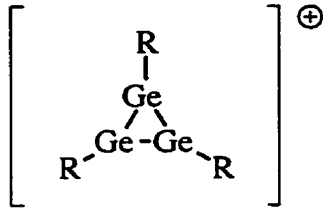

**1.16**

R = $Si(^tBu)_3$

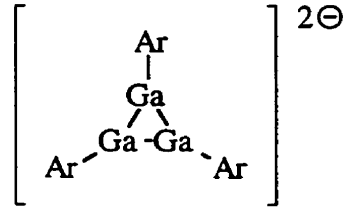

**1.17**

Ar = DMesp

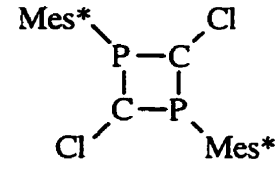

**1.18**

Sterically demanding ligands are typically described as "kinetic shields" which implies that the stabilization afforded by the substituents is kinetic in origin, i.e. that the bulky group restricts access to the reactive site in an unstable species A (Figure 1.2) (thus causing a large activation barrier, $E_a$) and thereby prevents formation of a more stable species B. Although this is certainly the case in some systems[38], such a view of sterically demanding substituents neglects the potentially significant and sometimes dominant thermodynamic stabilization these ligands provide for other low-coordinate systems. The notion that multiple-bonded main group compounds are "kinetically stabilized" arises from

isodesmic enthalpic comparisons of π-bonds versus σ-bonds (*vide supra*). For heavier main group elements (n > 2), the bond energy of a double bond to an element is found to be less than twice the energy of two single bonds, thus isodesmic comparisons always predict that the fully σ-bonded compound will be thermodynamically favoured. The fault in the logic of the simple isodesmic method is the implicit assumption that all other interactions and bond energies in both the π-bonded and σ-bonded compounds are the same and can thus be ignored. Although this assumption may be acceptable for systems with small substituents, the steric interaction between large ligands can not be ignored.

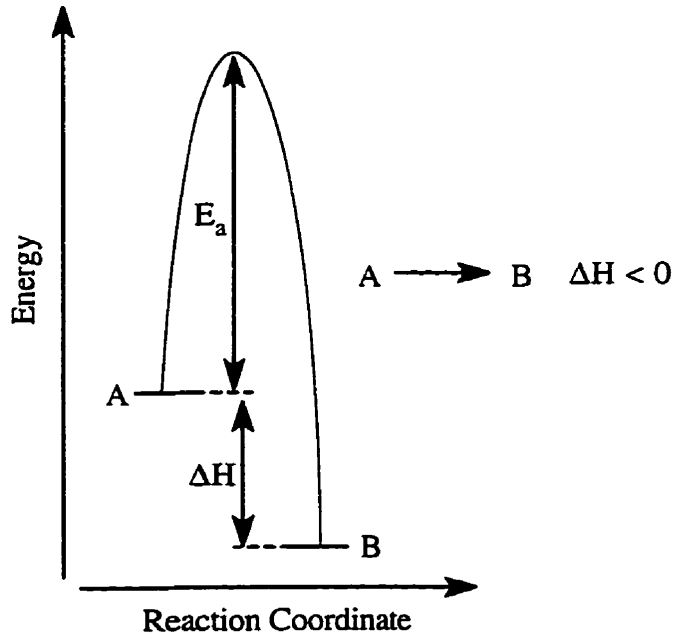


**Figure 1.2.** Schematic reaction energy diagram.

Molecular mechanics and semi-empirical calculations performed by our group have demonstrated that bulky ligands thermodynamically stabilize double-bonded systems

versus cyclic oligomers. [39] The steric strain caused by the proximity of bulky substituents in the dimeric or oligomeric species significantly destabilizes these fully σ-bonded structural alternatives with respect to the π-bonded monomers (Table 1.3). This strain energy more than overcomes the difference in single (2 x C-C: 670 kJ/mol)[9] and double bond energies (C=C: 630 kJ/mol)[9] for the system and renders the mutiple bonded system thermodynamically stable with respect to its oligomers. Because the multiple bonded species are thermodynamically favoured over their oligomeric alternatives the activation barrier separating them, no matter how large it may be, is irrelevant: the "kinetic shield" is redundant. Qualitative dimerization energy diagrams as a function of substituent size are depicted in Figure 1.3.

**Table 1.3.** Calculated enthalpies of the cyclodimerization of *trans*-RHC=CRH (kJ/mol).

| R | MM3 | AM1 |
|---|---|---|
| H | -85 | -142 |
| Me | -83 | -77 |
| tBu | -7 | -23 |
| Ph | +19 | -47 |
| Mes | +68 | +46 |
| Tip | +282 | +173 |
| Mes* | +395 | +475 |

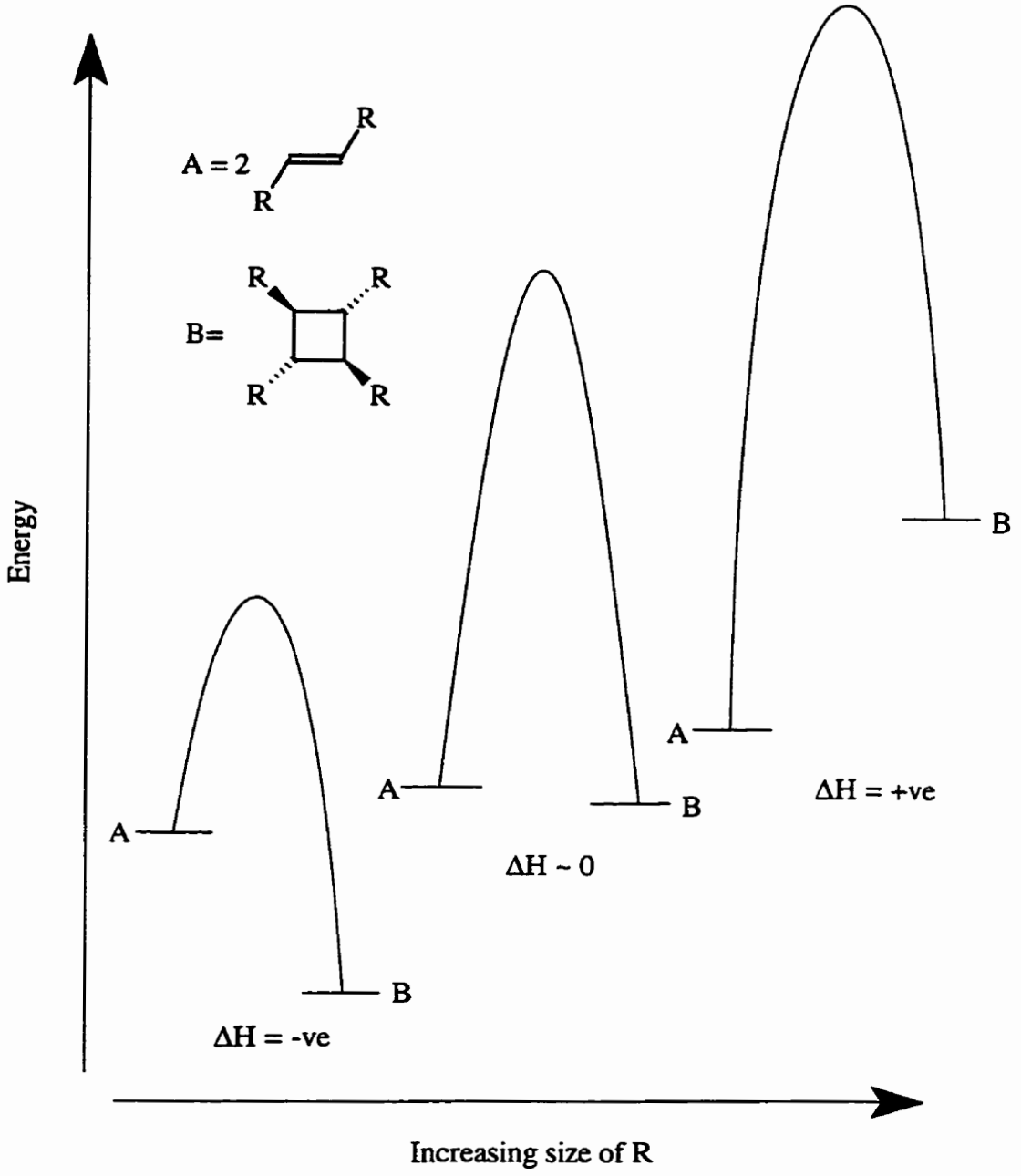


**Figure 1.3.** Qualitative reaction energy diagrams as a function of substituent size.

Unequivocal experimental evidence for the thermodynamic effects of bulky substituents is also found in the literature. Equilibrium constants for the reaction of $I_2$ with various diselenides **1.19** (Figure 1.4) were measured by du Mont *et al* [40] and show that the supposedly unattainable R-Se-I **1.20** compounds[41] are thermodynamically favoured ($K_{eq}$ is greater than one thus $\Delta G$ is negative) when R is a bulky substituent. The favourability of the iodoselenides is found to increase with the size of the substituent because of the steric strain imposed on the starting diselenides. The results of this study are indicative of the "tunability" of sterically demanding substituents: the different sizes of bulky substituents allow the researcher to control the bonding in a particular molecule by the appropriate choice of bulky group. The concept of "tunability" and steric control of chemical bonding is examined in this thesis.

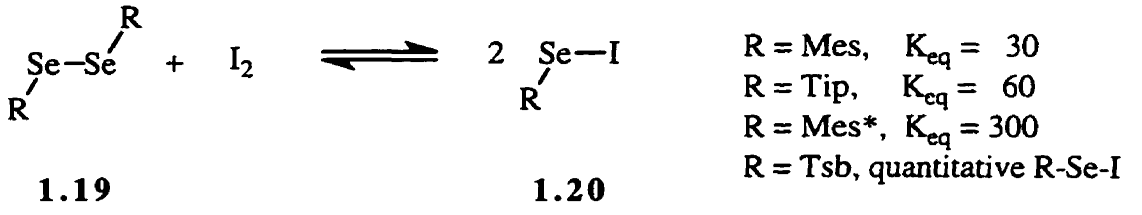


**Figure 1.4.** Reaction of diselenides with iodine.

An example from our own lab that also illustrates the thermodynamic stability confered to multiple bonded systems by bulky substituents is that of the spontaneous formation of an iminophosphine from a trisaminophosphine.[42] Aminoiminophosphines **1.21** typically react with primary amines to form trisaminophosphines **1.22** (or the P(V) isomeric diaminoiminophosphoranes **1.23**, depending on the substituent R) as expected

from comparison of P=N (300 kJ/mol σ + 185 kJ/mol π = 485 kJ/mol) and P-N (300 kJ/mol x 2 = 600 kJ/mol) bond energies. However, preparation of Mes* substituted trisaminophosphine **1.24** results in the spontaneous elimination of amine and the formation of aminoiminophosphine **1.25** — apparently causing the formation of a less stable product from a more stable starting material. The relative thermodynamic stability of the compounds in this system are obviously altered by the inclusion of the bulky Mes* ligand and the multiple bonded iminophosphine (with an equivalent of amine) is the most energetically stable situation because of the large steric strain in the trisaminophosphine.

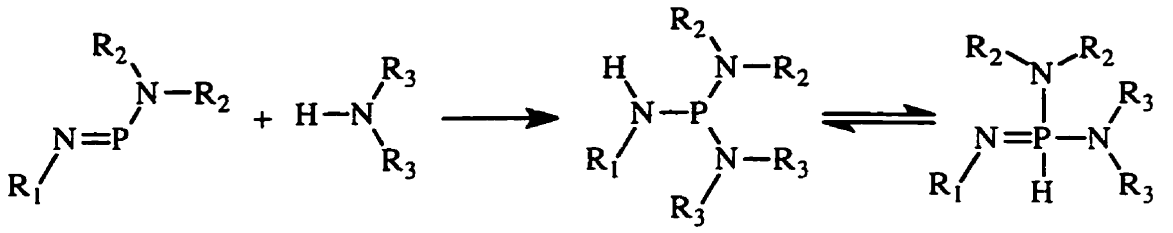

**1.21** **1.22** **1.23**

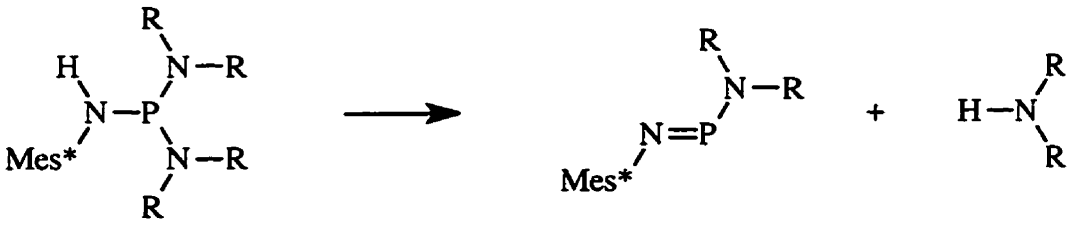

**1.24** **1.25**

The effects and limitations of bulky substituents are further examined in this thesis, however it must be re-emphasized that the use of such ligands has allowed for the isolation and characterization of compounds that were once thought to be "non-existent".[41] The experimental and theoretical studies of such compounds, especially the heavier main group analogues of organic compounds, demand the conclusion that the bonding observed

for the second row elements (i.e. organic chemistry) is the exception to the rule.[9,14,24] Because of the practicality and historical dominance of organic chemistry, a guiding focus of main group chemistry has been (and is) to mimic the well known chemistry of organic compounds. The preconceptions about chemical bonding drawn from organic chemistry (e.g. double bonded species must be planar, triple bonded compounds must be linear) should be ignored when descending the periodic table, however the differences and similarities between organic and main group chemistry are compared most effectively through the examination of analogous species. Consequently, the compounds examined in this thesis, where applicable, are considered in the context of organic analogues.

## 1.5 Thesis Overview

This thesis consists of seven additional chapters which describe studies of a variety of low-coordinate bonding environments containing group 15 atoms. The first three chapters relate results regarding pnictogenium cations and the final chapters examine low-coordinate compounds that are only attainable through the use of sterically demanding substituents. Highlights include the isolation of the first monomeric non-Hückel arsenium cation, the isolation of the first acyclic arsenium cation, the observation of an equilibrium which appears to defy Le Chatelier's principle, and the formation of the first arsenic-nitrogen triple bond.

Chapter 2 is a synthetic and theoretical study of cyclic phosphenium and arsenium cations which describes and explains the structural differences observed in these species. Chapter 3 describes the remarkable difference in the cycloaddition behaviour of these cations which is explained through the use of *ab initio* calculations. The use of the moderately bulky Fmes substituent as a stabilizing ligand for pnictogenium cations is examined in Chapter 4. Chapter 5 begins the examination of steric control of low-

coordinate pnictogen compounds with a study of the effects of ligand bulk in a series of analogous iminoaminopnictines, diazadipnictidines and trisaminopnictines. The use of sterically demanding groups is further examined in Chapter 6, which describes the remarkable "non-Le Chatelier" behaviour of a phosphazonium cation and its diazadiphosphetidine dimer. Chapter 7 details the synthesis of versatile iminoarsines which allow for the expansion of low-coordinate arsenic chemistry. Suggestions for future research are summarized in the conclusion sections of each chapter and the experimental details of the research reported in this thesis are found in Chapter 8.

# Chapter 2. Pnictogenium Cations (I): The Synthetic and Theoretical Examination of the Structure and Bonding of Phosphenium and Arsenium Cations

## 2.1 Introduction

The structural simplicity of systems containing coordinatively unsaturated (low-coordinate) centres makes them attractive for reactivity studies. Interest in carbenes **2.1a**[43] and the analogous systems **2.1** and **2.2** stems from their intriguing electronic structure, fascinating reactivity (e.g. electrophilic and nucleophilic behaviour) and corresponding synthetic utility (e.g. achiral and chiral[44] ligands in homogeneous catalysts[45]).[14,46,47] Isolable examples are known for carbenes **2.1a**,[46,48,49,50,51] silylenes **2.1b**,[52] germylenes **2.1c**,[52,53] stannylenes **2.1d** [52,53] and plumbylenes **2.1e**.[54]

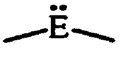

**2.1a** E = C
**b** E = Si
**c** E = Ge
**d** E = Sn
**e** E = Pb

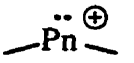

**2.2a** Pn = N
**b** Pn = P
**c** Pn = As
**d** Pn = Sb
**e** Pn = Bi

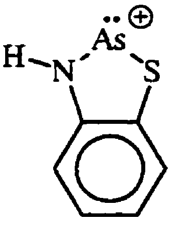

**2.3**

In this context, the cationic group 15 analogues (pnictogenium cations) **2.2** have attracted attention due to their structure and bonding analogy with carbenes. Numerous phosphenium **2.2b** derivatives have been reported[55,56,57] since their initial discovery[58] and isolation[59,60] establishing them as a principal focus in the development of phosphorus chemistry. Despite the identification of various arsenium cations **2.2c**,[61,62,63,64] few examples have been comprehensively characterized and the heavier congeneric systems,

stibenium cations **2.2d**[65] and bismuthenium cations **2.2e**,[66] are rarely mentioned in the literature. The use of a Hückel aromatic framework in **2.3** allowed for the isolation of the first arsenium derivative.[61b] However, in the absence of such charge delocalization, heterolytic As-Cl bond cleavage from the chloroarsolidines **2.4Cl** and **2.5Cl** provided dimeric structures **2.8** in the solid state,[63] in contrast to the phospholidinium **2.7** analogue.[60]

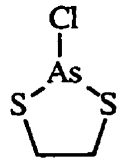

**2.4Cl**

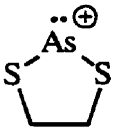

**2.4**

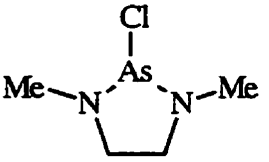

**2.5Cl**

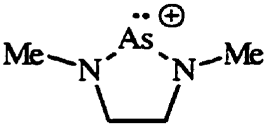

**2.5**

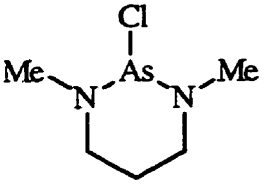

**2.6Cl**

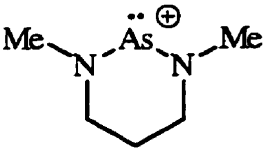

**2.6**

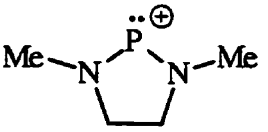

**2.7**

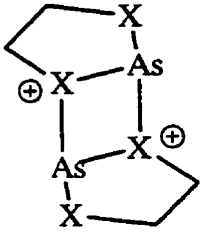

X = N(Me), S

**2.8**

This chapter presents the preparation and structures of the six-membered diazarsenane **2.6Cl** and the tetrachlorogallate salt of the corresponding diazarsenanium cation **2.6**, which is the first non-Hückel arsenium cation that is clearly monomeric in the solid state.[67] In addition, the surprising behaviour of arsenium cations is investigated through the use of high level *ab initio* calculations which confirm the singlet ground state of the cations, and explain the observation of monomeric arsenium cation **2.6**.

## 2.2 Chlorodiazarsenane and Diazarsenanium Tetrachlorogallate

The halide ion abstraction technique illustrated in Figure 2.1, now commonplace in the preparation of phosphenium salts,[55] is also applicable for the formation and isolation of arsenium derivatives.

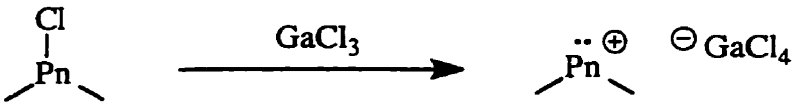


**Figure 2.1.** Preparation of pnictogenium cation by halide abstraction.

The first examples, **2.4**[$GaCl_4$] and **2.5**[$GaCl_4$], were shown to adopt novel dimeric structures **2.8** in the solid state.[63] The identical synthetic procedure was extended to the six-membered (cyclohexane derivative) diazarsenane framework to assess the generality of the bonding and reactivity observed in **2.4**[$GaCl_4$] and **2.5**[$GaCl_4$].[68]

2-Chloro-1,3-dimethyldiaza-2-arsenane **2.6Cl** reacts with $GaCl_3$, in an essentially identical fashion to the arsolidine **2.5Cl**,[63] to give 1,3-dimethyldiaza-2-arsenanium **2.6** tetrachlorogallate. Compounds **2.6Cl** and **2.6**[$GaCl_4$] have been comprehensively characterized and crystallographic views of the solid state structures are illustrated in Figures 2.3 and 2.4, respectively. The structure of 2-chloro-1,3-dimethyldiaza-2-arsolidine **2.5Cl** (-60°C; Figure 2.2) is also described for comparison. Selected bond lengths and angles for the three compounds are compared with those for **2.5**$_2$[$GaCl_4$]$_2$[63] in Table 2.1.

**Table 2.1** Selected bond lengths(Å) and angles (°) for **2.5**$_2$[$GaCl_4$]$_2$[63], **2.6**[$GaCl_4$], **2.5Cl**, and **2.6Cl**.

| **2.5**$_2$[$GaCl_4$]$_2$[63] | | **2.6**[$GaCl_4$] | | **2.5Cl** | | **2.6Cl** | |
|---|---|---|---|---|---|---|---|
| | | | | As(1)-Cl(1) | 2.390(5) | As(1)-Cl(1) | 2.357(2) |
| As(1)-N(1) | 1.752(5) | As(1)-N(1) | 1.68(3) | As(1)-N(1) | 1.77(1) | As(1)-N(1) | 1.796(4) |
| As(1)-N(2) | 1.949(4) | As(1)-N(2) | 1.67(2) | As(1)-N(2) | 1.830(8) | As(1)-N(2) | 1.803(5) |
| N(2)-C(4) | 1.506(8) | N(2)-C(2) | 1.505(12) | N(2)-C(4) | 1.47(1) | N(1)-C(3) | 1.459(8) |
| N(2)-C(2) | 1.500(9) | N(2)-C(3) | 1.487(12) | N(2)-C(2) | 1.46(1) | N(1)-C(5) | 1.456(8) |
| N(1)-C(3) | 1.487(8) | N(1)-C(1) | 1.489(12) | N(1)-C(3) | 1.44(1) | N(2)-C(1) | 1.459(8) |
| N(1)-C(1) | 1.462(8) | N(1)-C(5) | 1.489(12) | N(1)-C(1) | 1.43(1) | N(2)-C(4) | 1.465(7) |
| | | | | | | | |
| | | | | Cl(1)-As(1)-N(1) | 100.8(3) | Cl(1)-As(1)-N(1) | 99.8(2) |
| | | | | Cl(1)-As(1)-N(2) | 97.8(3) | Cl(1)-As(1)-N(2) | 99.1(2) |
| N(1)-As(1)-N(2) | 87.2(2) | N(1)-As(1)-N(2) | 102.2(11) | N(1)-As(1)-N(2) | 87.8(4) | N(1)-As(1)-N(2) | 98.4(2) |
| As(1)-N(2)-C(2) | 107.6(3) | As(1)-N(2)-C(3) | 126(2) | As(1)-N(2)-C(2) | 108.7(7) | As(1)-N(1)-C(3) | 121.9(4) |
| As(1)-N(2)-C(4) | 114.9(4) | As(1)-N(2)-C(2) | 121(2) | As(1)-N(2)-C(4) | 116.8(7) | As(1)-N(1)-C(5) | 113.7(4) |
| C(2)-N(2)-C(4) | 110.9(4) | C(3)-N(2)-C(2) | 113(2) | C(2)-N(2)-C(4) | 113.9(9) | C(3)-N(1)-C(5) | 112.3(5) |
| As(1)-N(1)-C(1) | 116.2(4) | As(1)-N(1)-C(5) | 130(2) | As(1)-N(1)-C(1) | 115.9(7) | As(1)-N(2)-C(1) | 121.1(4) |
| As(1)-N(1)-C(3) | 124.4(4) | As(1)-N(1)-C(1) | 121(2) | As(1)-N(1)-C(3) | 124.4(8) | As(1)-N(2)-C(4) | 113.2(4) |
| C(1)-N(1)-C(3) | 119.1(5) | C(1)-N(1)-C(5) | 108(2) | C(1)-N(1)-C(3) | 119(1) | C(1)-N(2)-C(4) | 112.6(5) |
| N(1)-C(1)-C(2) | 106.0(5) | N(1)-C(5)-C(4) | 109(2) | N(1)-C(1)-C(2) | 107.4(9) | N(2)-C(1)-C(2) | 112.0(5) |
| N(2)-C(2)-C(1) | 107.2(5) | N(2)-C(3)-C(4) | 113(2) | N(2)-C(2)-C(1) | 107.4(9) | N(1)-C(3)-C(2) | 111.3(5) |
| | | C(3)-C(4)-C(5) | 113(3) | | | C(1)-C(2)-C(3) | 113.1(5) |

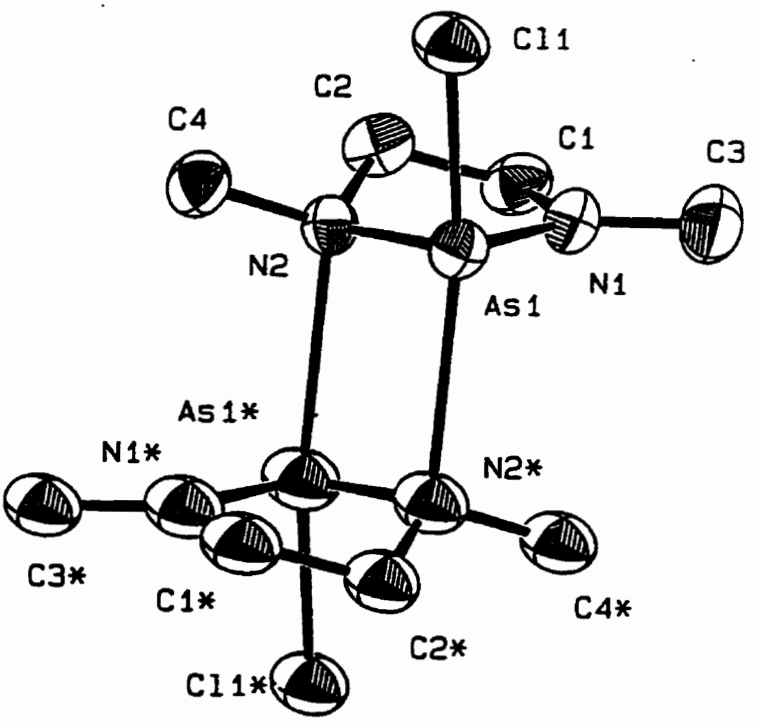


**Figure 2.2.** Molecular structure of **2.5Cl**.

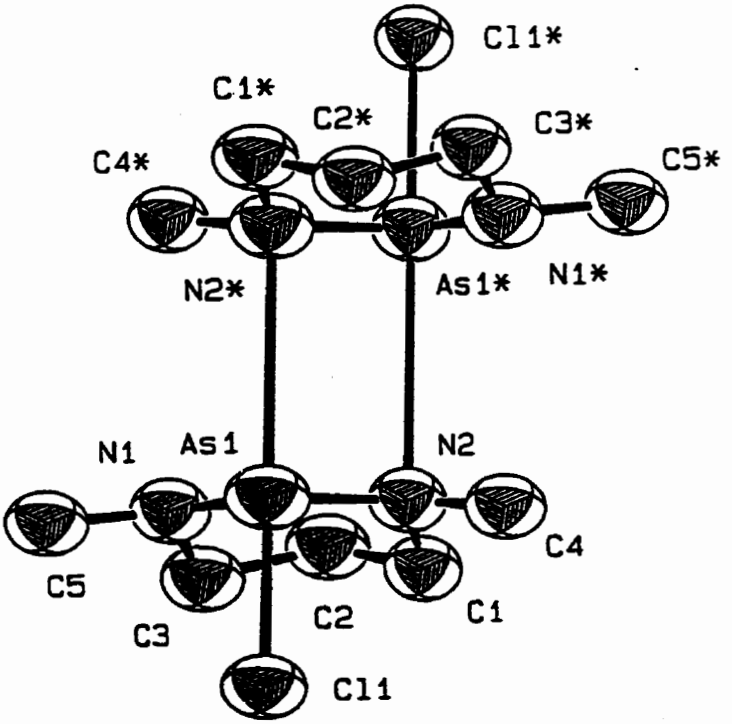


**Figure 2.3.** Molecular structure of **2.6Cl**.

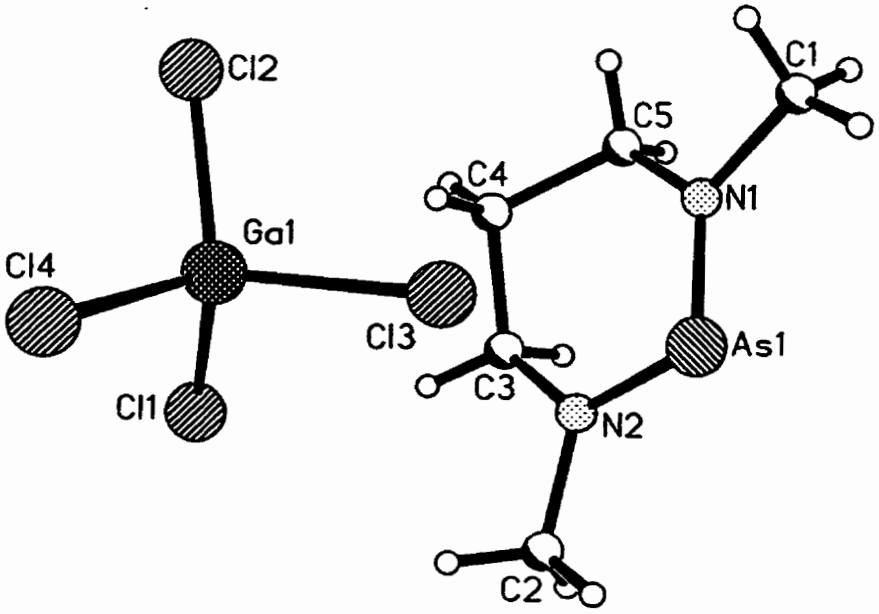


**Figure 2.4.** Molecular structure of **2.6**[$GaCl_4$].

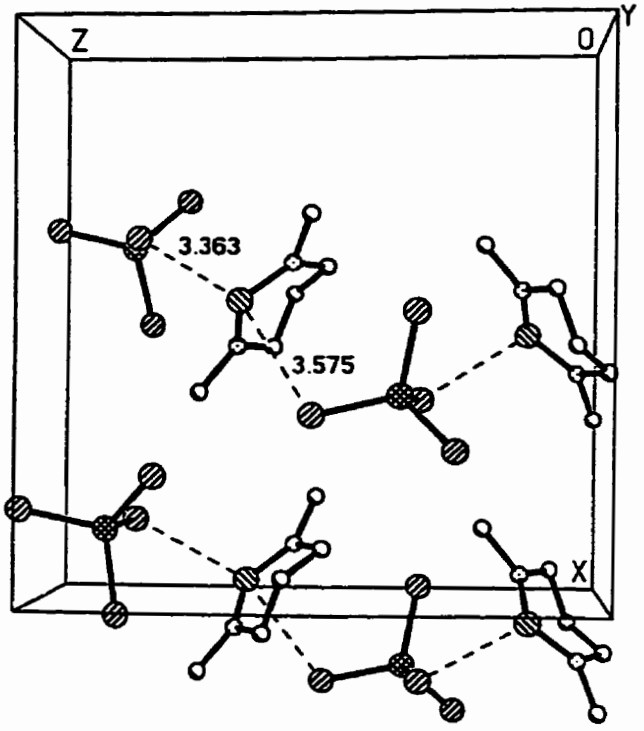


**Figure 2.5.** Packing diagram of **2.6**[$GaCl_4$].

Crystals of **2.6**[$GaCl_4$] were of poor quality and provided only limited data. Nevertheless, the distinctly ionic structure of **2.6**[$GaCl_4$] (Figure 2.4) shows no evidence of interaction between cations (shortest intercationic As-N 5.62(2)Å (Figure 2.5) in contrast to the dimeric **2.8** structure of **2.5**[$GaCl_4$] (as well as **2.4**[$GaCl_4$]). This implies that the association between monomers in **2.8** is weak, consistent with the relatively long intermonomer bonds observed. Furthermore, the $^1H$ NMR spectroscopic data for **2.5**[$GaCl_4$], which were interpreted as indicating a monomer-dimer equilibrium in solution,[63] are ambiguous and are also consistent with the presence of only monomeric arsenium units in solution. Cation-anion contacts [3.363(9)Å and 3.58(1)Å] are within the sum of the van der Waals' radii for As and Cl [As, 2.0 Å; Cl, 1.7 Å][69], but are significantly longer than the As-Cl bonds in **2.5Cl** [2.390(5)Å] and **2.6Cl** [2.357(2)Å], and are comparable to the cation-anion contacts observed in the structure of **2.5**[$GaCl_4$] [3.296(2)Å and 3.424(2)Å][63]. The resulting "coordination polymer" lattice of **2.6**[$GaCl_4$] is reminiscent of the solid state structures observed for [$Me_2Si(\mu\text{-}N^tBu)_2Pn$][$GaCl_4$] (Pn = Sb, Bi) **2.9**,[65d] however the As-Cl contacts in **2.6**[$GaCl_4$] (*vide supra*) are clearly more consistent with separate cations and anions than are the covalent Pn-Cl bonds in **2.9**. The As-N bonds (1.68(3) and 1.67(2) Å) are significantly shorter than the shortest bond of **2.5**$_2$[$GaCl_4$]$_2$ (1.752(5) and 1.949(4) Å)[63], shorter than the As-N bonds in the Hückel aromatic arsenium cations **2.3**[$GaCl_4$] (1.776(4) Å) and **2.10** [$GeCl_5$]$_{1/2}Cl_{1/2}$ (1.810(9) and 1.812(9) Å)[67] and are on the order of the formal As=N bond (1.707(2) Å) in FmesAs=NFmes [70] implicating a significant degree of π-bonding over the N-As-N unit.

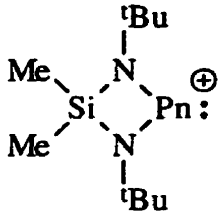

**2.9**

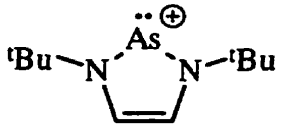

**2.10**

In spite of the monomeric structure observed for **2.6**[$GaCl_4$], the neutral arsenane **2.6Cl** also adopts a dimeric arrangement involving a four-membered $As_2N_2$ intermonomer contact which is similar to that of the corresponding arsolidines **2.4Cl** and **2.5Cl** as well as the dications **2.8**. Such arrangements contrast that observed for related chloroarsines[61b,65d] which involve four-membered $As_2Cl_2$ contacts. The intermonomer contact is significantly shorter in **2.5Cl** [As-N' 2.84(1)Å] than in **2.6Cl** [As-N' 3.250(5)Å], and both are substantially longer than observed for **2.5**$_2$[$GaCl_4$]$_2$ [2.103(8)Å].[63] These interactions are well within the sum of the van der Waals' radii for As and N (As, 2.0 Å;N, 1.5 Å)[69] and impose a pseudo-tetracoordinate environment on N(2). The shorter interaction in **2.5Cl** has a measurable impact on the structural features of the arsolidine heterocycle, which exhibits slight differences in the As-N bond lengths as well as the geometries at the nitrogen centres. N(1) is essentially planar (sum of the angles 359.3°), while N(2) is clearly pyramidalised (sum of the angles 339.4°). The geometrically indistinguishable nitrogen centres of **2.6Cl** have bond angle sums [N(1), 348°; N(2), 347°] that are substantially greater than expected for an $sp^3$ (328.5°) hybridized site. In this context, the relatively long[71] As-Cl bonds (**2.5Cl**, 2.390(5) Å; **2.6Cl**, 2.357(2) Å) and relatively short endocyclic As-N bonds (**2.5Cl**, 1.77(1) Å, 1.870(8) Å; **2.6Cl**, 1.796(4)

Å, 1.803(5) Å; typical range 1.82-1.88 Å)[72] in both compounds imply a degree of As-N π-bonding.

The $^1$H NMR spectra for **2.6Cl** (δ: 2.88m, 2.63s, 1.94m) and **2.6**[$GaCl_4$] (δ: 3.49m, 3.34s, 2.29m) are interpreted as very similar AA'BB'CD spin systems and differ only in chemical shift, with the salt exhibiting the expected deshielding. Consistent with integration values, the lower frequency multiplet is assigned to the aza-methylene protons and the singlet to the methyl protons. Spectra recorded at -80°C were not significantly different.

## 2.3 Theoretical Assessment of Phosphenium and Arsenium Cations

### 2.3.1 Introduction

The experimental results above and previous studies of such species illustrate significant differences between arsenium cations and all other carbenoids. All structural studies of pnictogenium cations reveal monomeric units in the solid state except in the case of arsolidinium **2.5** salts (and the dithia derivatives) which adopt dimeric solid state structures **2.8**.[63] The observation of a monomeric structure for the arsenanium salt **2.6**[$GaCl_4$] implies a small (if any) dimerization energy for **2.5**.[62] In addition, arsenium cations dimerize in a different manner than most group 14 carbenoids which dimerize to make E=E double bonds.

A rationale for the solid state structural differences of group 14 and 15 carbene analogues has recently been described in the context of the "Carter-Goddard-Malrieu-Trinquier Model" (CGMT);[14] however, the vast majority of the data model structurally simple and nonisolable model compounds. In an attempt to understand the factors

governing the structure and the dimerization behaviour of cations **2.7**, **2.5** and **2.6**, we have performed quantum chemical investigations of model cations **2.7'**, **2.5'** and **2.6'**; these confirmed the singlet ground state multiplicity and explained the enigma of arsenium dimerization.

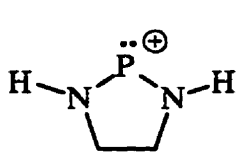

**2.7'**

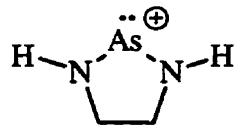

**2.5'**

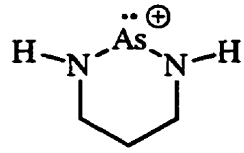

**2.6'**

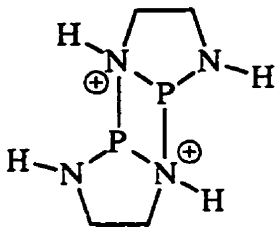

**2.21'**

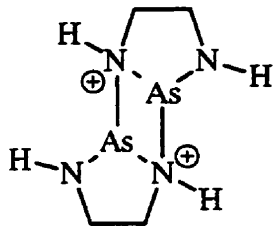

**2.22'**

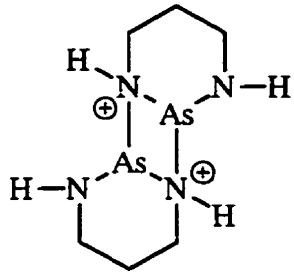

**2.23'**

### 2.3.2 Theoretical Methods and Results

All calculations in this thesis were performed on an IBM RS6000/580 workstation using the Gaussian94 set of programs.[73] Unless specified otherwise, the geometry of each species was optimized by the Hartree-Fock (HF) method using the 6-311G* basis set and all energies were calculated using full second-order Møller-Plesset (MP2) perturbation theory with the 6-311G* basis set. Model compounds were restricted to the highest appropriate symmetry; structural parameters are listed in Tables A.2 and A.3 in Appendix A. All energy minima were confirmed by 3N-6 positive eigenvalues of the Hessian matrices and the total energies include the HF/6-311G* zero-point vibrational energies

(MP2/6-311G*//HF/6-311G* + 0.9 ZPVE (HF)) which are listed in Table A.1. Molecular orbital (MO) analyses, spin densities and charge distributions were determined through the use of Mulliken population analysis and natural bond orbital analysis [74] (NBO) the results of which are listed in Tables A.4 and A.5.

**Table 2.2** Calculated enthalpies (kJ/mol) of dimerizations and singlet-triplet energy splittings for cyclic pnictogenium cations. UMP2 denotes UMP2/6-311G*//UHF/6-311G* + 0.90 ZPVE, UHF denotes UHF/6-311G* + 0.90 ZPVE.

| Reaction | UMP2 | UHF |
|---|---|---|
| **2.7' + 2.7' → 2.21'** | 277.44 | 337.27 |
| **2.7' s → 2.7' t** $C_1$ | 307.60 | 195.47 |
| **2.7' s → 2.7' t** $C_2$ | 288.02 | 209.96 |
| **2.7' s → 2.7' t** ($C_s \rightarrow C_{2v}$) | 290.20 | 210.15 |
| **2.5' + 2.5' → 2.22'** | 206.70 | 260.63 |
| **2.5' s → 2.5' t** $C_1$ | 249.14 | 123.46 |
| **2.5' s → 2.5' t** $C_2$ | 237.71 | 143.00 |
| **2.5' s → 2.5' t** ($C_s \rightarrow C_{2v}$) | 240.14 | 143.66 |
| **2.6' + 2.6' → 2.23'** | 247.92 | 294.00 |

### 2.3.3 Multiplicity of the Ground State for Diazaphosphenium and Diazaarsenium cations

Various factors govern the stability of pnictogen salts including: the solvent, the presence of base-stabilization (inter- or intramolecular), the nature of the counter anion, and the steric and electronic influence of the substituents adjacent to the di-coordinate site. The relative stabilities of such compounds may be assessed by the measurement of the lifetimes of species and their resistance to rearrangement or addition reactions. The isolation of $[GaCl_4]$ or $[AlCl_4]$ salts of pnictogenium cations **2.2** is perhaps surprising in view of

typical Lewis adduct chemistry ($R_2ClPn \rightarrow ECl_3$) of phosphines and arsines, and is indicative of the significance of the crystal lattice energy term in defining their stability. Studies using conventional *ab initio* methods typically ignore these external factors, however such studies do yield insight regarding the inherent stability of such species and thus may be extremely valuable in the understanding of results observed experimentally.

Several topical quantum chemical studies of ylidenes **2.1** have provided substantial insight into their structure and bonding.[75,76,77] Electronic structure models have also been established for the group 15 carbene analogues **2.2**[56,78,79,80,81,82,83,84,85] which indicate that most, including all those possessing adjacent $\pi$-electron donor substituents, have a singlet ground state ($[NH_2]$ is an exception)[86]. In this context, we have performed full geometry optimizations and frequency calculations at the HF/6-311G* level of theory for model cations **2.7'** and **2.5'** with singlet ($C_2$ symmetry) and triplet ground states ($C_1$, $C_2$, $C_s$, and $C_{2v}$ symmetries). These geometries were then used to obtain single-point UMP2 energies. Calculated structural parameters for **2.7'** are compared with experimentally determined values for **2.7** in Figure 2.6. The energies, zero-point vibrational energies (ZPVE), and number of imaginary frequencies for singlet and triplet cations **2.7'** and **2.5'** are listed in Table A.1[§] and selected structural parameters are listed in Table A.2.

---

§ In all tables the following format is used: **compound number** multiplicity label (s - singlet; d - doublet; t - triplet) symmetry (numbered when more than one structure of that symmetry)

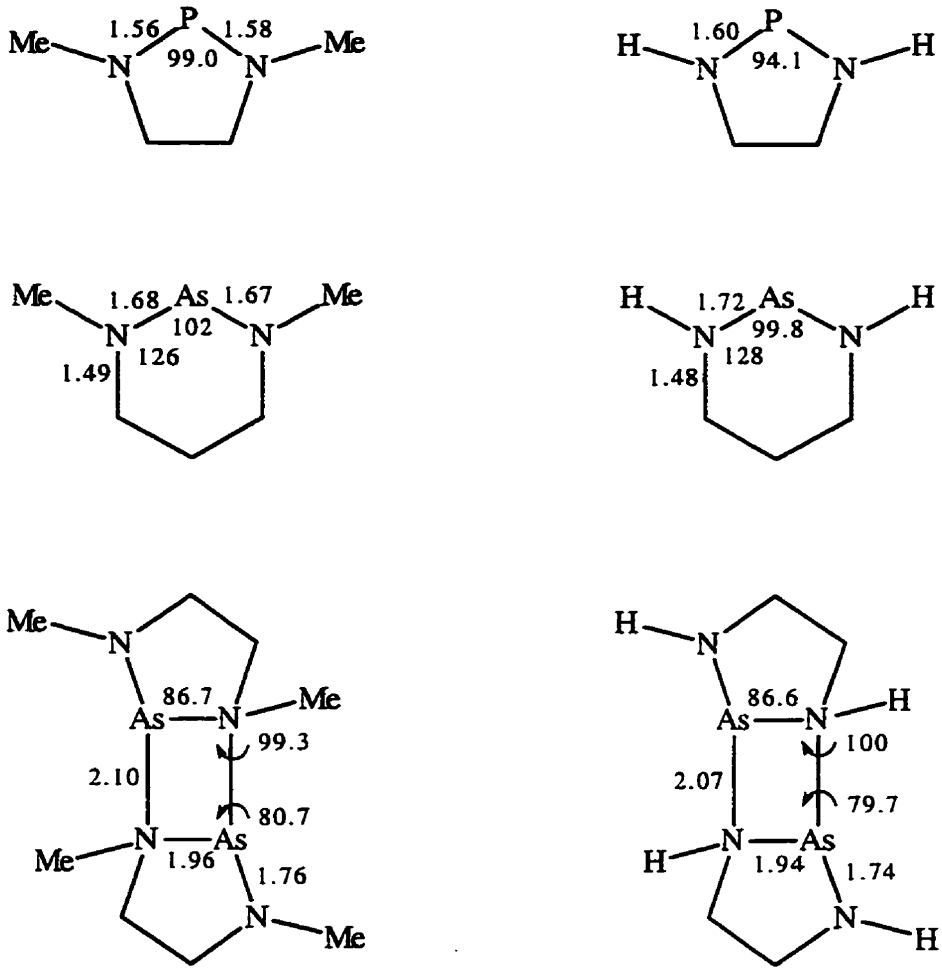


**Figure 2.6.** Comparison of experimental (left) and theoretical (right) structures. Bond lengths in Å, and angles in degrees.

The singlet states of the phospholanium **2.7'** and arsolanium **2.5'** cations are lower in energy than the corresponding triplet states by 308 kJ/mol and 249 kJ/mol, respectively, in qualitative agreement with previous quantum chemical investigations of structurally simpler pnictogenium cations.[14,78,80,83,85] The singlet-triplet splittings are much larger than those calculated for the cations [$PH_2$] (68.2, 81.6 and 56.9 kJ/mol[80] and 67.4 kJ/mol[78]) and [$AsH_2$] (87.9, 111.3 and 86.6 kJ/mol[80]). Nevertheless, the splitting in **2.7'** is consistent with those calculated for the cations [HPF] (178.2 kJ/mol), [$PF_2$] (351.5 kJ/mol),[78] [$PBr_2$] (159.20 kJ/mol),[85] as is the splitting in **2.5'** with those for [$AsCl_2$] (229.7 kJ/mol) and [$AsBr_2$] (182.8 kJ/mol).[83] These similarities are probably due to the π-donor substituents in **2.7'**, **2.5'**, [HPF] and [$PF_2$] (and to a lesser extent in the systems with the weaker π-donors, Cl and Br) which therefore stabilize the singlet state by π-donation.[80,87]

The inclusion of the pnictogen center in a five-membered ring imposes a small N-Pn-N bond angle (85°-95°) which is also predicted to stabilize the singlet state relative to the triplet state for carbenes,[88] although the optimized structures for the triplet states of **2.7'** and **2.5'** have even more acute N-Pn-N angles than do the singlets. To assess the validity of this observation at the HF/6-311G* level of theory, the energies of a series of simple acyclic pnictogenium cations [$H_2N$-Pn-$NH_2$] (**2.11'** Pn = P, **2.12'** Pn = As) were studied on the $C_{2v}$ energy hypersurface. The lowest singlet and triplet states were allowed to optimize with no constraints and the results show that the singlet species is substantially favoured in each case ($E_{s \rightarrow t}$: **2.11'**, 395.8 kJ/mol; **2.12'**, 325.2 kJ/mol). The triplet

species are optimized with more acute N-Pn-N angles for both phosphenium (104.8° vs. 90.0°) and arsenium cations (101.4° vs. 87.5°), however both triplet cations are not true minima (2 imaginary frequencies for both P and As). In addition, the effect of the N-Pn-N bond angle on the energy of the cations on the $C_{2v}$ singlet and triplet surfaces was examined by fixing the bond angle and allowing all other parameters to optimize. The results of these calculation are illustrated in Figure 2.7 and show that there exists only one minimum for each singlet cation and two "minima" for each of the triplet surfaces. Frequency analysis of each stationary point reveals that the only true minima (N imag = 0) on the P triplet surface are at 140° and 150° which are each more than 100 kJ/mol higher in energy than the lowest energy structure on the $C_{2v}$ surface. Full MP2/6-311G* optimizations for both $[(H_2N)_2Pn]$ triplet cations yield nearly identical structures to those of the HF/6-311G* optimizations thus the inclusion of electron correlation does not predict that $C_{2v}$ triplet cations are stable minima or alter the conclusions drawn from the HF calculations.

The Mulliken and NBO charges listed in Table A.4 show a concentration of positive charge at the pnictogen center and a localization of negative charge on the N atoms in both systems. The experimentally observed stability may be due to the internal Coulombic stabilization of the "negative-positive-negative" charge distribution for the N-Pn-N fragment (Pn = P, As), consistent with the conclusions of Wiberg based on an *ab initio* study of allylic systems.[89] This phenomenon is likely due to the σ-electronegative (and π-donating) stabilizing effect of an atom such as N, and in this context the vast majority of isolable pnictogenium systems have two nitrogen atoms adjacent to the pnictogen atom.[90]

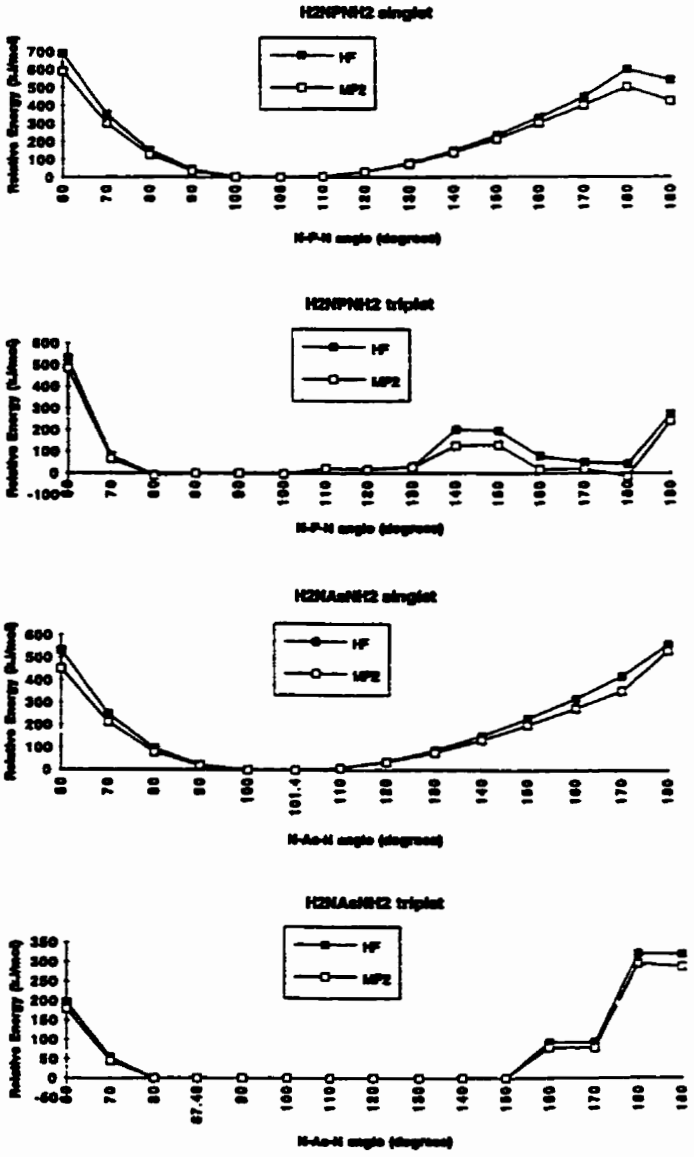


**Figure 2.7.** Plots of energy versus N-Pn-N angle for acyclic pnictogenium cations $[H_2N\text{-}Pn\text{-}NH_2]$.

In contrast to the previous reports, [78,80,83,85] the UHF optimized minima for the triplet states of **2.7'** and **2.5'** (N imag = 0) have $C_1$ symmetry and consist of a partial N-Pn multiple bond (three electron bond; Pn = P,As) and a nitrogen based radical. However at the UMP2 level, the $C_1$ geometry is higher in energy than both the $C_2$ (N imag = 1; $E_{s \rightarrow t}$

UMP2 = 288 kJ/mol) and $C_s$ (optimizes to $C_{2v}$; N imag = 2; $E_{s \rightarrow t}$ UMP2 = 290 kJ/mol) structures. This indicates that the UHF and MP2 energy hypersurfaces are not parallel in the case of the triplet species which is likely a consequence of the introduction of electron correlation in MP2 calculations. As expected, the singlet species are not as susceptible to the effects of electron correlation as is evident from the optimization of **2.7'** at the full MP2/6-311G* level of theory which yields a nearly identical structure and energy (6.85 kJ/mol lower) as that of **2.7'** at MP2/6-311G*//HF/6-311G* optimization.

The charge and spin distributions shown in Tables A.4 and A.5, respectively, are similar for triplets **2.7'** and **2.5'** ($C_1$ symmetry ; N imag=0) with positive charge localized on the pnictogen atom and negative charge on the nitrogen atoms. The charge on the pnictogen center is significantly lower for the triplet than for the singlet in each case (**2.7'** P: singlet, 1.12; triplet 0.77; **2.5'** As: singlet, 1.16; triplet, 0.82) and the negative charges on the nitrogen atoms are no longer equal (**2.7'** triplet N: -0.86 and -0.50; **2.5'** triplet N: -0.50 and -0.87). Analysis of electron spin density shows that the unpaired electrons are also found almost exclusively in the N-Pn-N moieties. The structural parameters, spin density and NBO analyses suggest that each triplet cation contain a Pn-N multiply-bonded (three electron bond) radical (sum of spin densities on Pn and N, **2.7'**:1.01 and **2.5'**: 0.98) cation and a separated nitrogen radical (spin density, **2.7'**:1.11 and **2.5'**: 1.13).

In an attempt to understand the difference in the symmetry and bonding of triplets **2.7'** and **2.5'**, calculations were performed on the singlet and triplet ground states of $NH_3$ **2.13'**, $[H_2NPH]$ **2.14'**[79], $[H_2NAsH]$ **2.15'**, and the doublet ground states of $[NH_3]^{+\bullet}$ **2.16'**, $[H_2NPH]^{\bullet}$ **2.17'** and $[H_2NAsH]^{\bullet}$ **2.18'**. All appropriate symmetries were examined for each species and the energies, the number of imaginary frequencies and the ZPVEs are listed in Table A.1. Structural parameters are listed in Table A.2.

**Table 2.3.** Calculated enthalpies (kJ/mol) of isogyric reactions and singlet-triplet energy splittings for acyclic pnictogenium cations. UMP2 denotes UMP2/6-311G*//UHF/6-311G* + 0.90 ZPVE, UHF denotes UHF/6-311G* + 0.90 ZPVE.

| Reaction | UMP2 | UHF |
|---|---|---|
| **2.13'** s + **2.14'** t $C_s$ #1 → **2.13'** t + **2.14'** s | 252.55 | 268.26 |
| **2.13'** s + **2.14'** t $C_s$ #2 → **2.13'** t + **2.14'** s | 274.08 | 335.69 |
| **2.13'** s + **2.14'** t $C_{2v}$ → **2.13'** t + **2.14'** s | 242.39 | 236.02 |
| **2.13'** s + **2.14'** t $C_1$ → **2.13'** t + **2.14'** s | 317.41 | 320.69 |
| **2.13'** s + **2.14'** t $C_s$ #2 → **2.16'** d + **2.17'** d $C_s$ #1 | 20.32 | 21.44 |
| **2.13'** s + **2.14'** t $C_s$ #2 → **2.16'** d + **2.17'** d $C_s$ #2 | 57.16 | 45.74 |
| **2.13'** s + **2.14'** t $C_s$ #2 → **2.16'** d + **2.17'** d $C_{2v}$ | 318.04 | 179.53 |
| **2.13'** s + **2.14'** t $C_s$ #2 → **2.16'** d + **2.17'** d $C_1$ | 22.24 | 22.73 |
| **2.13'** s $D_{3h}$ + **2.14'** t $C_s$ #1 → **2.16'** d + **2.17'** d $C_1$ | -18.60 | -66.25 |
| **2.13'** s + **2.15'** t $C_s$ #1 → **2.13'** t + **2.15'** s | 250.74 | 263.41 |
| **2.13'** s + **2.15'** t $C_s$ #2 → **2.15'** t + **2.15'** s | 306.39 | 382.42 |
| **2.13'** s + **2.15'** t $C_{2v}$ → **2.15'** t + **2.15'** s | 109.77 | 115.51 |
| **2.13'** s + **2.15'** t $C_1$ → **2.15'** t + **2.15'** s | 306.41 | 382.41 |
| **2.13'** s + **2.15'** t $C_s$ #2 → **2.16'** d + **2.18'** d $C_s$ #1 | 46.11 | 62.40 |
| **2.13'** s + **2.15'** t $C_s$ #2 → **2.16'** d + **2.18'** d $C_s$ #2 | 298.86 | 254.70 |
| **2.13'** s + **2.15'** t $C_s$ #2 → **2.16'** d + **2.18'** d $C_s$ #3 | 70.25 | 76.46 |
| **2.13'** s + **2.15'** t $C_s$ #2 → **2.16'** d + **2.18'** d $C_{2v}$ | 493.94 | 547.16 |
| **2.13'** s + **2.15'** t $C_s$ #2 → **2.16'** d + **2.18'** d $C_1$ | 45.91 | 61.73 |
| **2.13'** s $D_{3h}$ + **2.15'** t $C_s$ #1 → **2.16'** d + **2.18'** d $C_1$ | -29.05 | -78.82 |
| **2.13'** s $C_{3v}$ → **2.13'** t | 511.34 | 454.76 |
| **2.13'** s $D_{3h}$ → **2.13'** t | 492.03 | 433.21 |

Models **2.13'**, **2.14'** and **2.15'** are not consistent with the results obtained for triplets

**2.7'** and **2.5'** and predictably confirm that triplet ammonia is much less favourable than singlet ammonia and has a much larger singlet-triplet splitting ( 511.7 kJ/mol) than both **2.13'** and **2.14'**. An isodesmic comparison of the singlet and triplet species is thus unproductive, however an isogyric comparison of the doublet species **2.16'**, **2.17'** and **2.18'** to **2.13'**, **2.14'**, and **2.15'** accurately reproduces the behaviour observed in triplets **2.7'** and **2.5'**. The lengths for the shorter Pn-N bond in triplets **2.7'** and **2.5'** are consistent with those of doublets **2.17'** and **2.18'** respectively (**2.7'** t $C_1$: 1.66 Å, **2.17'** $C_1$: 1.694 Å; **2.5'** t $C_1$: 1.783 Å, **2.18'** $C_1$: 1.83), which are also shown to be partial multiple bonds through NBO analysis (approximately 3 electron bonds) in each case. The length of the **2.7'** t $C_1$ N(3)-H(5) bond (1.005 Å) [**2.5'** t $C_1$ N(2)-H(4) (1.005 Å)] (the hydrogen bonded to the nitrogen atom not involved in multiple bonding) is most closely reproduced by the 1.008 Å N-H bond in the ammonium radical cation **2.16'**. The structures of triplet cations **2.7'** and **2.5'** are thus best explained as a combination of distinct radical and radical cation units; however, the reason for the adoption of this structure remains unclear. A possible rationalization is found in the reaction energies shown in Table 2.3. Isogyric reaction energies show that singlet ammonia and the lowest energy triplet cation are favoured over all of the combinations of doublet species; however, if the singlet and triplet species are restricted to the symmetries observed in cations **2.7'** and **2.5'** (planar $R_2N$-Pn-$NR_2$ moiety), the doublet species are favoured ( 18.6 kJ/mol Pn = P; 29.0 kJ/mol Pn = As).

### 2.3.4 Dimerization of Pnictogenium Cations

Carbenes and their analogues are by definition formally subvalent (dicoordinate) and electron deficient and, as such, they are susceptible to dimerization to enable the adoption of a "normal" co-ordination number and valence octet. For example, group 14

carbenoids without π-donor substituents (including carbenes with π-donors) dimerize to form olefin-type compounds **2.19**.[14,91] Certain heavier carbene analogues bearing π-donor groups are predicted[14,92] and observed[14,93] to form bridged dimers **2.20**, which may be considered σ-bonded alternatives to the corresponding multiply-bonded monomers (2 or 4 π-electron systems), or mutual donor-acceptor complexes of the monomers.

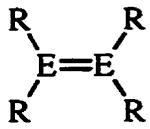

**2.19**

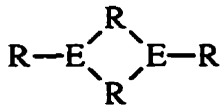

**2.20**

π-Bonding is weaker for heavier elements (n > 2) so that 4 single bonds (4 σ-bonds) are energetically favoured over 2 double bonds (2 σ-bonds and 2 π-bonds) as illustrated in Figure 2.8.

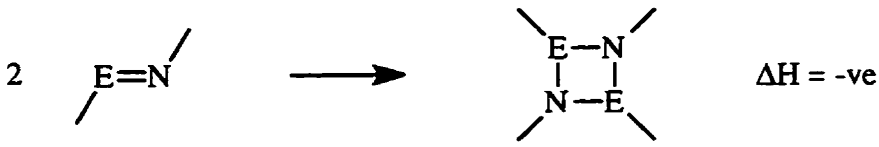


**Figure 2.8.** Cyclo-dimerization reaction of multiply-bonded compounds.

This prediction arises from the assumption that π-overlap decreases as n increases, although Schleyer has shown that it is actually the increase in the energy of planarization with increasing n that decreases the favourability of π-interactions.[94] The experimentally observed dimers of arsolanium cations[63] in contrast to the universally monomeric structures of phospholanium salts are consistent with such trends. However, our isolation

and characterization of monomeric arsenanium salt **2.6** [$GaCl_4$] implies that the centro-symmetric dimer **2.8** $[GaCl_4]_2$ (space group: $P2_1/n$) is likely a function of crystal packing.[62] Step-like dimeric structures analogous to that of cation **2.8** have been observed in centro-symmetric space groups for compounds involving elements from Groups 13,[95] 14,[96] and 15.[62] To further evaluate and quantify the dimerization reaction the structures of dimers **2.21'**, **2.22'** and **2.23'** have been optimized at the HF/6-311G* level with restriction to $C_i$ symmetry (*vide supra*). The UMP2 energies obtained at these geometries and their ZPVE values are listed with those of the monomers **2.7'**, **2.5'** and **2.6'** in Table A.1. Selected calculated structural features are compared with those observed experimentally (X-ray crystallographic studies) in Figure 2.6.[60,64,63,62] The structures of cations **2.7**, **2.8** and **2.6** are very closely approximated by the optimized geometry of **2.7'**, **2.22'** and **2.6'**, respectively. All bond lengths are within the estimated standard deviations obtained experimentally and all angles are within 5° of the experimentally determined values.

The energy of dimerization for the arsolanium cation **2.5'** is calculated to be +206.7 kJ/mol confirming that the monomer is favoured in the gas phase in contrast to the experimentally observed solid-state structure **2.8**. An experimental observation consistent with the unfavourability of dimerization is found in the case of the six-membered ring analogue of **2.5**[$GaCl_4$]. The arsenanium cation in salt **2.6** [$GaCl_4$] is unquestionably monomeric in the solid state (space group: $Pca2_1$): the closest intermolecular As-N contact is 5.62 Å despite the weak dimer structure observed for the chloroarsine **2.6Cl** (space group: $P2_1/n$).[62] The energy of dimerization of **2.6'** to centrosymmetric dimer **2.23'** is calculated to be +247.9 kJ/mol, almost 20% more than that of **2.5'** which shows that 6-

membered cyclic **2.6'** is more stable *vis à vis* dimerization than is 5-membered cyclic **2.5'** and may imply that **2.6'** is an inherently more stable carbenoid environment. A possible explanation for the seemingly enhanced stability of **2.6'** is that the less restricted 6-membered ring allows the N-As-N angle (99.8° in **2.6'**) to approach the optimum angle (101.4° in the acyclic analogue, *vide supra*) whereas the smaller ring constrains the N-As-N angle to be significantly more accute (89.6° in **2.5'**). In the acyclic model, changing the angle at the arsenic atom from 100° to 90° results in a destabilization of 17.9 kJ/mol (35.8 kJ/mol for the two molecules that form the dimer, *vide infra*), which represents almost the entire difference between the dimerization energies of **2.5'** and **2.6'**.

Similarly, the phosphenium cation in salt **2.7** [$GaCl_4$] is monomeric (space group: $P2_1$) and the calculated energy of dimerization (+277.4 kJ/mol) is greater than those for **2.5'** or **2.6'**, however the rationale for the significant difference in dimerization energies between the phosphenium and arsenium systems is different. The relative stability of the phosphenium cation in comparison to the analogous arsenium species with respect to dimerization is consistent with more favourable N-P (2p-3p)π-bonding versus N-As (2p-4p)π-bonding in the respective monomers.

An estimate of the dimerization activation energy was obtained through the use of the generalized transition state method[97] in which the dimerization process is assumed to proceed *via* the deformation of each monomeric unit to the structure in which it is found in the dimer followed by the coupling of two of these "proto-dimeric" moieties. In most systems where dimerizations occur the energy of the deformation of each monomer (the energy which is denoted $\Delta E_{prep}$) is generally endoenthalpic and the coupling is exoenthalpic. The energy of coupling is divided into two terms: $\Delta E°$ (the energy of the

stabilizing electrostatic interactions and the destabilizing repulsive interaction between the two fragments) and $\Delta E_{el}$ (the energy of the stabilizing interaction of filled and empty orbitals on each fragment).[98] The dimerization energy can be expressed as:

$$\Delta E_{dimerization} = E_{dimer} - 2\,E_{monomer} \qquad (2.1)$$

and,

$$\Delta E_{dimerization} = 2\,\Delta E_{prep} + \Delta E^{\circ} + \Delta E_{el} \qquad (2.2)$$

The dimerizations studied in this work are all highly endothermic (*vide supra*) and analysis of the relative contributions to the dimerization energy using equation (2) offers valuable insight into the cause of this endothermicity. In all three systems, the term ($\Delta E^{\circ} + \Delta E_{el}$) is negligible (**2.7'**: 10.4 kJ/mol; **2.5'**: 25.6 kJ/mol; **2.6'**: 3.0 kJ/mol) which is likely because of the repulsion caused by the positive charge on each fragment (destabilizing) and the lack of purely filled or empty $\pi$-orbitals in the monomeric fragments (some $\pi$-delocalization is still present in the monomer fragments in their dimer respective geometries). Thus the dominant factor contributing to $\Delta E_{dimerization}$ is $\Delta E_{prep}$, the energy of distorting the monomers from their most stable geometry to the geometry observed in the dimer. The distortion energy is very large for each monomer ($\Delta E_{prep}$: **2.7'**: 133.5 kJ/mol; **2.5'**: 90.6 kJ/mol; **2.6'**: 122.4 kJ/mol) and precludes the formation of the dimers. Note that this distortion energy may also be used as a gauge for the relative stabilities of **2.5'** and **2.6'** in that the 6-membered ring containing the more favourable arsenium N-As-N angle requires 35% more energy to distort than does the relatively less stable 5-membered ring.

## 2.4 Conclusions

The diazarsenanium tetrachlorogallate salt adopts a monomeric structure in the solid state in contrast to the corresponding arsolidinium salt. Diaza-pnictogenium cations are calculated to have singlet ground states in agreement with experimental observations and consistent with previous calculations on structurally simpler acyclic cations, while the calculated models of the triplet species contrast those of previous theoretical studies. HF/6-311G* geometry optimizations (gas phase) accurately predict the molecular structures of **2.7**, **2.8** and **2.6** which were previously determined experimentally by X-ray crystallography. Dimerization reactions of cyclic diazapnictogenium cations are predicted to be unfavourable in the gas phase because of the requisite distortion of the stable monomeric forms. These conclusions are based on the energetics of the cations obtained from *ab initio* calculations and ignore all interactions such as those with the anions or solvent that are found in condensed phases. The experimentally observed dimer of the arsolanium cation **2.5** is concluded to be a crystal packing phenomenon which is likely dominated by the large difference in crystal lattice energy between (+1) (-1) salts and (+2) $(-1)_2$ salts.

Suggested future work is the synthesis and structural characterization of 5-and 6-membered cyclic diamino-stibenium and bismuthenium cations which will provide for a more complete understanding of the structure and bonding of pnictogen carbenoids.

# Chapter 3. Pnictogenium Cations (II): Synthetic and Theoretical Investigation of the Unprecedented Arsenium Cycloaddition Reactivity

## 3.1 Introduction

Carbenoids have generally been considered to be transient species and their existence was proven by means of trapping reactions with appropriate reagents. One of the most common class of reagents used for the trapping of singlet carbenoids is butadienes which add to carbenoids *via* [4 + 2] cheletropic cycloadditon reactions.[57] In this chapter, the rapid, regiospecific and quantitative cycloaddition reactions of the gallate salts of cations **3.1** (**2.7**),[64] **3.2** (**2.5**) and **3.3** (**2.6**) with 2,4-dimethylbutadiene are described. The products obtained illustrate the monomeric behaviour of both arsenium cations in solution (see Chapter 2) and show a dramatic contrast in the reactivity of phosphenium and arsenium cations.

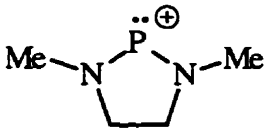


**3.1**

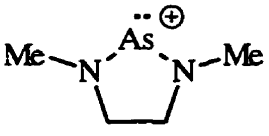


**3.2**

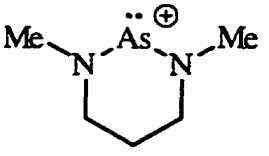


**3.3**

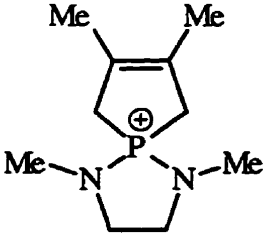


**3.1BD**

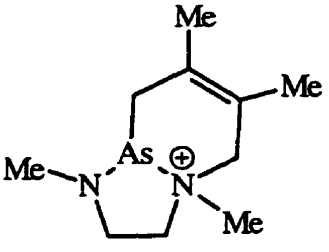


**3.2BD**

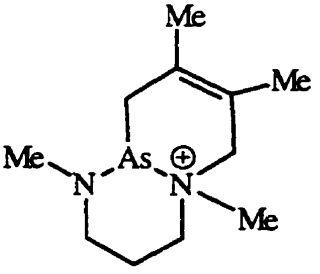


**3.3BD**

Phosphenium salt **3.1**[$GaCl_4$] reacts with 2,3-dimethylbutadiene to give the gallate salt of the spirocyclic cation **3.1BD** whereas both **3.2**[$GaCl_4$] and **3.3**[$GaCl_4$] react with the diene to yield the Diels-Alder type adducts **3.2BD**[$GaCl_4$] and **3.3BD**[$GaCl_4$], respectively. **3.2BD**[$GaCl_4$] has been structurally characterized, and the related structure of the cycloadduct **3.3BD**[$GaCl_4$] is confirmed by 2D NMR.

*Ab initio* calculations predict the observed reactivity and allow for the prediction of the cycloaddition behaviour of unknown stibenium and bismuthenium cations.

## 3.2 Diazarsenium-Butadiene Cycloaddition

Compounds **3.2**[$GaCl_4$] and **3.3**[$GaCl_4$] react rapidly with 2,4-dimethylbutadiene in $CH_2Cl_2$ to give a single product, as shown by $^1H$ NMR spectra of the reaction mixtures. The isolated products are spectroscopically similar and an X-ray crystallographic study of the product from **3.2**[$GaCl_4$] reveals a tetrachlorogallate salt of cycloadduct **3.2BD**, in which the diene is assymmetrically bound to the arsolidinium heterocycle (across one of the As-N bonds).

The bicyclic structure of the cation is shown in Figure 3.1 and selected bond lengths and angles are given in Table 3.1. The cross-ring As(1)-N(2) bond is significantly longer [2.056(10) Å] than that of As(1)-N(1) [1.797(11) Å], and is comparable (within experimental error) to the corresponding bond observed in the dication **3.2$_2$ (2.8)** (As - tetracoordinate N, 1.949(4) Å; As - tricoordinate N, 1.752(5) Å.) The cross-ring bond in **3.2BD** is anomalously long in comparison to the As-N bonds in **3.2Cl (2.5Cl)**, **3.3Cl (2.6Cl)** and **3.2$_2$**[$GaCl_4$]$_2$, and may be considered an intramolecular donation to an amino-alkyl-arsenium centre. Consistently, intermolecular donor interactions to the

dithiarsolidinium cation are also long,[63] as are those to phosphenium centres [99]. In the other extreme, the bicyclic structure of **3.2BD** can be viewed as an ammonium-arsine.

**Table 3.1.** Selected bond lengths (Å) and angles (°) for **3.2BD**[$GaCl_4$].

| | |
|---|---|
| As(1)-N(1) | 1.797(11) |
| As(1)-N(2) | 2.056(10) |
| N(1)-C(1) | 1.50(2) |
| N(1)-C(3) | 1.49(2) |
| N(2)-C(2) | 1.50(2) |
| N(2)-C(4) | 1.53(2) |
| N(1)-As(1)-N(2) | 89.3(4) |
| As(1)-N(2)-C(2) | 104.2(8) |
| As(1)-N(2)-C(4) | 107.8(9) |
| C(2)-N(2)-C(4) | 109.7(11) |
| As(1)-N(1)-C(1) | 110.0(9) |
| As(1)-N(1)-C(3) | 117.2(10) |
| C(1)-N(1)-C(3) | 112.6(12) |
| N(1)-C(1)-C(2) | 107.4(12) |
| N(2)-C(2)-C(1) | 106.4(11) |

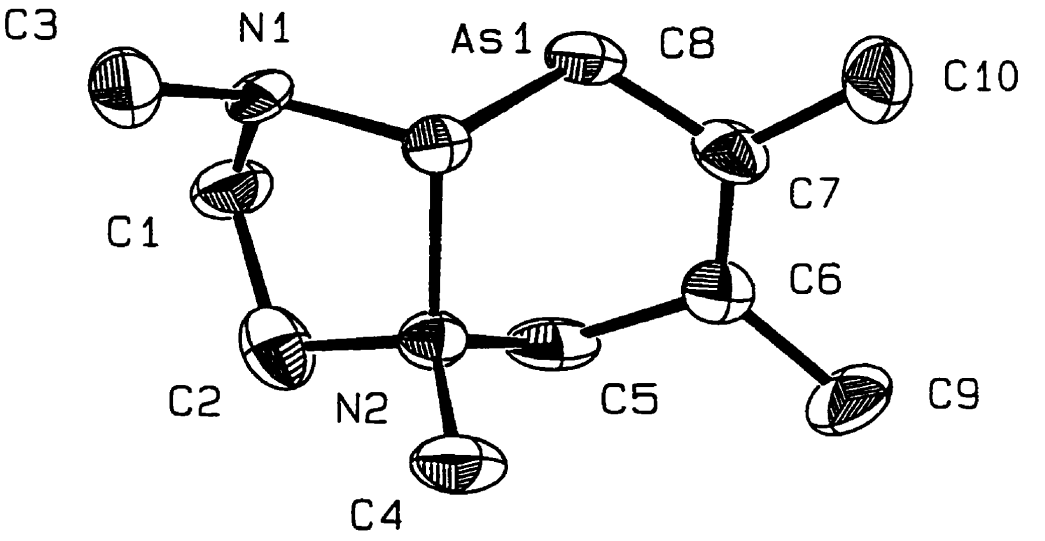


**Figure 3.1.** Molecular structure of **3.2BD**[$GaCl_4$].

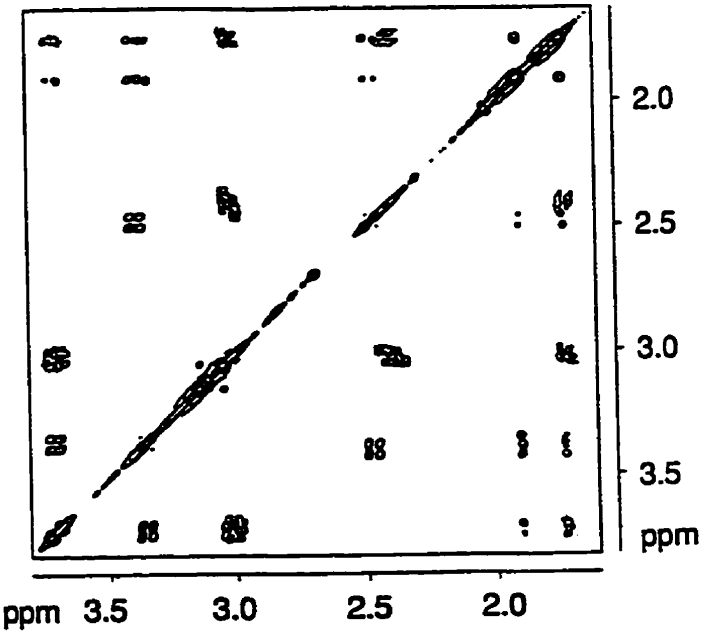


**Figure 3.2.** ($^1H$, $^{13}C$) COSY spectrum of **3.3BD**.

The complex $^1$H NMR spectra of **3.2BD**[$GaCl_4$] (previously reported[100]) and **3.3BD**[$GaCl_4$] (Figure 3.2) in $CD_2Cl_2$ were resolved by COSY techniques at 400 MHz. In the spectrum of **3.3BD**[$GaCl_4$], methyl groups 1, 2, 3 and 4 are observed as singlets at 1.90, 1.74, 3.05 and 3.14 ppm, respectively. The six methylene protons are observed in the usual region, with the signals for those closest to the nitrogen atoms farther downfield. While it has been possible to identify the signals produced by each of the protons in a vicinal pair, it has not been possible to identify which of the two protons is responsible for each of the signals. Protons 1 and 2 are observed as multiplet signals at 3.01 and 3.71 ppm. Likewise, protons 3 and 4 exhibit multiplets at 1.74 and 2.39 ppm. Protons 5 and 6 exhibit a doublet at 3.36 ppm and a multiplet at 3.69 ppm, while protons 7 and 8 each produce a doublet at 2.47 ppm and 3.39 ppm. Finally, protons 9 and 10 each produce multiplet signals at 3.01 ppm and 3.71 ppm.

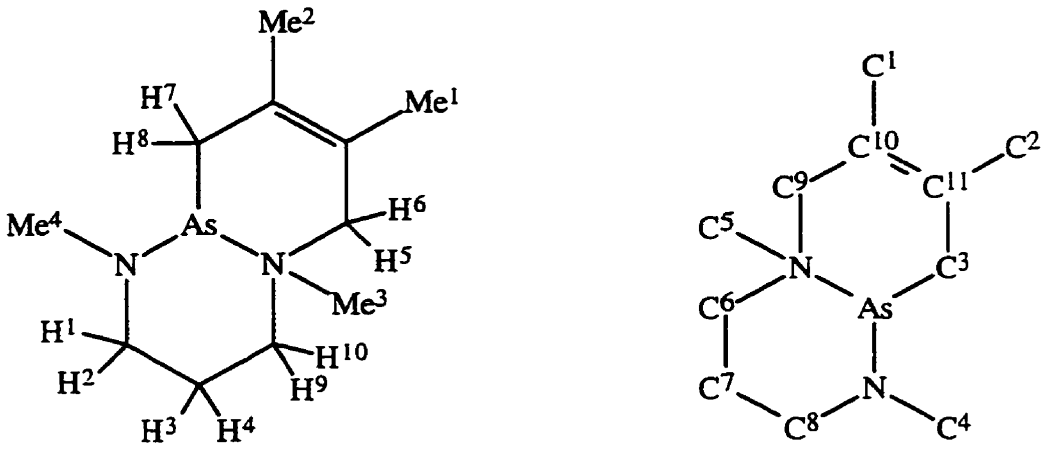


**Legend for NMR assignments.**

A ($^1$H, $^{13}$C) HETCOR spectrum has allowed for unambiguous assignment of the

carbon signals for **3.3BD**[$GaCl_4$] (Figure 3.2) by Dr. G. Wu: 1, 22.2 ppm; 2, 19.0 ppm; 3, 33.1 ppm; 4, 43.9 ppm; 5, 48.9 ppm; 6, 57.4 ppm; 7, 19.5 ppm; 8, 45.6 ppm; and 9, 65.0 ppm. Two quaternary carbon signals were found at 123.3 and 124.6 ppm. The lower field signal is presumably due to carbon 10.

Formation of cations **3.2BD** and **3.3BD** are in contrast to the butadiene cycloaddition reaction observed for the diazaphospholidinium cation **3.1**, which results in the oxidative cycloaddition phosphonium product **3.1BD** as shown unambiguously by multinuclear NMR spectra ($\delta$ $^{13}C$: 16.4 (d, $^{3}J_{P\text{-}C}$ 15.3 Hz, Me-C), 31.2 (d, $^{1}J_{P\text{-}C}$ 66.3 Hz, C-As), 32.0 (d, $^{2}J_{P\text{-}C}$ 6.7 Hz, Me-N), 50.1 (d, $^{2}J_{P\text{-}C}$ 6.7 Hz, $CH_2$-N), 128.5 (d, $^{2}J_{P\text{-}C}$ 12.4 Hz, C=C) ppm; $\delta$ $^{31}P$: 89.6 ppm).[101] At first glance, the arsenium cycloaddition reactions may be classified as Diels-Alder type reactions with the As-N unit behaving as a "hetero-dienophile", and in the context of reactions observed for phosphaalkynes,[102] phosphaalkenes[103] and phosphinines.[104] However, qualitative MO analysis reveals that the frontier orbital symmetries are incompatible (Figure 3.3). The HOMO of the diene and the LUMO of the dienophile can be considered of appropriate symmetry (Figure 3.3 (**a**)) for the observed product structure, and likely represent the dominant interaction which determines the structure of the transition state in a "normal electron-demand" process.[105] Nevertheless, a node at the arsenic centre in the HOMO for the other frontier orbital interaction (Figure 3.3 (**b**)) raises questions about the concertedness of the reaction and the Diels-Alder classification. To understand the differences observed in the butadiene cycloaddition behaviour of these species a thorough *ab initio* investigation was performed.

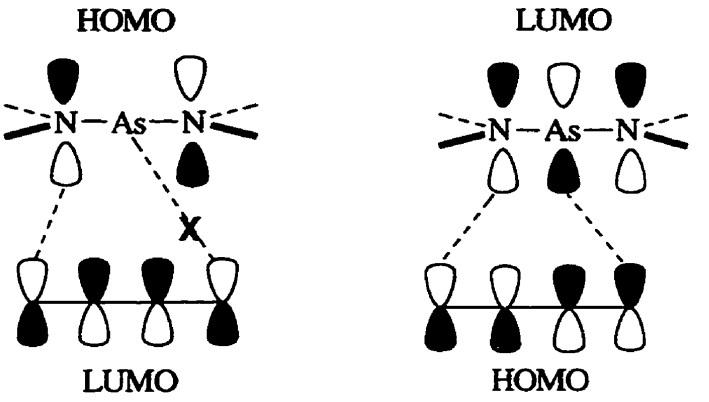


**Figure 3.3.** Qualitative frontier MO analysis for a pnictogenium cation and *cis*-1,3-butadiene.

## 3.3 Theoretical Assessment of Pnictogenium-Butadiene Cycloaddition Reactions

Cycloaddition reactions are of immense utility to synthetic chemists[106] and the theoretical principles that explain pericyclic reactions have been studied extensively since Woodward and Hoffmann's seminal articles in 1965.[107] The cycloaddition behaviour of phosphenium cations is well documented[19,57] including reactions with 1,3-dienes which give phospholenium cations **3.4**, and based on a number of stereospecific experimental results, Cowley proposed that the reaction proceeds *via* a [2+4] disrotatory cheletropic mechanism.[55]

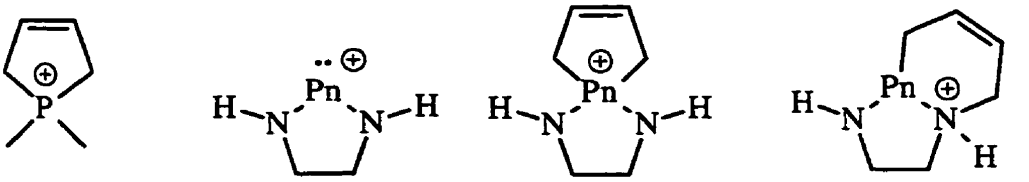


**3.4** **3.1'** (Pn = P) **3.2'** (Pn = As) **3.5'** (Pn = P) **3.7'** (Pn = As) **3.6'** (Pn = P) **3.8'** (Pn = As)

The observed products in the reaction of carbenes,[108] silylenes, germylenes[53,108,109] and stannylenes with 1,3-dienes[108,109,110] are similar. However, data for the cycloaddition reactivity of heavier low-coordinate pnictogen species are limited.[111] Cations **3.2** and **3.3** are the only carbene analogues that have been observed to react with butadiene to form a Diels-Alder type product.[62,63]

The Diels-Alder (DA) reaction[112] is probably the most well known pericyclic reaction and has been thoroughly investigated synthetically and theoretically.[113] The [2+2] and [4+2] cycloaddition reactivity of methylene has been studied theoretically,[114] however in spite of the dramatic contrasts which are unambiguously experimentally demonstrated for phospholanium and arsolanium cations, we are unaware of *ab initio* studies for the cycloaddition behaviour of pnictogenium cations. To model these reactions we have optimized the structures of cycloaddition products **3.5'**, **3.6'**, **3.7'** and **3.8'** and all minima were found to have the expected $C_1$ symmetry. Their UMP2 energies, and ZPVE values are tabulated with those of cations **3.1'** and **3.2'** and those of trans-1,3-butadiene in Table A.1. The structure of **3.8'** is compared to that of **3.2BD** in Figure 3.4. Calculated reaction enthalpies are listed in Table 3.2.

**Table 3.2.** Calculated enthalpies of cycloaddition reactions UMP2 denotes UMP2/6-311G*//UHF/6-311G* + 0.90 ZPVE, UHF denotes UHF/6-311G* + 0.90 ZPVE. (All enthalpies in kJ/mol.)

| Reaction | UMP2 | UHF |
|---|---|---|
| **3.1'** + *trans*-1,3-butadiene → **3.5'** | -163.74 | -138.11 |
| **3.1'** + *trans*-1,3-butadiene → **3.6'** | -112.20 | -61.59 |
| **3.2'** + *trans*-1,3-butadiene → **3.7'** | -85.92 | -59.23 |
| **3.2'** + *trans*-1,3-butadiene → **3.8'** | -144.45 | -93.06 |

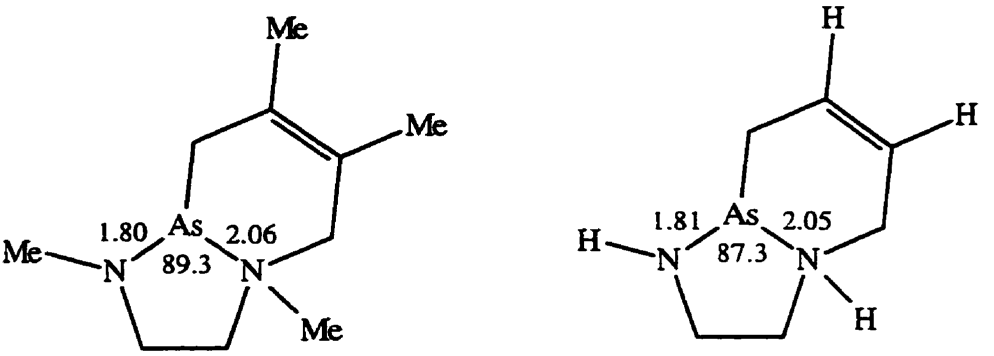


**Figure 3.4.** Comparison of experimental and theoretical structural parameters for **3.2BD** and **3.8'**.

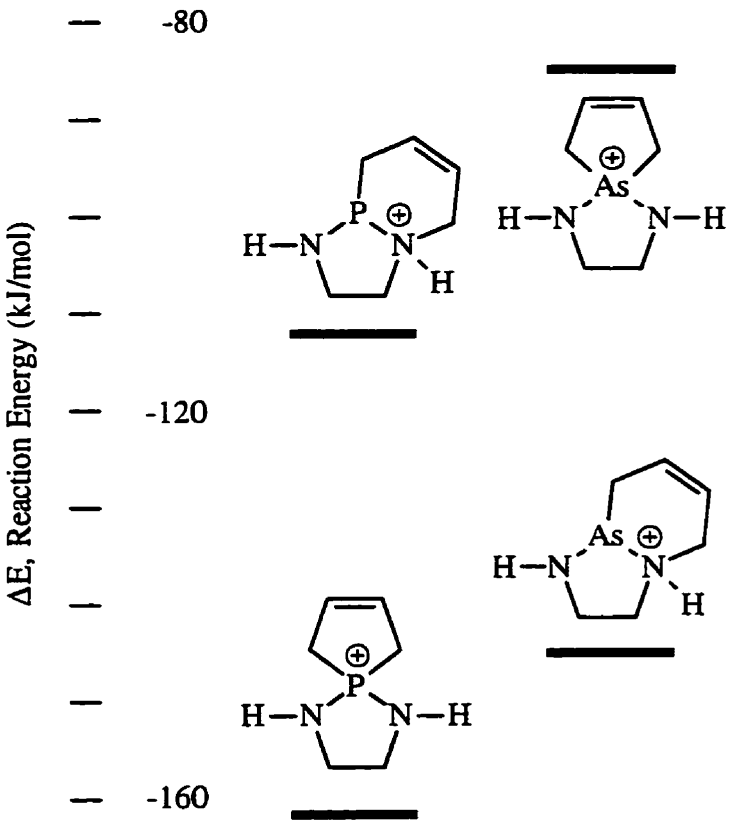


**Figure 3.5.** Schematic representation of the cycloaddition reaction energies (kJ/mol) for the reaction of pnictogenium cation with *trans*-1,3-butadiene.

The experimentally observed butadiene cycloaddition products for both **3.1'**, and **3.2'** are calculated to be the thermodynamically favoured product with respect to the other possible cycloaddition product in each system. Reaction of **3.1'** with trans-butadiene to give **3.5'** (-163.7 kJ/mol) and **3.6'** (-112.2 kJ/mol) are both exothermic but the Diels-Alder product **3.6'** is more than 50 kJ/mol higher in energy. The theoretical model also mimics the experimental observations for arsolanium derivatives predicting that the formation of **3.7'** from **3.2'** has a calculated reaction enthalpy of -85 kJ/mol, while the formation of arsonium **3.8'** is more exothermic (-144.5 kJ/mol). A graphical representation of the results is given in Figure 3.5.

These conclusions validate the necessity of such a high level computational study, as a comparison of empirical bond energies ([all energies in kJ/mol] 2 P-C (552) bonds vs. P-C (276) and C-N (314) and 2 As-C bonds (458) vs. As-C (229) and C-N (314))[115] predict a DA-type product for both pnictogenium cations. Interestingly, the DA-type product has not even been observed in butadiene reactions with iminophosphines, which contain a formal P-N double bond.[116] Phosphorus and arsenic have nearly identical spectroscopic electronegativity values (P: 2.253, As: 2.211 Pauling Units)[4] and the calculated charge distributions in **3.1'** and **3.2'** (*vide supra*) are not significantly different so that the contrasting cycloaddition behaviour is not likely controlled by either property. The most probable explanation arises from the different oxidation potentials of phosphorus and arsenic. Whereas phosphorus(III) oxidizes preferentially to the P(V) state (*ca.* -50 kJ/mol) , the corresponding oxidation of arsenic(III) is unfavourable (*ca.* +100 kJ/mol) thus formal oxidation product **3.7'** is unstable with respect to structural isomer **3.8'**.[117] *Ab intio* calculations of the reaction $PnH_3 + H_2 \rightarrow PnH_5$ give $\Delta H$ values of 189.5 (P), 228.4 (As), 210.0 (Sb) and 305.4 (Bi) kJ/mol and correctly predict that As(V) and Bi(V)

are significantly less favourable than P(V).[8] The relative instability of the As(V) oxidation state is due to the "d-block contraction" (Chapter 1) and results in the preferential formation of the adduct with the tricoordinate arsenic center. The Pn(III) to Pn(V) oxidation for antimony (*ca.* +100 kJ/mol) and bismuth (*ca.* +300 kJ/mol) (very large due to relativistic effects) leads to the prediction that bismuthenium and possibly stibenium cations will also react in a similar fashion to the arsenium cations however these reactions have not as yet been examined experimentally. Unambiguous prediction is not possible for antimony because the atom is more readily oxidized than either As or Bi and thus may form cheletropic adducts.

The rapid, quantitative and regiospecific reactions observed experimentally imply concerted reaction mechanisms thus symmetries of the calculated frontier orbitals were examined in this context.

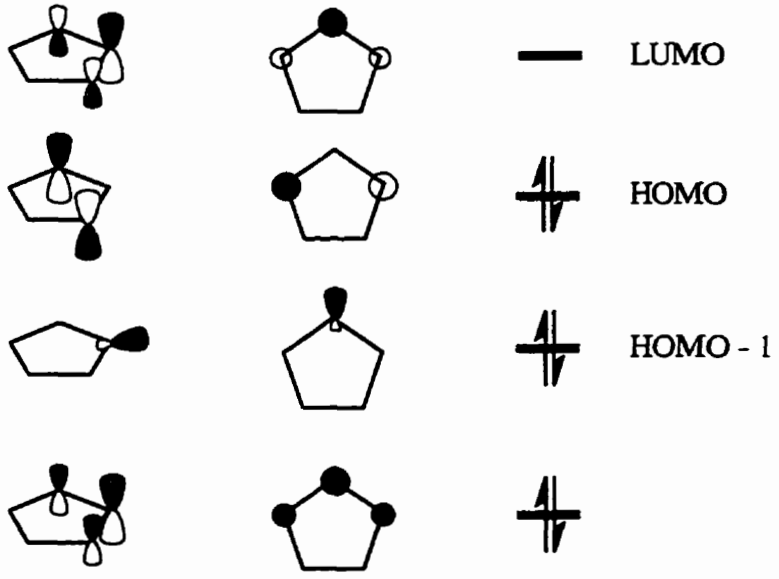


**Figure 3.6.** Qualitative depiction of calculated molecular orbitals in **3.1'** and **3.2'**. Energy spacings and orbital sizes are not to scale.

The frontier orbitals that we have determined for cations **3.1'** and **3.2'** are consistent with previous results[56] and correspond to an "allylic-type" π-system with the additional $\sigma_n$ non-bonding ($a_1$) MO (the "lone pair" ) lower in energy than the $\pi_n$ HOMO ($a_2$). As such these systems cannot be considered truly isolobal with singlet carbenes which feature a $\sigma_n$ HOMO.[14] Of the possible frontier orbital interactions only that of the diene HOMO and pnictogenium LUMO is allowed. The pnictogen "lone pair" MO (HOMO -1) has the same symmetry (A) as the HOMO but the large energy difference between the HOMO and HOMO-1 (182.0 kJ/mol for **3.1'**, 207.9 kJ/mol for **3.2'**) and the node at the Pn center in the HOMO may preclude a contribution of the lone pair in the frontier interaction (although orbital mixing is still a possibility). The π-type and "lone pair" frontier orbital interactions are qualitatively illustrated in Figures 3.7 and 3.8 and are consistent with both cheletropic and Diels-Alder type mechanisms involving the diene HOMO and the pnictolanium LUMO, while neither mechanism has a symmetry allowed diene-LUMO — ene-HOMO interaction. If the "lone pair" molecular orbital (HOMO -1) is used in the frontier orbital interactions instead of the true "ene" HOMO (as for carbenes),[14] it becomes apparent that both HOMO-LUMO interactions (diene-pnictolanium and pnictolanium-diene) are of the appropriate symmetry for bond formation.

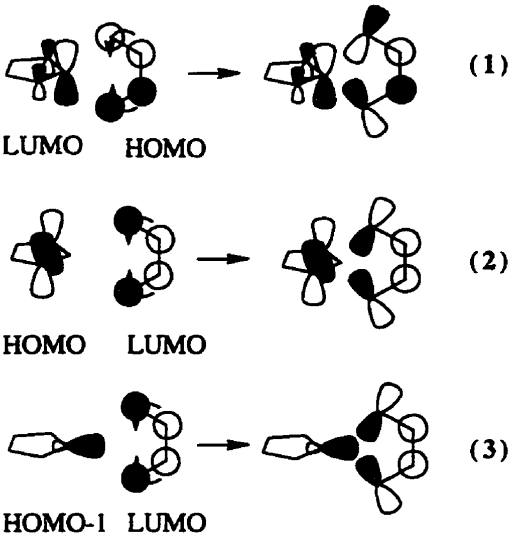


**Figure 3.7.** Pnictogenium LUMO - butadiene HOMO cheletropic interaction.

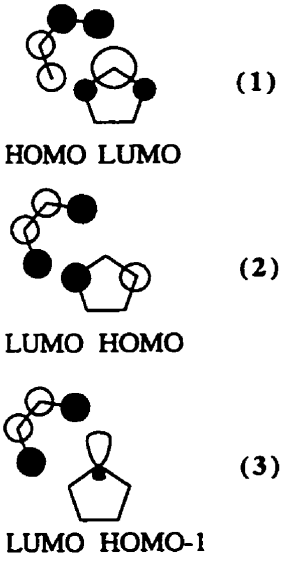


**Figure 3.8.** Pnictogenium LUMO - butadiene HOMO Diels-Alder interaction.

## 3.4 Conclusions

Both salts undergo quantitative Diels-Alder like cycloaddition reactions with 2,3-dimethylbutadiene, involving one As-N bond as the olefin, and contrasting the observations for the corresponding phospholidinium cation and all other reported carbene analogues (*vide supra*). The dramatic contrast observed in the quantitative butadiene cycloaddition reactions of phosphenium (formal cheletropic cycloaddition → phosphonium cation) and arsenium (formal Diels-Alder cycloaddition → arsinoamonium cation) cations have been modeled by determining the absolute energies of structures **3.1'**, **3.2'**, **3.5'**, **3.6'**, **3.7'**, and **3.8'** (UMP2/6-311G*//UHF/6-311G* + 0.90 ZPVE). The relative energies of cycloaddition products **3.5'** and **3.6'** (52 kJ/mol), and **3.7'** and **3.8'** (-59 kJ/mol) are consistent with the experimental observations and indicate that the observed products are thermodynamically favoured in each case. The anomalous butadiene cycloaddition behaviour of arsenium cations is rationalized in terms of the relative instability of the As(V) oxidation state. The theoretical data obtained does not allow for analysis of the mechanism of the reactions of **3.1** or **3.2** and it is possible that arsenium cations react with dienes to form spirocyclic adducts (**3.7**), which rapidly rearrange to the thermodynamically favoured DA-type adducts (**3.8**).

Future work on this project should be the *ab initio* modelling of the transition states of the cycloaddition reactions and the spirocyclic adduct → DA-type adduct rearrangement. This will specify the mechanism of the cycloaddition reactions; however, more computing power is required before such a study is undertaken. In addition, the cycloaddition reactivity of stibenium and bismuthenium cations should be examined with a synthetic study.

# Chapter 4. Evaluation of the 2,4,6-Tris(trifluoromethyl)phenyl as a Stabilizing Ligand for Pnictogenium Cations

## 4.1 Introduction

As suggested in Chapter 1, the stabilization of low-coordinate and electron deficient species is often necessary to allow for their isolation.[10,11,12,14] The isolation of stable carbenes and their analogues — those that do not oligomerize or decompose at ambient conditions in an inert atmosphere — has been effected through the use of various substituents which have one (or both) of two methods of stabilization. The cations of Chapters 2 and 3 are isolable because of "electronic stabilization", which implies that electron density from the substituent is imparted to the electron deficient atom and results in a reduction of the electron deficiency at that site. Such stabilization is provided by electron rich substituents such as those containing nitrogen, sulfur or oxygen either adjacent to the low-coordinate site or fixed in a position conducive to such a donation. Similar stabilization may also be effected by hyperconjugative interactions in ligands without "lone pairs" of electrons.[118] The concept of "steric stabilization" is discussed in detail in Chapter 1 (and in the upcoming chapters) and implies that the ligation of a sterically demanding substituent to an electron deficient atom results in a relatively less reactive species.

The 2,4,6-tris(trifluoromethyl)phenyl substituent (fluoromes, Fmes) has properties that allow for both electronic and steric stabilization of low-coordinate compounds and has been used extensively to stabilize a wide variety of potentially reactive main group and transition metal species. The chemistry of sterically demanding fluorinated substituents including Fmes has been reviewed by Witt and Roesky[119] and the chemistry of the Fmes substituent up to 1992 is summarized in a review by Edelmann,[120] however the numerous references to "unpublished results" and non-refereed contributions (Ph.D. theses and a

poster) detract from the value of this reference source. The interesting coordination chemistry of the C-F unit in Fmes and other fluorinated ligands is summarized by Herbert Plenio in a recent review.[121] It is estimated by the method of Bondi[5] that the steric bulk of this ligand is, not surprisingly, between that of the Mes and Dip (more accurately Tip) substituents, however the stabilizing effect of the coordinative interactions of $CF_3$ has allowed for the isolation of compounds that are unstable even with the larger substituents Dip, Tip and Mes*.

The parent arene 1,3,5-tris(trifluoromethyl)benzene was synthesized by McBee and Leech in 1947 by the photochemical chlorination of mesitylene followed by fluorination with HF at 200°C for 20 hours.[122] Proton, carbon and fluorine NMR spectra of the arene in $CDCl_3$ were reported by Takahashi *et.al.* in 1985 [$\delta^1$H, 8.10 ppm; $\delta^{13}$C, 123.4 ppm (q, $^1J_{C\text{-}F}$ 272 Hz, $\underline{C}F_3$), 126.2 ppm (s, $\underline{C}$-H), 134.0 ppm (q, $^2J_{C\text{-}F}$ 35 Hz, $\underline{C}$-$CF_3$); $\delta^{19}$F -64.0 ppm].[123] The lithiated arene FmesLi **4.1** was first synthesized in 1950 by McBee and Sanford[124] and a superior synthesis was reported by Chambers *et al.* in 1987,[125] as shown in Figure 4.1. This method is nearly identical to a seldom referenced much earlier (1970) Russian synthesis.[126]

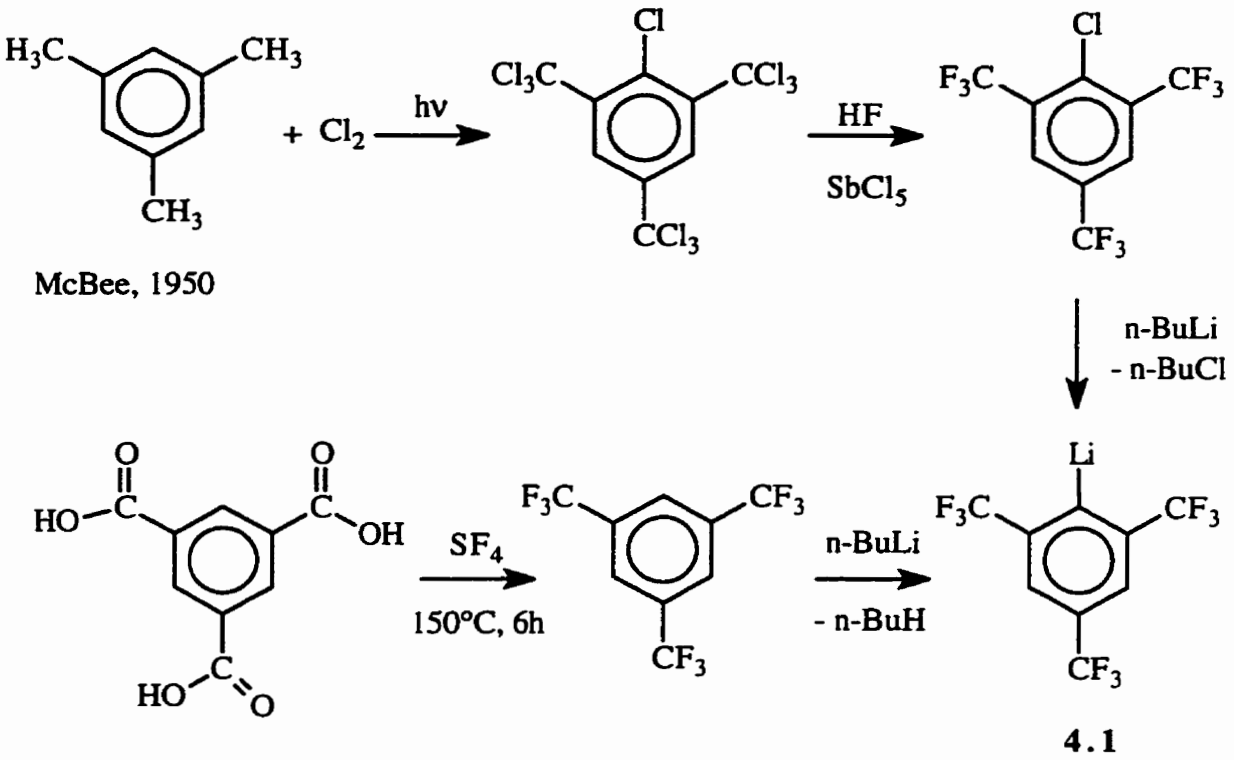


**Figure 4.1.** Synthesis of FMesLi.

The structure of the etherate adduct of this versatile reagent (Figure 4.2) illustrates the feature of this substituent that distinguishes it from all other common bulky ligands: the potential for electronic stabilization *via* electron donation from the F atoms on the ligand. X-ray crystallographic analysis reveals a dimeric structure in which the lithium atoms adopt a distorted trigonal bipyramidal geometry with very short Li-F contacts in the axial positions — the first example of coordination of a $CF_3$ moiety to a Li ion.[127] Although stable in ether, FmesLi is thermally unstable in THF and temperatures above -78°C result in the deposition of LiF.[127] Likewise, lithiation of more sterically congested $CF_3$ substituted arenes such as 1,2,3,5-tetrakis(trifluoromethyl)benzene or 1,2,4,5-tetrakis

(trifluoromethyl)benzene results in the decomposition of the fluorinated ligand.[128,129]

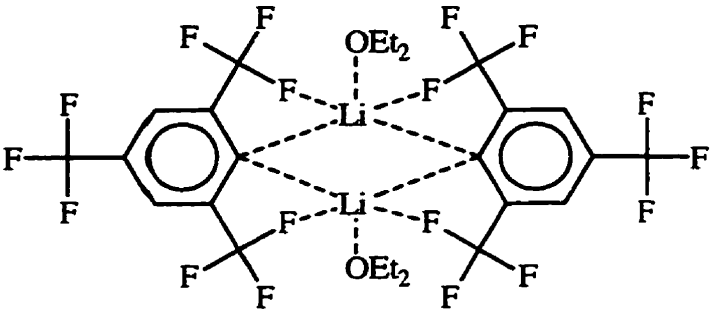


**Figure 4.2.** Drawing of [Li] coordination in FmesLi•$OEt_2$.

Donation of electron density to electron deficient sites *via* the ortho-$CF_3$ groups is the most important property of the Fmes ligand. This intramolecular donation is critical for the stabilization of such reactive species and it tends to counteract the substantial electron withdrawing nature of the ligand.

The FmesLi reagent may be used to prepare synthetically useful bulky reagents as illustrated in Figure 4.3.[130] Several Fmes substituted main group compounds have been synthesized and crystallographically characterized; some interesting examples from group 13 include monomeric air and moisture stable triaryl gallium and indium compounds **4.2**,[131,132] the rare diindane **4.3**,[132] and the remarkable Fmes phenoxides **4.4** (M = In, Th) which were the first examples of dicoordinate indium and thallium centers.[133,134] A remarkable carbenoid obtained through the use of the Fmes substituent is digermylene **4.5**.[135]

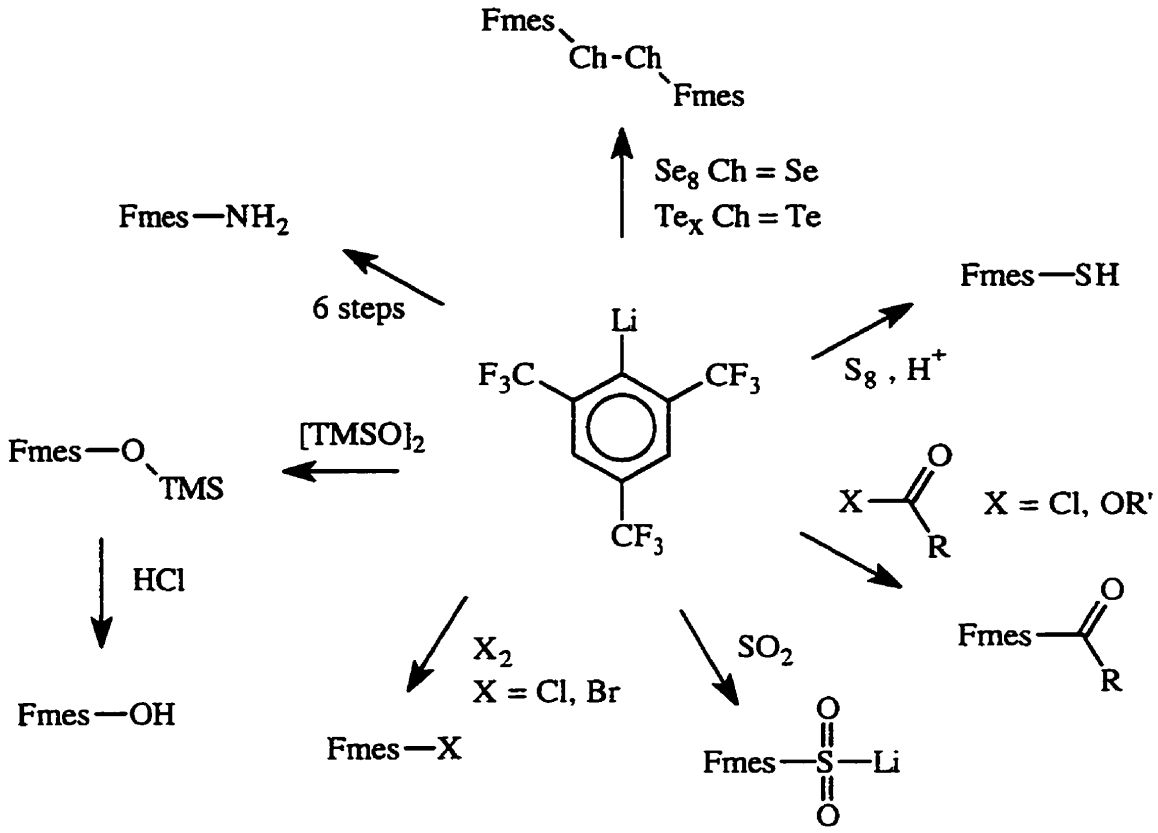


**Figure 4.3.** Synthesis of ligands containing Fmes.

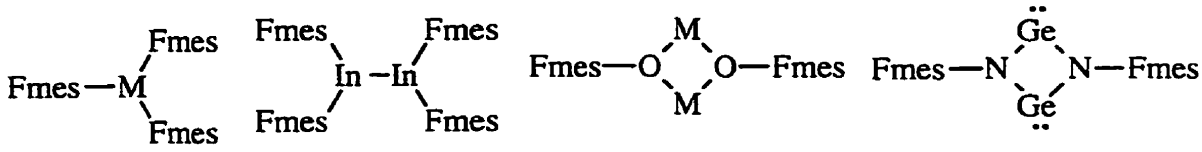


M = Ga, In

M = In, Tl

**4.2** **4.3** **4.4** **4.5**

Compounds containing dicoordinate group 14 environments **4.6** are of direct relevance to this thesis and were isolated by Bender *et al.*,[136] Grützmacher *et al.*[137] and Edelmann *et al.*[138] from the reaction of two equivalents of LiFmes to $ECl_2$ (1,4-dioxane

adducts for E = Sn, Ge) as illustrated in Figure 4.4. The great strength of the Si-F bond (and high probability of rearrangement isomerization) renders the silicon derivative unlikely. This prediction is supported by the result of the reaction of two equivalents of FmesLi with $SiCl_4$ which results in the formation of $Fmes_2SiF_2$, a product that must arise from the decomposition of Fmes ligands in the reaction mixture.[120]


**4.6**

**Figure 4.4.** Synthesis of $Fmes_2E$.

The carbene analogues are remarkably resistant to oligomerization, although the Sn derivative has also been crystallized as a distannene "dimer",[139] in contrast to the Dip or Tip analogues that are found to be trimeric in the solid state (and in monomer - dimer - trimer equilibrium in solution).[140] The authors postulate that the presence of four close E-F contacts (each between 70 and 80% of the respective E-F van der Waals' radii in all three derivatives) provide weak but sufficient internal "base stabilization" to prevent the oligomerization typically observed in such systems. Observation of temperature dependent $^{19}F$-$^{117}Sn$ and $^{19}F$-$^{119}Sn$ couplings in variable-temperature $^{19}F$ NMR experiments — the magnitudes of the coupling constants (239.5 Hz and 228.5 Hz respectively at 30°C) are inversely proportional to temperature — provides evidence for the persistence of the E-F contacts in solution.[137] A $^{207}Pb$-$^{19}F$ coupling constant of 358 Hz was also observed, but a temperature dependence was not evaluated.[138] The magnitudes of these coupling constants

are too large to be assigned as $^4J_{E\text{-}F}$ coupling and are consistent only with "through space" coupling. This conclusion is in contrast to that of Zuckermann *et.al.* based on the appearance of the bands due to the ligand in the infrared spectrum of [(2,6-bis(trifluoromethyl)phenyl]$_2$Sn.[141] All three carbenoids exhibit the expected bent geometry at E and contain relatively long E-$C_{ipso}$ bonds and the Fmes groups are twisted from coplanarity. Analysis of the structural parameters of the three carbene analogues lead the investigators to conclude that the orientation of the Fmes substituents is not defined by the minimization of steric repulsion between the ortho-$CF_3$ groups but by the maximization of E-F interactions.

The Fmes substituent has numerous advantages over other bulky groups for the isolation of carbene analogues. It prevents oligomerization reactions (*vide supra*) observed for derivatives with all smaller and some larger groups. The bulkier Mes* substituted stannylene **4.7** is monomeric, but rearranges irreversibly in solution at room temperature to the less strained alkyl isomer **4.8** and thus is only stable at low temperature.[142]

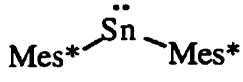


**4.7**

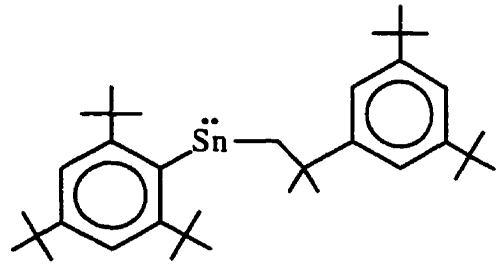


**4.8**

Bulky groups, usually needed to prevent oligomerization, are equally effective in preventing or retarding the reaction of the carbenic centers, particularly in the ligation of the compounds to transition metals.[136] Finally, substituents with heteroatom linkages to the carbenic center often undergo cleavage or reaction at the E-X (X = heteroatom) bond when

reacted with transition metals and other reagents.[136] Thus the Fmes ligand allows for the isolation of thermally stable monomeric carbenoids that are not rendered unreactive by the steric bulk of the ligand.

A number of group 15 Fmes reagents have been prepared by the reaction of FmesLi with $PnX_3$ (Pn = P, As, Bi; X = Cl, F), the results of which are illustrated in Figure 4.5.

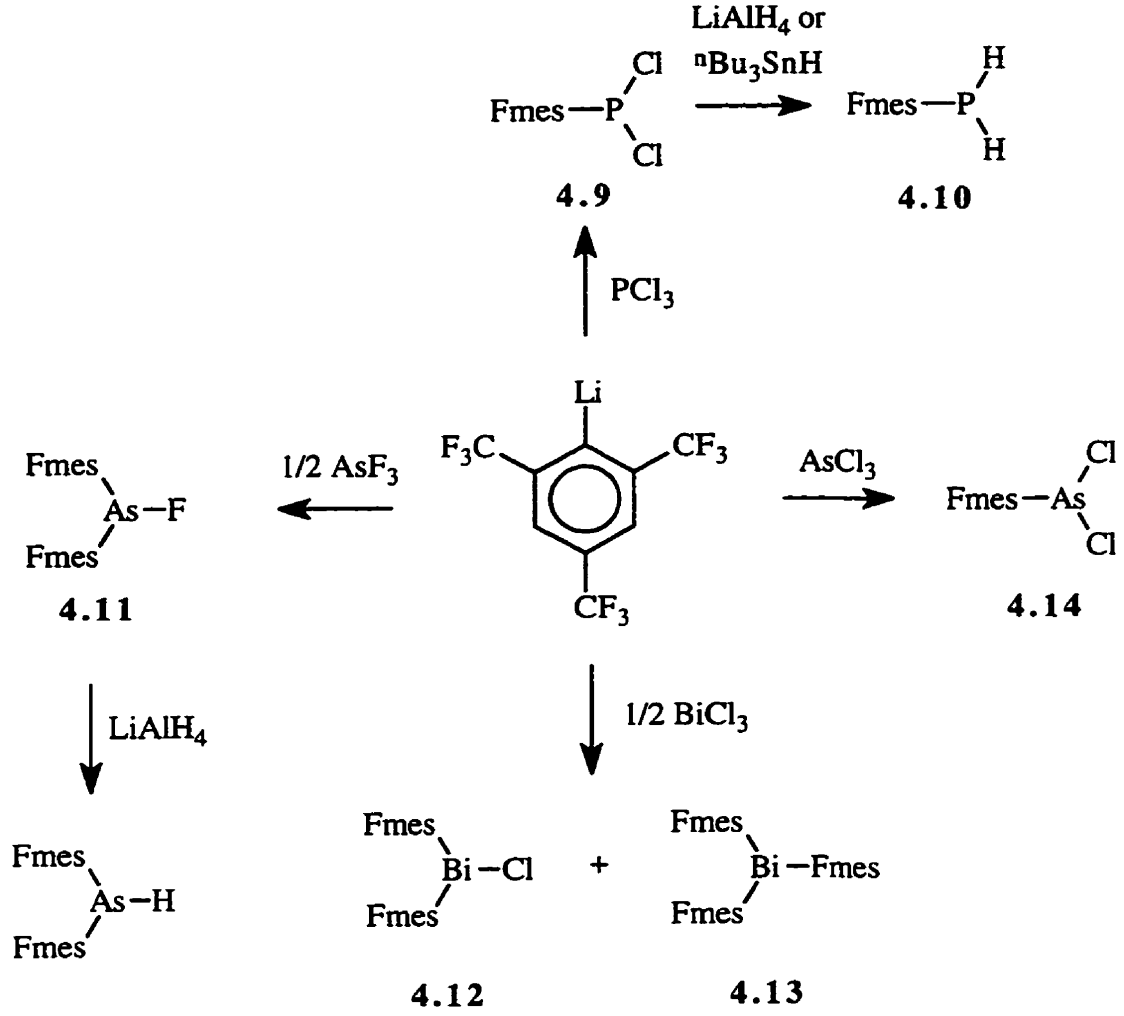


**Figure 4.5.** Synthesis of compounds containing the [Fmes-Pn] fragment.

Reaction of one equivalent of FmesLi with $PCl_3$ results in the formation of the colourless liquid $FmesPCl_2$ **4.9** which can be converted into $FmesPH_2$ **4.10** by $LiAlH_4$ or $^nBu_3SnH$.[143] Attempts to make $FmesPnX_2$ from the equimolar reaction of FmesLi with $AsF_3$ or $BiCl_3$ resulted in the isolation of the disubstituted (and mostly trisubstituted for Bi) compounds **4.11**, **4.12** and **4.13** (the yields of these reactions are improved by modifying the stoichiometry of FmesLi).[143,144] All species were identified by multinuclear NMR and mass spectrometry. Both bismuth compounds **4.12** and **4.13** have been structurally analyzed and each exhibits a pyramidal geometry about the bismuth atom and five close Bi-F contacts (range: 2.867 - 3.298Å).[144] Reaction of $AsCl_3$ with one equivalent FmesLi gives the colourless liquid monosubstituted dichloroarsine **4.14**.[70, 144]

Reagents **4.9** to **4.14** have allowed for the preparation of compounds containing low-coordinate pnictogen centers. Reaction of $FmesPCl_2$ with $FmesPH_2$ in the presence of DBU resulted in the formation of diphosphene **4.15**,[143] which is unusually stable in air; however, it readily reacts with one-eighth of an equivalent of $Se_8$ to yield the selenodiphosphirane **4.16**.[145] $FmesPCl_2$ was reacted with one equivalent of perfluoroaniline resulting in the formation of diazadiphosphetidine **4.17**, the dimer of the desired iminophosphine.[146] Synthesis of Fmes substituted iminophosphine **4.18** (Pn = P) and, more significantly, the analogous iminoarsine (Pn = As) is accomplished by the reaction of FmesN(H)K with $FmesPnCl_2$, although the major product in each reaction is phosphine (arsine) **4.19**.[70, 144,142] Iminoarsine **4.18** is the only example of a stable diaryl iminoarsine; the only other known compound with an As=N bond is

Mes*N(H)As=NMes*.[147] Finally, attempts to prepare FmesN=PnCl (Pn = P, As) resulted in the formation of diazadiphosphetidine (diazadiarsetidine) **4.20**.[135]

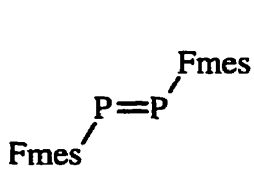

**4.15**

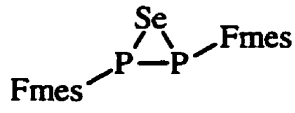

**4.16**

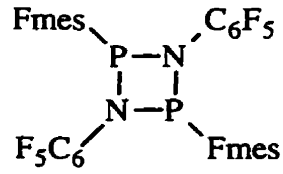

**4.17**

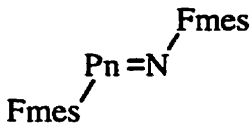

**4.18**

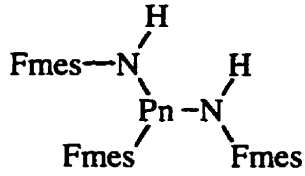

**4.19**

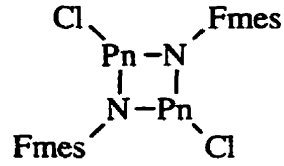

**4.20**

Pn = P, As

Our interest in pnictogenium cations and the reported isolation of the bisFmes substituted stannylene, germylene and plumbylene carbenoids prompted a study of their isoelectronic group 15 analogues. The synthetic method is illustrated in Figure 4.6 and consists of the preparation of pnictine derivatives $Fmes_2PnCl$ **4.21** (Pn = P, As, Sb, Bi) followed by halide abstraction using either $GaCl_3$ or AgOTf to yield salts of the cations $[Fmes_2Pn]$ **4.22** (Pn = P, As, Sb, Bi).

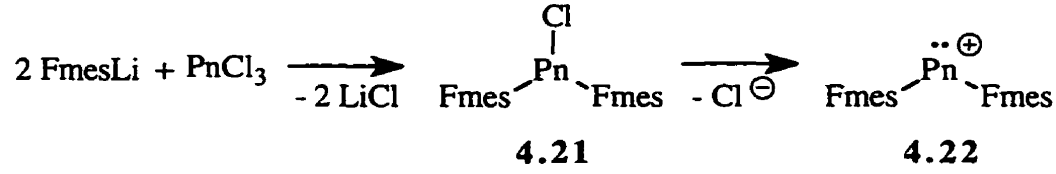

**4.21** **4.22**

**Figure 4.6.** Synthesis of $Fmes_2PnOTf$ compounds.

## 4.2 $Fmes_2PnCl$ Derivatives

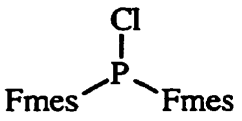


**4.23**

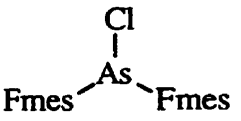


**4.24**

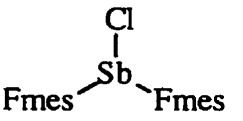


**4.25**

Reaction of two equivalents of FmesLi prepared *in situ* with $PCl_3$ in diethyl ether gives an orange solution which yields clear liquid $FmesPCl_2$ after removal of solvent and vacuum distillation.[143] The dichlorophosphine was fully characterized by multinuclear NMR ($\delta^{31}P$: 144.8 ppm, septet, $^4J_{P\text{-}F}$ = 61.0 Hz; $\delta$ $^{19}F$: -53.4 ppm, d, $^4J_{P\text{-}F}$ = 61.0 Hz, 2 F; - 64.3 ppm, s, 1F; $\delta^1H$: 8.4 ppm, s) however the reaction also resulted in a minor amount (< 1 % by $^{31}P$ NMR integration) of $Fmes_2PCl$ **4.23**. Small colourless needle-shaped crystals were isolated from the distillation residue characterized as $Fmes_2PCl$ by IR (*vide infra*) and multinuclear NMR ($\delta^{31}P$: 74.8 ppm, tridecaplet (9 lines visible), $^4J_{P\text{-}F}$ = 42.0 Hz, *c.f.* $Ph_2PCl$: $\delta^{31}P$: 80.5 ppm[148]).[149] The distinct favourability of $FmesPCl_2$ over $Fmes_2PCl$ is likely due to steric strain caused by the presence of two bulky Fmes groups on the relatively small phosphorus atom (Chapter 5 describes such an argument in detail).

The analogous reaction of $AsCl_3$ with two equivalents FmesLi gives $Fmes_2AsCl$ **4.24** which was purified by recrystallization from ether, then sublimation, followed by recrystallization from n-hexane to yield colourless needle-shaped crystals. The three purification steps are required to remove by-products such as $FmesAsCl_2$ and mostly

$^{n}Bu_xAsCl_{x-3}$ resulting from excess $^{n}$BuLi used in the *in situ* preparation of FmesLi. The product is characterized as $Fmes_2AsCl$ on the basis of multinuclear NMR, vibrational spectra (*vide infra*), elemental analysis and X-ray crystallography. The $^{1}H$ NMR spectrum contains a single deshielded ($\delta$ = 8.10 ppm) peak for the equivalent protons at the meta position of the Fmes groups and the signals in the $^{13}C$ NMR spectrum exhibit the expected one- and two-bond C-F coupling constants. The $^{19}F$ NMR spectrum displays only two peaks at $\delta$ -54.5 ppm and $\delta$ -63.9 ppm with a 2:1 integration. Although **4.24** recrystallizes in both monoclinic ($P2_1/a$) and orthorhombic ($P2_12_12_1$) space groups, the molecular structure is essentially identical in each crystal form. The molecular structure is shown in Figure 4.7 and selected bond lengths and angles are listed in Table 4.1.

**Table 4.1.** Selected bond lengths (Å) and angles (°) for $Fmes_2AsCl$ **4.24** ($P2_12_12_1$ form).

| | |
|---|---|
| As-Cl | 2.1920(12) |
| As-C(11) | 2.023(4) |
| As-C(21) | 2.016(4) |
| As-F(18) | 2.823(2) |
| As-F(13) | 2.849(2) |
| As-F(22) | 2.984(3) |
| As-F(23) | 3.018(3) |
| As-F(29) | 3.143(3) |
| C(11)-As-C(21) | 107.53(16) |
| C(11)-As-Cl | 100.57(12) |
| C(21)-As-Cl | 92.04(11) |

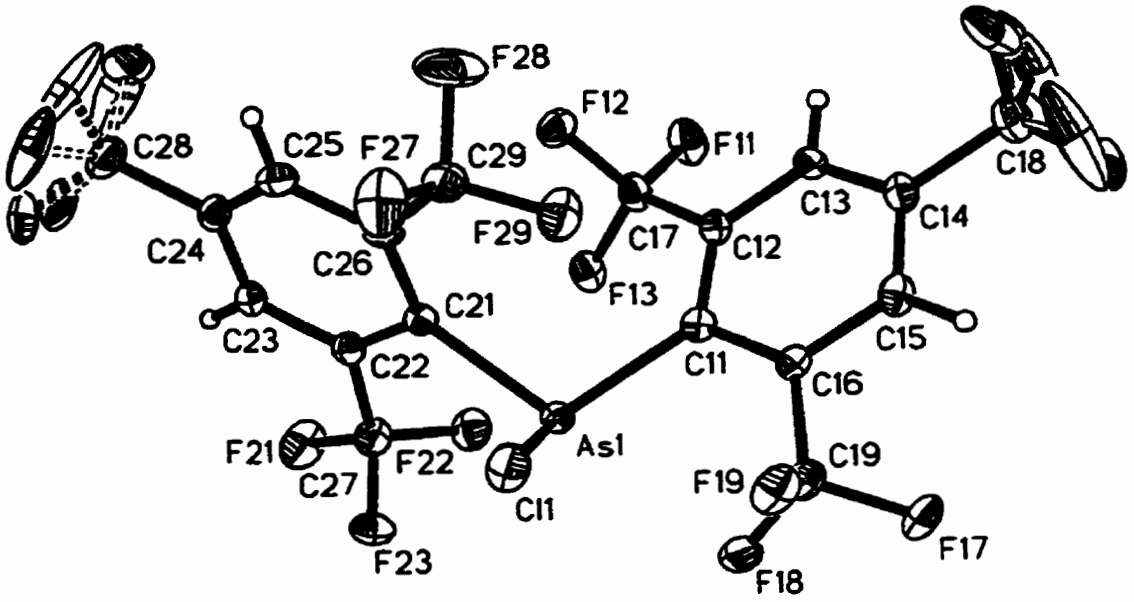


**Figure 4.7.** Molecular structure of $Fmes_2AsCl$.

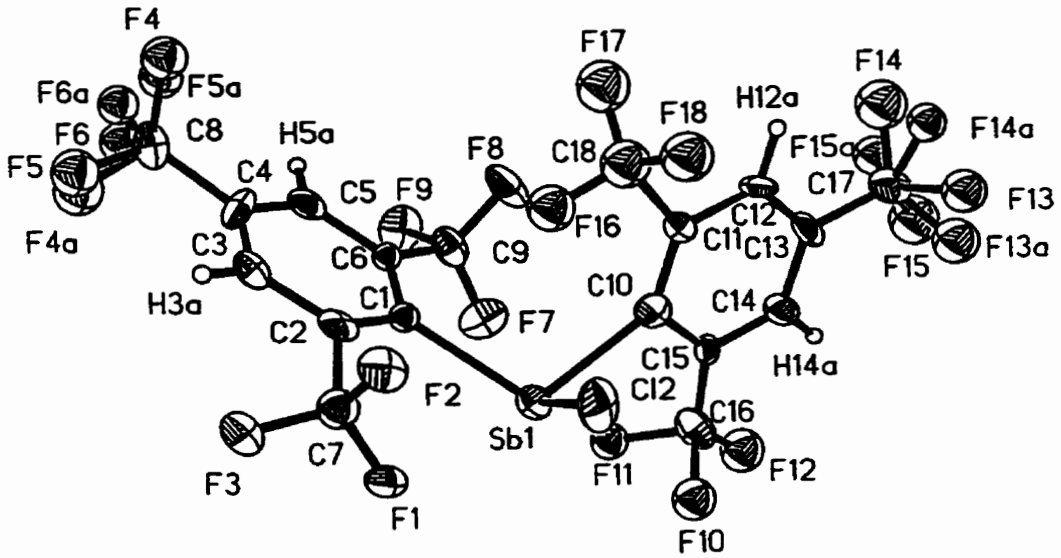


**Figure 4.8.** Molecular structure of $Fmes_2SbCl$.

The As-Cl bond length (2.1920(12) Å) is typical of As(III)-Cl bonds in chlorodiarylarsines ($Ph_2AsCl$ : 2.26(2) Å;[150] 10-chloro-5,10-dihydrophenarsazine: 2.301(4) Å[71], 2.270 Å[151]; 10-chlorophenothiarsenin: 1.923(3) Å,[152] and shows no indication of the "proto-ionization" observed in the diaminoarsines discussed in Chapter 1. The other structural features of **4.24** are similar to those of $Ph_2AsCl$[150][As-C: **4.24**, 2.023(4) and 2.016(4) Å; $Ph_2AsCl$, 1.97(4) Å); C-As-C: **4.24**, 107.53(16)°; $Ph_2AsCl$, 105(2)°] and are thus unexceptional.

Reaction of $SbCl_3$ with two equivalents of FmesLi in ether furnishes $Fmes_2SbCl$ **4.25** as very large (10 mm diameter, 4 mm thick) hexagon shaped crystals upon recrystallization. Multinuclear NMR data ($^{19}F$, $^{1}H$, $^{13}C$), vibrational spectra (FT-IR and FT-Raman) and elemental analysis are consistent with the formulation $Fmes_2SbCl$. The $^{19}F$ NMR spectrum consists of two peaks (δ -55.3 ppm and δ -63.9 ppm) with a 2:1 integration ratio. The crystals were carefully cut to obtain a single crystal X-ray structure of this compound shown in Figure 4.8. The diarylchlorostibine crystallizes in the monoclinic space group $P2_1/c$ and pertinent bond lengths and angles are listed in Table 4.2. The structure shows significant disorder in both para-$CF_3$ groups (typically observed in structures containing the Fmes substituent) which Dr. T. S. Cameron refined by splitting each group into two rigid bodies. The Sb-Cl bond length in **4.25** (2.368(8)Å) is comparable to the average Sb-Cl single bond length of 2.32Å, however the Sb-C distances are long [2.241(11)Å and 2.298(12)Å] even in comparison to those of bulky triarylstibines such as Sb(2,6-dimethylphenyl)$_3$ (Sb-C, 2.190Å). Fmes substitution also results in a very large C-Sb-C bond angle (107.6(6)°) which is significantly wider than even that of

dimesitylstibine, $Mes_2SbH$ (101.7°).[153] The antimony center exhibits the typical pyramidal geometry of neutral Sb(III) compounds (the sum of the angles at Sb is 297.2°) in the primary coordination sphere and also has a secondary coordination sphere of five Sb-F contacts, typical of main group Fmes derivatives (*vide supra*). These bonds range from 2.804Å (80% of the van der Waals radii) to 3.113Å (88% of the van der Waals radii).

**Table 4.2.** Selected bond lengths (Å) and angles (°) for $Fmes_2SbCl$ **4.25**.

| | |
|---|---|
| Sb-Cl | 2.368(8) |
| Sb-C(1) | 2.241(11) |
| Sb-C(10) | 2.298(12) |
| Sb-F(1) | 2.892 |
| Sb-F(5) | 2.804 |
| Sb-F(10) | 3.073 |
| Sb-F(11) | 3.052 |
| Sb-F(16) | 3.113 |
| C(1)-Sb-C(10) | 107.6(6) |
| C(1)-Sb-Cl | 101.9(5) |
| C(10)-Sb-Cl | 87.7(5) |

Reaction of two equivalents of FmesLi with $BiCl_3$ results in the formation of both colourless crystalline $Fmes_2BiCl$ **4.12** and primarily bright yellow crystalline $Fmes_3Bi$ **4.13**.[144] $Fmes_2BiCl$ was obtained through the ligand exchange reaction of 2 equivalents of $BiFmes_3$ with one equivalent of $BiCl_3$ in THF.[144] Several days of stirring results in the loss of the yellow colour typical of the triaryl bismuthine and removal of solvent *in vacuo* yields a pale grey white solid that is characterized by $^{19}F$ NMR as a mixture of $BiFmes_3$

(*ca.* 35%) and $Fmes_2BiCl$ (*ca.* 65%). The compounds are easily distinguished on the basis of $^{19}F$ and $^{1}H$ NMR. The $^{19}F$ NMR spectrum of $BiFmes_3$ in $CD_2Cl_2$ consists of a very broad singlet at δ -56.9 ppm ($w_{1/2} \approx 50$ Hz) from the ortho $CF_3$ groups and a singlet at δ -63.8 ppm corresponding to the para $CF_3$ groups. The spectrum of **4.12** has a much sharper ($w_{1/2} \approx 12$ Hz) singlet for the ortho $CF_3$ fluorine atoms at δ -56.3 ppm and a singlet from the para $CF_3$ groups also at δ -63.8 ppm. Roesky showed that the breadth of the more deshielded signal in the trisubstituted bismuthine results from hindered rotation of the Fmes groups (rotation barrier = 38 kJ/mol) as evidenced by a variable-temperature NMR study.[144] The $^{1}H$ NMR spectrum of the mixture of both species confirms the ratio of the products.

Infrared (Figure 4.9) and Raman (Figure 4.10) spectra of $Fmes_2PnCl$ derivatives (Raman spectrum for **4.12** was not obtained) allow for the tentative assignment of the Pn-Cl stretching frequencies for each compound. Each spectrum exhibits many bands arising from the Fmes substituents however, as expected, there are significant differences in the region of 500 - 250 $cm^{-1}$. The assigned frequencies of the Pn-Cl stretch are: IR: P-Cl, 434 $cm^{-1}$; As-Cl, 390 $cm^{-1}$; Sb-Cl, 351 $cm^{-1}$; Bi-Cl, 305 $cm^{-1}$; Raman: P-Cl, 437 $cm^{-1}$; As-Cl, 388 $cm^{-1}$; Sb-Cl, 349 $cm^{-1}$. The relative intensity of the Pn-Cl stretches in the infrared spectra increases dramatically as the mass of the Pn atom increases which may be caused by the increase in the dipole moment of the Pn-Cl fragment as the electronegativity of Pn decreases down the periodic table.

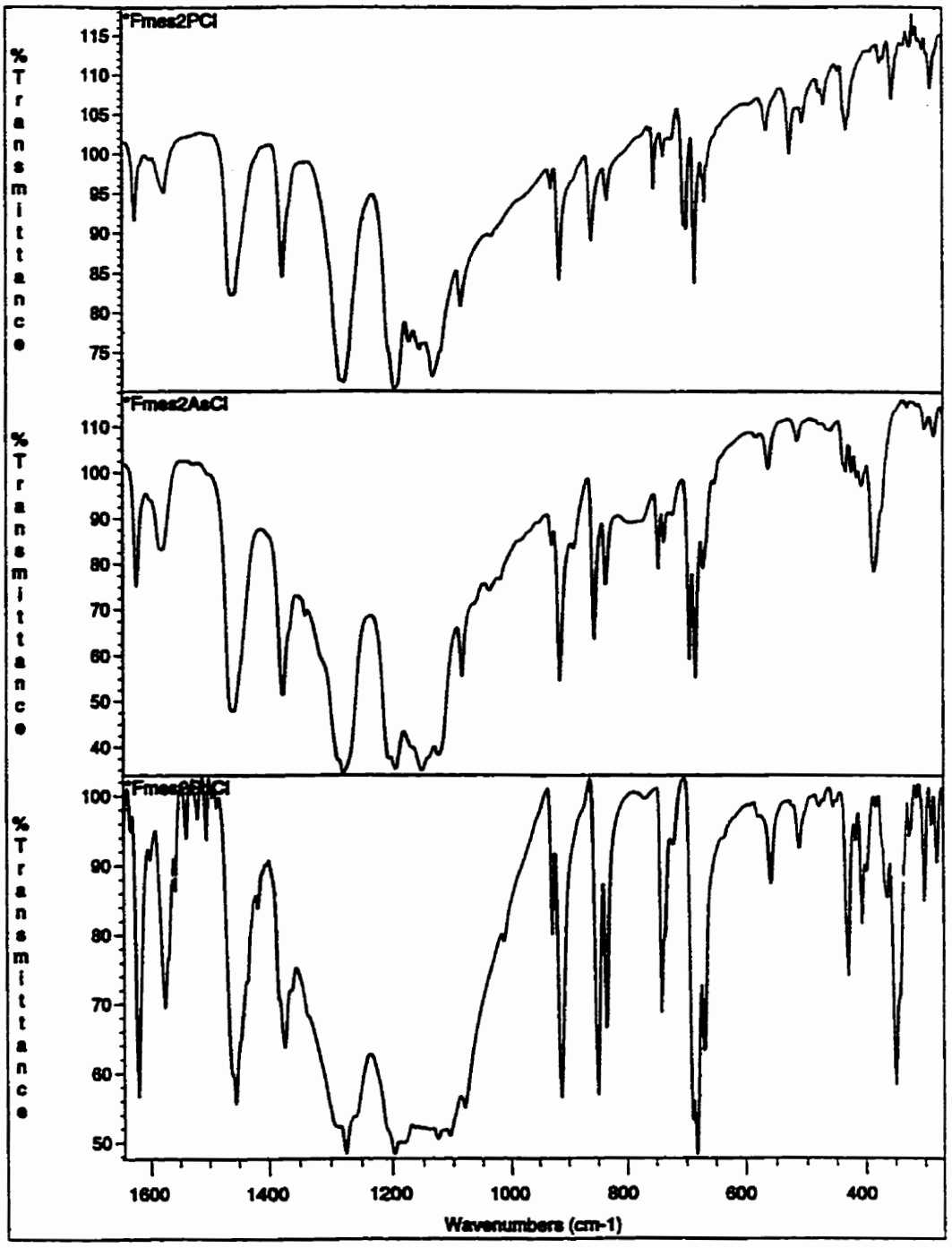


**Figure 4.9.** IR spectra of $Fmes_2PnCl$ compounds. Top: Pn = P; Middle, Pn= As; Bottom, Pn = Sb.

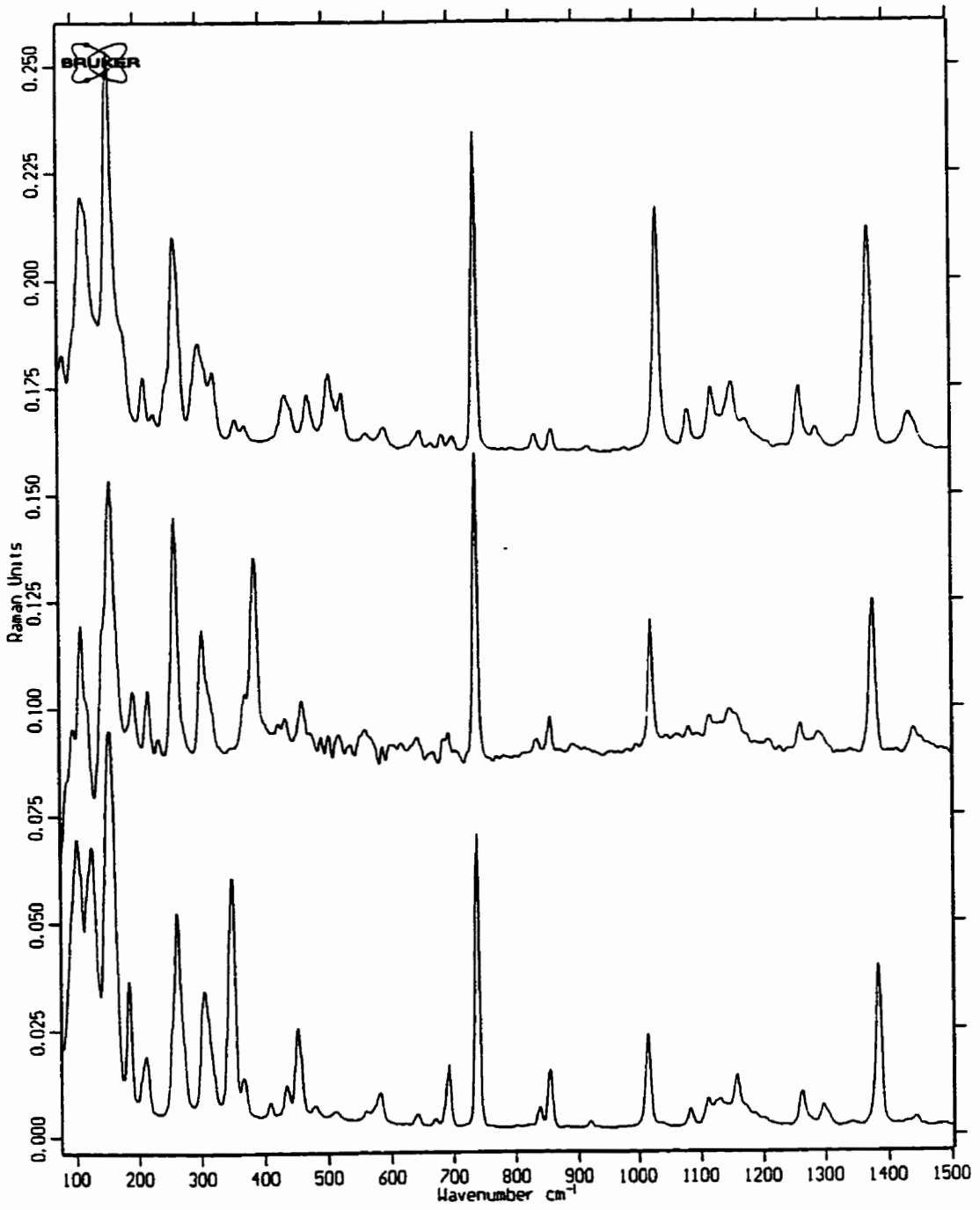


**Figure 4.10.** Raman spectra of $Fmes_2PnCl$ compounds. Top: Pn = P; Middle, Pn= As; Bottom, Pn = Sb.

## 4.3 [$Fmes_2Pn$] Derivatives

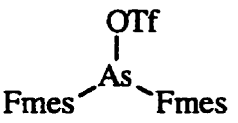


**4.26**

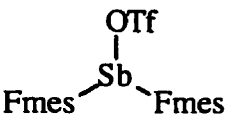


**4.27**

Reactions of $Fmes_2PnCl$ with silver triflate (AgOTf) or TMS-OTf in hydrocarbon solvent were examined as potential routes to ionic [$Fmes_2Pn$][OTf] derivatives. Chloride abstraction from $Fmes_2SbCl$ was also attempted with $GaCl_3$. Both reactions offered surprising results.

Combination of $FmesPCl_2$ in dichloromethane with an equimolar solution of $GaCl_3$ gave a lilac solution which rapidly turned very pale orange. $^{31}P$ and $^{19}F$ NMR spectra contained only peaks corresponding to the starting phosphine. $Fmes_2PCl$ was not isolated in sufficient quantity to allow for reactivity studies.

Reaction of $Fmes_2AsCl$ with an equimolar amount of AgOTf in hexane gave a yellow solution with white solid. Aliquots of the solution were removed and NMR analysis revealed a small amount of $Fmes_2AsOTf$ **4.26** (typically < 5%) and $Fmes_2AsCl$ (95-100%). Removal of the solvent *in vacuo* over 5 days yielded pale yellow needles of $Fmes_2AsCl$ (characterized by IR, m.p., NMR, and X-ray crystallography). Similarly, reaction of $Fmes_2AsCl$ with TMS-OTf in n-hexane gave only the starting material $Fmes_2AsCl$ (NMR). These results are in stark contrast to the reaction of $Mes_2AsCl$ with AgOTf, which affords $Mes_2AsOTf$ quantitatively (characterized by multinuclear NMR), and indicate that Fmes substitution precludes the formation of the desired triflate

compound. Although the reason for the relative "inertness" of $Fmes_2AsCl$ is not readily apparent, it is likely that the bulk of the Fmes ligands prevents the approach of the triflate reagent (kinetic stabilization) or that the increased steric strain in $Fmes_2AsOTf$ renders this derivative unstable with respect to $Fmes_2AsCl$ (thermodynamic stabilization).

The reaction of $Fmes_2SbCl$ with equimolar $GaCl_3$ in dichloromethane produced a lilac solution which rapidly faded to pale yellow. Multinuclear NMR of the reaction mixture showed no change from the starting stibine and crystals isolated from this solution were identified as $Fmes_2SbCl$ (IR, NMR, X-ray crystallography). In contrast, reaction of $Fmes_2SbCl$ with AgOTf in hexane results in the quantitative ($^{19}F$ NMR) formation of $Fmes_2SbOTf$ **4.27**. The reaction mixture $^{19}F$ NMR spectrum consists of a very broad (*ca.* 33 Hz in $CD_2Cl_2$ and 26 Hz in hexane) singlet at -55.7 ppm, a sharp singlet at -63.8 ppm and a sharp singlet at -77.3 ppm with an integration ratio of 4:2:1. The breadth of the signal of the ortho-$CF_3$ fluorine atoms is indicative of the increased crowding at the Sb center caused by the replacement of the Cl atom with the larger OTf ligand which hinders the rotation of the Fmes ligands. Removal of hexane yielded small colourless prism-shaped crystals and vibrational spectra of these show the disappearance of the Sb-Cl stretch consistent with the formation of $Fmes_2SbOTf$. X-ray crystallographic analysis of $Fmes_2SbOTf$ shows the molecule to be a covalent rather than ionic compound. The molecular struture is depicted in Figure 4.11 and selected bond lengths and angles are listed in Table 4.3.

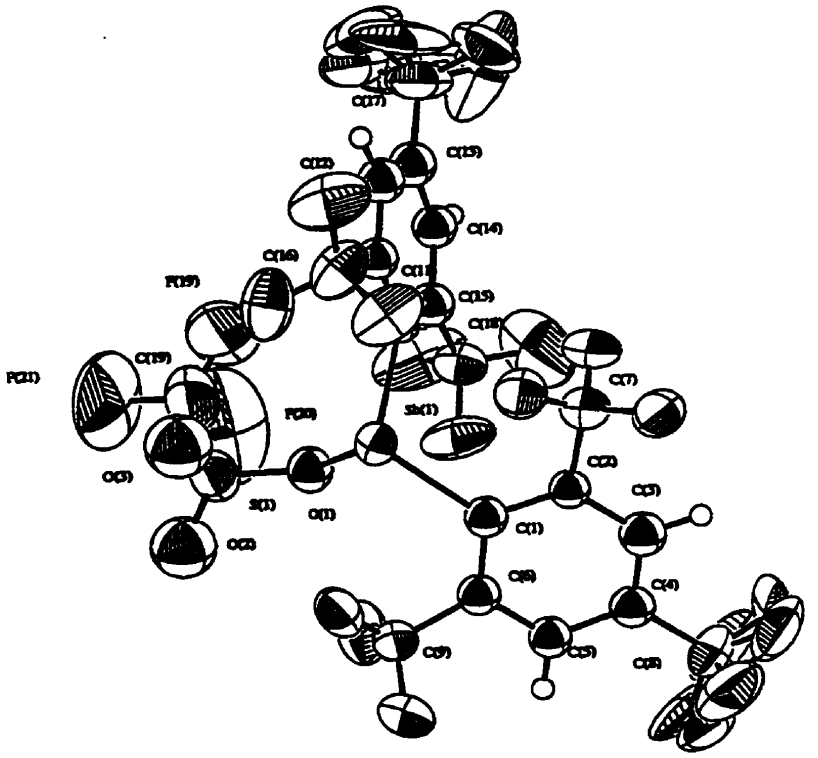

**Figure 4.11.** Molecular structure of $Fmes_2SbOTf$.

**Table 4.3.** Selected bond lengths (Å) and angles (°) for $Fmes_2SbOTf$ **4.27**.

| | | | |
|---|---|---|---|
| Sb-O(1) | 2.082(8) | C(1)-Sb-C(10) | 105.3(4) |
| Sb-C(1) | 2.21(1) | C(1)-Sb-O(1) | 94.8(4) |
| Sb-C(10) | 2.23(1) | C(10)-Sb-O(1) | 87.7(4) |
| O(1)-S | 1.513(9) | O(1)-S-O(2) | 114.6(6) |
| O(2)-S | 1.40(1) | O(1)-S-O(3) | 109.9(6) |
| O(3)-S | 1.41(1) | O(2)-S-O(3) | 119.2(7) |
| S-C(19) | 1.66(2) | O(1)-S-C(19) | 100.6(8) |
| Sb-F(2) | 2.733(8) | O(2)-S-C(19) | 111(1) |
| Sb-F(9) | 2.884(7) | O(3)-S-C(19) | 99(1) |
| Sb-F(10) | 3.17(1) | | |
| Sb-F(11) | 3.025(9) | | |
| Sb-F(17) | 3.131(7) | | |

The Sb-O bond length (2.082(8)Å) is almost exactly the sum of Pauling's Sb and O covalent bond radii[154] (Sb: 1.41Å, O: 0.66Å; sum, 2.07Å) although a search of the Cambridge Structural Database (CSD) reveals very few Sb(III)-O compounds.[155] The covalent bond is in contrast to the coordinative bond observed in the similar group 14 carbenoid complex $(FmesS)_2Pb$-THF[156] (Pb-O, 2.495(10)Å, sum of covalent radii 2.20Å,[6] sum van der Waals radii 3.50Å[157]) and calculated group 14 carbenoid complexes.[158] In addition, the structural parameters of the triflate moiety are clearly indicative of a covalently bound triflate substituent (rather than an ionic triflate anion). There are two short S-O bond lengths (1.40(1)Å and 1.41(1)Å) typical of S=O double bonds and a longer single S-O bond (1.513(9)Å) to the oxygen atom bound to the Sb center, in contrast to an anionic triflate group such as that in $[Mes^*NH_3][OTf]$ which exhibits nearly equal S-O bond lengths intermediate between those of single and double S-O bonds (1.440(8)Å, 1.432(9)Å and 1.436(8)Å). The C-Sb-C angle in **4.27** is 2.3° smaller than in the chlorinated precursor (*vide supra*). This is indicative of the increased steric requirements of the OTf ligand versus those of the Cl atom; however, the sum of the angles at the Sb atom decreases by almost 10° (287.8° vs. 297.2°). The geometry of the Sb atom is thus similar to those observed in $Ph_2SbOAc$ (sums of angles at Sb: 270.8° and 268.9Å) or $Ph_2SbOSbPh_2$ (sums of angles at Sb: 283.0° and 283.4°).[159,160] $Fmes_2SbOTf$ also displays five Sb-F contacts in the range of 2.733(8)Å to 3.131(7)Å making this compound and its chlorinated precursor (*vide supra*) the only reported compounds containing such Sb-F bonding.

The isolation of the covalent stibine rather than an ionic stibenium triflate can be rationalized in terms of the relative basicities of anionic [OTf] and that of a covalently

bonded F atom. Although the triflate anion is a very weak base (and relatively poor nucleophile), it is still a stronger base than the covalently bonded fluorine atoms on the $CF_3$ groups of the Fmes substituent and thus [OTf] more likely to react with the unstabilized cationic Sb center. The steric bulk of the Fmes substituents alone is not large enough to kinetically stabilize the cation by preventing the approach of the triflate anion thus the thermodynamically preferred covalent stibine is formed in the non-polar hydrocarbon solution.

The analogous reactions with $Fmes_2BiCl$ were not attempted because sufficiently pure $Fmes_2BiCl$ could not be isolated.

## 4.4 Conclusions

The results of the above syntheses and previous work by other groups allow for several conclusions to be drawn regarding the stabilizing effect of the Fmes substituent. Firstly, although the Fmes substituent is capable of stabilizing neutral group 14 carbenoids, it is not sufficient to stabilize their positively charged group 15 analogues. The explanations for these observations are twofold and derive from the structure and electronic properties of the ligand. Fluoromes is a highly electron-withdrawing substituent and, as such, is effective in stabilizing electron deficient species by diminishing the likelihood of oxidation. However the ligand does not allow for resonance or Coulombic stabilization of cationic centers (see Chapter 2). The results of this chapter indicate that the presence or absence of formal charge affects the relative stability of the isoelectronic series of aryl substituted carbenoids. This conclusion is consistent with that of Cramer *et. al.* based on a recent *ab initio* examination of the series ArEMe ($E = B^-$, C, $N^+$).[161]

Furthermore, the ligand does not provide sufficient steric bulk to kinetically prevent reactivity of the electron deficient site and thus the relative stability of Fmes substituted

compounds depends primarily on the effectiveness of the intramolecular contacts between the ortho-$CF_3$ groups and the electron deficient site. The necessity of fluorine atom proximity to the electron deficient site explains the failure of this substituent in stabilizing more reactive moieties that are not directly bonded to the ligand. For example, Roesky's attempted synthesis of FmesN=Pn-Cl (Pn = P, As)[142] was destined to result in the dimers that were isolated because the presence of the nitrogen atom between the low-coordinate Pn atom and the Fmes substituent prevents the necessary F-Pn interactions that would stabilize the double bonded compound and prevent dimerization. In addition, the contacts to the electron deficient site must be able to donate enough electron density to render oxidation, oligomerization or undesired reactions thermodynamically unstable with respect to the low-coordinate alternative. Although the Fmes ligand does provide such stabilization for the neutral group 14 carbenoids, the diphosphene and the iminopnictines, the electron density donated by the fluorine atoms is clearly not sufficient to compete with that of an anionic base in the case of the positively charged group 15 carbenoids.

The presence of a positive charge in the group 15 derivatives makes them highly susceptible to reaction with anions such as [OTf], the Fmes groups do not possess sufficient steric bulk to stabilize the cation kinetically and the close Pn-F contacts do not provide sufficient base stabilization to prevent cation-anion combination. The combination of these factors results in the isolation of covalent pnictines and derivatives derived from these as opposed to pnictogenium cations.

The conclusions reached from this work suggest that Fmes should be more effective in stabilizing anions than the neutral species that have been isolated. This suggests that carbenoid anions [$Fmes_2M$] **4.28** for M = B, Al, Ga, In, Tl are interesting synthetic targets for future study. Such compounds will allow for a more complete understanding of carbenic bonding through comparison with the now well established

group 14 and 15 analogues. Compounds **4.28** would also be useful synthons and may allow for synthesis of new varieties of multiple-bonded main group compounds *via* reactions with species such as group 14 and 15 carbenoids, phosphaalkynes, iminopnictines, and phosphazonium cations.

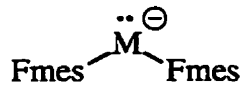


**4.28**

# Chapter 5. Steric Control of Low Coordinate Bonding Environments (I): The Steric Scale for Iminoaminopnictines, Diaminopnictazanes and Trisaminopnictines

## 5.1 Introduction

New structure and bonding imposed or stabilized by the presence of sterically demanding substituents has been a principal theme of inorganic chemistry for 20 years (Chapter 1). There are numerous bulky substituents (Chapter 1),[162] but Mes* is the most often used ligand (and one of the most sterically demanding) and has been responsible for the realization of heavier (n > 2) elements of Groups 13,[163] 14[164] and 15[165] in low-coordinate environments.

This work[166] establishes some boundaries for the limits of substituent steric strain by the Mes* substituent with the isolation and characterization of the trisaminostibine, $Sb(N(H)Mes^*)_3$ **5.1c** and trisaminobismuthine, $Bi(N(H)Mes^*)_3$ **5.1d**. The phosphorus **5.1a** and arsenic **5.1b** analogues are inaccessible and the use of the slightly less bulky Dip substituent results in the isolation of stibazane (diaminostibetidine) $[DipN(H)SbNDip]_2$ **5.3c**. Examination of the products obtained by these analogous lithiation reactions as well as others reported in the literature offers insight into the thermodynamic consequences of substituent steric strain. In doing so, this study provides guidelines for the steric control of structure and bonding in N-Pn-N compounds and thus allows for the establishment of a "steric scale" of the stability of such systems.

## 5.2 Synthesis and structure of $Pn(N(H)Mes^*)_3$ (Pn = Sb and Bi) and $[DipN(H)SbNDip]_2$

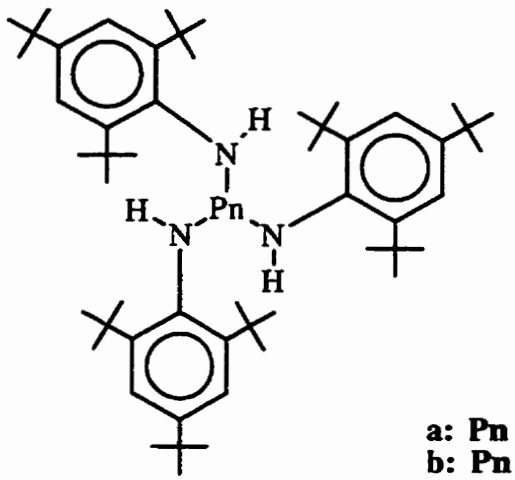

5.1

**a: Pn = P**
**b: Pn = As**
**c: Pn = Sb**
**d: Pn = Bi**

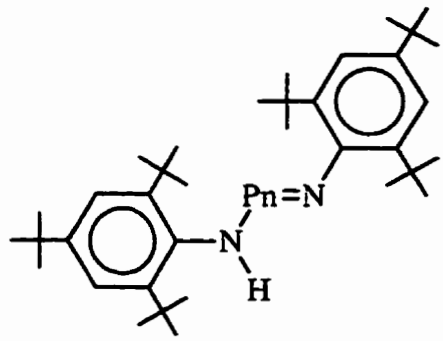

5.2

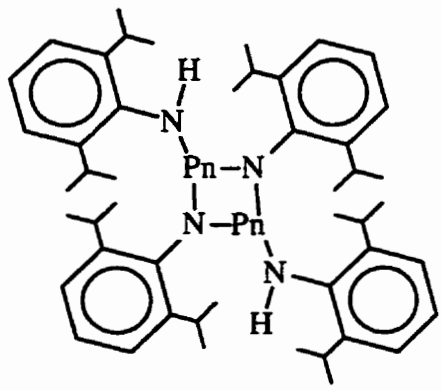

5.3

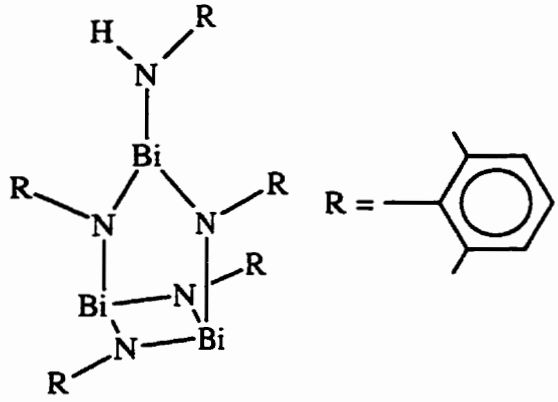

5.4

Reactions of $SbCl_3$ or $BiCl_3$ with three equivalents of LiN(H)Mes* occur rapidly at room temperature to give $Sb(N(H)Mes^*)_3$ **5.1c** and $Bi(N(H)Mes^*)_3$ **5.1d**, respectively. We envisage the reaction to occur according to equation 5.1 (*vide infra*), and $^1H$ NMR spectra of the reaction mixtures show the presence of the product and LiN(H)Mes* only. It

was not possible to promote completion of the reactions, and isolated yields are low. The compounds have been comprehensively characterized by numerous techniques including X-ray crystal crystallogaphy. The structures of **5.1c** and **5.1d** are isomorphous and selected structural parameters for these and stibazane **5.3c** are listed in Table 5.1. A crystallographic view of $Sb(N(H)Mes^*)_3$ is shown in Figure 5.1 and illustrates the substantial steric crowding imposed by the Mes* substituents, which is manifest in the severe distortion from a symmetric pyramidal geometry at the pnictogen center in both structures with N-Pn-N bond angles varying over a range of 19° (**5.1c**: 85.6(2)°-104.4(3)°; **5.1d**: 82.7(6)°-106.7(6)°).

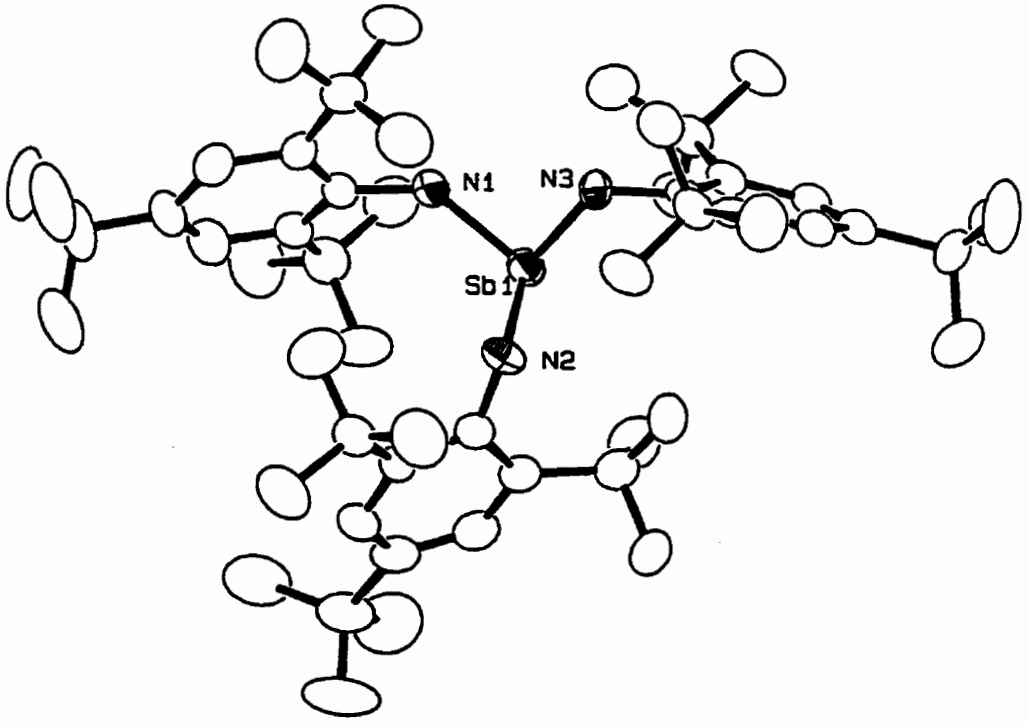


**Figure 5.1.** Molecular structure of $Sb[N(H)Mes^*]_3$.

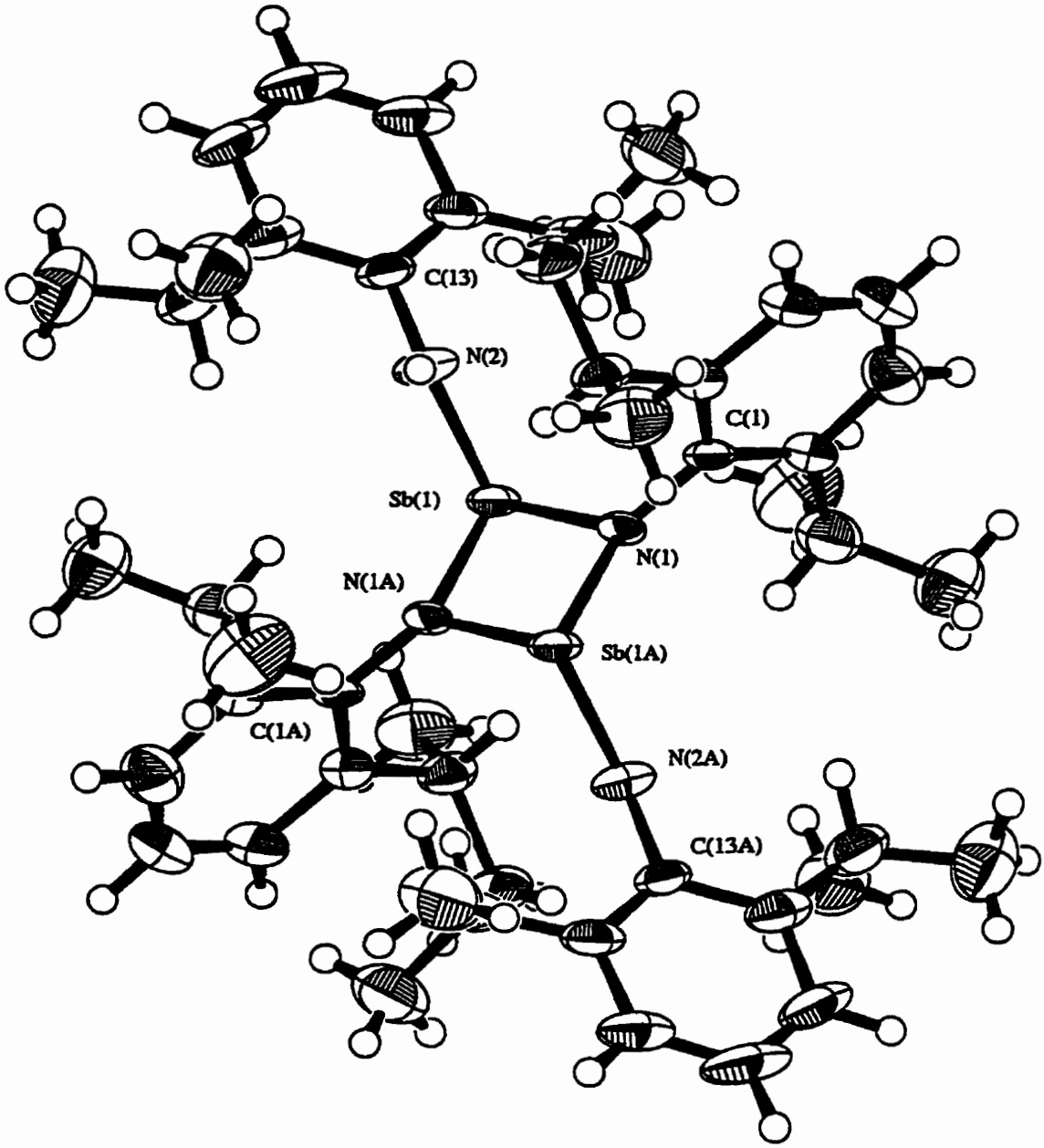


**Figure 5.2.** Molecular structure of $[DipN(H)SbNDip]_2$.

**Table 5.1.** Selected bond lengths (Å) and angles (°) for **5.1c**, **5.1d** and **5.3c**.

| | | | |
|---|---|---|---|
| **5.1c** | | | |
| Sb(1)-N(1) | 2.041(6) | N(1)-Sb(1)-N(3) | 85.6(2) |
| Sb(1)-N(3) | 2.048(6) | N(1)-Sb(1)-N(2) | 104.4(3) |
| Sb(1)-N(2) | 2.064(6) | N(3)-Sb(1)-N(2) | 99.9(2) |
| N(1)-C(1) | 1.423(9) | C(1)-N(1)-Sb(1) | 137.8(5) |
| N(2)-C(7) | 1.421(9) | C(7)-N(2)-Sb(1) | 117.4(5) |
| N(3)-C(13) | 1.442(8) | C(13)-N(3)-Sb(1) | 119.9(4) |
| | | | |
| **5.1d** | | | |
| Bi(1)-N(1) | 2.14(2) | N(1)-Bi(1)-N(3) | 106.7(6) |
| Bi(1)-N(3) | 2.179(14) | N(1)-Bi(1)-N(2) | 82.7(6) |
| Bi(1)-N(2) | 2.214(13) | N(3)-Bi(1)-N(2) | 98.5(5) |
| N(1)-C(1) | 1.47(2) | C(1)-N(1)-Bi(1) | 136.6(11) |
| N(2)-C(7) | 1.45(2) | C(7)-N(2)-Bi(1) | 114.8(10) |
| N(3)-C(13) | 1.49(2) | C(13)-N(3)-Bi(1) | 113.2(10) |
| | | | |
| **5.3c** | | | |
| Sb(1)-N(1) | 2.064(6) | N(1)-Sb(1)-N(1A) | 77.7(3) |
| Sb(1)-N(1A) | 2.032(6) | Sb(1)-N(1)-Sb(1A) | 102.3(3) |
| Sb(1)-N(2) | 2.032(6) | N(1)-Sb(1)-N(2) | 97.3(3) |
| N(1)-C(1) | 1.414(9) | N(1A)-Sb(1)-N(2) | 99.0(3) |
| N(2)-C(13) | 1.414(9) | Sb(1)-N(1)-C(1) | 125.0(4) |
| | | Sb(1A)-N(1)-C(1) | 128.8(5) |
| | | Sb(1)-N(2)-C(13) | 127.0(6) |

To my knowledge there are no previous structural reports for trisaminostibines.[167] The closest example is the trisiminostibine $Sb(NCPh_2)_3$ [Sb-N, 2.081(7), 2.074(7), 2.077(7)Å][168] which has Sb-N bond lengths slightly longer than those of $Sb(N(H)Mes^*)_3$ [Sb-N, 2.041(6), 2.048(6), 2.064(6)Å]; the latter are typical of amino N-Sb covalent bonds.[169] Structural studies on homoleptic trisaminobismuthines are rare,[170] but reveal

consistent Bi-N bond lengths [$Bi(NMe_2)_3$: 2.189(18), 2.180(21)Å; $Bi(NPh_2)_3$: 2.17(2), 2.16(3), 2.26(3); 2.28(2), 2.12(2), 2.21(4)Å]. The bonds in $Bi(N(H)Mes^*)_3$ are comparable [2.14(2), 2.179(14), 2.214(13)Å] and all of these bond lengths are significantly shorter than examples of coordinate N→Bi bonds.[171]

In contrast, the analogous reaction of three equivalents of the slightly less bulky amide DipN(H)Li with $SbCl_3$ results in the quantitative formation of stibazane $[DipN(H)SbNDip]_2$ **5.3c** and one equivalent of $DipNH_2$. The centrosymmetric structure of **5.3c** (Figure 5.2) consists of a planar 4 member Sb-N-Sb-N ring with pendant N(H)Dip moieties attached to the antimony centers. The bond lengths (Sb-N(1): 2.064(6)Å, Sb-N(1A): 2.032(6)Å (cyclic) and Sb-N(2): 2.032(6)Å (exocyclic)) and angles (N(1)-Sb-N(1A): 77.7(3)°, Sb(1)-N(1)-Sb(1A): 102.3(3)° (cyclic) and N(1)-Sb(1)-N(2): 97.3(3)°, N(1A)-Sb(1)-N(2): 99.0(3)° (exocyclic)) are consistent with those of the only other reported stibazanes $[Me_2NSbNR]_2$ (R = 3,4,5-trimethyoxyphenyl and 4-methylpiperidine).[172,173] The Sb-N bond lengths in these compounds are in the range of 2.019(5)Å to 2.068(5)Å, the cyclic N-Sb-N angles are 73.6(2)° and 75.8° and the cyclic Sb-N-Sb angles are 106.4(2)° and 104.2(2)°. The ring nitrogen atoms are nearly planar (sum of angles 356.1°) and the aryl groups are almost perpendicular to the N-Sb-N-Sb ring (94.7°).

## 5.3 Structure Defined by Steric Strain for [N-Pn-N] Species

The isolation of $Sb(N(H)Mes^*)_3$ **5.1c** and $Bi(N(H)Mes^*)_3$ **5.1d** is consistent with previous structural reports for the sterically encumbered homoleptic trithiolates $Sb(SDip)_3$[174] (Dip = 2,6-diisopropylphenyl) and $Bi(SMes^*)_3$.[175] However, they are in

contrast to the established analogous chemistry for phosphorus and arsenic. The reaction of $PnCl_3$ (Pn = P, As) with three equivalents of LiN(H)Mes* is reported to give the aminoiminopnictines, Mes*N=P(H)NMes* **5.2a** and Mes*N=As(H)NMes* **5.2b** (the first example of a stable aminoiminoarsine),[147] rather than the trisaminopnictines $Pn(N(H)Mes^*)_3$. The driving force for these reactions is likely the formation and precipitation of LiCl and the concomitant formation of $Mes^*NH_2$ (for Pn = P and As) as illustrated in equations (5.1) and (5.2).

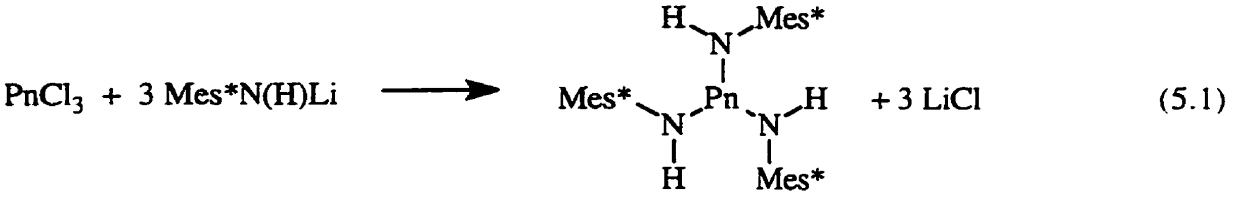


(5.1)

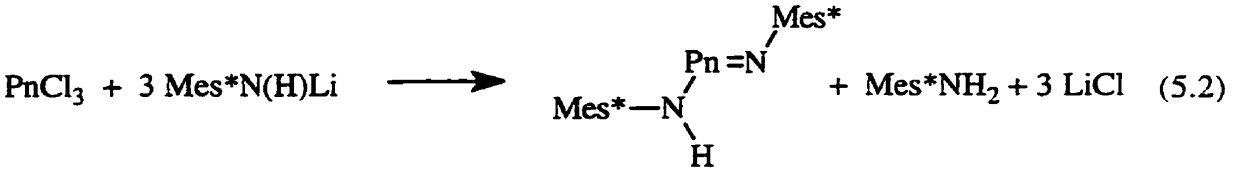


(5.2)

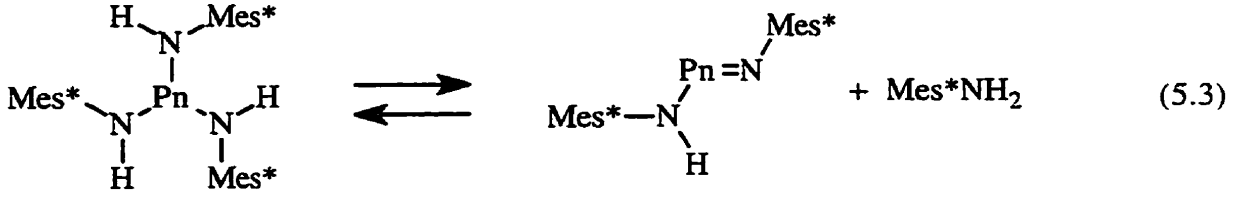


(5.3)

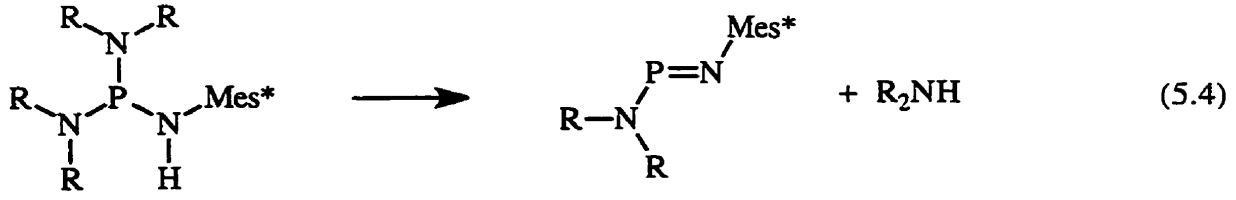


(5.4)

Furthermore, I have examined mixtures of **5.2a** with excess $Mes^*NH_2$ by $^{31}P$ NMR spectroscopy and do not observe any reaction. Together, these observations imply that the trisaminophosphine **5.1a** and trisaminoarsine **5.1b** are thermodynamically unstable with respect to $Mes^*NH_2$ and **2a** or **2b**, respectively (equation (5.3)). Indeed, Burford *et al.* have previously reported the spontaneous elimination of secondary amines from trisaminophosphines possessing a single Mes* substituent [equation (5.4)],[42] demonstrating the thermodynamic consequences of substituent steric strain (Chapter 1).

The favourable formation of **5.1c** and **5.1d** can be superficially understood in terms of the more spacious trisamino-stibine and -bismuthine environment by comparison with the trisamino-phosphine or -arsine. The Pn-N bond lengths offer the most obvious comparison. The Sb-N bonds in $Sb(N(H)Mes^*)_3$ [2.041(6), 2.048(6), 2.064(6)Å] and the Bi-N bonds in $Bi(N(H)Mes^*)_3$ [2.14(2), 2.179(14), 2.214(13)Å] are all in excess of 2 Å, while examples of trisaminophosphines[176,177] (including $\{N(H)Mes^*\}P\{NCPh_2\}_2$[178] containing the Mes* substituent) and trisaminoarsines[179] reveal a substantially more restricted pnictogen environment (P-N, 1.68-1.73 Å; As-N, 1.79-1.89 Å). We* therefore expect equation (2.3) for **5.1a** and **5.1b** to be exothermic due to the release of substituent strain energy upon elimination of $Mes^*NH_2$, consistent with previous experimental observations.[42] Minimization of substituent steric strain in **5.1c** and **5.1d** and adoption of fully σ-bonded structures is presumably responsible for their relative stability.

Report of the heterocyclic bismuthazane **5.3d**[180] introduces another interesting comparison. The compounds **5.3b** (Pn = As),[181] **5.3c** (Pn=Sb) and **5.3d** (Pn = Bi) can

---

* N. Burford and the author

be considered dimers of the iminoaminopnictine DipN=Pn(H)NDip (Dip = 2,6-diisopropylphenyl), derivatives of **5.2b**, **c** and **d**, respectively. Their formation from $PnCl_3$ and LiN(H)Dip is independent of reaction stoichiometry, implying thermodynamic preference over the trisaminopnictine $Pn(N(H)Dip)_3$, and illustrating the delicate energetic distinction between frameworks **5.1**, **5.2** and **5.3**. The replacement of a methyl group from each ortho $^t$butyl group of the Mes* substituent offers enough steric relief to allow for the association of the iminoaminopnictine units, as is clearly evident in the crystal structures of **5.3c** and **5.3d**.[180] Arrangement **5.3** represents a structural alternative to the double bonded iminoaminopnictine species allowing for a tricoordinate pnictogen center, avoidance of Pn=N π-interactions and less steric strain than is present in a trisamino-framework, $Pn(N(H)Dip)_3$. Such a structure is precluded by the extra methyl group ($^t$butyl rather than $^i$propyl) in the Mes* substituent and the trisamino- **5.1** framework therefore becomes the most thermodynamically favourable structure. Another interesting comparison is provided by the Bi-N cluster **5.4** formed from the analogous reaction of 3 equivalents of the even less bulky amide RN(H)Li (R = 2,6-dimethylphenyl) with $BiCl_3$.[182] The structure of **5.5** consists of a Bi-N-Bi-N ring similar to that of **5.3d** where an RN(H)Bi moiety bridges the two exocyclic R-N fragments. The authors report that the identical reaction with $SbCl_3$ results in the formation of a structure analogous to that of **5.3c** but do not offer any experimental details ("unpublished results").

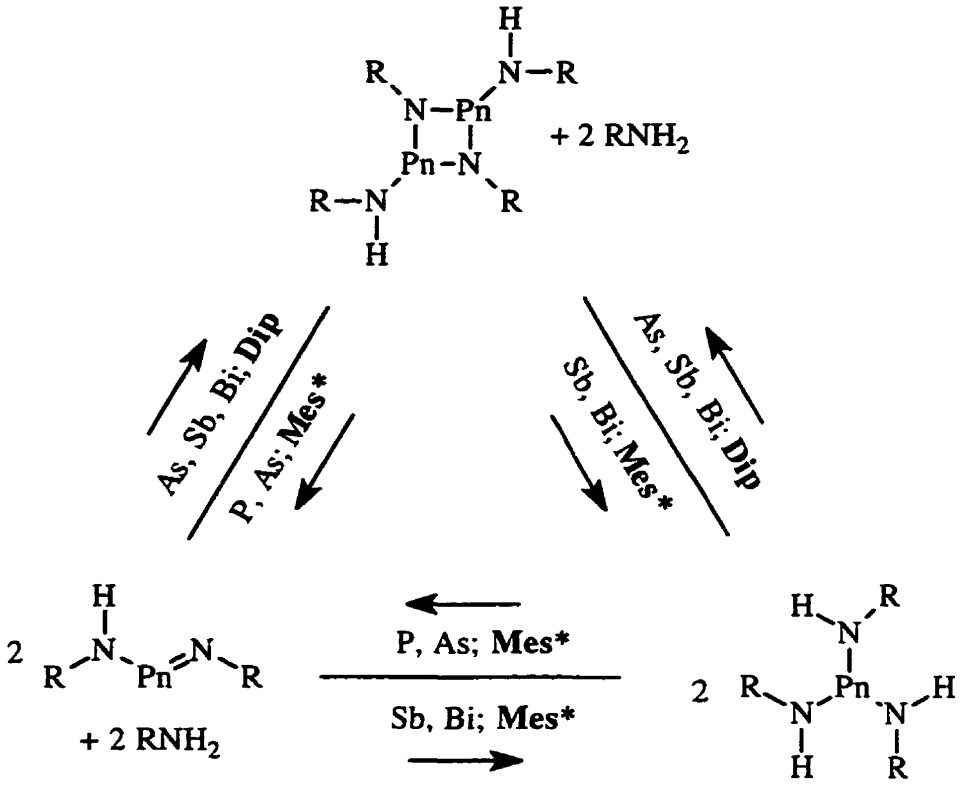


**Figure 5.3.** Schematic representation of the steric control of N-Pn-N bonding.

Overall the relationship between substituent size and the type of structure adopted is illustrated schematically in Figure 5.3 and can be understood as follows. For small substituents (Me, Et, $^{i}$Pr, etc.) steric factors are relatively unimportant thus the more energetically favourable trisaminopnictine structure is observed when Pn = P, As, Sb, and Bi. With the Mes* ligand (a large amount of steric bulk), the smaller pnictogen atoms (P and As) favour the π-bonded iminoaminopnictine framework because the steric strain of the trisaminopnictine or pnictazane structures renders them thermodynamically unfavourable (this also allows for the exothermic formation of one equivalent of Mes*$NH_2$). The larger pnictogen atoms allow for larger separation between Mes* substituents and adopt the fully σ-bonded triaminopnictine structure to avoid the less energetically favourable π-bonding

and because the pnictazane framework is precluded by the $^t$Bu groups of the ligand. Slightly smaller bulky ligands (Dip and 2,6-dimethylphenyl) result in the formation of pnictazanes (Pn = As, Sb, Bi) (or the similar Bi cluster) because the cyclic structure allows for a fully σ-bonded framework with less steric strain than the trisaminopnictine alternative and allows for the concomitant formation of one equivalent of $RNH_2$. For phosphorus, the smallest of these atoms, the Dip substituent is likely still bulky enough to yield the π-bonded iminoaminophosphine (although P forms π-bonds more readily than any of its heavier congeners).

## 5.4 Conclusions

Sterically congested trisaminopnictines $Sb(N(H)Mes^*)_3$ and $Bi(N(H)Mes^*)_3$ offer useful comparisons with the unstable phosphorus and arsenic analogues and with the compounds formed from similar reactions using less sterically demanding ligands. The results provide guidelines for the control of structure and bonding in N-Pn-N bonded systems through the use of Mes* and other bulky substituents.

The conclusions in this chapter suggest a variety of possible future projects. Substituents larger than Mes* such as Tbt, DMesp or DTipp (Chapter 1) should be used to synthesize iminoaminopnictines containing Sb and Bi. Alternatively, the use of secondary lithium amides containing the Mes* ligand (e.g. Mes*N(TMS)Li or Mes*N(Me)Li) may also allow for the synthesis of compounds containing the N=Pn (Pn = Sb or Bi) moiety.

*Ab initio* studies of the reactions studied in this chapter should be performed when sufficient computing power is available to allow for the efficient calculation of molecules bearing large substituents. Such calculations will provide for the quantification of the "steric scale" forwarded in this chapter.

# Chapter 6. Steric Control of Low Coordinate Bonding Environments (II): Investigations of the Iminophosphine-Diazadiphosphetidine Dimerization and the Observation of "Non-Le Chatelier" Behaviour

## 6.1 Introduction

The previous chapter provides a framework for the steric control of N-Pn-N bonding environments in which the observed bonding in the compounds is determined by the relative thermodynamic stability of the various structural alternatives. This chapter describes the dimerization of iminophosphines — systems in which both kinetic and thermodynamic effects are found to be important.

From a kinetic perspective, the steric shield provided by bulky substituents is envisaged as hindering the approach of molecules and preventing oligomerization and other types of reaction. The ethene dimerization described in Chapter 1 provides a simple theoretical model to address the thermodynamic consequences of substituent steric strain; however, estimates of the steric influence on reaction kinetics are far more difficult to quantify. The large number of atoms in the sterically demanding ligands outlined in Chapter 1 make *ab initio* calculations of transition states impractical or impossible at the current time: calculations of transition states would allow for quantification of activation barriers for reactions of compounds containing sterically demanding substituents. We have therefore turned our attention to the synthetic study of the facile monomer-dimer relationship between iminophosphines[165m] and diazadiphosphetidines to gain a qualitative understanding of the kinetic influences of bulky ligands.

Iminophosphines **6.1** containing 3p(P(III))-2p(N) $\pi$-bonds have been extensively studied synthetically and theoretically.[116,165m] Although other dimeric structures have

been identified,[183] the symmetric cyclic 1,3,2,4-diazadiphosphetidine **6.2** dimers (also known as phosphazanes) are most common and represent one of the most extensively studied series of inorganic compounds.[184] A [2+2] cycloaddition monomer/dimer equilibrium is well established for some RNPR derivatives,[185] but is considered irreversible for others.[186] Without exception, iminophosphines bearing the Mes* substituent on the nitrogen atom do not dimerize at ambient temperature.[187]

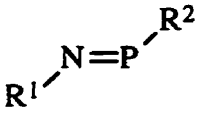

**6.1**

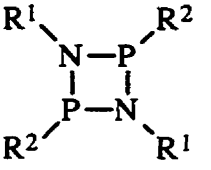

**6.2**

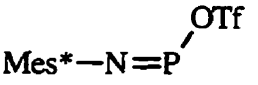

**6.3**

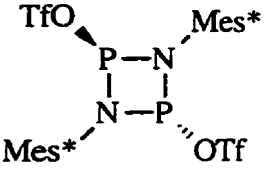

**6.4**

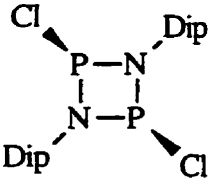

**6.6**

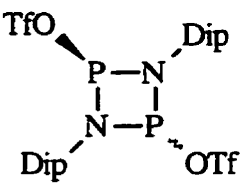

**6.7**

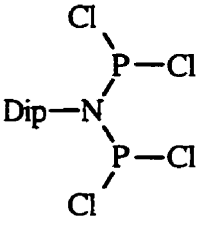

**6.8**

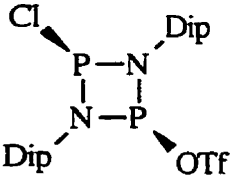

**6.9**

This chapter details the isolation of a monomer-dimer mixture in the solid state for the iminophosphine Mes*N=P-OTf **6.3** (or phosphazonium triflate [Mes*N≡P][OTf]), which was first crystallographically characterized by Niecke *et al.*[188] We have observed the consistent formation of $[Mes^*N{=}P\text{-}OTf]_2$ **6.4** as a significant co-product of Mes*N=P-OTf **6.3** in the reaction of iminophosphine Mes*N=P-Cl **6.5** with $AgOSO_2CF_3$ (AgOTf). The diazadiphosphetidine **6.4** has been characterized by X-ray crystallography, vibrational spectroscopy, solid-state NMR and *ab initio* calculations. A

solution-state $^{31}P$ NMR signal is not detected for the dimer (when dissolved in one of several different solvents). To assess the significance of the Mes* substituent in the relative stability of dimer **6.4** and monomer **6.3**, we have also synthesized analogous compounds with the slightly less bulky 2,6-diisopropylphenyl (Dip) substituent. The dimeric analogue of **6.5**, $[DipN{=}P\text{-}Cl]_2$ **6.6**, was reacted with AgOTf to produce dimeric $[DipN{=}P\text{-}OTf]_2$ **6.7** exclusively. Interestingly, attempted preparation of **6.6** *via* the reaction of $DipNH_2$ and $PCl_3$ in the presence of base (*cf.* **6.5**) yields $DipN(PCl_2)_2$ **6.8** instead of **6.6**.

## 6.2 Synthesis and Structures of Iminophosphines and Diazadiphosphetidines

Iminophosphine **1** was first prepared and structurally characterized by Niecke together with a series of other iminophosphines containing the Mes*N=P-O- fragment.[188] Although we have used the same reagents, our handling and isolation procedures differ in a number of ways. First all solution experiments were performed under vacuum instead of an argon atmosphere. Secondly, the crystallization was achieved at room temperature rather than at -30°C, and we believe that the *ca.* 50°C difference in temperature is a very significant factor in the formation of 1,3,2,4-diazadiphosphetidine **6.4**. Finally, the crystallization was carried out in normal room light rather than in the dark; however, we feel that this is likely an insignificant difference as phosphetidines are also observed in the absence of light. Our isolation procedure provides a mixture containing a vast majority of large dark orange crystals **6.3** and a minority (est. 5% or less) of small clear yellow crystals **6.4** with a combined yield of 83% ($^{31}P$ NMR spectra of the reaction mixture shows quantitative formation of **6.3**). While it has been possible to isolate each type of

crystal by the Pasteur method, the individual yields are not meaningful. Dimerization is also observed when crystals of purified **6.3** are redissolved in fresh hexane and recrystallized. This observation implies that no catalysts are present to facilitate the dimerization. Barring self-catalysis, the only possible catalysts present in the initial reaction mixture are Ag(OTf) and AgCl.[189,190]

Both **6.3** and **6.4** have been spectroscopically characterized and their respective structures have been determined by X-ray crystallography. Dr. T. S. Cameron's solution of the structure for the orange crystals is identical with that assigned to **6.3** by Niecke.[188] The yellow crystals are shown to have the molecular structure **6.4**, which is a head-to-tail [2+2] dimer of **6.3**. The significant difference between the molecular structure of each crystal form is responsible for the different unit cell parameters, volume and the twinning of **6.4**. Although both forms adopt the same space group, the angle $\beta$ in **6.4** is nearly right (90.59(3)°). Crystal twinning is not apparent on a macroscopic level however sub-microscopic growth of inter-penetrating twins is possible, in which the twinned crystal contains many individual crystallites in two different orientations in unequal ratios.[191] Crystals with a monoclinic unit cell (such as that of **6.4**) and the unique angle of the unit cell, $\beta \approx 90°$, are prone to a specific type of twinning.[192] The crystal twins are related by the [1 0 0  0 -1 0  0 0 -1] symmetry operation, which is equivalent to a rotation about the crystallographic ***a*** axis (not a symmetry element in $P2_1/n$). This type of twin is classified as a *twin-lattice quasi-symmetry* (TLQS) twin, in which there are two reciprocal lattices which have slightly different orientations.[193] Drs. Cameron and Kwiatkowski have also determined the cell of a number of crystals of each type to confirm that the bulk of each sample is the same as the single crystals used for structural determination. In addition, the

solid-state $^{31}P$ CP/MAS NMR spectrum of bulk sample exhibits features consistent with twinning throughout the crystals of **6.4** (*vide infra*). Pertinent bond lengths and angles for **6.4** and **6.3** are listed in Table 6.1. The molecular structures of **6.3** and **6.4** are depicted in Figures 6.1 and 6.2, respectively and the packing of the unit cell is shown in Figure 6.3.

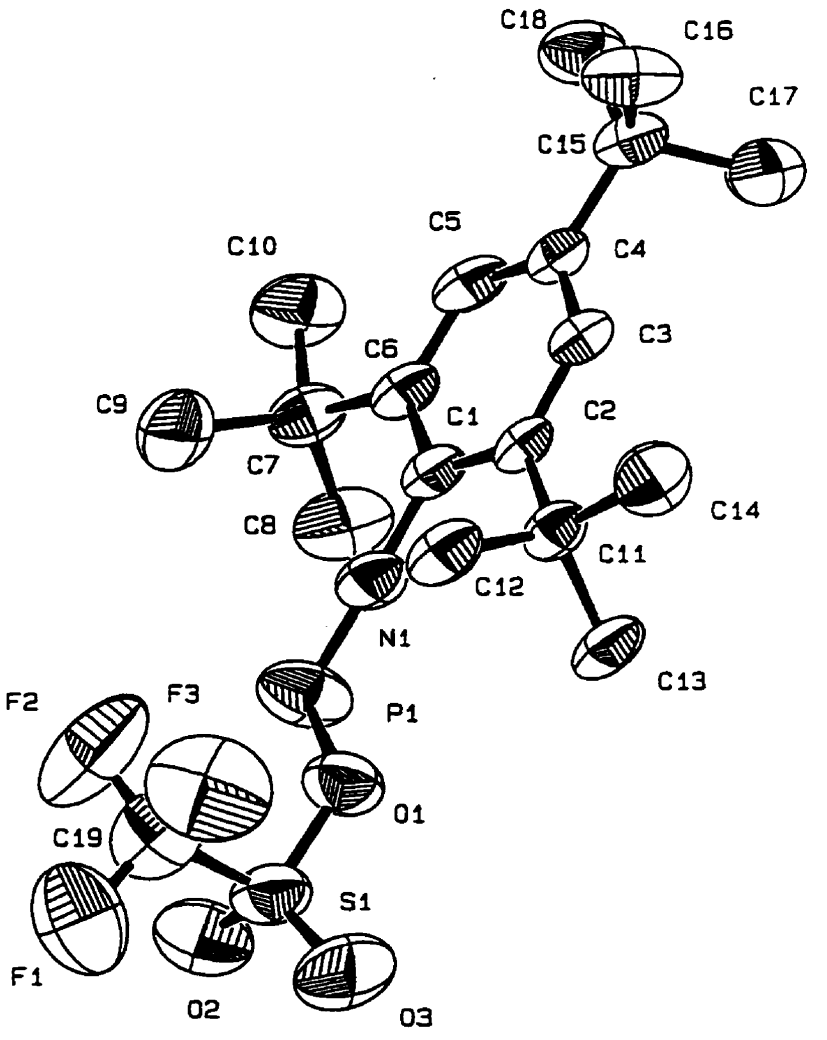


**Figure 6.1.** Molecular structure of Mes*N=P-OTf.

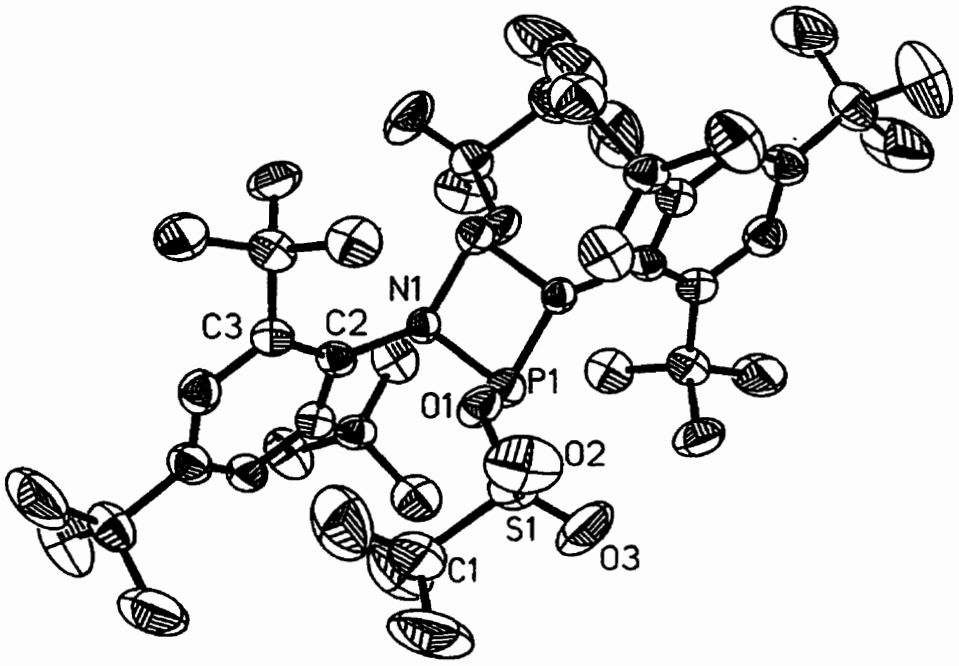


**Figure 6.2.** Molecular structure of $[Mes^*N{=}P\text{-}OTf]_2$.

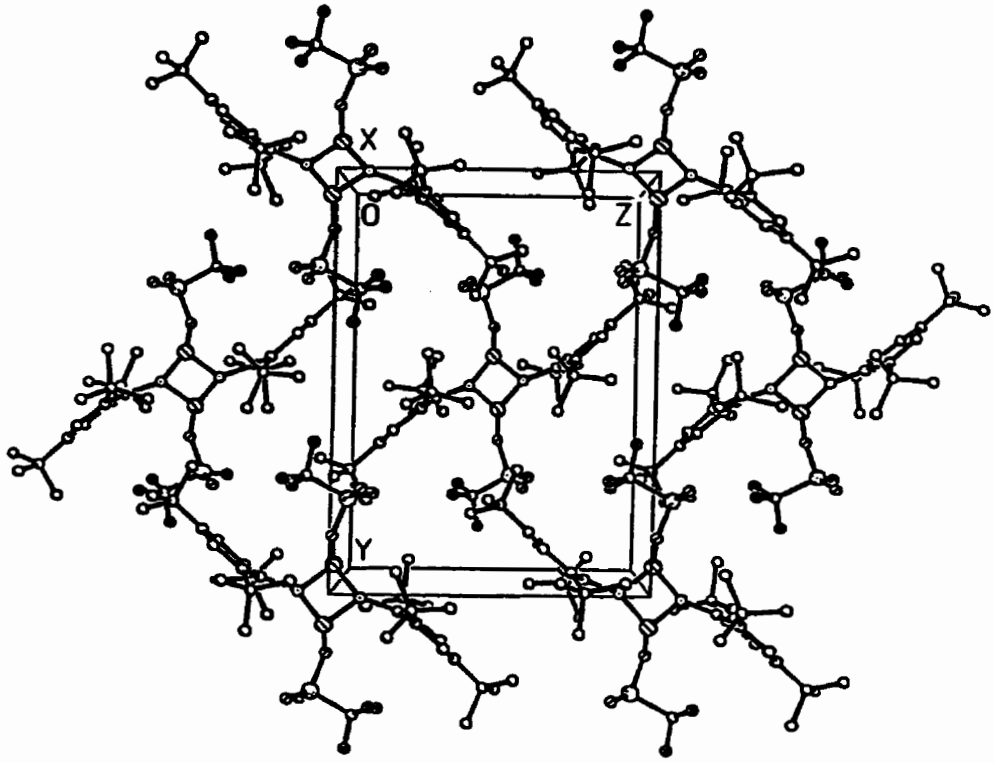


**Figure 6.3.** Packing diagram of $[Mes^*N{=}P\text{-}OTf]_2$.

**Table 6.1.** Selected bond lengths (Å) and angles (°) for **6.3** and **6.4**.

| | **6.4** | **6.3** | **6.3**[8] |
|---|---|---|---|
| P(1)-N(1) | 1.724 (4) | 1.477 (5) | 1.467 (4) |
| P(1)-N(1)' | 1.713 (4) | | |
| P(1)-P(1)' | 2.577 (3) | | |
| N(1)-C(2) | 1.462 (6) | 1.386 (7) | |
| P(1)-O(1) | 1.787 (3) | 1.926 (4) | 1.923 (3) |
| O(1)-S(1) | 1.550 (3) | 1.511 (4) | 1.499 (4) |
| | | | |
| C(2)-N(1)-P(1) | 119.7 (3) | 176.4 (4) | 176.4 (3) |
| N(1)-P(1)-O(1) | 95.7 (2) | 107.8 (2) | 108.4 (2) |
| P(1)-O(1)-S(1) | 124.3 (2) | 121.5 (3) | 121.9 (2) |
| N(1)-P(1)-N(1)' | 82.8 (2) | | |
| P(1)-N(1)-P(1)' | 97.2 (2) | | |
| | | | |
| C(3)-C(2)-N(1)-P(1) | 106.1 | 153 (6) | |
| C(2)-N(1)-P(1)-O(1) | 64.4 | -162 (6) | -158.4 |
| S(1)-O(1)-P(1)-N(1) | -158.4 | 168.3 (3) | 168.5 |

The dimer **6.4** adopts a nearly square PNPN moiety having crystallographically indistinguishable P-N bond lengths [1.713(4) Å and 1.724(4) Å], which are significantly shorter than a typical P-N single bond of 1.80 Å,[194] but are in stark contrast to the extremely short (1.477(5) Å) P-N bond in **6.3**. Each nitrogen centre in **6.4** is essentially planar [sum of the angles = 357.6(8)°] perhaps indicating some degree of π-bonding in the four-membered ring. The aromatic Mes* units are twisted 106.1° from the NPNP plane and are not able to conjugate with a PNPN π-system, consequently the C-N bond is longer [**6.4**: 1.462(6)Å , **6.3**: 1.386(7) Å].

The P-N-P bond angle [97.2(2)°] and N-P-N bond angle [82.8(2)°] are close to

right angles, while the C-N-P angles [140.7(3)°] and 119.7(3)° are markedly reduced from the nearly linear 176.4(4)° angle of the monomer. The bond lengths and angles are completely consistent with studies previously reported for P(III) 1,3,2,4-diazadiphosphetidines with a variety of substituents on the phosphorus and nitrogen atoms.[195,196,184] A search of the Cambridge Structural Database[197] yielded 40 structures with the following extrema: 1.655(6)Å[198] - 1.784(3)Å[199] for P-N bond lengths; 77.3(1)° - 89.4(3)° for N-P-N bond angles; and 91.1(1)° - 102.7(2)°[200] for P-N-P bond angles.

To date only two crystal structures of 1,3,2,4-diazadiphosphetidines that contain the Mes* substituent bound to the NPNP ring have been reported, both of which have only a single Mes* group directly bonded to the NPNP framework.[201,202] In these phosphetidines and dimer **6.4** the steric strain inherent in the molecules is manifest in the structure of the Mes* ligands themselves. All three structures contain Mes* units that are deformed such that the ipso aromatic carbon is not in the plane of the *ortho*, *meta*, and *para* aromatic carbons. This bend is best observed in the side-on view of the Mes* groups shown in Figure 6.3.

Other significant differences between the structures of compounds **6.3** and **6.4** include: a shorter P-O bond in the dimer [**6.4** 1.787(3) Å vs. **6.3** 1.926(4) Å ]; a longer S-O bond for the oxygen atom bonded to the phosphorus atom [**6.4** 1.550(3) Å vs. **6.3** 1.511(4) Å]; and a smaller O-P-N angle [**6.4** 95.7(2)° from **6.3** 107.8(2)°]. All of the listed structural parameters indicate an enhanced covalency in the dimer with respect to the monomer and are contrary to the expectations for the effects of steric impositions of the Mes* substituents.

The unprecedented dimerization of **6.3** suggests that the Mes* substituent is only just bulky enough to allow for the isolation of the monomeric iminophosphine in this system. Support for this hypothesis is provided by the results of the synthesis of

analogous compounds bearing the slightly smaller Dip substituent, in which one of the methyl groups on the *ortho*-$^t$butyl groups is replaced with a hydrogen atom. Reaction of $DipNH_2$ with $^n$BuLi followed by reaction with $NEt_3$ results in the formation of $[DipN{=}P\text{-}Cl]_2$ **6.6**, the dimeric analogue of **6.5**. The structure of **6.6** is depicted in Figure 6.4 and pertinent bond lengths and angles are listed in Table 6.2.

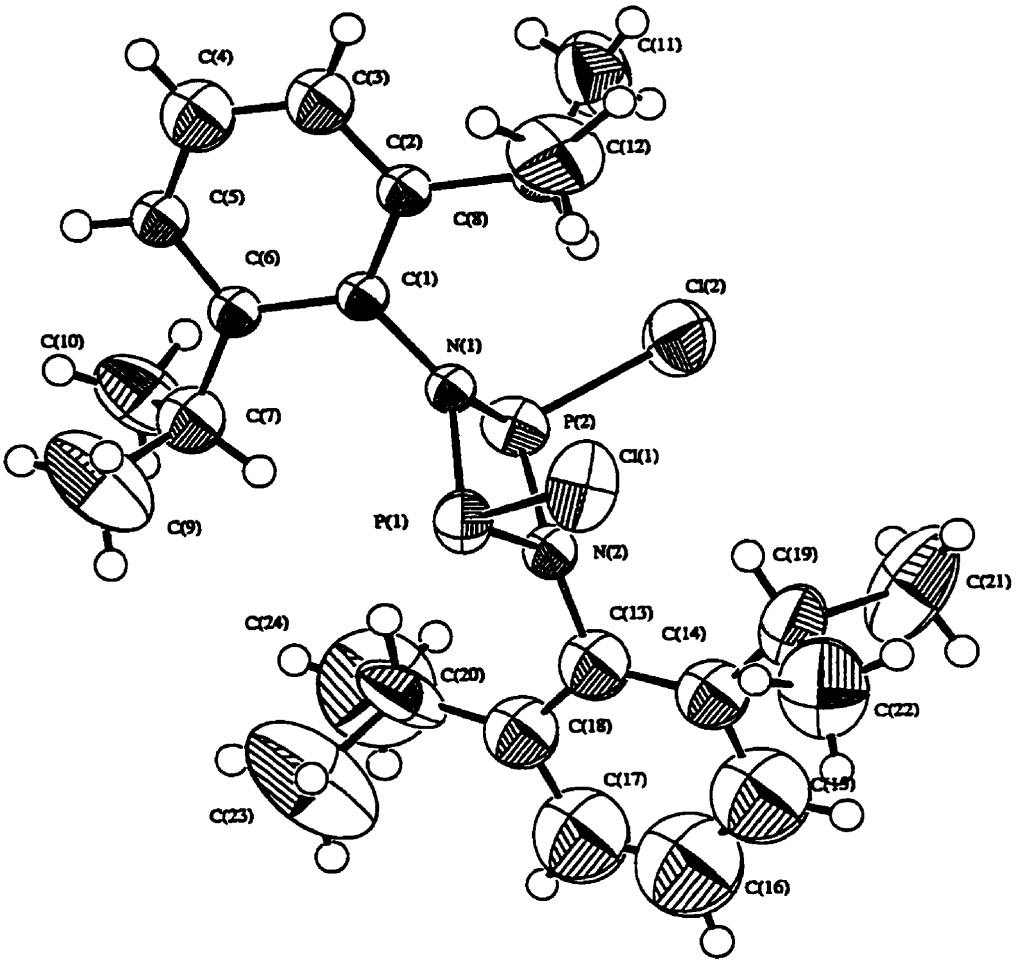


**Figure 6.4.** Molecular structure of $[DipN{=}P\text{-}Cl]_2$.

**Table 6.2.** Selected bond lengths (Å) and angles (°) for **6.6**, **6.7** and **6.8**.

| | **6.6** | **6.7** | **6.8** | **6.9** |
|---|---|---|---|---|
| P(1)-N(1) | 1.71 (1) | 1.694 (6) | 1.59 (3) | 1.72 (1) |
| P(1)-N(2) | 1.69 (1) | 1.695 (6) | | 1.67 (1) |
| P(2)-N(1) | 1.69 (2) | 1.707 (6) | 1.76 (2) | 1.71 (1) |
| P(2)-N(2) | 1.73 (1) | 1.698 (6) | | 1.72 (1) |
| N(1)-C(1) | 1.45 (2) | 1.457 (9) | 1.61 (4) | 1.43 (2) |
| P(1)-O(1) | | 1.784 (6) | | 1.814 (4) |
| P(2)-O(6) | | 1.763 (5) | | |
| O(1)-S(1) | | 1.512 (5) | | 1.5452 (2) |
| O(6)-S(2) | | 1.519 (6) | | |
| P(1)-Cl(1) | 2.071 (8) | | 2.11 (2) | |
| P(1)-Cl(2) | | | 2.03 (2) | |
| P(2)-Cl(1/3) | | | 2.01 (2) | 2.074 (5) |
| P(2)-Cl(2/4) | 2.085 (8) | | 2.06 (2) | |
| C(1)-N(1)-P(1) | 128 (1) | 129.3 (5) | 132 (2) | 128.9 (9) |
| C(13)-N(2)-P(2) | 125 (1) | 126.8 (5) | | 123.7 (9) |
| C(1)-N(1)-P(2) | 129 (1) | 127.0 (5) | 105 (2) | 129.7 (9) |
| N(1)-P(1)-O(1) | | 98.8 (3) | | 101.0 (4) |
| P(1)-O(1)-S(1) | | 121.8 (4) | | 119.3 (1) |
| N(1)-P(1)-N(2) | 81.3 (7) | 82.6 (3) | | 83.5 (5) |
| N(1)-P(2)-N(2) | 80.5 (7) | 82.1 (3) | | 82.2 (5) |
| P(1)-N(1)-P(2) | 98.6 (7) | 96.6 (3) | 122 (2) | 95.7 (6) |
| P(1)-N(2)-P(2) | 97.9 (8) | 96.9 (3) | | 97.1 (6) |
| N(1)-P(1)-Cl(1) | 103.2 (6) | | 102 (1) | |
| N(2)-P(1)-Cl(1) | 105.8 (6) | | | |
| N(2)-P(2)-Cl(2) | 103.2 (6) | | | 103.7 (4) |
| N(1)-P(2)-Cl(2/4) | 106.1 (6) | | 102 (1) | 105.4 (4) |
| C(2)-C(1)-N(1)-P(1) | 107 (2) | -103.2 (8) | | |
| C(1)-N(1)-P(1)-O(1) | | 97.5 (7) | | |
| S(1)-O(1)-P(1)-N(1) | | 176.1 (4) | | |

Dichlorodiazadiphosphetidine **6.6**, in contrast to most other N-aryl diazadiphosphetidines, is isolated in the *cis* conformation exclusively. The bond lengths and angles in **6.6** are typical of such species (P-N: 1.69 (2) - 1.73 (1) Å; P-Cl: 2.071 (8) and 2.085 (8); N-P-N: 81.3 (7) and 80.5 (7)°; P-N-P: 98.6 (7) and 97.9 (8)°) however, as in the case of **6.4**, the aryl groups are twisted nearly perpendicular (93.1°) to the "plane" of the NPNP ring as a consequence of the bulkiness of the Dip substituent. The nitrogen centers are not planar (sum of angles at N: 355.6° and 354.9°) as is typical of cis diazadiphosphetidines.

Reaction of **6.6** with two equivalents of AgOTf in hexane results in the formation of dimeric $[DipN{=}POTf]_2$ **6.7**, as predicted. Multinuclear NMR spectra show the presence of both *cis* [$^{31}$P: δ 177.5 ppm, $^{19}$F: δ -75.1 ppm *ca.* 75%] and *trans* [$^{31}$P: δ 273.9 ppm, $^{19}$F: δ -76.3 ppm *ca.* 25%] isomers in solution (*c.f.* **6.3**: $^{31}$P: δ 50.1 ppm; $^{19}$F: δ -78.3 ppm); however, we were only able to obtain a crystal structure of the dominant *cis* isomer as shown in Figure 6.5. Important bond lengths and angles are assembled in Table 6.2 and as in the case of diazadiphosphetidines **6.4** and **6.6** the structural parameters of the NPNP moiety are typical of such systems (P-N: 1.694 (6) - 1.707 (6) Å; N-P-N: 82.1 (3) and 82.6 (3)°; P-N-P: 96.6 (3) and 96.9 (3)°) and the aryl substituent is nearly perpendicular (97.7°) to the NPNP "plane". The nitrogen centers are not planar in the cis isomer (sum of angles: 352.9° and 353.3°). The P-O bond lengths (1.784 (6) and 1.763 (5)Å) in **6.7** are similar to those in **6.4** and are consistent with typical P-O single bonds. The interpretation of covalent bonding of the triflate group to the phosphetidine system is supported by the structural parameters of the triflate substituents and NMR spectroscopic features (*vide infra*). Each triflate group contains two short S-O bonds (1.419 (7) and 1.430 (7)Å in one and 1.413 (7) and 1.422 (7)Å in the other) and a longer S-O bond (1.512 (5)Å and 1.519 (6)Å) for the oxygen atom bonded to the

phosphorus atom. The N-P-O bond angles (98.8 (3) - 101.8 (3)°) and P-O-S angles (121.8 (4)° and 121.7 (3)°) are also consistent with those of **6.4**.

The reaction of one equivalent of AgOTf with **6.6** results in the formation of the expected cyclic "phosphenium cation" **6.9** as identified by multinuclear NMR. Somewhat surprisingly, the $^{31}P$ chemcial shift of the supposed dicoordinate phosphorus atom (δ 189.3 ppm ($^{2}J_{P-P}$ = 62.9 Hz, $^{4}J_{F-P}$ = 17.4 Hz)) is more shielded than that of the chloride substitued phosphorus atom (δ 203.2 ppm ($^{2}J_{P-P}$ = 62.9 Hz)) and both nuclei are more shielded than those in **6.6** (δ 211.5 ppm). The observation of $^{19}F$-$^{31}P$ coupling between the fluorine atoms of the $OSO_2CF_3$ group (confirmed by the 17.5 Hz splitting observed in the $^{19}F$ spectrum) and the phosphorus nuclei in the phosphetidine ring is another interesting spectroscopic feature of this molecule (also observed in *cis* and *trans* **6.7**) which indicates a significant interaction between the triflate group and the phosphetidine ring in solution. Such a coupling is not expected or observed in anionic triflate phosphenium salts, thus **6.9** is best described as a diazadiphosphetidine. The phosphetidine-type (covalent) bonding is confirmed by the molecular structure shown in Figure 6.6. Selected structural parameters are listed in Table 6.3. The bond lengths and angles for the NPNP fragment in **6.9** are typical of phosphetidines and do not require further comment. The compound exhibits a *cis* phosphetidine geometry and the structural parameters of the triflate group are similar to those of the covalent species **6.4** and **6.7** (one long S-O bond: 1.5452 (2)Å and two short S-O bonds: 1.4207(3)Å and 1.4119(2)).

Surprisingly, the attempted preparation of DipN=PCl using the same synthetic procedure as used for the synthesis of **6.5** results in the formation of bulky tetrachlorodiphosphine $DipN(PCl_2)_2$ **6.8**.[184] Although this compound results from the

formal addition of $PCl_3$ to DipN=PCl, it is more likely that it is formed from the reaction $DipN(H)PCl_2$ and $PCl_3$ with the loss of HCl. The molecular structure of **6.8** is illustrated in Figure 6.7 and selected bond lengths and angles are listed in Table 6.3. The outstanding features of **6.8**, which crystallizes with two almost identical molecules in the asymmetric unit, are the planarity of the nitrogen center (sum of angles 359° and 360°) and that the P-N-P fragment is perpendicular to the plane of the aryl group — characteristics typical of all such compounds.[184] This molecule may be of interest to transition metal chemists because it is a highly functionalizable "Nixon" ligand with more steric bulk than those being used currently.[184] Such ligands are typically used to stabilize coordination complexes of metals in low (0 or negative) oxidation states thus a ligand with significant steric bulk may allow for the synthesis of new complexes.[184,203,204]

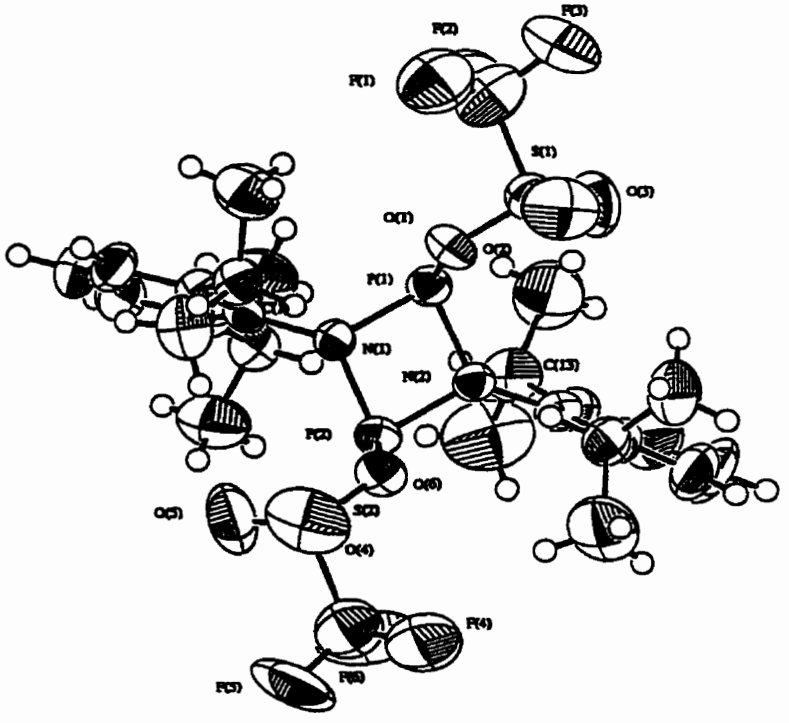

**Figure 6.5.** Molecular structure of $[DipN=P\text{-}OTf]_2$.

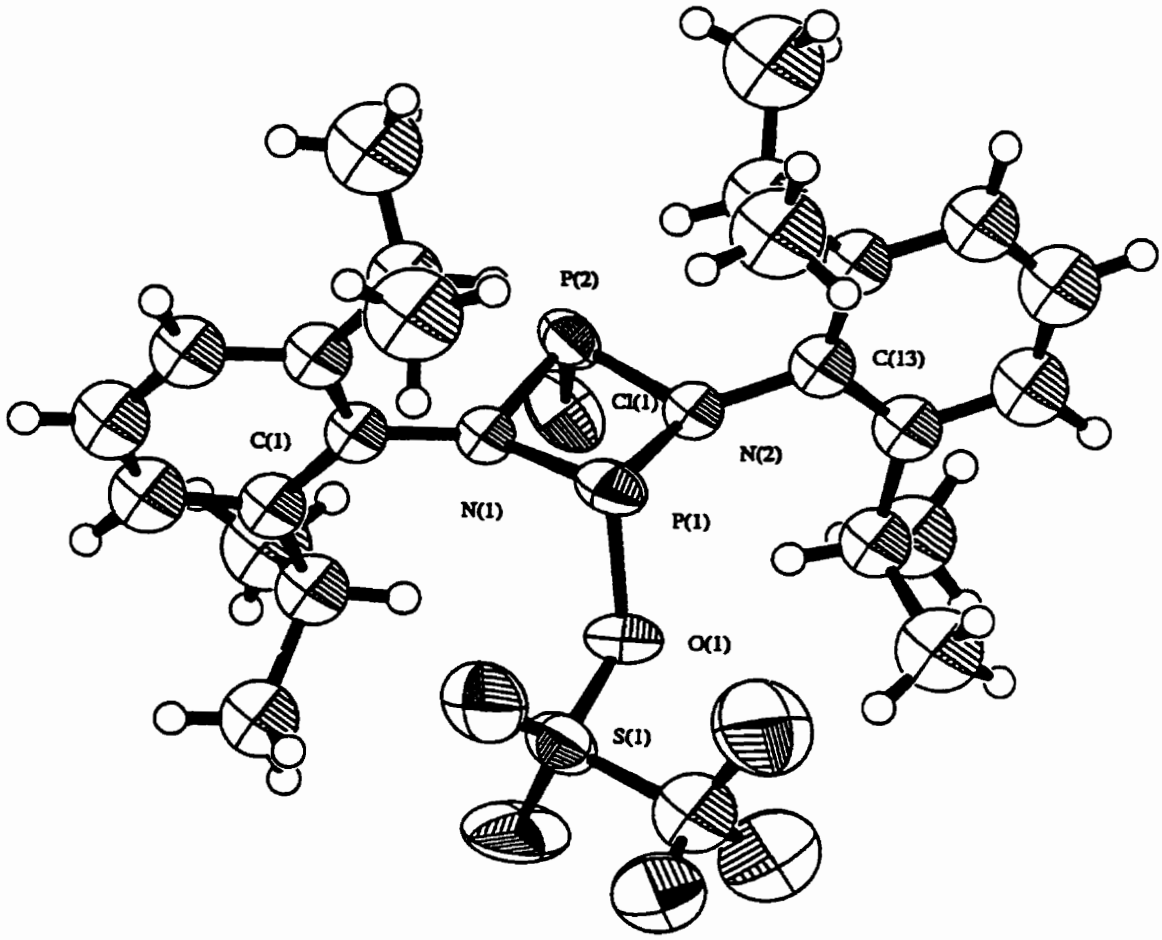


**Figure 6.6.** Molecular structure of Cl-P(μ-NDip)$_2$P-OTf.

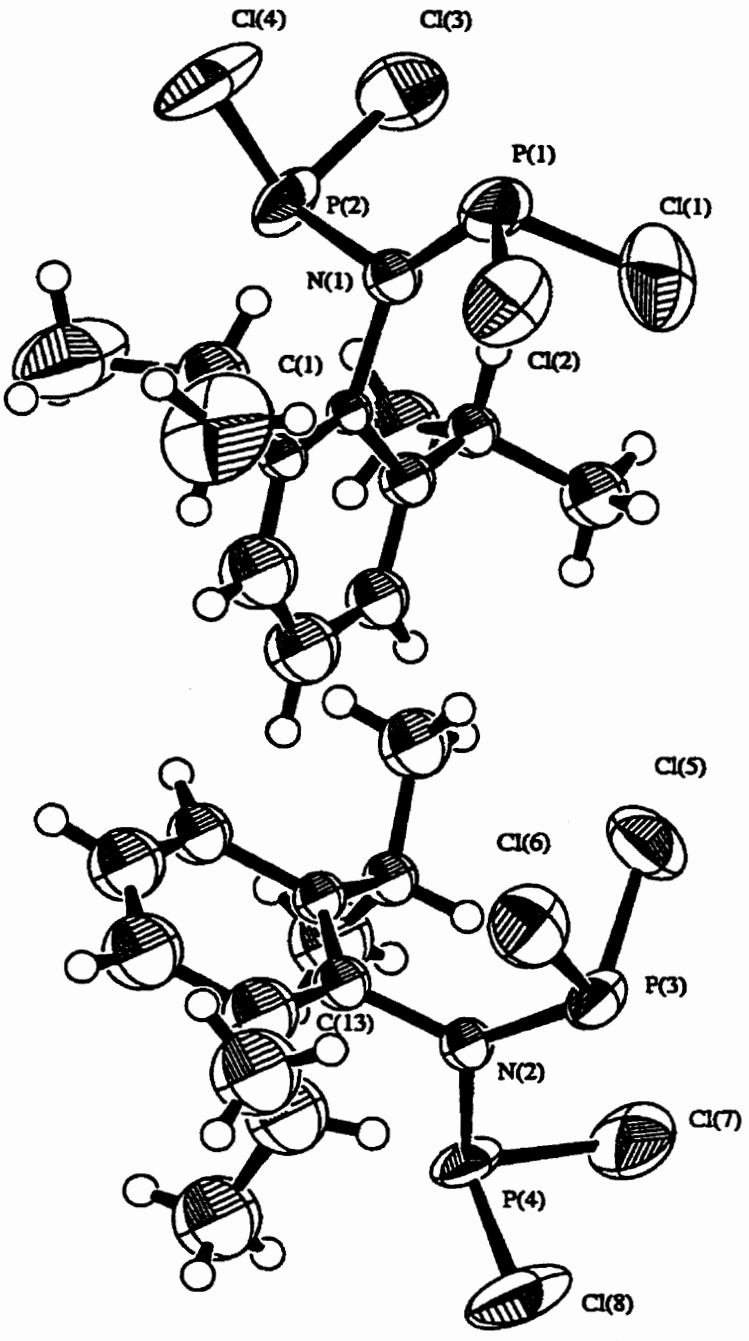


**Figure 6.7.** Molecular structure of $DipN(PCl_2)_2$.

## 6.3 Vibrational Spectra of Iminophosphines and Diazadiphosphetidines

Although the Raman spectrum of **6.4** is much less intense than that of **6.3**, the spectra of **6.3** and **6.4** are similar. The most obvious exception is the band at 1475 $cm^{-1}$ in the region of the P-N stretch which we have assigned for **6.3**.[205] This difference is indicative of the change in the P-N bonding from the highly polarizable essentially linear (triple bond-like) geometry in **6.3** which allows for conjugation with the Mes* aromatic system to the single (or partially delocalized) P-N bond in **6.4** that can not be conjugated. The characteristic stretch for the P≡N triple bond is present in **6.3** and absent in **6.4**. Although we are reluctant to assign the P-N stretch for **6.4**, the Raman spectrum of $^{15}N$ labelled **6.4** does not contain the prominent band at 995 $cm^{-1}$ but shows a new band at 874 $cm^{-1}$. The spectrum also shows significant shifts of the bands at 768 $cm^{-1}$ (to 758 $cm^{-1}$) and 132 $cm^{-1}$ (to 118 $cm^{-1}$).

The vibrational spectra of **6.6** are typical of such species exhibiting P-Cl bands at 496 and 421 $cm^{-1}$ (IR) and 496 and 419 $cm^{-1}$ (Raman). The IR spectrum of **6.7** shows the disappearance of both P-Cl bands and the appearance of bands at *ca.* 1030 $cm^{-1}$, 1163 $cm^{-1}$ and 1250 $cm^{-1}$, which are indicative of the OTf fragment.[61e] Similarly the spectra of **6.9** show the appearance of the OTf bands, however the P-Cl stretch is still observed.

## 6.4 Variable-Temperature Solution NMR of Mixtures of 6.3 and 6.4

Variable-temperature (VT) NMR studies of the crystallization mixture of **6.3** and **6.4** dissolved in hexane, toluene, diethyl ether and dichloromethane ($CH_2Cl_2$ and $CD_2Cl_2$) showed no indication of the [2+2] dimer or a [2+1] product in solution at any temperature. The expected chemical shift of the dimer (around 257 to 252 ppm, *vide infra*) was not

observed in any of the solvents at any temperature down to the freezing point of the solvents. In each solvent the only difference observed upon cooling the sample from 293 K was a progressive increase in shielding in the chemical shifts by a total of 2-3 ppm over the entire temperature range.

## 6.5 Solid-State $^{31}$P NMR of Mixtures of 6.3 and 6.4

Solid-state NMR is capable of providing information otherwise unobtainable from analogous solution-state NMR techniques, such as chemical shielding anisotropy, dipolar interactions between coupled nuclei, the orientation of the CS tensor and the detection of crystallographically non-equivalent sites within a crystalline sample. Solid-state $^{31}$P NMR has previously been used to probe the bonding in iminophosphines and related systems,[206,207,208,209] and solution $^{31}$P NMR studies have also been reported for such systems.[210,211]

Solid-state $^{31}$P NMR spectra were acquired under the conditions of cross-polarization (CP) and magic-angle spinning (MAS) at two different fields and the results were interpreted by R.W. Schurko. The spectra display signals for both the monomeric and dimeric forms of Mes*N=P-OTf in samples of the powdered crystals. Static $^{31}$P NMR spectra of **6.3** allow for the determination of the principal components and approximate orientation of the chemical shift (CS) tensor at the phosphorus nuclei. Experimental results are compared with theoretical chemical shift tensors calculated by means of high-level restricted Hartree-Fock (RHF) and density functional theory (DFT) *ab initio* computations. Pertinent information from the experimental and theoretical NMR studies is summarized in Table 6.4.

**Table 6.4.** Experimental and Calculated $^{31}P$ Chemical Shift Tensors.

| | 6.3 | | | 6.4 | | |
|---|---|---|---|---|---|---|
| | Exptl. | RHF | B3LYP | Exptl. | RHF | B3LYP |
| $\delta_{11}$ (ppm) | 223 | 320 | 312 | 456 | 439 | 583 |
| $\delta_{22}$ (ppm) | 207 | 181 | 217 | 324, 308 | 318 | 378 |
| $\delta_{33}$ (ppm) | -281 | -416 | -237 | -8 | -35 | 121 |
| $\delta_{iso}$ (ppm) | 49.7 | 28.3 | 97.3 | 257.3, 252.0 | 240.7 | 360.7 |
| $\Omega$ (ppm) | 504 | 736 | 549 | 464 | 474 | 462 |
| $\kappa$ | +0.94 | +0.62 | +0.65 | +0.43 | +0.49 | +0.11 |
| $\beta_{NMR}$ (°) | 21 | 11 | 11 | n/a | 45 | 45 |

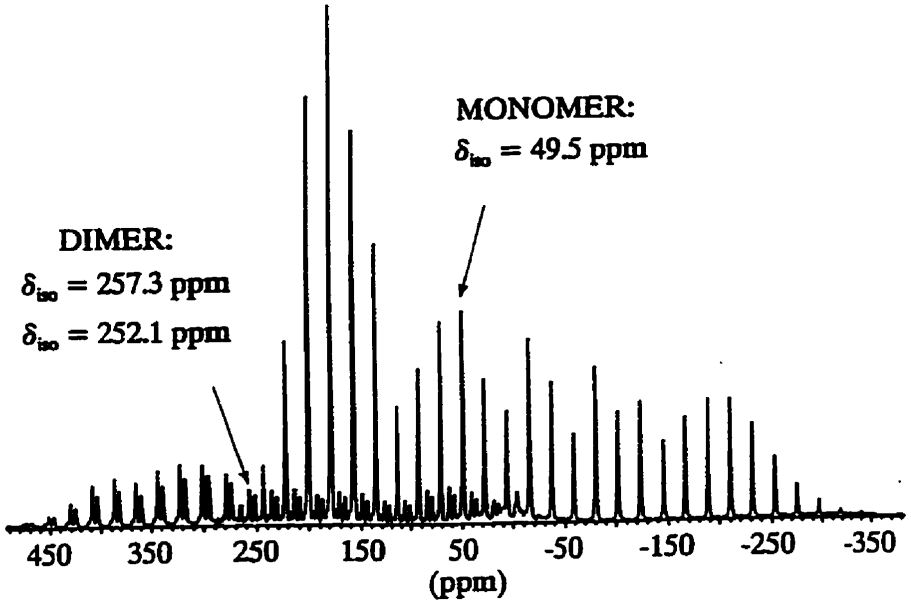


**Figure 6.8.** Solid-state $^{31}P$ CP/MAS NMR spectrum of the crystallization mixture of **6.3** and **6.4**.

Solid-state $^{31}P$ CP/MAS NMR spectra of the crystallization mixture of **6.3** and **6.4** display three distinct signals (see Figure 6.8). The most intense signal has an isotropic chemical shift of 49.7 ppm and a span of 504 ppm and is assigned to **6.3**. The observation of a single solution chemical shift of 50.1 ppm indicates that the structure of **6.3** is very similar in the solution and solid state. This is in stark contrast to Mes*N=P-I, which has $^{31}P$ chemical shifts of 218 ppm and 100 ppm in the solution and solid state, respectively.

The two other manifolds of spinning sidebands (*ca.* 0.8:1 integrated intensity) in the $^{31}P$ CP/MAS spectrum of the monomer/dimer mixture (see Figure 6.8) arise from a pair of magnetically non-equivalent phosphorus nuclei with isotropic chemical shifts of 257.3 and 252.1 ppm and are assigned to the dimer, **6.4**. Each site has a span of *ca.* 470 ppm. The isotropic solid-state chemical shift of **6.4** is similar to solution $^{31}P$ NMR chemical shifts recently reported for analogous diazadiphosphetidines, $[(t\text{-Bu})(Me_3Si\text{-HC})C\text{-N=P-Cl}]_2$, ($\delta(^{31}P)$ = 268.2 ppm),[212] $[Fmes\text{-N=P-Cl}]_2$ (Fmes = 2,4,6-tris(trifluoromethyl)-phenyl), (*cis*- and *trans*-isomers, $\delta(^{31}P)$ = 214.3 and 293.3 ppm, respectively),[135] and other *trans*-diazadiphosphetidines.[213] Within the unit cell, the phosphorus nuclei of each dimer unit are related by a centre of inversion, and should therefore be both crystallographically and magnetically equivalent; thus, under conditions of MAS one would expect to observe a single resonance.[214] The appearance of two separate $^{31}P$ NMR signals is surprising, but can be attributed to the twinning of the crystals of **6.4** (*vide supra*). There are two slightly different unit cells which give rise to nuclei which are in non-identical electronic environments (i.e. the nuclei are crystallographically inequivalent). Since chemical shielding is a property which is very sensitive to the

surrounding electronic environment, two separate signals are observed in the solid-state $^{31}P$ MAS NMR spectra. There is no indication of splitting due to $^{2}J_{P\text{-}P}$ coupling in the solid-state $^{31}P$ NMR spectra, which is consistent with the presence of a centrosymmetric [2+2] cycloaddition dimer and incompatible with any other dimeric forms.[165m]

Gauge-Including Atomic Orbital (GIAO)[215] calculations were performed on an IBM RS6000/580 workstation at the RHF/6-311G* and DFT(BL3YP)/6-311G* levels of theory using the Gaussian94 suite of programs.[73] Single point *ab initio* calculations were performed on the models PhN=P-OTf and $[PhN{=}P\text{-}OTf]_2$ using the geometries obtained from X-ray crystallography, since the optimized structure of PhN=P-OTf is substantially different from the X-ray structure observed in the solid state.[188] The $^{t}$butyl groups were replaced with hydrogen atoms placed along the C(aryl)-C($^{t}$Bu) axis. R.W. Schurko converted the absolute $^{31}P$ chemical shielding values to the $^{31}P$ chemical shift scale ($\delta(^{31}P$, 85% $H_3PO_4) = 0$ ppm) by subtracting the absolute shielding values from $\delta(^{31}P$, 85% $H_3PO_4) = 328.35$ ppm.[216]

For iminophosphines containing 3p(P(III))-2p(N) π-bonds, the chemical shielding at the phosphorus nucleus is largely influenced by the $n \rightarrow \pi^*$ transition energy, $E(n \rightarrow \pi^*)$, which is dramatically affected by changing the substituents at the phosphorus or nitrogen centers.[206,207,208] If the double-bond system is perturbed in such a manner that there is an increase in $E(n \rightarrow \pi^*)$, then the paramagnetic contribution to chemical shielding decreases, and the shielding at the phosphorus nucleus increases. The effects of a number of different

substituents at the phosphorus and nitrogen atoms on the phosphorous chemical shift have been catalogued and discussed in several publications.[116,165m,207,208,217]

The $^{31}P$ isotropic chemical shift of **6.3** (49.7 ppm) is the most shielded isotropic chemical shift reported for an iminophosphine. Iminophosphine derivatives with linear Mes*NP moieties tend to have very shielded chemical shifts ([Mes*N≡P][$AlCl_4$], $\delta_{iso}(^{31}P)$ = 77 ppm and Mes*N=P-I, $\delta_{iso}(^{31}P)$ = 100 ppm) relative to systems with a bent geometry at the nitrogen atom.[206,207] In the case of [Mes*N≡P][$AlCl_4$], the most shielded component of the CS tensor is found to lie approximately along the direction of the P-N internuclear vector (i.e., $\beta_{NMR} = 0$). [Mes*N≡P][OTf] **6.3**, [Mes*N≡P][$AlCl_4$] and Mes*N=P-I have approximate cylindrical symmetry ($C_{\infty v}$) about the $C_{ipso}$-N-P fragment (i.e. $C_{ipso}$-N-P bond angles are ca. 180°) in the solid-state. In molecules with $C_{\infty v}$ symmetry, there is no paramagnetic contribution to shielding when the symmetry axis is parallel to the direction of the magnetic field, and a maximum paramagnetic contribution when the symmetry axis is perpendicular to the magnetic field direction,[218] accounting for the highly shielded values of $\delta_{33}$ in [Mes*N≡P] derivatives. For **6.3**, $\delta_{33}$ is not exactly along the P-N bond ($\beta_{NMR} = 21°$) because of the presence of substituents (i.e., the Mes* and triflate groups) which do not conform with $C_{\infty v}$ symmetry.[207] $^{31}P$ NMR spectra of stationary samples of formally double-bonded P-N systems consistently display a negative skew (i.e. $\kappa = 3(\delta_{22} - \delta_{iso})/\Omega$ = negative),[207] whereas the formally triply-bonded systems

have a high positive skew, with the CS tensor having axial or near-axial symmetry.[206,207] The positive value of the skew in **6.3**, $\kappa = +0.94$, is in accordance with this trend, since there is an almost linear P-N bond. The skew indicates that the CS tensor is nearly axially symmetric, which would be expected due to the high local symmetry at the phosphorus nucleus.

## 6.6 Interpretation of Observations - Steric Inhibition of Le Chatelier's Principle ?

Monomer-dimer equilibria are observed in solution, in the liquid phase or in the gas phase for many types of inorganic systems, with the minimal thermodynamic difference between monomer and dimer species responsible for the observation of both species. For example, radical species such as NO and $NO_2$ associate *via* relatively weak N-N (and O-O) bonds.[13] The strong alkene multiple bond is destabilized with respect to two carbene monomers with the introduction of aza-[48,49] or amino-substituents,[50] and the varying steric bulk of substituents is seen to tune the relative stability of alkene analogues such as distannenes and digermenes with respect to carbene analogues.[14,219] In each of these cases, the relative thermodynamic stabilities of the monomer and dimer are sufficiently different such that only one structural isomer is isolated under a specific set of conditions, as predicted by Le Chatelier's principle.

$$\mathbf{A}_{\text{solution}} \rightleftharpoons \mathbf{B}_{\text{solution}} \xrightarrow[\text{Recrystallization}]{} \mathbf{B}_{\text{solid}}$$

**Figure 6.9.** The equilibrium of **A** and **B** is forced to the right by the recrystallization of **B** (diminishing the concentration of **B** in solution).

Le Chatelier's principle, a tenet of chemistry, states: "when a system in chemical equilibrium is disturbed by a change of temperature, pressure, or a concentration, the system shifts in equilibrium composition in a way that tends to counteract this change of variable."[220] In practical terms, the principle asserts that as the concentration of one component in an equilibrium is reduced the system adjusts so as to maintain the equilibrium. In the case of recrystallization, Le Chatelier's principle usually provides for the isolation of a single product (see Figure 6.9). As the least soluble component **B** begins to crystallize at its saturation concentration (reducing the concentration of **B** in solution thus making $Q < K_{eq}$), the system shifts to the right to maintain the equilibrium which results in the concomitant reduction in the concentration of **A**. Because **B** is constantly being removed from the system, the concentration of **A** is continually being reduced until it is completely removed from the reaction mixture, and only **B** is isolated. Although Le Chatelier's principle is generally applicable, the results of this chapter demonstrate that the chemical behaviour it predicts will only be observed if the kinetics of the equilibrium reaction allow for equilibration on the timescale of the reaction or recrystallization.

A summary of the experimental observations is mandated before discussion of the conclusions drawn. Only **6.3** is observed in solution and both **6.3** and **6.4** are formed by recrystallization from hexane. Relatively rapid recrystallization results in the formation of **6.3** whereas slower recrystallization results in the isolation of increasing amounts of **6.4**. Preliminary experiments indicate that the presence of quinuclidine in a dichloromethane solution of **6.3** results in the isolation of crystalline **6.4** exclusively.[221] The analogous system with the slightly smaller Dip substituent yields only dimeric structures for both **6.6** and **6.7** in solution as well as the solid-state. In addition, quantum chemical calculations show that the arrangement of atoms in **6.3** (two moles; Ph instead of Mes*) is 43.4 kJ/mol (HF/6-311G*) or 15.8 kJ/mol (B3LYP/6-311G*) less stable than in **6.4** ( Ph instead of

Mes*) in the gas phase at 0 K.

The observation of two (or more) crystal forms for a particular compound is certainly not unprecedented (*vide supra*), however the isolation of crystals of both monomeric and dimeric forms from one recrystallization is rare. Generally, each crystalline form is obtained under a different set of reaction conditions. The most relevant example of another system in which both monomeric and dimeric structures have been obtained from the same reaction conditions is that of $Fmes_2Sn$ and its "dimer".[139,222] In this example, there are no significant differences in the structural parameters of the monomer and the monomeric unit in the "dimer" structure (which is in stark contrast to the structures of typical distannenes). The observations suggest that the "dimeric" arrangement is imposed by crystal packing forces. Conversely, the dimerization of **6.3** results in drastic changes in the structure and bonding (*vide supra*) and results in a molecular structure which is comparable to those of other diphosphetidines.

The observation of only **6.3** in solution upon the dissolution of a mixture of **6.3** and **6.4** clearly indicates that the monomer is thermodynamically favoured in solution. This is expected on the basis of the increased entropy (which is explicitly neglected in the 0K *ab initio* calculations) of two monomers versus a single dimer molecule. Solvation by donor solvents is expected to increase the stability of the monomer as is dissolution in polar solvents; however, only **6.3** is observed in essentially non-polar hexane. The isolation of any **6.4** in the crystalline state implies that this form is more stable than is crystalline **6.3**, as the solution is composed of exclusively **6.3**. The conclusion that crystalline **6.4** is more stable is in accord with the theoretical calculations of the molecules although such calculations only model the molecules and neglect all intermolecular solid-state interactions. In addition, the exclusive isolation of phosphetidines **6.6**, **6.7** and **6.9** with the slightly less bulky Dip substituent demonstrates the energetic preference of the fully σ-bonded

phosphetidine arrangement — behaviour which is definitively demonstrated for P-N compounds with less bulky substituents.

The rate of recrystallization influences the relative amounts of monomer and dimer. Overnight removal of hexane results in the almost complete formation of **6.3** whereas prolonged (one week) recrystallization at nearly constant volume (similar to recrystallization using a Soxhlet apparatus) produces nearly pure crystals of **6.4**. Niecke's exclusive recrystallization of **6.3** at -30°C from hexane and the other observations above are consistent with the postulate that **6.3** is the kinetically preferred crystalline form whereas **6.4** is the thermodynamically favoured crystal.

These results suggest the presence of an equilibrium between **6.3** and **6.4** in solution that favours **6.3** although small amounts of **6.4** must be present in solution to allow for the formation of **6.4** crystals. A large activation energy between **6.3** and **6.4** is expected due to the bulk of the Mes* substituent which acts as a kinetic shield and because of the change in the angle at the nitrogen atom that is required in the transition state structure involves distorting a conjugated π-system. A significant activation barrier explains the observed behaviour of the reaction between quinuclidine and **6.3** to form **6.4** exclusively. The addition of σ-donor bases to Mes*N=P-OTf results in σ-complexes of the phosphorus atom, which exhibit a significant decrease in the $C_{ipso}$-N-P angle and a slight lengthening of the N-P and N-C bonds; the compounds adopt a more typical iminophosphine geometry. This complexation presumably reduces the dimerization activation barrier as it eliminates the energy requirement for angle deformation and the resultant bond lengthening reduces the steric strain in the transition state. As such quinuclidine acts as a catalyst (although not necessarily in minute concentrations) for the recrystallization of **6.4**.

The apparent inhibition of Le Chatelier's principle is the observation of both types

of crystals from the same reaction mixture. We propose that the behaviour observed is caused by the steric bulk of the Mes* substituent. The relative energies of the monomeric and dimeric components and the energy of the activation barrier between **6.3** and **6.4** is dependent on the size of the substituent. Ligands smaller than Mes* thermodynamically favour diazadiphosphetidines whereas larger groups are predicted to thermodynamically favour the monomeric iminophosphine. The Mes* ligand gives a system in which both constituents are of very similar energy with the monomer favoured in solution and the dimer favoured in the solid-state. The large activation barrier prevents rapid interconversion of **6.3** and **6.4** *on the timescale of the recrystallization* and does not allow for the exclusive formation of either type of crystal as would be expected on the basis of Le Chatelier's principle. Other factors such as concentration and solubility are also likely to influence the equilibrium, however we believe that the timescale of the reaction is the most significant factor.

## 6.7 Conclusions

Monomeric and dimeric forms of Mes*N=P-OTf have been synthesized and isolated in crystalline form. X-ray crystal structures reveal solid-state structures which are consistent with the other characterization data.

The dimerization of Mes*N=P-OTf is an example of a system in which the kinetic and thermodynamic influences of bulky subsituents are exposed. It is a case where the relative thermodynamic stabilities of two structural alternatives are very similar and, as such, represents a key example in the spectrum of dimerization reactions controlled by relative steric bulk. On one end of this spectrum (systems with small substituents) steric interactions are relatively unimportant so the thermodynamic stabilities of the compounds are controlled by relative $\sigma$- and $\pi$-bond energies — dimers are favoured and kinetic

stabilization is required for the isolation of multiply-bonded compounds. On the other end of the spectrum (systems with very bulky groups) the differences in bond energies are insignificant compared to the energetic consequences of steric strain thus the thermodynamic stabilities are controlled by the steric demands of the ligands —monomers are favoured and kinetic stabilization is redundant. The dimerization reported above sits in the middle of this spectrum and thus provides unprecedented information about the kinetic and thermodynamic effects of bulky groups.

# Chapter 7. The Nascent Chemistry of the [Mes*N=As] Moiety

## 7.1 Introduction

### 7.1.1 Diazonium Cations

The diazonium cation **7.1** is a synthetically useful organic functional group that has an extensive chemistry and has been studied since the middle of the 19th century. [223,224] Diazonium cations are isoelectronic with nitriles and consist of a nitrogen-nitrogen triple bond with a monocoordinate terminal nitrogen atom and a dicoordinate nitrogen center having a formal positive charge. *Ab initio* calculations on diazonium cations reveal that the electronic structure of the cations is not accurately represented by the conventional Lewis structure - the positive charge is predominantly found on the terminal nitrogen atom and on the carbon atom bonded to the diazonium group thus the most accurate representation of the electronic structure of [ArN≡N] is that of a higly polarized N≡N molecule coordinated to a phenyl cation.[225]

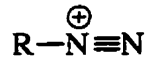

**7.1**

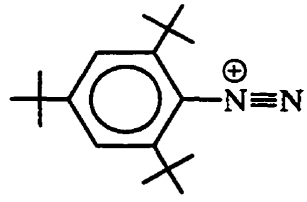

**7.2**

Diazonium cations are generally synthesized in the presence of HCl which yields the chloride salts; such salts are generally explosive. The chloride anion can be exchanged for another anion *via* metathesis reactions with salts such as $NaBF_4$ yielding more stable salts. [226,227]

Diazonium cations are linear with a C-N-N angle between 169.9° and 180° with the vast majority closer to 180°.[228] The nitrogen-nitrogen bond lengths fall within the range 1.083(3) Å to 1.11(5) Å[227] which is on the order of the nitrogen-nitrogen bond length in $N_2$ of 1.09768(5) Å, thus diazonium cations are usually considered to have a nitrogen-nitrogen triple bond. Dinitrogen is one of the most stable leaving groups and isotopic labelling experiments with one $^{14}N$ and one $^{15}N$ have shown that the monocoordinate nitrogen (α) and the dicoordinate nitrogen (ß) exchange positions at ambient temperature.[229] The proposed mechanism shown in Figure 7.1 is modeled by high level *ab initio* calculations and involves the formation of a phenyl cation followed by the subsequent recapture of the nitrogen molecule before the species are separated by solvent.[225] The potential for the loss of $N_2$ is a unique feature of diazonium cations in comparison with heavier diazonium analogues and results in important differences in the chemistry and the potential danger of these species (*vide infra*).

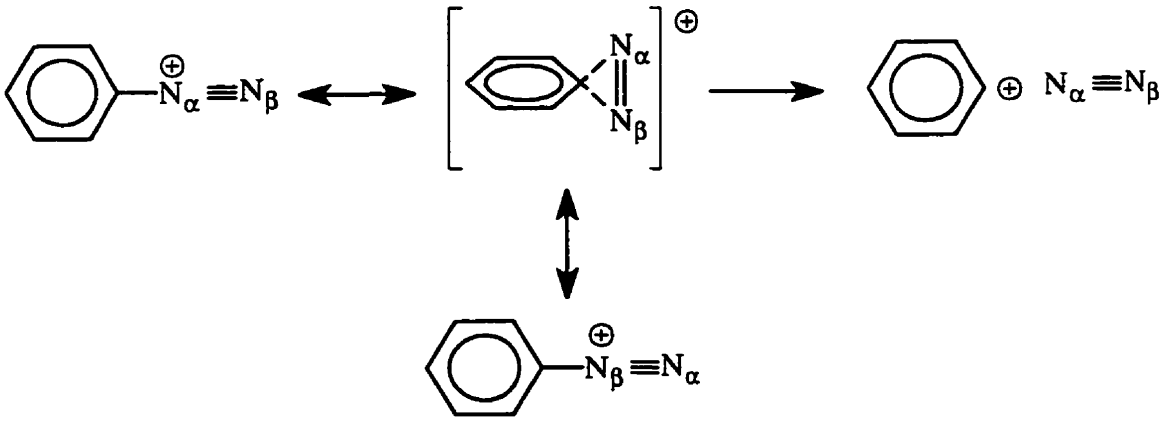


**Figure 7.1.** Mechanism for N atom exchange in [PhN≡N].

The synthesis of the supermesityldiazonium cation [Mes*N≡N] **7.2** (analogous to the compounds in this thesis) cannot be effected by the standard methods and is accomplished either by the reaction of $NO^{\bullet}$ with $Mes^*NH_2$[230] or by the decomposition of Mes*N=N-O-C(O)R.[231] This cation is unstable and readily ejects a molecule of $N_2$ to form a reactive aryl cation which rapidly abstracts a hydrogen atom from the ortho-$^t$Bu group.

Diazonium cations generally react as electrophiles through the terminal nitrogen and the major classes of reactions involving diazonium cations that are relevant to this thesis are summarized in Figure 7.2. More extensive discussions of diazonium chemistry can be found in several books [224,226,232] and review articles.[233]

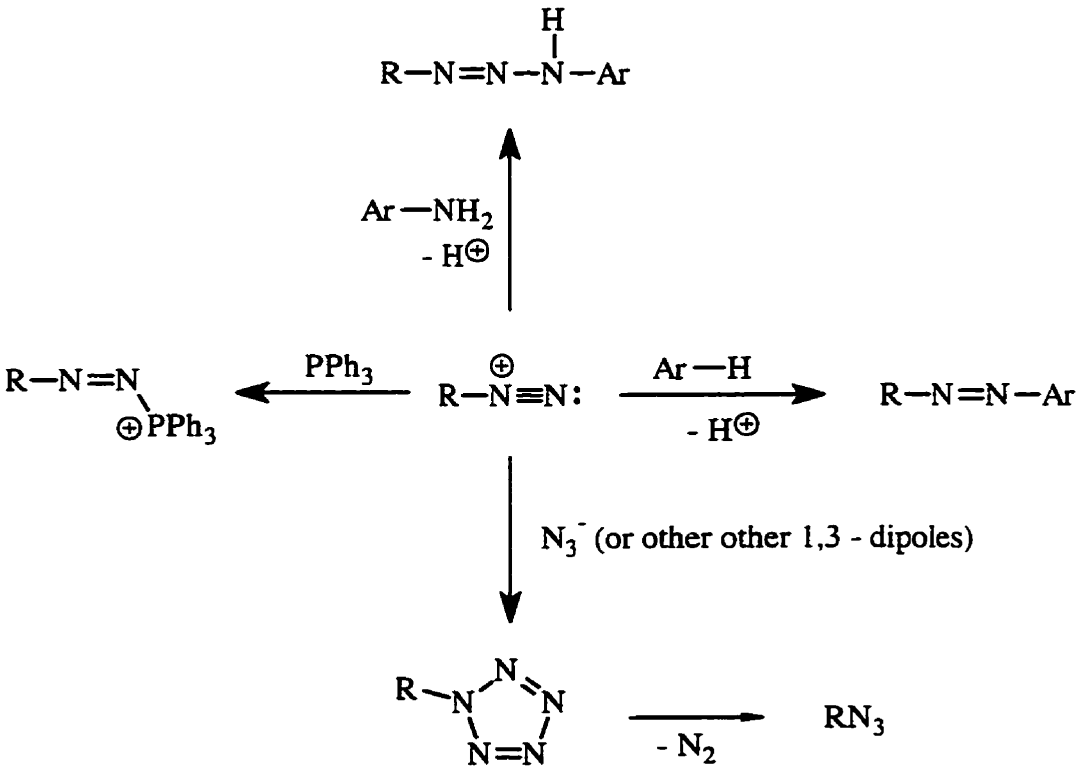


**Figure 7.2.** Diazonium cation reactivity.

### 7.1.2 Phosphazonium Cation and Phosphaalkynes

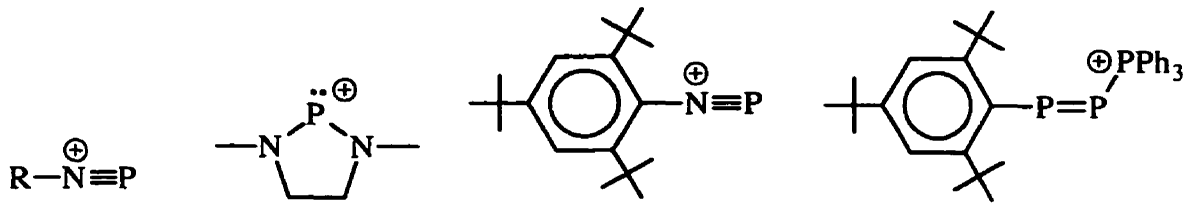

7.3 7.4 7.5 7.6

Phosphazonium cations (iminophosphenium cations) **7.3** are isovalent with diazonium cations and contain a terminal phophorus atom. Phosphazonium cations with terminal nitrogen and dicoordinate phosphorus have not been reported, thus the exchange of mono- and di-coordinate pnictogens observed in diazonium cations does not occur for the heavier analogues. This observation may be understood in terms of bond energies, in which a C-N bond is energetically favoured over a C-P bond, thus the observed compounds [RN≡P] are thermodynamically more favourable than the alternative [RP≡N] isomer. *Ab initio* calculations allow for quantification of this observation and predict that for R = Me [RN≡P] is 253 kJ/mol lower in energy than [RP≡N].[234] The large difference in the stability of the isomers is rationalized by the difference in their ability to adopt the stabilizing (+)(-)(+) charge distribution: P is much more electropositive than N and thus the most stable structure is that with a terminal P atom. The loss of $P{\equiv}N_{(g)}$ is not as favoured (For R = Me, [RN≡P] is 241 kJ/mol more stable towards this loss than is [RN≡N]) thus phosphazonium cations do not exhibit the explosive nature of their lighter analogues and [RN≡P] is also calculated to be stable with respect to the loss of cyclic $(P{=}N)_3$ by 374 kJ/mol.[234] Phosphazonium cations have only been isolated with the Mes*

ligand although the cation [MeN≡P] has been observed in mass spectra of the phosphenium cation **7.4 (2.7)**.

Phosphazonium cation **7.5** is prepared as $[MCl_4]$ (M = Al or Ga) or [OTf] salts *via* halide ion abstraction from the versatile iminophosphine Mes*N=P-Cl [235] using reagents such as $Al_2Cl_6$, $GaCl_3$, and AgOTf. The gallate ($[GaCl_4]$) and digallate ($[Ga_2Cl_7]$) salts only crystallize in the presence of arenes, and it has been shown that the arene is, in fact, π-coordinated to the phosphorus center and is not only a solvent of recrystallization.[236] The N-P bond length is dependent on the arene and counter ion, and is observed to be in the range of 1.463-1.529 Å[237]. The P-N bond is typically considered a triple bond because of its linearity, bond length (the spectroscopically determined bond length for $P{\equiv}N_{(g)}$ is 1.491 Å[238] and that of cationic $[PN]_{(g)}$ is 1.57 Å[239]), the conclusions of *ab initio* calculations and $^{31}P$ NMR data (Chapter 6). The $^{31}P$ NMR chemical shift of the phosphazonium cation is dependent on whether it is in solution or the solid state, the counter anion present and, if applicable, the arene to which it is coordinated; the range of observed chemical shifts is δ 50 - 95 ppm.[237] Vibrational spectra (IR and Raman) of phosphazonium cations and other compounds containing the Mes*N≡P moiety reveal that the N-P stretch is typically between 1420 -1530 $cm^{-1}$ and that there is a qualitative correlation between the bond angle, the vibrational frequency and the intensity of the band; — the frequency and intensity increase as the angle approaches 180°.[205] We have also postulated that the presence of significant $^5J_{P\text{-}H}$ coupling is an indication of a linear $C_{ipso}$-N-P unit of [Mes*N≡P] species in solution. The $^5J_{P\text{-}H}$ coupling can only arise if the phosphorus atom

is in the plane of the arene ring as the coupling is transmitted *via* the aromatic π-system. Such a conclusion is consistent with the results of previous calculations on isoelectronic Ar-C≡P systems.[240] In the case of the Mes* substituent, the ortho-$^t$Bu groups prevent geometries with a significantly non-linear C-N-P moiety from being coplanar with the aromatic ring (typically the $C_{ipso}$-N-P plane is perpendicular to that of the ring) and thus coupling is not observed in such systems. The chemistry of the phosphazonium cation is summarized in Figure 7.3.[241]

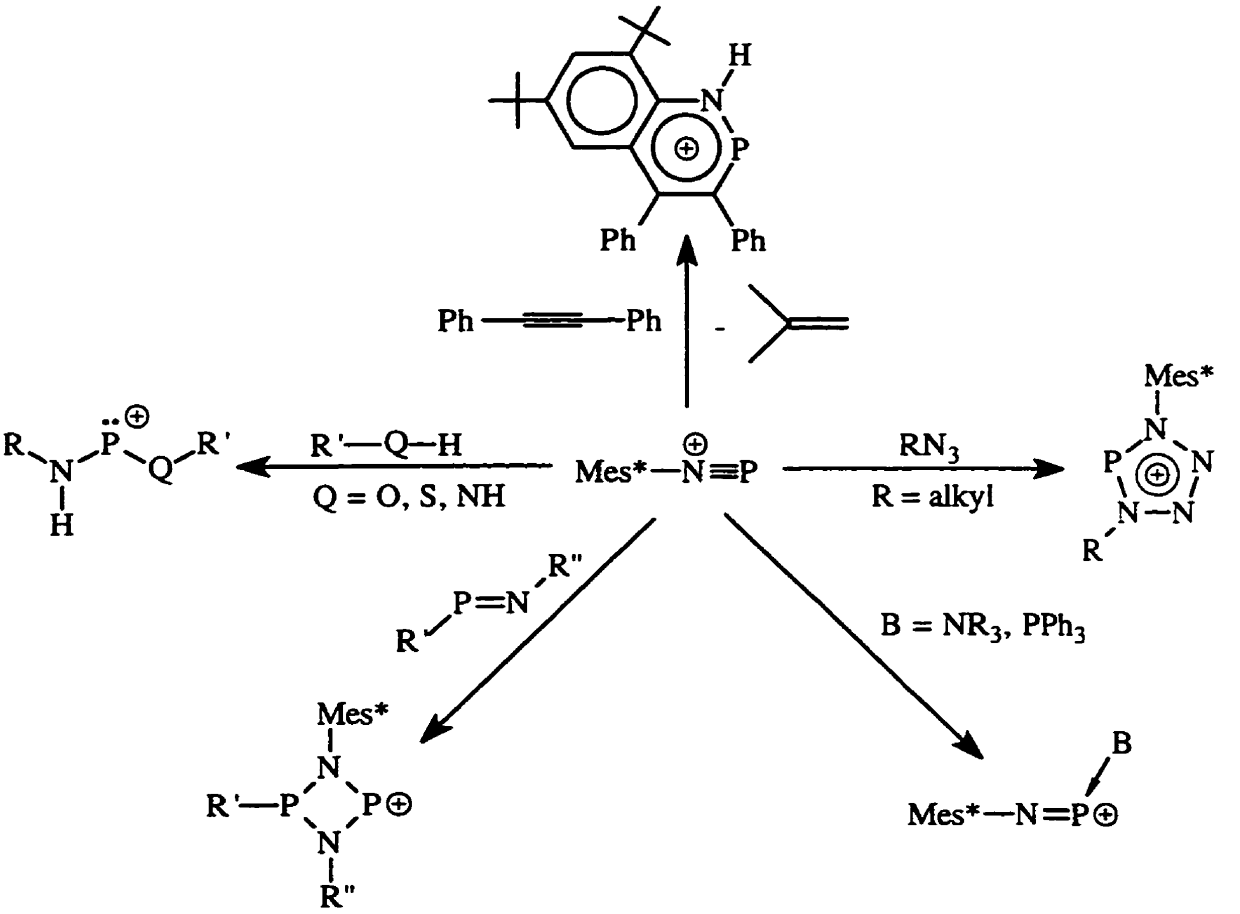


**Figure 7.3.** [Mes*N≡P] Chemistry.

Diphosphazonium cation, **7.6**, (phosphanetriylphosphonium cation) has been reported,[242] but the diphosphazonium moiety is not linear with the C(1)-P(1)-P(2) angle of 98.8° and in fact has a *trans* geometry about the P(1)-P(2) double bond (2.025 Å) and the P(1)-P(2)-P(3) angle is 96.78°. A cation proposed to contain the [R-P≡P] moiety is [$^{i}Pr_2$NP≡P] which has only been observed in mass spectra.[243] *Ab initio* calculations confirm that [R-P≡P] is significantly less stable than [R-N≡P] because of the reduction in the dipole moment of the P≡P moiety and concomitant loss of the stabilizing (+)(-)(+) charge distribution.[234]

## Phosphaalkynes

R—C≡P:

**7.7**

Phosphaalkynes, **7.7**, are the direct analogues of nitriles and alkynes, and they are the most extensively studied of all the low-coordinate phosphorus compounds yet prepared.[102] $^{31}$P NMR chemical shifts for the variety of observed phosphaalkynes are extremely shielded for the same reason (linear $C_{ipso}$-C-P fragment) as are those of [Mes*N≡P] cations (*vide supra*) and fall in the range of 34.4 to -69.2 ppm relative to 85% $H_3PO_4$. The chemistry of phosphaalkynes is extensive and well documented in several review articles[244] and books.[102,243]

### 7.1.3 Heavier Isovalent Analogues

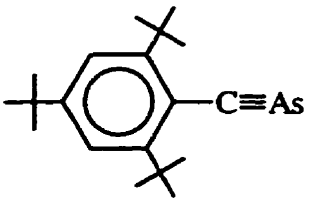


**7.8**

A monomeric arsaalkyne Mes*C≡As **7.8** analogous to phosphaalkynes has also been isolated through the use of the Mes* substituent.[245] The compound was prepared by the reaction depicted in Figure 7.4, and the driving force is the elimination of TMS-O-TMS.

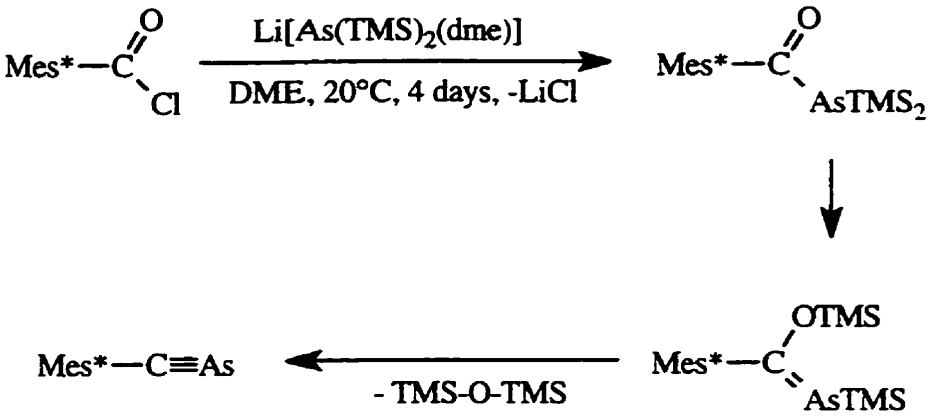


**Figure 7.4.** Mechanism for the synthesis of Mes*C≡As.

Attempts to make arsaalkynes with smaller substituents result in the formation of oligomers such as the arsacubane $(^{t}BuCAs)_4$.[246] "Free" arsaalkynes without sterically demanding substituents can only be studied in the gas phase.[247] Calculations for RC≡Pn (Pn = N, P,

As, Sb) **7.9** predict that these species are stable (in the gas phase) and that the heavier homologues (Pn = As, Sb) will react in a similar fashion to the corresponding phosphaalkyne.[240,248]

### 7.1.4 Mass Spectrometric Identification of [Mes*N≡Pn]

Electron ionization mass spectrometry (EIMS) studies of the aminoiminopnictines (**7.10** (**5.2a**) (Pn = P) and (**5.2b**) (Pn = As)) and trisaminopnictines (**7.11** (**5.1c**) (Pn = Sb) and (**5.1c**) (Pn = Bi)) (Chapter 5) by means of a collaboration with G.B. Yhard have resulted in the observation of the series of [Mes*N≡Pn] cations (E = P, As, Sb) as prominent ions in the 70 eV spectra.

The stibazonium (m/z 380, 12% and m/z 382, 8%) and bismazonium (m/z 468, 35%) cations have not been reported previously and thus represent the first examples of such species. The formation of these cations can be rationalized as shown in Figure 7.5. It is also noteworthy that both pnictogenium cations [Mes*NHPnNHMes*] **7.12** are also observed in the spectra.

The phosphazonium (m/z 290, 100%) and the arsenoazonium (m/z 334, 100%) cations are the base peaks in their respective spectra and are thus the most stable on the timescale of the experiment (*ca.* 10 microseconds). The formation of these cations can be rationalized as shown in Figure 7.5. All of the observed cations were identified unambiguously through the use of MS/MS and accurate mass determination. The only arsenoazonium cation previously observed in mass spectra was [MeN≡As], reported by this research group in 1994.[249]

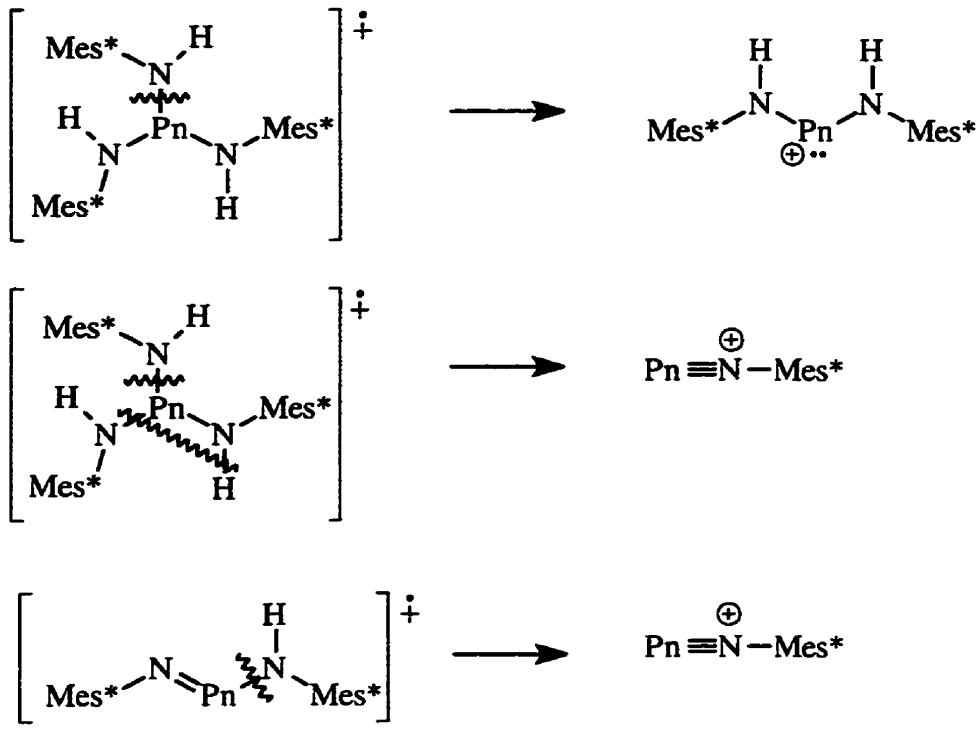

**Figure 7.5.** Mechanism for the formation of cations by EIMS.

The observation of these diazonium cation analogues as relatively stable species and the isolation of isoelectronic Mes*C≡As (although it is neutral and therefore less reactive) suggested that compounds of the type [Mes*N≡Pn] should be synthetically accessible, as should be the ideal precursors to such compounds Mes*N=Pn-Cl, thus we undertook the synthesis of these compounds. Two synthetic methods were studied in the synthesis of Mes*N=As-Cl which are summarized in Figures 7.6 and 7.7.

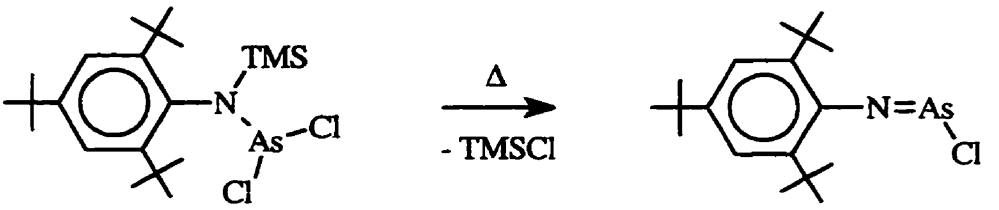


**Figure 7.6.** Synthesis of Mes*N=As-Cl from Mes*N(TMS)$AsCl_2$.

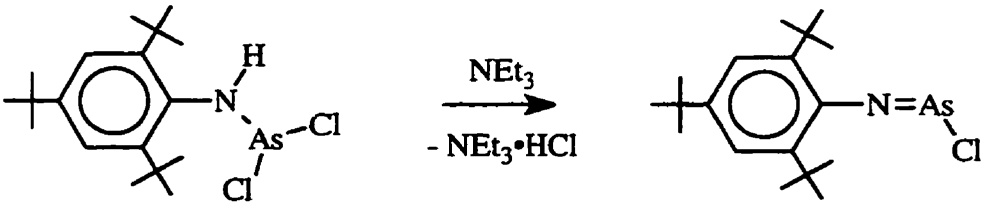


**Figure 7.7.** Synthesis of Mes*N=As-Cl from Mes*N(H)$AsCl_2$.

## 7.2 Synthesis of Potential Iminoarsine Precursors

### 7.2.1 Mes*N(TMS)$PnCl_2$ (Pn = P, As, Sb)

Reaction of a pale yellow ethereal solution of Mes*N(TMS)Li with $PCl_3$ (Figure 7.8) results in the formation of orange crystals characterized as Mes*N(TMS)$PCl_2$ **7.13** by multinuclear NMR, vibrational spectroscopy and X-ray crystallography.

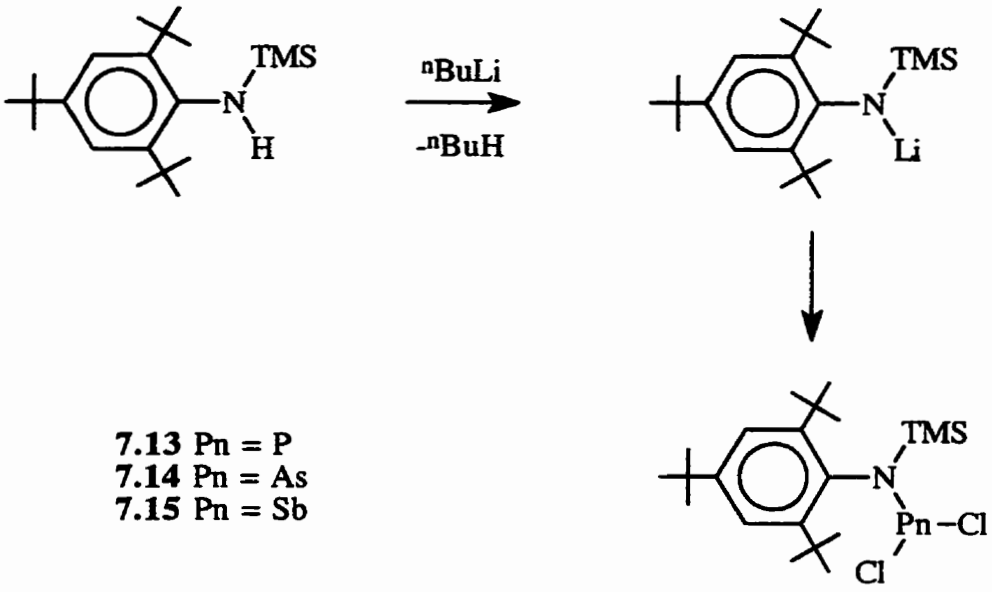


**7.13** Pn = P
**7.14** Pn = As
**7.15** Pn = Sb

**Figure 7.8.** Synthesis of Mes*N(TMS)$PnCl_2$.

The molecular structure of **7.13** is shown in Figure 7.9 and pertinent structural parameters are listed in Table 7.1. The bond lengths and angles are unexceptional, however the nitrogen center exhibits a planar geometry (sum of angles 360°) which is enforced by the steric demands of the *ortho*-$^t$butyl groups of the Mes* substituent. The plane defined by P-N-Si sits perpendicular (90.7°) to that of the Mes* group for the same reason.

**Table 7.1.** Selected bond lengths (Å) and angles (°) for Mes*N(L)$PnCl_2$ compounds **7.13** (Pn = P, L = TMS), **7.14** (Pn = As, L=TMS) and **7.17** (Pn = As, L=H).

| | **7.13** | **7.14** | **7.17** |
|---|---|---|---|
| Pn-Cl(1) | 2.08(1) | 2.208(2) | 2.231(3) |
| Pn-Cl(2) | 2.12(1) | 2.239(2) | 2.171(3) |
| Pn-N | 1.68(2) | 1.809(4) | 1.789(6) |
| N-C(1) | 1.55(3) | 1.491(6) | 1.423(9) |
| N-Si | 1.80(2) | 1.797(4) | |
| Cl(1)-Pn-Cl(2) | 91.6(5) | 91.09(7) | 94.0(1) |
| Cl(1)-Pn-N | 100.6(8) | 101.2(1) | 108.0(2) |
| Cl(2)-Pn-N | 108.4(8) | 107.2(1) | 96.1(2) |
| Pn-N-C(1) | 114(1) | 113.6(3) | 119.8(5) |
| Pn-N-Si | 130(1) | 127.7(2) | |
| Ar-N-Pn-Si (torsion) | 90.70 | 92.18 | |

Similarly, the reaction of Mes*N(TMS)Li with $AsCl_3$ in ether results in the formation of pale yellow crystals Mes*N(TMS)$AsCl_2$ **7.14**. These crystals can be obtained either by recrystallization from ether or hexane or by sublimation under dynamic vacuum. Proton and $^{13}C$ NMR spectra confirmed the presence of the Mes*N(TMS) unit in the product and vibrational spectra indicated the presence of the $AsCl_2$ moiety (*vide infra*). Crystallographic analysis of the compound confirmed the formulation determined spectroscopically and the molecular structure is shown in Figure 7.10 with pertinent structural parameters listed in Table 7.1. The structure of **7.14** is isomorphous to that of the phosphorus analogue and, similarly, the bond lengths and angles are typical. The geometry about the nitrogen atom is planar (sum of angles 359.9°) and the As-N-Si plane makes an angle of 92.18° with that of the aryl ring of the Mes* substituent.

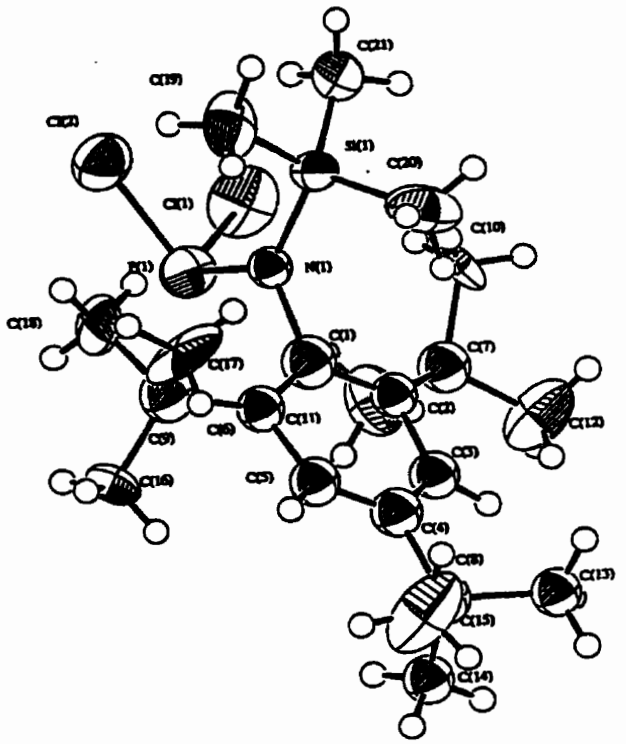

**Figure 7.9.** Molecular structure of Mes*N(TMS)$PCl_2$.

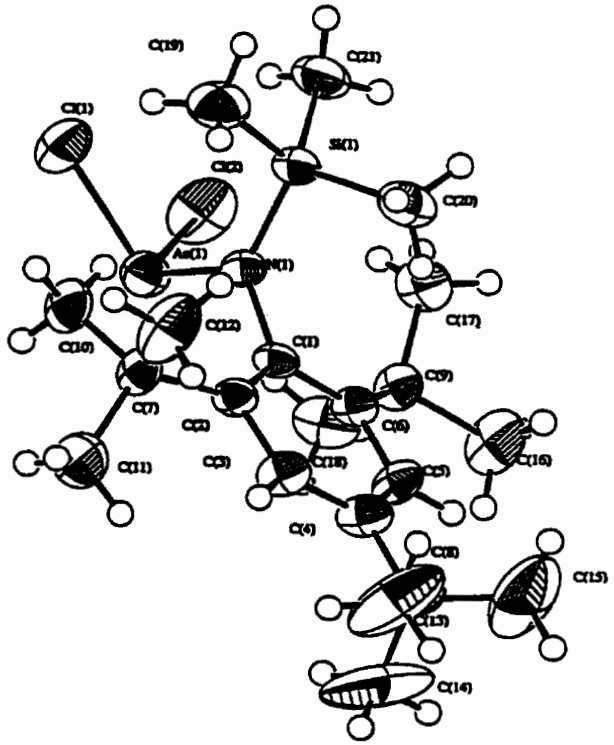

**Figure 7.10.** Molecular structure of Mes*N(TMS)$AsCl_2$.

The analogous reaction of Mes*N(TMS)Li with $SbCl_3$ in ether results in the formation of a peach coloured solid upon removal of solvent. Attempted recrystallization was unsuccessful and resulted in the isolation of a mixture of Mes*N(TMS)$SbCl_2$ **7.15** and, surprisingly, crystals characterized as Mes*$NH_2$•$SbCl_3$ **7.16**. The proton NMR spectrum of the mixture reveals that Mes*N(TMS)$SbCl_2$ is the major component of the mixture (overall intensity *ca.* 70%) while Mes*$NH_2$•$SbCl_3$ accounts for the other signals observed. Although the vibrational spectra of both compounds are very similar, there are significant differences between the spectra of each. In contrast to the IR spectrum of **7.15** (*vide infra*), the spectrum of **7.16** shows one very broad Sb-Cl stretching band at 300-340 $cm^{-1}$ and is missing the very strong band at 865 $cm^{-1}$ (stretching in the TMS group). The spectrum also contains N-H stretching bands at 3516 and 3443 $cm^{-1}$. Similarly the Raman spectrum of **7.16** exhibits a broad peak centered at 340 $cm^{-1}$ (Sb-Cl stretches) and a weak band at 3459 $cm^{-1}$ from the N-H vibration.

The IR spectra of **7.13**, **7.14** and **7.15** are similar, most notable is an intense broad band at *ca.* 800-900 $cm^{-1}$ caused by the TMS group stretching, and allow for the identification of the Pn-Cl stretching (P-Cl, 378 and 320 $cm^{-1}$; As-Cl, 364 and 321 $cm^{-1}$; Sb-Cl, 339 and 314 $cm^{-1}$). The Raman spectra shown in Figure 7.11 likewise allow for such a comparison and the assigned vibrational frequencies are: P-Cl, 376 and 325 $cm^{-1}$; As-Cl, 362 and 322 $cm^{-1}$; Sb-Cl, 338 and 313 $cm^{-1}$.

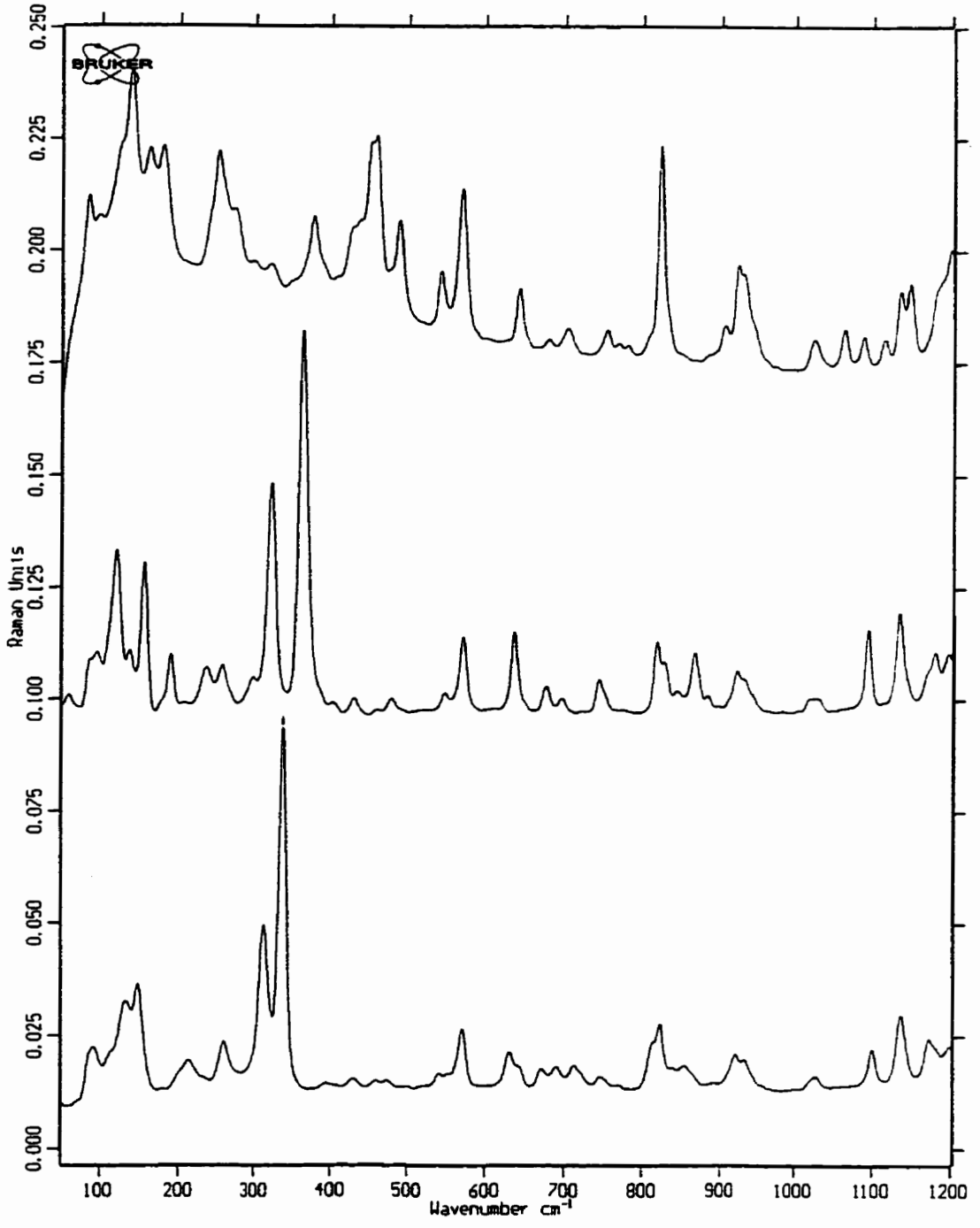


**Figure 7.11.** Raman spectra of **7.13** (Top), **7.14** (Middle) and **7.15** (Bottom).

### 7.2.2 Mes*N(H)AsCl$_2$

Reaction of Mes*N(H)Li with AsCl$_3$ in ether results in the formation of a peach coloured solution which yields a peach coloured solid characterized as Mes*NHAsCl$_2$ **7.17**. The vibrational spectra confirm the presence of the AsCl$_2$ (bands at 361 and 332 cm$^{-1}$) and N-H (3406 cm$^{-1}$)moieties and the $^1$H NMR spectrum exhibits peaks assigned to the Mes*NH fragment (singlets at δ 1.30 (9H, p-$^t$Bu), 1.51 (18H, o-$^t$Bu), 5.85 (H, broad, N-H), 7.38 (2H, Ar-H) ppm). The molecular structure of **7.17** is shown in Figure 7.12 and selected structural parameters are listed in Table 7.1.

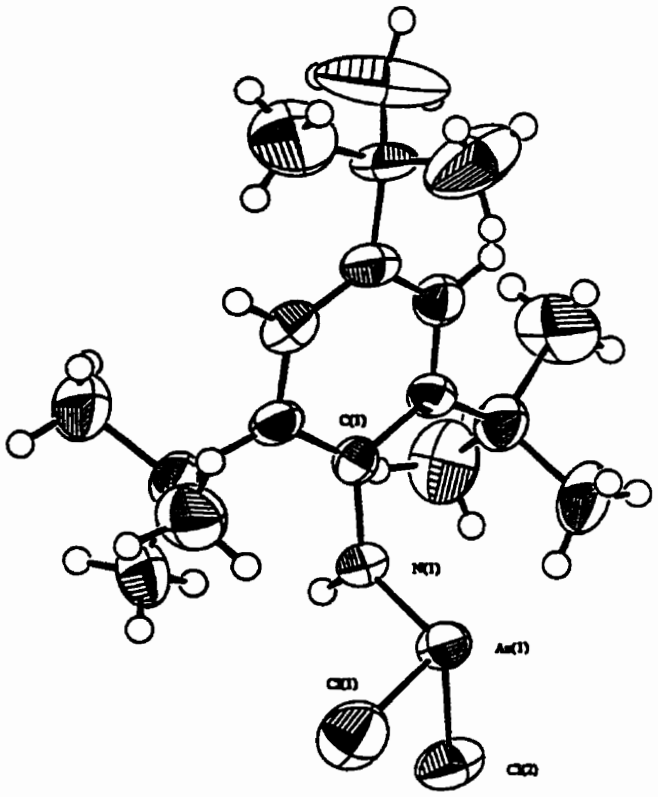

**Figure 7.12.** Molecular structure of Mes*N(H)AsCl$_2$.

## 7.3 Mes*N=As-Cl

The synthesis of Mes*N=P-Cl **7.18** by the thermal elimination of TMS-Cl from $Mes^*N(TMS)PCl_2$[250] was performed to determine if the proposed reaction scheme (Figure 7. 8) would be effective for the synthesis of the unknown compounds Mes*N=Pn-Cl (Pn = As, Sb). Thermolysis of orange $Mes^*N(TMS)PCl_2$ *in vacuo* (static) resulted in the formation of a dark red solid with a $^{31}P$ NMR chemical shift of δ 137 ppm (*ca.* 65%, Mes*N=P-Cl) as well as decomposition products at δ 153 ppm (<5%) and δ 221 ppm (*ca.* 35%).

Thermolysis of solid $Mes^*N(TMS)AsCl_2$ at 130°C *in vacuo* (static) results only in the sublimation of the pale yellow starting material (confirmed by $^1H$ and $^{13}C$ NMR spectra); however, thermolysis at 190°C in a sealed tube under a nitrogen atmosphere results in the formation of a dark red/brown solid, the Raman spectrum of which shows only one As-Cl stretch at 302 $cm^{-1}$ and the proton and $^{13}C$ NMR spectra show loss of the TMS substituent and indicate formation of **7.19** in greater than 90% yield (by integration of the $^1H$ NMR spectrum).

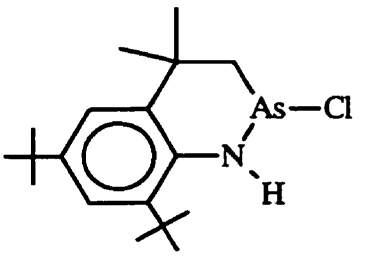


**7.19**

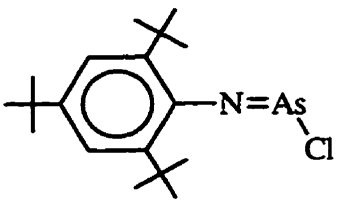


**7.20**

Heterocycle **7.19** is the cyclo-decomposition product of Mes*N=As-Cl **7.20** and its formation is discussed in more detail below. Likewise, the thermolysis of

$Mes^*N(TMS)AsCl_2$ in THF-$D_8$ solution at 126°C shows the formation of TMS-Cl (δ 0.41 ppm) and the steady formation of cyclo-decomposition product **7.19**. The decomposition product observed is indicative of the formation of Mes*N=As-Cl and suggests that the thermal elimination of TMS-Cl is not the ideal method to be used in the isolation of the iminoarsine.

Reaction of $Mes^*NHAsCl_2$ with triethylamine in toluene results in the precipitation of colourless solid ($NEt_3$•HCl) and the formation of a red wine coloured solution. The reaction mixture $^1H$ NMR spectrum is consistent with the loss of the proton on the nitrogen atom and formation of Mes*N=As-Cl. Heating of such a mixture during filtration results in the formation of significant amounts of cyclo-decomposition product **7.19** in accord with the formation of chloroiminoarsine **7.20**. Filtration and slow removal of solvent results in the formation of yellow crystals which were analyzed by X-ray crystallography to confirm the structure of heterocycle **7.19**. The molecular structure is depicted in Figure 7.13 and selected structural parameters are listed in Table 7.2, however the structural features of **7.19** are not unusual. The hydrogen atom on the nitrogen atom was located in a difference Fourier map by Dr. T. S. Cameron. Although a crystallographic analysis of **7.20** has not yet been possible, the structure of **7.19** confirms the formation of **7.20** by the methods used.

**Table 7.2.** Selected bond lengths (Å) and angles (°) for heterocycle **7.19**.

| | | | |
|---|---|---|---|
| As-Cl | 2.274(2) | Cl-As-N | 104.1(2) |
| As-N | 1.814(4) | Cl-As-C(18) | 94.6(2) |
| As-C(18) | 1.943(6) | N-As-C(18) | 95.7(2) |
| N-C(1) | 1.421(6) | As-N-C(1) | 125.1(4) |
| N-H | 1.02 | As-N-H | 108.3 |
| As-C(18)-C(9) | 114.6(4) | C(1)-N-H | 114.1 |

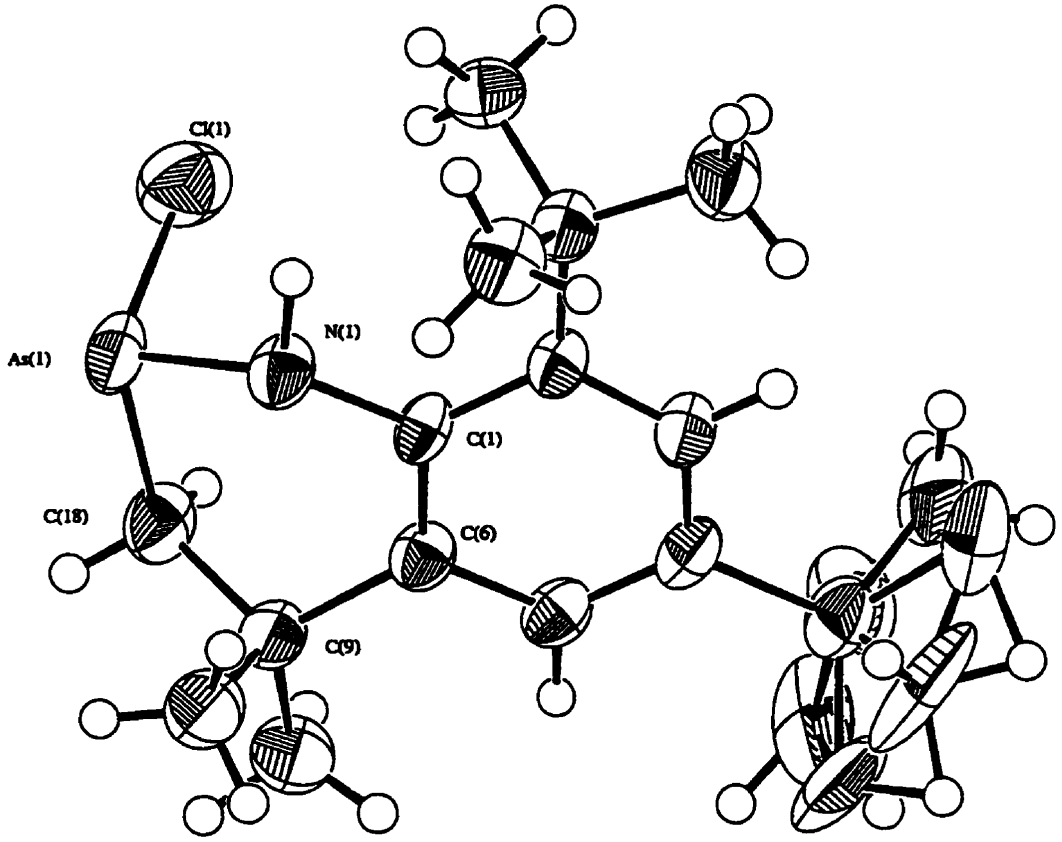


**Figure 7.13.** Molecular structure of heterocycle **7.19**.

The analogous reaction of $Mes^*NHAsCl_2$ with pyridine in toluene results in the formation of a peach coloured reaction mixture and addition of $NEt_3$ results in the precipitation of colourless triethylammonium chloride. The mixture is characterized as a mixture of Mes*N=As-Cl **7.20**, heterocycle **7.19** and Mes*N=As-Cl•pyr **7.21**, which is analogous to Mes*N=P-Cl•pyr[251]

Reaction of $Mes^*NHAsCl_2$ with $NEt_3$ in the presence of $PPh_3$ results in the instantaneous formation of a red wine coloured mixture and the precipitation of colourless triethylammonium chloride. The product is characterized as Mes*N=As-Cl•$PPh_3$ **7.22** by $^1H$ and $^{31}P$ NMR spectroscopy. The persistence of the red colour (Mes*N=As-Cl) is rationalized by analogy to the $PPh_3$ adduct of Mes*N=P-OTf which is found to dissociate in solution.

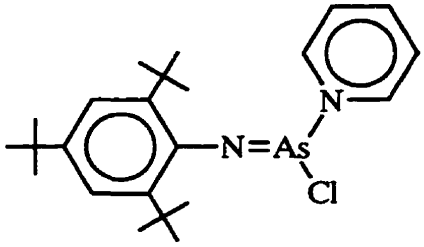


**7.21**

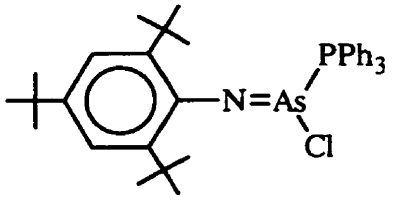


**7.22**

## 7.4 Synthetic Utility of $Mes^*N(TMS)AsCl_2$

Reaction of $Mes^*N(TMS)AsCl_2$ with LiOAr (Ar = 2,6-di-$^t$butyl-4-methylphenyl) in ether or toluene (Figure 7.14) results in the formation of a pale pink solution and the precipitation of LiCl. Slow removal of solvent after filtration results in the isolation of

colourless crystals characterized as Mes*N(TMS)As(Cl)OAr **7.23** (and a minute amount of Mes*N=As-OAr **7.24** is indicated by the pink colour). Reaction of **7.23** with TMS-OTf[252] gives dark purple **7.24** *via* the elimination of TMS-Cl as demonstrated by $^{1}H$ NMR spectroscopy.

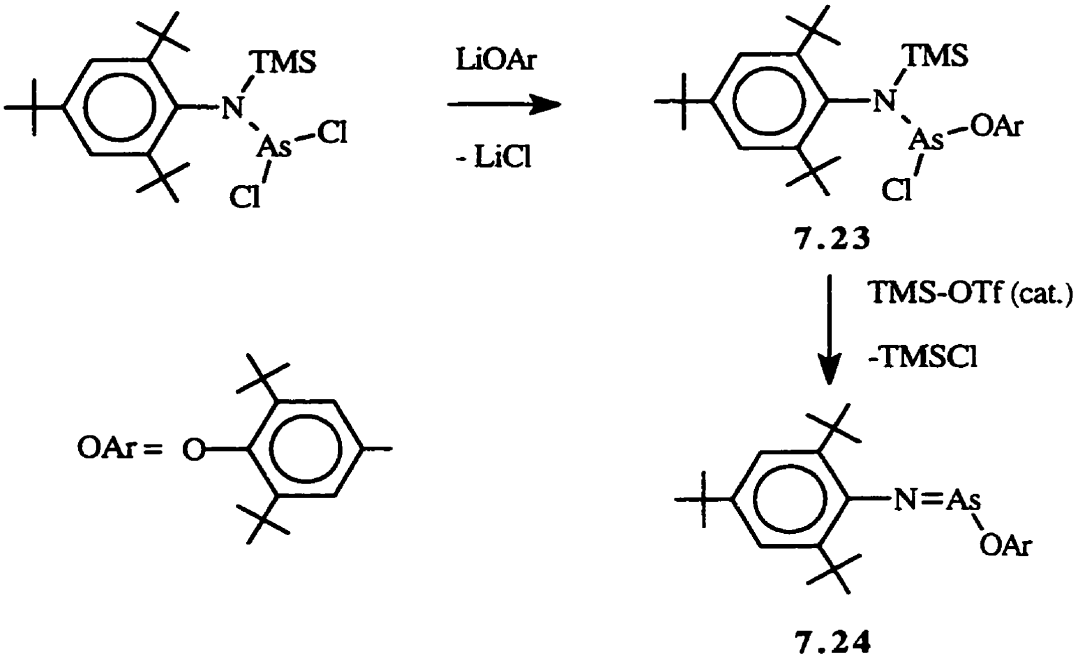


**Figure 7.14.** Synthesis of Mes*N=As-OAr.

The metathesis reaction of silver triflate and Mes*N(TMS)$AsCl_2$ in hexane in the dark affords a yellow reaction mixture. The $^{19}F$ NMR spectrum reveals a single peak at δ -78 ppm indicative of the triflate unit and the $^{1}H$ NMR spectrum of this mixture in $CD_2Cl_2$ after removal of volatiles *in vacuo* shows complete loss of the TMS fragment and formation of Mes*N=As-OTf **7.25** (*ca.* 80% of the total integration) . The other *ca.* 20% of the signal intensity is found in the peaks attributable to the cyclo-decomposition product of

**7.25**, cyclic arsenium triflate **7.26** and a very small amount of **7.27** (*vide infra*). Slow removal of solvent results in the formation of yellow (major product) and small orange crystals; the proton NMR of this mixture of crystals reveals that the ratio of **7.25** to **7.26** changes to *ca.* 1:10 thus the yellow crystals are the heterocyclic compound.

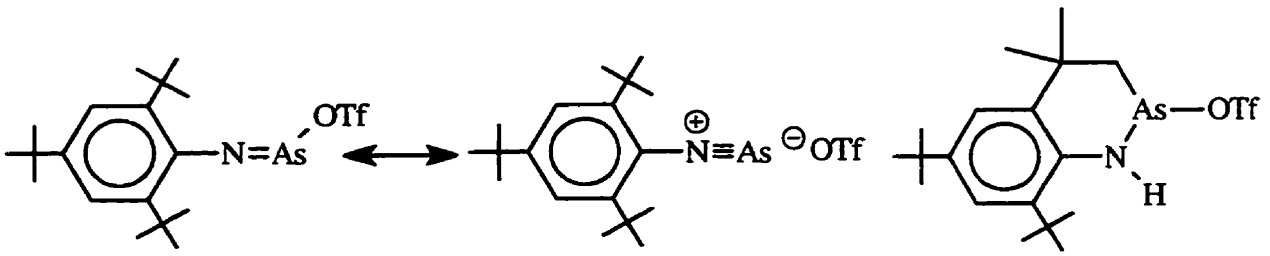


**7.25** **7.26**

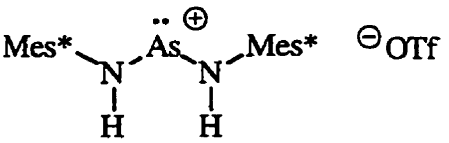


**7.27**

It is of note that **7.26** represents the first reported arsenium cation containing a carbon bonded to the divalent arsenic center, however a structural characterization of the compound is required before conclusions about its structure and bonding are drawn. Cyclo-decomposition reactions of the type shown in Figure 7.15 are not uncommon in Mes* substituted subvalent species and reaction with the ortho-$^{t}$Bu groups has been observed in systems such as [Mes*P≡C],[253] [Mes*AsO],[254] [Mes*P(H)PMes*][255] and [Mes*N≡P][$GaCl_4$].[256]

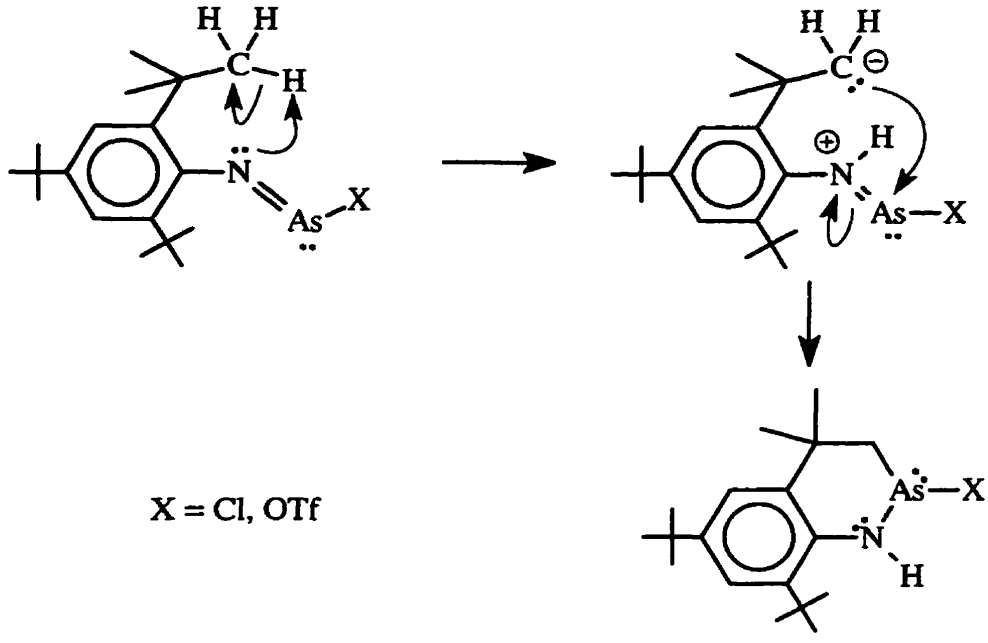


**Figure 7.15.** Cyclo-decomposition reaction for **7.20** and **7.25**.

Reaction of silver triflate and Mes*N(TMS)$AsCl_2$ in diethyl ether gives a yellow/orange solution. After the removal of volatiles *in vacuo* $^1H$, $^{13}C$ and $^{19}F$ NMR spectra were obtained in $CD_2Cl_2$ which confirm the formation of Mes*N=As-OTf **7.25** and show the presence of one equivalent of diethylether. The observation of one equivalent of ether and **7.25** after the removal of volatiles suggests the formation of a 1:1 adduct of the form Mes*N=As-OTf•$OEt_2$ (or diethyl ether may be a solvent of recrystallization).

The AgOTf metathesis reactions in both hexane and toluene also result in the formation of an unexpected and remarkable compound derived from Mes*N=As-OTf. When the reaction is performed in toluene the only crystalline product obtained is characterized as arsenium cation [Mes*NHAsNHMes*][OTf] **7.27**. Proton NMR identifies this product unambiguously with singlet signals at δ 1.33 (18H, p-$^t$Bu), 1.56

(36H, o-$^t$Bu), 7.52 (4H, Ar-H), and 8.50 (broad, 2H, N-H) ppm and the structural assignment is confirmed by the results of X-ray crystallographic analysis. The molecular structure of **7.27** is depicted in Figure 7.16 and selected structural parameters are listed in Table 7.3.

**Table 7.3.** Selected bond lengths (Å) and angles (°) for [Mes*N(H)AsN(H)Mes*][OTf] **7.27**.

| | |
|---|---|
| As-N(1) | 1.765(7) |
| As-N(2) | 1.768(7) |
| N(1)-C(1) | 1.47(1) |
| N(2)-C(19) | 1.46(1) |
| S-O(1) | 1.42(1) |
| S-O(2) | 1.47(2) |
| S-O(3) | 1.45(2) |
| N(1)-As-N(2) | 99.2(3) |
| As-N(1)-C(1) | 121.6(6) |
| As-N(2)-C(19) | 122.7(6) |

Consistent with the structural comparison of the phosphorus analogues, the structure of the cationic fragment is almost identical to that of Lappert's Mes*N=AsNHMes* **7.28 (5.2b)** [147](see Chapter 5); the As-N bonds (1.765(7)Å and 1.768(7)Å) are short compared to typical As-N bonds of 1.82-1.88Å (Chapter 2) and the N-As-N angle is 99.2(3)° in remarkably good agreement with the calculated structural parameters for [$H_2NAsNH_2$] (As-N: 1.724Å, N-As-N: 101.35°) (see Chapter 2) despite the replacement of the bulky Mes* group with a hydrogen atom. The formation of [Mes*NHAsNHMes*][OTf] is surprising in that there are no hydrogen atoms bonded to the nitrogen atoms in the starting materials.

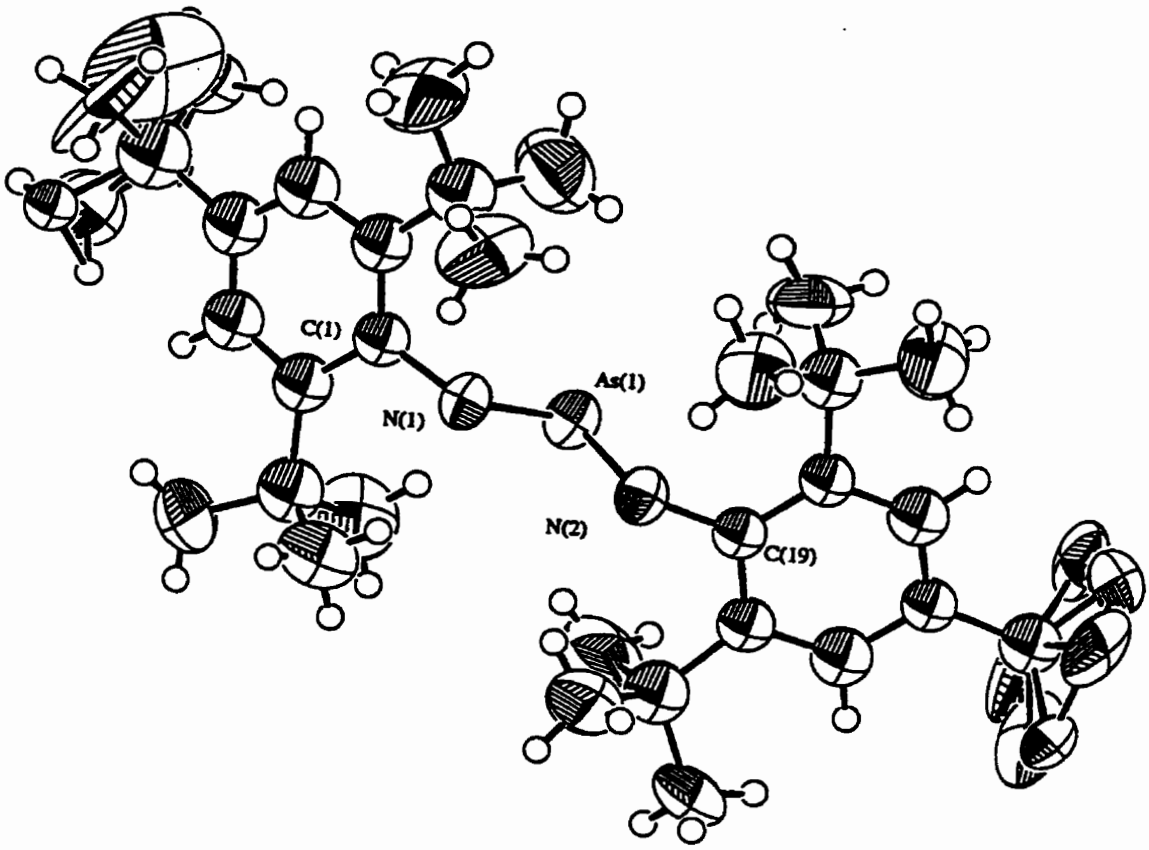


**Figure 7.16.** Molecular structure of [Mes*N(H)AsN(H)Mes*][OTf].

*In situ* formation of Mes*$NH_2$ would result in the formation of **7.27** *via* reaction with Mes*N=As-OTf accompanied by a 1,3-hydrogen shift as observed in the analogous reaction of Mes*N=P-OTf with Mes*$NH_2$. This mechanism suggests that [Mes*NHAsNHMes*][OTf] will be formed when Mes*N(TMS)$AsCl_2$ is reacted with AgOTf in the presence of Mes*$NH_2$. The rational synthesis of **7.27** has been accomplished by the protonation of **7.28** with triflic acid. [Mes*NHAsNHMes*][OTf] is the first isolated example of an acyclic arsenium salt and, as such, represents an important development in our understanding of the chemistry of sub-valent arsenic compounds.

*Ab initio* calculations (UMP2/6-311G*//HF/6-311G*) on the species [HN≡As], [N≡AsH], and the Me-H addition product [$H_2$N–As-Me] reveal that [HN≡As] is 337 kJ/mol more stable than the As-H isomer (which is not a minimum on the $C_{\infty v}$ energy hypersurface). In addition, the calculations show that the reaction of [HN≡As] with methane to form [$H_2$N–As-Me] is exothermic by 110 kJ/mol in agreement with the observation of the cyclodecomposition products. The energies of these products and selected structural parameters are listed in Table 7.4.

**Table 7.4.** *Ab initio* calculation results for pnictazonium cations, isomerization reactions and methane addition reactions. Energies are in hartrees unless otherwise specified and selected structural parameters (bond lengths (Å), bond angles (°)) are given.

| Compounds | HF energy | ZPVE | UMP2 energy | N imag |
|---|---|---|---|---|
| HNP | -395.4802466 | 0.0160990 | -395.7561557 | 0 |
| NPH | -395.3041028 | 0.0092970 | -395.6155941 | 0 |
| $H_2NPMe$ ($C_1$) | -435.7388477 | 0.0693800 | -436.1503258 | 0 |
| $H_2NPMe$ ($C_2$) | -435.7388603 | 0.0692790 | -436.1504968 | 1 |
| HNAs | -2288.8776193 | 0.0148200 | -2289.1597786 | 0 |
| NAsH | -2288.6979939 | 0.0082230 | -2289.0255507 | 2 |
| $H_2NAsMe$ ($C_2$) | -2329.1473248 | 0.0678890 | -2329.5559587 | 0 |
| methane | -40.2026372 | 0.0473090 | -40.3492510 | 0 |
| Isomerizations | E(MP2) + 0.9*ZPVE | | | |
| HNP → NPH | 352.97 kJ/mol | | | |
| HNAs → NAsH | 336.82 kJ/mol | | | |
| Reactions | | | | |
| HNP + $CH_4$ → $H_2NPMe$ ($C_1$) | | -103.82 kJ/mol | | |
| HNAs + $CH_4$ → $H_2NAsMe$ ($C_2$) | | -109.60 kJ/mol | | |
| Structural parameters | | | | |
| HNP | N-P: 1.4284 | H-N: 0.9986 | | |
| HPN | N-P: 1.4415 | H-P: 1.408 | | |
| $H_2NPMe$ ($C_1$) | N-P: 1.5871 | P-C: 1.8057 | N-P-C: 103.37 | |
| $H_2NPMe$ ($C_2$) | N-P: 1.5881 | P-C: 1.8048 | N-P-C: 103.63 | |
| HNAs | N-As: 1.549 | H-N: 0.9996 | | |
| HAsN | N-As: 1.5533 | H-As: 1.4964 | | |
| $H_2NAsMe$ ($C_2$) | N-As: 1.549 | As-C: 0.9996 | N-As-C: 99.61 | |
| methane | C-H: 1.083 | | | |

The chemistry of the N=As fragment is now ripe for examination. The two

compounds containing N=As bonds that were synthesized previously (Mes*N=AsN(H)Mes* and FmesN=AsFmes) did not allow for the systematic development of the chemistry of multiple bonded arsenic-nitrogen species. The syntheses of Mes*N(TMS)$AsCl_2$ **7.14**, Mes*N=As-Cl **7.19** and Mes*N=As-OAr **7.24** provide three synthetically useful reagents that allow for the synthesis of almost any compound containing the [Mes*N=As] moiety. Reaction of **7.14** or **7.19** with lithiated (LiGrp) or Grignard reagents (BrMgGrp) will result in the formation of Mes*N(TMS)As(Cl)Grp **7.29** and Mes*N=As-Grp **7.30**, respectively as depicted in Figure 7.17.

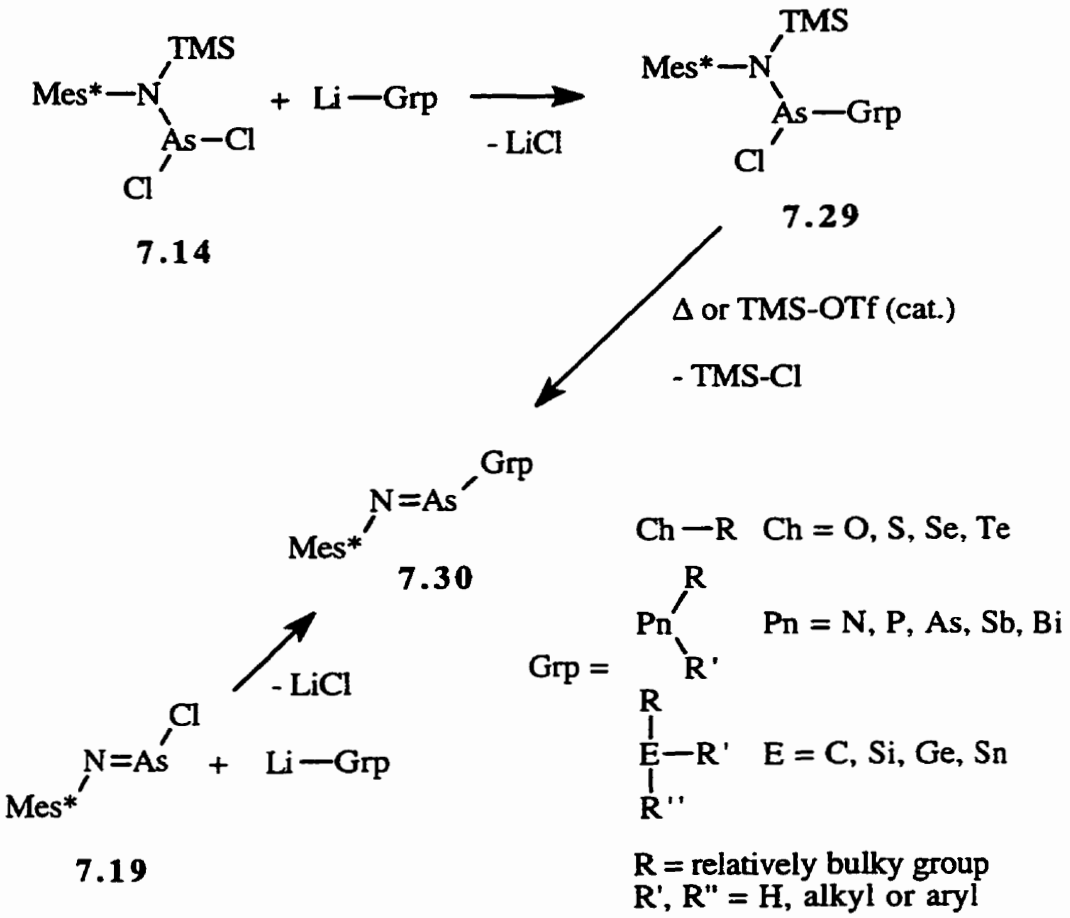


**Figure 7.17.** Potential reactivity of Mes*N(TMS)$AsCl_2$ and Mes*N=As-Cl.

Thermal or catalytic elimination of TMS-Cl from **7.29** will also result in **7.30**. Similarly, reaction of **7.24** with bases that are stronger than Li-O-Ar will result in the elimination of Li-O-Ar and the subsequent formation of new [Mes*N=As] compounds as shown in Figure 7.18.

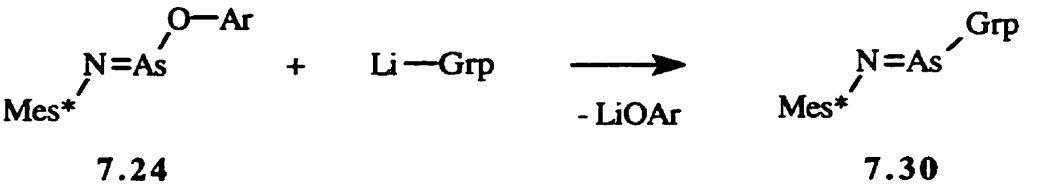


**7.24** **7.30**

**Figure 7.18.** Potential reactivity of Mes*N=As-OAr (Grp as defined in Figure 7.17 without Ch-R congeners).

## 7.5 Conclusions

$Mes^*N(TMS)AsCl_2$ is an excellent precursor to N=As bonds through lithiation or metathesis reactions because the reaction of the reaction products with TMS-OTf results in the elimination of TMSCl. This observation is significant in that it suggests that the isolation of the much more reactive Mes*N=As-Cl molecule is not necessary as the starting material to access a multitude of multiply bonded systems. Likewise the isolation of the first phenoxyiminoarsine Mes*N=As-OAr provides another useful starting material for similar syntheses as the OAr unit should be easily displaced by stronger nucleophiles such as $LiNR_2$ or LiR. It is also apparent that the cation [Mes*N≡As] is very reactive and must be made in presence of coordinating reagents to allow for convenient isolation.

Furthermore, the decomposition/reaction products isolated in preparations of Mes*N=As-OTf represent novel bonding environments for arsenium cations including the first alkyl substituted arsenium cationic unit ($CH_2$-As-NH) in **7.26** and the first acyclic

arsenium cation [Mes*NHAsNHMes*][OTf] **7.27**.

Together the results of this study double the number of known iminoarsines, provide several synthetic routes to new iminoarsines, provide evidence for the formation of the first As-N triple bond and expand the number and bonding environments of arsenium cations. This represents a very significant development in the chemistry of subvalent pnictogen compounds.

Future work on this project should include the crystallographic characterization of the synthesized iminoarsines and the formation of new iminoarsines by the methods described above. The chemistry of these species should be examined thoroughly and compared to and contrasted with the extensive and interesting chemistry of the [Mes*N=P] fragment. Studies of cycloaddition reactivity, coordination chemistry (as a donor and/or acceptor), [1,3] hydride shift reactivity, and ligand exchange reactions should all be undertaken. The observed structures, bonding and reactivity of products should be rationalized through the use of high level *ab initio* calculations. In addition, the electronic (UV-vis) spectra of these compounds should be examined as the compounds synthesized to date all have very intense and distinctive colours. Such spectroscopic studies, in combination with other characterization data, may lead to a better understanding of the similarities and differences of the π-bonding of [Mes*N=P] and [Mes*N=As] containing molecules.

Furthermore, the synthetic methods used to make [Mes*N=As] compounds should also be used with Mes*N(TMS)$SbCl_2$ to make compounds containing the [Mes*N=Sb] fragment. Isolation of such compounds would be particularly valuable because the potential for oxidation of the antimony atom (which is not to be expected for As or Bi) allows for the exploration of multiple bonding of Sb(V). Compounds such as those depicted in Figure 7.19 are unknown and, as such, represent exciting synthetic targets.

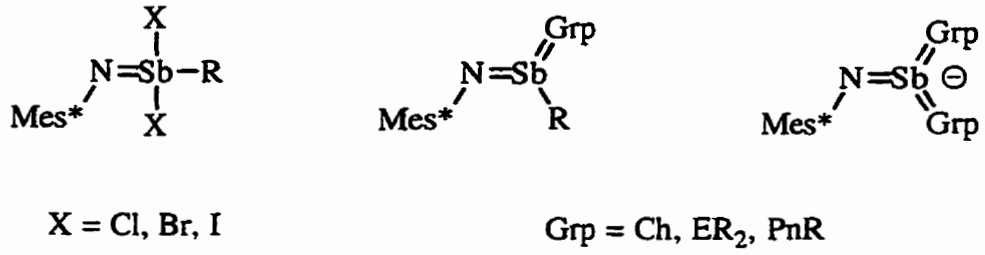


**Figure 7.19.** Synthetic targets containing Sb(V).

# Chapter 8. Experimental Procedures

## 8.1 The Handling of Air Sensitive Reagents

Unless otherwise indicated, all reactions were performed using methods developed for use with reagents that are air or moisture sensitive. The basic vessels and techniques most commonly employed in our laboratory are described in the literature;[257,258] however, a more detailed description of recrystallization techniques is given in this chapter. Drawings of the compounds described in this chapter are listed on the next pages for the reader's benefit.

**Caution:** All of the materials described in this thesis are potentially toxic or carcinogenic and due care should be taken when working with these chemicals. Vacuum reactors and tubes sealed under vacuum may implode if they are damaged or not handled properly.

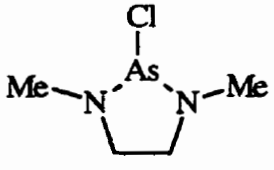


**2.5Cl**

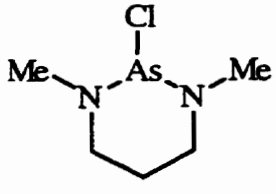


**2.6Cl**

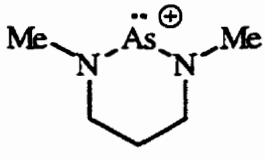


**2.6**

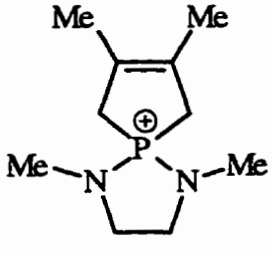


**3.1BD**

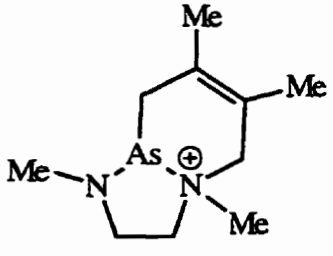


**3.2BD**

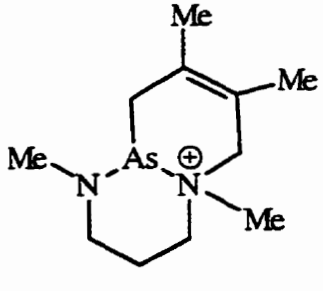


**3.3BD**

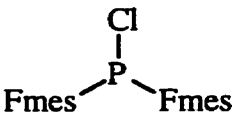


**4.23**

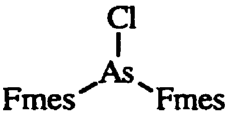


**4.24**

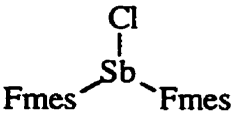


**4.25**

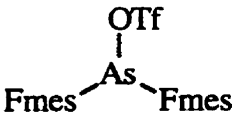


**4.26**

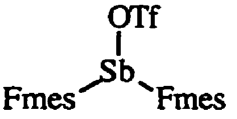


**4.27**

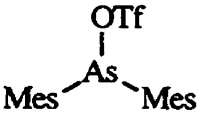


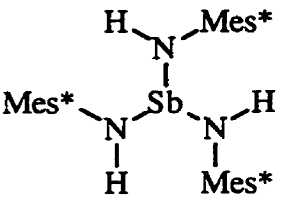


**5.1c**

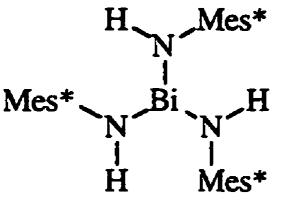


**5.1d**

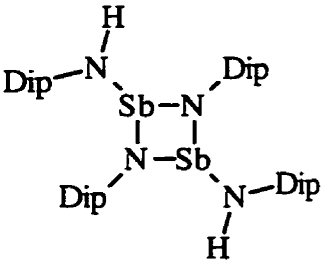


**5.3c**

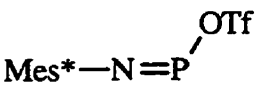


**6.3**

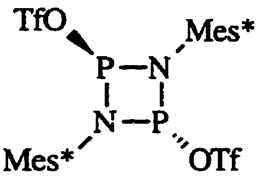


**6.4**

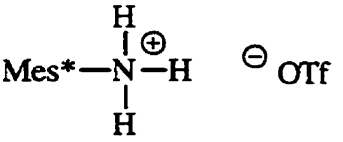


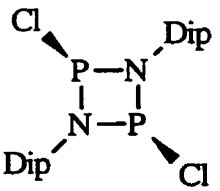


**6.6**

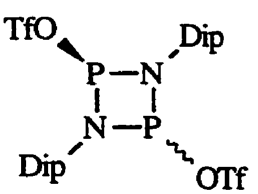


**6.7**

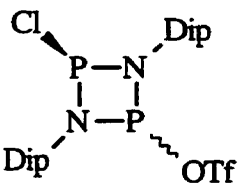


**6.9**

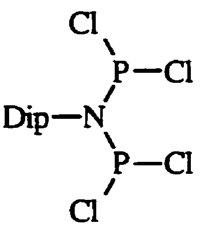


**6.8**

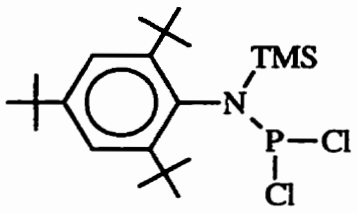


7.13

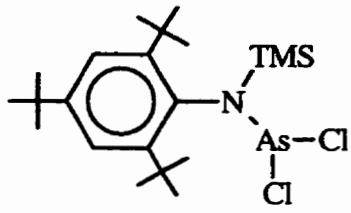


7.14

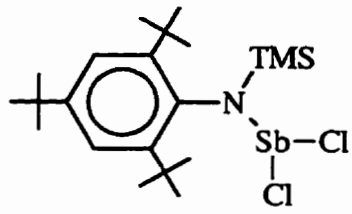


7.15

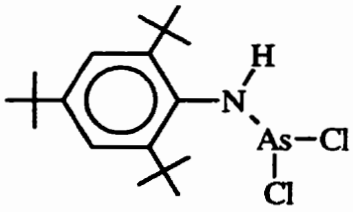


7.17

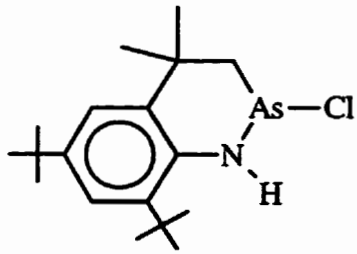


7.19

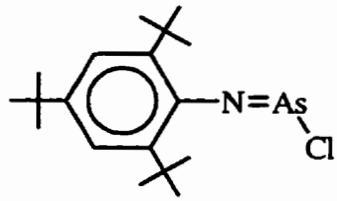


7.20

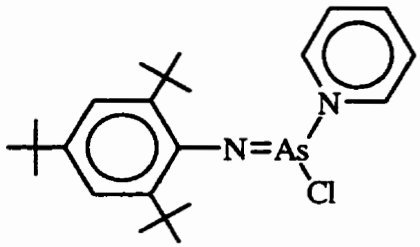


7.21

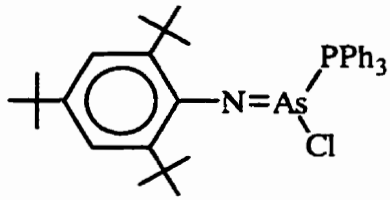


7.22

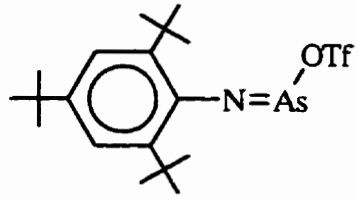


7.25

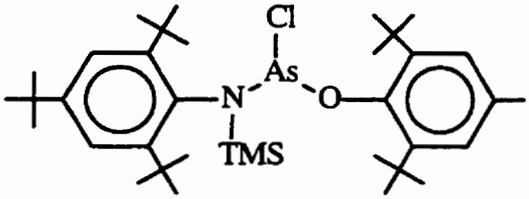


7.23

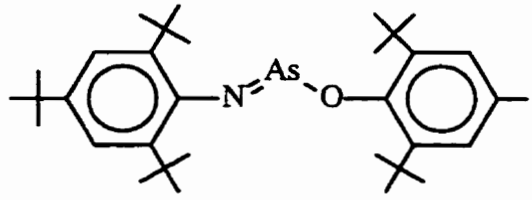


7.24

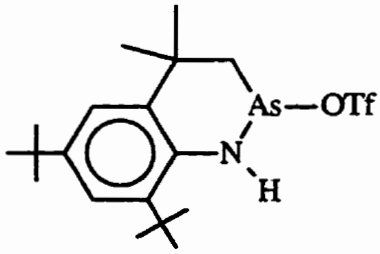


7.26

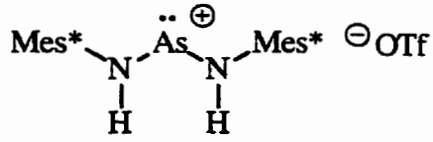


7.27

## 8.2 General Procedures

Solvents were dried over sodium and benzophenone (diethyl ether, THF, benzene, toluene); $CaH_2$ and $P_2O_5$ ($CH_2Cl_2$); $P_2O_5$ ($CCl_4$); or, $CaH_2$ ($CHCl_3$, hexane, pentane), degassed, and stored in evacuated bulbs. Solid reactants were handled in a VAC Vacuum/Atmospheres or Innovative Technology nitrogen-filled glove box. Reactions were performed in evacuated ($10^{-3}$ Torr) reactors and all glassware was flame-dried before use. Melting points were obtained on a Fisher-Johns apparatus and are uncorrected. Elemental analyses were performed by Beller Laboratories, Gottingen, Germany. Infrared spectra were recorded as Nujol mulls (solids) or neat liquids on CsI plates using a Nicolet 510P FT-IR spectrometer. Raman spectra were recorded on a Bruker RFS100 Raman spectrometer with the samples sealed under nitrogen in melting point tubes. Solution $^{1}H$, $^{31}P$, $^{19}F$ and $^{13}C$ NMR spectra were recorded on a Bruker AC-250 MHz or a Bruker AMX400 spectrometer with samples flame-sealed in 5mm Pyrex tubes or commercial thin walled NMR tubes. All chemical shifts are reported in parts per million (ppm) relative to an external standard; tetramethylsilane for $^{1}H$ and $^{13}C$ spectra, 85% $H_3PO_4$ for $^{31}P$ NMR spectra, $CCl_3F$ for $^{19}F$. All $^{13}C$, $^{19}F$ and $^{31}P$ spectra were obtained under conditions of broad band proton decoupling {$^{1}H$} unless otherwise indicated. Variable-temperature (VT) NMR studies utilized equilibration times of ten minutes at each temperature. $^{1}H$ and $^{13}C$ NMR samples of reaction mixtures were prepared by decanting an aliquot of the reaction mixture into an NMR tube, removing the volatiles *in vacuo*, and introducing an appropriate amount of deuterated solvent ($CD_2Cl_2$, THF-D8) *in vacuo*. Solid-state NMR spectra were obtained and interpreted by R. W. Schurko and R. E. Wasylishen using Bruker double-air-bearing MAS probes on Bruker AMX-400 (9.4 T) and MSL-200 (4.7 T) spectrometers.

Powdered crystalline samples were carefully packed in 4 mm (AMX-400) and 7 mm (MSL-200) rotors under an inert atmosphere. Typical rotor speeds ranged from 6 to 8 kHz. NMR spectra were acquired with proton-phosphorus cross-polarization under conditions of Hartman-Hanh matching. The proton 90° pulse width was set to 2.5 μs, with a contact time and recycle delay of 5 ms and 6 s, respectively. Between 900 and 1000 transients were acquired for each spectrum. Crystals suitable for X-ray structure determination were carefully selected or cut and mounted in thin wall glass capillaries in the dry box, and subsequently sealed under nitrogen. Structure determination and refinement was performed at the Dalhousie Crystallography Center (DALX) by Dr. T. S. Cameron, Dr. Witold Kwiatkowski, Katherine Robertson, or Susan Lantos using a Rigaku AFC5R diffractometer. Mass spectra were performed by G. Bradley Yhard on either a VG Analytical Quattro or a VG Autospec mass spectrometer at a nominal ionization energy of 70 eV (EIMS). Samples were introduced to the spectrometer *via* a standard heated solids probe in a nitrogen filled glove bag (Aldrich Atmos Bag) sealed to the front of the mass spectrometer[249].

2,4,6-Tri$^t$butylaniline, N-(trimethylsilyl)-2,4,6-tri$^t$butylaniline, 2,6-diisopropylaniline, 1,3,5-tris(trifluoromethyl)benzene, ethylene sulfide, methylamine, N,N'-dimethyl-1,3-propanediamine, bismuth (III) chloride, silver trifluoromethanesulfonate, $^n$butyllithium (1.6 M in hexane) (Aldrich) and $Mes_2AsCl$ (Quantum Design) were used without further purification. Antimony trichloride (Aldrich) was twice sublimed *in vacuo* prior to use. Arsenic trichloride (Aldrich), phosphorus trichloride (Aldrich), 2,3-dimethyl-1,3-butadiene (Aldrich) and trimethylsilyl trifluoromethanesulfonate were distilled *in vacuo* prior to use. Triethylamine (BDH) was dried over $CaH_2$ and distilled prior to use. Gallium trichloride (Aldrich) was sublimed *in*

*vacuo* before use.

## 8.3 Recrystallization Methods

A variety of recrystallization methods are typically used with our glass reactors (called "bridges"); these are detailed below. In each of the methods described, the solvent (and other volatiles) is removed until *ca.* 1-5 ml remain. The remaining solution is carefully decanted from the solid material then the crystals are washed by "cold spot back distillation": the reaction vessel is held on an angle such that solvent will drain from the bulb containing the crystals into the body of the reactor then liquid nitrogen "steam" or a cotton swab soaked in liquid nitrogen is used to distill *ca.*1-5 ml of solvent onto the solid. The washing is typically repeated three to five times.

The "tap recrystallization" method involves slow solvent removal from a concentrated solution (in a static vacuum) in one bulb of the reactor ("bridge") by slowly dripping cold tap water onto the adjacent empty bulb. The rate of dripping may be adjusted (from less than 1 drop per second to a rapid flow) to change the rate of solvent removal. Typically the flow of water is tuned to allow for the removal of volatiles over a two to three day period. This method allows for the greatest flexibility in recrystallization rate for all volatile solvents, but the reproduction of exact recrystallization conditions is difficult.

The "soft liquid nitrogen" recrystallization is a similar static vacuum method in which the volatiles are removed by placing the adjacent bulb in the cold fumes at the top of a dewar of liquid nitrogen. A more rapid removal of solvent is obtained by the "hard liquid nitrogen" method, in which the adjacent bulb is immersed in a dewar of liquid nitrogen. The latter method is often necessary when the recrystallization solvent has low vapour pressure or if the reaction mixture has turned into an oil.

The most effective solvent removal is obtained by the "hard vacuum" recrystallization in which the reaction mixture is subjected to dynamic vacuum. This

method is used almost exclusively for mixtures that have become oils and the resultant solid is often not crystalline.

Another method is "heating and cooling" in which the volume of the recrystallization mixture is reduced by the "hard vacuum" method until the appearance of solid. The mixture is then stirred and warmed with either a stream of hot water or a blow-drier until the solid dissolves and then the mixture is allowed to slowly cool to room temperature. If the solid obtained from the cooling is not crystalline, the heating and cooling cycle is repeated.

Thermally unstable compounds and oily recrystallization mixtures sometimes require the use of the fridge freezer following the solvent removal to promote crystal formation.

## 8.4 Specific Procedures

$NMeCH_2CH_2NMeAsCl$, $[NMeCH_2CH_2NMeAs]_2$ $[GaCl_4]_2$, $NMeCH_2CH_2CH_2NMeAsCl$,[63,62] **3.2BD** $[GaCl_4]$,[64] $[NMeCH_2CH_2NMeP][GaCl_4]$,[60] Mes*N(H)As=NMes*,[147] Mes*N=P-OTf,[188] Mes*N=P-Br, Mes*N=P-I,[235] $Fmes_3Bi$, $Fmes_2BiCl$,[144] and $FmesPCl_2$[143] were prepared according to procedures found in the literature. Mes*N(H)P=NMes* was synthesized by the reaction of Mes*NPCl[235] with Mes*NHLi[237].

### Preparation of $N(Me)CH_2CH_2CH_2N(Me)AsCl$, 2.6Cl.

Under a continuous stream of dry nitrogen gas a solution of N,N'-dimethyl-1,3-propanediamine (4.96 g, 48.5 mmol) and triethylamine (*ca.* 25 ml) in diethyl ether (20 ml)

was slowly added (45 min) dropwise to a solution of $AsCl_3$ (8.80 g, 48.5 mmol) in diethyl ether (125 ml) in a 3-neck flask. Immediate reaction produced a copious white precipitate, the mixture was stirred overnight then filtered under nitrogen and the solid was washed with two portions (25 ml) of fresh ether. The washings were added to the filtrate and the volume of the solution was reduced (90%) by removal of the solvent *in vacuo*. Cooling to -18°C produced colourless crystals, which were recrystallized from fresh ether and characterized as 2-chloro-1,3-dimethyl-cyclo-1,3-diaza-2-arsahexane (referred to as 2-chloro-1,3-diaza-1,3-dimethyl-2-arsenane), 5.81 g, 27.6 mmol, 57%; m.p. 47.0-48.5°C;

IR ($cm^{-1}$): 2744m, 2718m, 2702m, 2687w, 1276vs, 1227vs, 1207m, 1146vs, 1133vs, 1125vs(sh), 1091s, 1050vs, 1037vs, 941vs, 925s, 891s, 837vs, 570vs, 540m, 414m, 361vs, 342m, 320w, 285s(sh), 263vs, 239vs, 233vs;

$^1H$ NMR ($CD_2Cl_2$): 2.88 ($CH_2N$, m, 4H), 2.63 ($CH_3$, s, 6H), 1.94 ($CH_2$, m, 2H);

$^{13}C$ NMR ($CD_2Cl_2$): 48.4 ($CH_2N$), 40.3 ($CH_3$), 27.8 ($CH_2$).

Crystal data: Monoclinic, space group: $P2_1/n$ (#14), a = 7.206(1) Å, b = 9.650(1) Å, c = 13.021(2) Å, $\beta$ = 99.61(2)°; V = 892.8(2) $Å^3$, $D_{calc}$ = 1.566 $g/cm^3$, $R_1$ = 0.0259.

**Preparation of $[N(Me)CH_2CH_2CH_2N(Me)As]$ $[GaCl_4]$, 2.6$[GaCl_4]$.**

A solution of chloroarsenane **2.6Cl** (0.44 g, 2.1 mmol) in $CH_2Cl_2$ (20 ml) was slowly added to a solution of $GaCl_3$ (0.37 g, 2.1 mmol) in $CH_2Cl_2$ (40 ml) over a period of 15 minutes. Approximately 90% of the solvent was removed *in vacuo* and the solution was cooled to 5°C to produce yellow crystals characterized as 1,3-dimethyl-1,3-diaza-2-

arsenanium tetrachlorogallate, 0.39 g, 1.0 mmol, 48%; m.p. 52.0-54.5°C;

Anal. Calcd.: C, 15.53; H, 3.13; N, 7.25%;

Found: C, 15.97; H, 3.29; N, 7.35%;

IR ($cm^{-1}$): 1347w, 1284vs, 1242vs, 1205s, 1184w, 1152vs, 1118vs, 1102m, 1084s, 1049vs, 1040vs, 955vs, 913w, 879s, 862m, 806w, 752w, 601s, 588s, 551w, 493w, 387vs(sh), 378vs, 362vs, 339vs, 301w, 266w, 255w, 232s;

$^1H$ NMR ($CD_2Cl_2$): 3.49 ($CH_2N$, m, 4H), 3.34 ($CH_3$, s, 6H), 2.29 ($CH_2$, m, 2H);

$^{13}C$ NMR ($CD_2Cl_2$): 51.6 ($CH_2N$), 42.6 ($CH_3$), 26.2 ($CH_2$);

Crystal data: Orthorhombic, space group: $Pca2_1$ (#29), a = 14.432(3) Å, b = 6.7580(14) Å, c = 13.905(3) Å; V = 1356.2(5) $Å^3$, $D_{calc}$ = 1.893 $g/cm^3$, $R_1$ = 0.0505.

**Recrystallization of $N(Me)CH_2CH_2N(Me)AsCl$, 2.5Cl.**

**2.5Cl** was distilled *in vacuo* into sample tubes and stored in a refrigerator (4°C) for weeks resulting in the sublimation of large colourless crystals onto the walls of the tube. The crystals were mounted in a nitrogen filled glove bag under a stream of cold nitrogen (liquid nitrogen boil-off). The crystal structure of **2.5Cl** (m.p.≈ 19°C) was determined at low temperature (-60°C).

Crystal data: Monoclinic, space group: $P2_1/n$ (#14), a = 6.959(7) Å, b = 9.23(2) Å, c = 12.14(2) Å, β = 95.4(1)°; V = 777(4) $Å^3$, $D_{calc}$ = 1.681 $g/cm^3$, $R_1$ = 0.0431.

**Preparation of 3.3BD[$GaCl_4$].**

A solution of 2,3-dimethyl-1,3-butadiene (0.24 g, 2.9 mmol) in $CH_2Cl_2$ (6 ml) was added over a period of 4 minutes to a solution of **2.6**[$GaCl_4$] (0.86g, 2.2 mmol) in $CH_2Cl_2$ (90 ml) prepared *in situ*. The mixture was allowed to stir for 20 minutes. The solvent was entirely removed *in vacuo* to give a viscous yellow oil which solidified upon standing overnight and was characterized as 1-azonia-1,3,4,7-tetramethyl-7-aza-6-arsabicyclo[4.4.0]dec-3-ene tetrachlorogallate, **3.3BD**[$GaCl_4$], 0.85 g, 1.8 mmol, 82%; m.p. 83.5-87.5°C;

IR ($cm^{-1}$): 1343w, 1313m, 1301m, 1286w, 1267m, 1234m, 1204s, 1200s, 1184m, 1156vs, 1135s, 1123m, 1097w, 1074m, 1051m, 1042s, 1029m, 1003s, 982vs, 946s, 913s, 884s, 847vs, 806w, 788w, 770vs, 738w, 657m, 611m, 583s, 548w, 503s, 405m(sh), 381vs(br), 365vs, 343s, 317m, 288w, 257w;

$^1H$ NMR (ppm, $CD_2Cl_2$): 3.71 (m, 3H), 3.69 (m, 3H), 3.39 (d, 1H), 3.36 (d, 1H), 3.14 (s, 3H), 3.05, (s, 3H), 3.01 (m, 2H), 2.47 (d, 1H), 2.39 (m, 1H), 1.90 (s, 3H), 1.74 (m, 1H); See Chapter 3 for 400 MHz COSY analysis;

$^{13}C$ NMR (ppm, $CD_2Cl_2$): 124.6, 122.8, 65.0, 57.4, 48.9, 45.6, 43.9, 33.1, 22.2, 19.5, 19.0;

$^1H$ and $^{13}C$ NMR spectra of the reaction mixture show **3.3BD[$GaCl_4$]** as the only product.

**NMR identification of $[MeN(CH_2)_2MeNPCH_2(C(Me))_2CH_2][GaCl_4]$, 3.3BD.**

A colourless solution of dimethylbutadiene (3 ml, mmol) in dichloromethane (5 ml) was added to a pale yellow solution of $[MeN(CH_2)_2MeNP][GaCl_4]$ (0.046 g, 0.14 mmol) in dichloromethane (5ml) resulting in the disappearance of the yellow colour and the formation of an opaque white mixture. An aliquot was decanted into an NMR tube and volatiles were removed *in vacuo* and the resultant white solid was dissolved in $CD_2Cl_2$.

$^1H$ NMR (ppm, $CD_2Cl_2$): 1.86 (d, $^3J_{H-H}$ 1.22 Hz, Me-C), 2.80 (d, $^3J_{P-H}$ 10.99 Hz, Me-N), 2.8-2.9 (m, $CH_2$-P), 3.42 (d, $^3J_{P-H}$ 8.85 Hz, $CH_2$-N);

$^{13}C$ NMR (ppm, $CD_2Cl_2$): 16.4 (d, $^3J_{P-C}$ 15.3 Hz, Me-C), 31.2 (d, $^1J_{P-C}$ 66.3 Hz, C-As), 32.0 (d, $^2J_{P-C}$ 6.7 Hz, Me-N), 50.1 (d, $^2J_{P-C}$ 6.7 Hz, $CH_2$-N), 128.5 (d, $^2J_{P-C}$ 12.4 Hz, C=C);

$^{31}P$ NMR (ppm, $CD_2Cl_2$): 89.6 (s).

**Preparation of $Fmes_2PnCl$ (Pn = As, Sb).**

In a typical reaction, a solution of $^nBuLi$ (1.6 M in hexane) was slowly added through a septum to a cooled (0°C) equimolar solution of tris(trifluoromethyl)benzene in diethyl ether (50 ml) under nitrogen in one chamber of the reactor. This was stirred and allowed to warm to room temperature then stirred for an additional 3-4 hours, producing a dark orange solution which was then added over a period of 15 minutes to a stirred solution of $PnCl_3$ (0.5 equivalents) in diethyl ether (30 ml) producing yellow solutions and depositing a white precipitate (LiCl). The reaction mix was frozen, the reactor was

evacuated and the mixtures were allowed to stir for 2 days then filtered to yield clear yellow solutions. Diethyl ether was removed slowly by the "tap method" to yield crystalline material.

**Purification and Characterization of $Fmes_2AsCl$, 4.24.**

The crude yellow solid was sublimed at 75°C under dynamic vacuum to yield a white solid coated by yellow oil. This mixture was recrystallized from hexane by the tap method to yield colourless rod shaped crystals; yield 0.718 g, 1.1 mmol, 13% (first crop), m.p. 98-100°C.

Anal. Calcd. C, 32.14; H, 0.60; Cl, 5.27%;
Found C, 32.20; H, 0.70; Cl, 5.12%;

IR ($cm^{-1}$): 3377 vw(br), 3100w, 3087w(sh), 2727w, 2671w(br), 2279w(br), 1844w, 1668w, 1624m, 1581w, 1341m(sh), 1279s, 1207s(sh), 1195s, 1153s, 1125s, 1085s, 1039m, 930w(sh), 916s, 891w(sh), 857m, 836m, 792w(br), 747m, 736w, 695m, 692m(sh), 685s, 671m, 652w(sh), 562w, 435w, 424w, 417w, 408w, 387m;
Raman ($cm^{-1}$) 225 mW (poor scatterer): 110m, 158s, 193w, 217w, 260s, 304m, 388s, 461w, 739s, 857w, 1022m, 1588m, 1625s, 1665w, 3089m;
$^1H$ NMR (ppm, $CD_2Cl_2$): 8.10 (s);
$^{13}C$ NMR (ppm, $CD_2Cl_2$): 122.6 (q, $^1J_{C-F}$ 277.0Hz, p-$CF_3$),123.4 (q, $^1J_{C-F}$ 276.1Hz, o-$CF_3$), 128.7 (s(br), C-H), 133.3 (q , $^2J_{C-F}$ 34.8Hz, $C_o$), 136.3 (q, $^2J_{C-F}$ 34.5Hz, $C_p$), 147.5 (s, $C_i$);

$^{19}F$ NMR (ppm, $CD_2Cl_2$): -54.5 (s, 2F), -63.9 (s, 1F).

Two crystalline forms were identified:

Crystal data: Monoclinic, space group: $P2_1/a$ (#14), a = 8.705(9) Å, b = 30.38(1) Å, c = 8.167(4) Å, β = 91.53(6)°; V = 2159(2) $Å^3$, $D_{calc}$ = 2.069 $g/cm^3$, $R_1$ = 0.067.

Crystal data: Orthorhombic, space group: $P2_12_12_1$ (#19), a = 9.782(1) Å, b = 25.772(2) Å, c = 8.751(2) Å; V = 2206.2(5) $Å^3$, $D_{calc}$ = 2.025 $g/cm^3$, $R_1$ = 0.043.

and a low-temperature structure at 130(2) K:

Crystal data: Orthorhombic, space group: $P2_12_12_1$ (#19), a = 8.6646(2) Å, b = 9.69650(10) Å, c = 25.4076(6) Å; V = 2134.65(7) $Å^3$, $D_{calc}$ = 2.093 $g/cm^3$, $R_1$ = 0.033.

**Characterization of $Fmes_2SbCl$ 4.25.**

Large hexagon shaped pale yellow crystals; yield 0.688 g, 0.96 mmol, 41%, m.p. 112-113°C.

Anal. Calcd. C, 30.05; H, 0.56; Cl, 4.93%;

Found C, 30.23; H, 0.67; Cl, 4.86%;

IR ($cm^{-1}$): 3096w, 3083w, 1844w, 1623s, 1577m, 1559w, 1419w, 1279s, 1200s, 1129s, 1108.5s, 1082s(sh), 1015w(sh), 930m, 915s, 852s, 837m, 742m, 691s(sh), 684s, 670s,

560w, 432m, 408w, 401w(sh), 366w, 351s, 302w;

Raman ($cm^{-1}$) 166 mW (poor scatterer): 101s, 126s, 155s, 184m, 211w, 262s, 304m, 349s, 367w, 434w, 451w, 581w, 691w, 738s, 854w, 1014w, 1157w, 1261w, 1383m, 1624m, 3084m;

$^{1}H$ NMR (ppm, $CD_2Cl_2$): 8.22 (s);

$^{13}C$ NMR (ppm, $CD_2Cl_2$): 122.8 (q, $^{1}J_{C-F}$ 272.8Hz, p-$CF_3$), 124.1 (q, $^{1}J_{C-F}$ 276.1Hz, o-$CF_3$), 128.3 (s(br), $C_m$-H), 133.9 (q , $^{2}J_{C-F}$ 34.8Hz, $C_o$), 137.8 (q, $^{2}J_{C-F}$ 32.9Hz, $C_p$), 151.9 (s(br), $C_i$);

$^{19}F$ NMR (ppm, $CD_2Cl_2$): -55.3 (s, 2F), -63.9 (s, 1F).

Crystal data: Monoclinic, space group: $P2_1/c$ (#14), a = 8.296(3) Å, b = 30.430(8) Å, c = 8.779(3) Å, $\beta$ = 94.03(3)°; V = 2210.9(2) $Å^3$, $D_{calc}$ = 2.161 $g/cm^3$, $R_1$ = 0.0834.

**Attempted preparations of $Fmes_2As$-OTf, 4.26.**

$Fmes_2As$-Cl (0.182 g, 0.27 mmol) and AgOTf (0.079 g, 0.31 mmol) were placed in one bulb of a reactor under a very fine fritted glass filter. Hexane (10 ml) was distilled onto the solids and the mixture was allowed to stir for 3 days in the dark. NMR spectra of the reaction mixture show the presence of $Fmes_2As$-Cl (>95%) and signals corresponding to $Fmes_2As$-OTf: $^{19}F$ NMR (ppm, $CD_2Cl_2$): -55.3 (s(br), 4F), -63.9 (s, 2F), -78.0 (s, 1F). The reaction mixture was filtered to yield a clear yellow solution which was slowly concentrated by the tap method of recrystallization. This produced pale yellow crystals

characterized as $Fmes_2As$-Cl (starting material by NMR, IR, Raman and crystal structure).

A colourless solution of TMSOTf (2.456 g, 11.1 mmol) in n-hexane (2 ml) was added to a colourless solution of $Fmes_2As$-Cl (0.195 g, 0.29 mmol) in n-hexane (5 ml). The resultant pale yellow solution was stirred for 3 days. An aliquot of the reaction mixture was placed in an NMR tube and volatiles were removed *in vacuo* and the yellow microcrystalline product was dissolved in $CD_2Cl_2$. Multinuclear NMR spectra show only peaks assigned to $Fmes_2As$-Cl.

**Preparation of $Fmes_2Sb$-OTf, 4.27.**

$Fmes_2Sb$-Cl (0.248 g, 0.34 mmol) and AgOTf (0.096 g, 0.37 mmol) were placed in one bulb of a reactor under a very fine fritted glass filter. Hexane (10 ml) was distilled onto the solids and the mixture was allowed to stir for 3 days in the dark. The reaction mixture was filtered to yield a clear yellow solution which was slowly concentrated by the tap method of recrystallization. This produced very pale yellow diamond shaped crystals; yield 0.04 g, 0.05 mmol, 14% (initial yield), m.p. 125.5-126.5°C;

IR ($cm^{-1}$): 3105w, 3087w, 2726w, 1625w, 1578w, 1377s, 1280s, 1268s(sh), 1238m(sh), 1220s(sh), 1198s, 1171s, 1183s(sh), 1152s(sh), 1140s, 1084m, 1077m, 1013w, 942m(sh), 932s, 916s, 852m, 836w, 767w, 742m, 693m, 685m, 672w, 628m, 603w, 571w, 559w, 537w, 515w, 431w, 408w, 384w, 366w;
Raman ($cm^{-1}$) 110 mW (poor scatterer): 157s, 184m, 212m, 262s, 306m, 434w, 456w, 574w, 693w, 739w, 767m, 856w, 931w, 1018m, 1085w, 1042w(br), 1238w; 1264w, 1384, m, 1626m, 1796w(br), 1862w(br), 3090m;

$^{1}H$ NMR (ppm, $CD_2Cl_2$): 8.32 (s);

$^{13}C$ NMR (ppm, $CD_2Cl_2$): only 124.1 (q, $^{1}J_{C-F}$ 276.1Hz, o-$CF_3$) and 128.9 (s(br), $C_m$-H);

$^{19}F$ NMR (ppm, $CD_2Cl_2$): -55.7 (s(br), 4F), -64.0 (s, 2F), -77.3 (s, 1F).

Crystal data: Orthorhombic, space group: $P2_12_12_1$(#19), a = 16.172(4) Å, b = 17.758(2) Å, c = 9.119(1) Å; V = 2618.8(6) $Å^3$, $D_{calc}$ = 2.113 $g/cm^3$, $R_1$ = 0.043.

**Preparation of $Mes_2AsOTf$.**

$Mes_2AsCl$ (0.319 g, 0.92 mmol) and AgOTf (0.261 g, 1.02 mmol) were placed in one bulb of a reactor under a very fine fritted glass filter. Hexane (30 ml) was distilled onto the solids and the mixture was allowed to stir for 3 days in the dark resulting in a very pale yellow solution and a white precipitate. The mixture was filtered and the product was characterized as $Mes_2As$-OTf by $^{1}H$ and $^{19}F$ NMR spectroscopy (the $^{1}H$ NMR spectrum contains several minor unidentified signals):

$^{1}H$ NMR (ppm, $CD_2Cl_2$): 2.19 (s (broad), 6H), 2.29 (s, 3H), 6.92 (s, 2H);

$^{19}F$ NMR (ppm, $CD_2Cl_2$): -77.9 (s).

*c.f.* $Mes_2AsCl$ :

$^{1}H$ NMR (ppm, $CD_2Cl_2$): 2.12 (s (sharp), 6H), 2.25 (s, 3H), 6.80 (s, 2H).

**Preparation of trisaminopnictines.**

In a typical procedure, a solution of $^{n}$BuLi (1.6 M in hexane) (ml) was slowly added through a septum to a cooled (0°C) solution Mes*$NH_2$ (*ca.* 5.0 g, 19.1 mmol) in diethyl ether (50 ml) under nitrogen in one chamber of the reactor. The resulting yellow solution with white solid was warmed to room temperature and then added over a period of 15 minutes to a stirred solution of $PnCl_3$ (*ca.* 6.3 mmol) in diethyl ether (30 ml) in the second chamber. The reaction mixture was frozen and evacuated and the septum bulb was replaced with a fritted receiver. The mixture was warmed to room temperature, stirred overnight and filtered. Crystalline samples were obtained by slow removal of solvent from the reaction mixture within the reaction vessel by passing a cool stream of water over the empty adjacent compartment (or placing it over liquid nitrogen) and distilling the volatiles *in vacuo* (static). Crystals were washed with cool hexane by cold spot back distillation.

**Characterization data for Sb(N(H)Mes*)$_3$, 5.1c.**

Cube shaped yellow crystals; yield 0.40 g, 0.44 mmol, 25 %; d.p. 197-200°C;

Anal. Calcd. C, 71.82; H, 10.05; N, 4.65%;
Found C, 72.00; H, 10.21; N, 4.65%;

IR ($cm^{-1}$): 3420m, 3403m, 3076w, 1602w, 1595sh, 1421s, 1390sh, 1335m, 1286m, 1257sh, 1239sh, 1220s, 1201sh, 1170m, 1141w, 1113m, 1019w, 909w, 877m, 837sh, 827m, 810m, 772m, 749w, 748w, 730w, 575w, 482sh, 460m;
Raman ($cm^{-1}$) 166 mW: 3421w, 3405w, 3087w, 2963s, 2904s, 2776w, 2707w, 1603m, 1463sh, 1445sh, 1426w, 1290m, 1264w, 1240sh, 1220sh, 1201w, 1176w, 1141w,

922w, 814w, 748w, 569w, 480sh, 458w, 254w, 143w, 105sh, 85sh;

$^1$H NMR (ppm, $CD_2Cl_2$): 1.26 (s, 9H), 1.31 (s, 18H), 5.07 (s, 1H), 7.11 (s, 2H);

$^{13}$C NMR (ppm, $CD_2Cl_2$): 31.7, 32.9, 34.5, 35.8, 123.1, 138.0, 140.3, 144.3.

Crystal data: Triclinic, space group: P-1 (#2), a = 11.491(5) Å, b = 24.652(7) Å, c = 10.002(5) Å, $\alpha$ = 98.38(3)°,$\beta$ = 96.44(5)°, $\gamma$ = 77.25(3)°; V = 2724(2) Å$^3$, $D_{calc}$ = 1.101 g/cm$^3$, $R_1$ = 0.0547.

**Characterization data for Bi(N(H)Mes*)$_3$, 5.1d.**

Dark orange/red crystals recrystallized from hexane; decomposition occurs in ether and $CH_2Cl_2$ over a period of days; yield, 0.18 g, 0.18 mmol, 11 %; d.p. 144-147°C;

Anal. Calcd. C, 65.49; H, 9.16; N, 4.24%;
Found C, 65.76; H, 9.41; N, 4.13%;

IR (cm$^{-1}$): 3406w, 3396w, 3076w, 1601w, 1420m, 1389m, 1376sh, 1285m, 1220s, 1200sh, 1166sh, 1113m, 1020w, 877m, 825w, 808w, 774m, 730w, 588w, 444w, 393w; Raman (cm$^{-1}$) 47 mW: 3405w, 3390w, 3086w, 2958s, 2904s, 2777w, 2705w, 1601s, 1463sh, 1445sh, 1421m, 1287sh, 1253m, 1220m, 1198sh, 1175sh, 1140m, 810m, 741sh, 727sh, 723m, 527s, 456sh, 443m, 393sh, 343w, 323w, 252w, 153w, 93s, decomposition at 166mW;

$^{1}$H NMR (ppm, $CD_2Cl_2$): 1.27 (s, 9H), 1.31 (s, 18H), 5.86 (s, 1H), 7.18 (s, 2H);

$^{13}$C NMR (ppm, $CD_2Cl_2$): 32.0, 33.0, 34.3, 35.5, 122.2, 139.2, 140.8, 145.9.

Crystal data: Triclinic, space group: P-1 (#2), a = 11.511(5) Å, b = 24.785(15) Å, c = 9.981(5) Å, $\alpha$ = 98.06(5)°,$\beta$ = 96.50(4)°, $\gamma$ = 77.40(5)°; V = 2742(2) Å$^3$, $D_{calc}$ = 1.200 g/cm$^3$, $R_1$ = 0.0619.

**NMR studies of Mes*N=PnN(H)Mes* with $Mes*NH_2$ (Pn = P or As).**

$^{31}$P NMR studies of equimolar mixtures of (N(H)Mes*)PNMes* with $Mes*NH_2$ in diethyl ether showed the presence of (N(H)Mes*)PNMes* only. $^{1}$H NMR studies of equimolar mixtures of (N(H)Mes*)AsNMes* with $Mes*NH_2$ in $CD_2Cl_2$ showed the presence of the starting materials only. In both cases, exposure of the samples to utrasound had no measurable effect.

**NMR studies of thermolysed samples of $Pn(N(H)Mes*)_3$ (Pn = Sb or Bi).**

Sealed samples of $Pn(N(H)Mes*)_3$ (E = Sb or Bi) in $CD_2Cl_2$ were heated (60°C) with ultrasound for several hours and then examined by $^{1}$H NMR spectroscopy. $Sb(N(H)Mes*)_3$ showed no change, while $Bi(N(H)Mes*)_3$ produced a white precipitate and $^{1}$H NMR signals corresponding to $Mes*NH_2$.

**Preparation of [DipN=Sb-N(H)Dip]$_2$, 5.3c.**

A pale yellow 1.6M solution of $^n$BuLi in hexane (15.5 ml, 24.8 mmol) was slowly added through a septum to a cooled (0°C) pale pink solution of degassed $DipNH_2$ (4.300 g, 24.3 mmol) in diethyl ether (60 ml). This was allowed to warm to room temperature then stirred for an additional six hours resulting in the formation of a bright yellow solution. The yellow mixture was added over a period of 30 minutes to a stirred colourless solution of $SbCl_3$ (1.658 g, 7.27 mmol) in diethyl ether resulting in the formation of a yellow solution and copious amounts of white precipitate (LiCl). The reaction mixture was allowed to stir for two days then filtered through a fiberglass frit resulting in a clear yellow solution. Removal of volatiles by the "tap method" resulted in the formation of bright yellow cube-shaped crystals which were washed repeatedly with hexane (more than 10 times) and characterized as [DipN=Sb-N(H)Dip]$_2$, yield 0.258 g, 0.273 mmol, 4% (initial yield), mp. 197-199°C.

IR ($cm^{-1}$): 3380w, 3053m, 1589w, 1428vs, 1363m, 1322s, 1312m(sh), 1300m, 1259m, 1240vs, 1232s(sh), 1190s, 1157w, 1108m, 1099m, 1057w(sh), 1052w, 1037w, 931w, 884m, 858m, 839m, 815w, 805w, 794m, 772vs, 757s, 696w, 669s, 641w, 514m, 402m, 362m;

$^1$H NMR (ppm, $CD_2Cl_2$): 0.88 (d, $^3J_{H-H}$ 6.71 Hz, 12H), 1.25 (d, $^3J_{H-H}$ 6.71 Hz, 12H), 2.73 (septet, $^3J_{H-H}$ 6.72 Hz, 2H), 4.30 (septet, $^3J_{H-H}$ 6.72 Hz, 2H), 5.15 (s, 2H), 6.86-7.20 (m, 12H);

$^{13}$C NMR (ppm, $CD_2Cl_2$): x, x, x, x, x, x;

Crystal data: Triclinic, space group: P-1 (#2), a = 11.104(1) Å, b = 11.779(1) Å, c = 10.292(4) Å, $\alpha$ = 96.53(2)°,$\beta$ = 98.64(2)°, $\gamma$ = 115.990(7)°; V = 1171.6(5) $Å^3$, $D_{calc}$ = 1.342 $g/cm^3$, $R_1$ = 0.045.

**Preparation of Mes*N=POTf, 6.3 and $[Mes*N=POTf]_2$, 6.4.**

Mes*N=P-OTf **6.3** was prepared using a variation of a method previously reported (Mes*$^{15}$N=P-OTf was prepared in the same manner).[188] Mes*N=P-Cl (0.766 g, 2.35 mmol) and AgOTf (0.651 g, 2.54 mmol) were placed in one compartment of a 2 compartment reactor vessel equipped with a glass frit. Hexane (50 ml) was distilled onto the mixture which was then stirred in the dark for 4 days. The dark orange reaction mixture was filtered into the second compartment. The fritted receiver was replaced with a clean flame-dried bulb. A mixture of large dark-yellow/orange crystals and small clear yellow crystals were obtained by slow removal of solvent from the reaction mixture by the tap method. The crystalline mixture was washed with cool solvent by cold spot back-distillation.[257] Yield: 0.852 g, 82.5%. Samples of each type of crystal were isolated by the Pasteur method under a microscope in a dry-box. Attempts to purify the products by sublimation resulted in the decomposition of both products as indicated by NMR, Raman, and melting point.

Orange crystals: d.p. (°C) 119-122 (dec.prod. melts at 192-197) assigned as **6.3** based on X-ray crystallographic analysis:

Crystal data for **6.3**: Monoclinic, space group: $P2_1/n$ (#14), a = 10.454(2) Å, b =

10.741(2) Å, c = 20.489 (2) Å, β = 97.834 (10)°; V = 2279.2 (5) $Å^3$, $D_{calc}$ = 1.281 $g/cm^3$, $R_1$ = 0.0580.

Clear yellow crystals: d.p. 111-113 (dec.prod. melts at 195-199) assigned as **6.4** based on X-ray crystallographic analysis:

Crystal data for **6.4**: Monoclinic, space group: $P2_1/n$ (#14), a = 11.368(2) Å, b = 16.429(3) Å, c = 12.013(2) Å, β = 90.59 (3)°; V = 2243.5 (7) $Å^3$, $D_{calc}$ = 1.301 $g/cm^3$, $R_1$ = 0.0468.

Elemental Analysis of Mixture:

Calcd.: C, 51.93; H, 6.65; N, 3.19 %;
Found: C, 51.20; H, 7.09; N, 3.09 %.

FT-IR:

**6.3**: 1599s, 1541w, 1424w(sh), 1415w(sh), 1398m, 1296w, 1266m, 1246m(sh), 1235vs, 1219m(sh), 1196vs, 1184vs, 1150vs, 1134s(sh), 1069w, 1022w, 914vs, 886s, 829w, 776w, 764w, 629s, 585m, 573w(sh), 532m, 514w, 374w, 356w, 259m.

**6.4**: 1617sh, 1598m, 1509w(br), 1404m, 1367vs, 1255s, 1203m, 1174m, 1140w, 1098w, 1020s, 919w, 883w(br), 827m(br), 766w(sh), 752m(sh), 722s, 629s, 608s,

574w, 520m, 501w, 444m, 364w.

FT-Raman (166mW):

**6.3**: 2971s, 2911s, 1598s, 1475vs, 1408m, 1368w, 1292w, 1266w, 1203w, 1134s, 1070s, 1029w, 926w, 823m, 781w, 764w, 571w, 254w, 143w, 103m.

**6.4**: 2966vs, 2913vs, 1601m, 1472m, 1445m, 1425wsh, 1294w, 1246w, 1223m, 1196m, 1150m, 1122w, 1024m, 995s, 928w, 832s, 758w, 574m, 132s, 73w.

Solution NMR of reaction mixture (hexane): $^{31}P$: 55.9 ppm; $^{19}F$: -78.3 ppm

Note: "crystal mixture" below denotes unseparated samples of isolated crystals dissolved in fresh solvent.

Solution NMR of crystal mixture ($CD_2Cl_2$): $^{31}P$: 50.1 ppm; $^{19}F$: -78.3 ppm; $^{1}H$ (ppm): 1.32 (s,9H), 1.49 (s,18H), 7.42 (s,2H); $^{13}C$ (ppm): 29.9, 31.1, 33.9, 36.2, 98.9, 123.1, 135.7, 140.0, 150.7.

Solution $^{31}P$ NMR of crystal mixture: (hexane): 55.9 ppm; ($Et_2O$): 51.4 ppm; ($CH_2Cl_2$): 50.0 ppm; (toluene): 51.7 ppm.

**Hydrolysis of Mes*N=P-OTf.**

A mixture of distilled water (0.02 g, 1.1 mmol) in $CH_2Cl_2$ (5 ml) was added to a

stirred orange solution of Mes*N=P-OTf (0.197 g, 0.45 mmol) in $CH_2Cl_2$ (20 ml) resulting in the immediate formation of a pale yellow reaction mixture. Aliquots were removed for analysis of the reaction mixture by NMR ($CH_2Cl_2$ and $CD_2Cl_2$) and slow removal of solvent resulted in the formation of clear colourless needle-shaped crystals characterized as [Mes*$NH_3$][OTf], yield 0.080g, 0.19 mmol, 43%, m.p. 193-196°C.

Anal. Calcd. C, 55.45; H, 7.84; N, 3.40%;
Found C, 54.52; H, 7.91; N, 3.61%;

IR ($cm^{-1}$): 3284w, 3175w(vbr), 2670w(br), 2589w(br), 1616w, 1598m, 1559w, 1539w(sh), 1515m(br), 1408w, 1422w, 1255s, 1223s, 1175s, 1109m, 1021s, 991m, 936w, 915w, 886w, 629m, 610w, 576w, 521m;
Raman ($cm^{-1}$) 166 mW: 86w, 139m, 253m, 320m, 347m, 356m(sh), 572m, 711w, 762m, 826s, 936w(br), 1030s, 1109w, 1145w, 1169w, 1201w, 1228w, 1242w, 1292w, 1447m, 1471m, 1519w, 1599w, 2729w, 2742w, 2803w, 2914s, 2969s, 3106w;

$^1H$ NMR (ppm, $CD_2Cl_2$): 1.30 (s, 9H), 1.54 (s, 18H), 7.43 (s, 2H), 8.61 (broad s, 3H);

$^{13}C$ NMR (ppm, $CD_2Cl_2$): 31.3, 31.7, 35.1, 123.8, 143.6, 151.7, 156.7, (q due to $CF_3$ group is not observed);
$^{19}F$ NMR (ppm, $CD_2Cl_2$): -78.9.

Crystal data: monoclinic, space group: $P2_1/c$ (#14), a = 8.872(2) Å, b = 11.806(2) Å, c =

21.064(2) Å, $\beta = 92.33(1)°$; V = 2204.5(6) $Å^3$, $D_{calc}$ = 1.237 $g/cm^3$, $R_1$ = 0.069.

Reaction mixture NMR:

$^1H$ NMR (ppm, $CD_2Cl_2$): 1.32 (s, 9H), 1.54 (s, 18H), 7.48 (s, 3H), 8.58 (broad s, 3H);

$^{31}P$ NMR (ppm, $CD_2Cl_2$, no decoupling): 4.45 (s), 8.50 (s), 11.51 (s), 15.44 (broad m);

$^{31}P$ NMR (ppm, $CH_2Cl_2$): 7.64 (broad s), 11.45 (s);

$^{19}F$ NMR (ppm, $CD_2Cl_2$): -78.9.

**Preparation of $[DipN=P-Cl]_2$, 6.6.**

A degassed sample of $DipNH_2$ (4.759g, 26.8 mmol) was dissolved in diethylether (40 ml) producing a pale pink solution and stirred at 0°C under nitrogen in a bulb equipped with a septum. A yellow solution of $^nBuLi$ in hexane (1.6 M, 17.0 ml, 27.2 mmol) was added to this resulting in the instant formation of a yellow solution which was allowed to warm to room temperature and stirred overnight. The resultant slurry of yellow solution and white solid was added over a period of 10 minutes to a stirred colourless solution of $PCl_3$ in pentane. Each aliquot added produced an orange colour which quickly faded to pale yellow upon mixing and resulted in the production of white solid. The mixture was stirred overnight then the pale yellow liquid was decanted from the solid and volatiles were removed *in vacuo* (dynamic) to yield a pale yellow oil ($DipN(H)PCl_2$). The oil was dissolved in pentane then frozen. Triethylamine (*ca.* 20 ml, large excess) was distilled onto this and the mixture was allowed to thaw then was stirred overnight. This resulted in a

yellow/orange liquid and copious amounts of white solid which was filtered to yield a clear orange solution. Removal of volatiles (liquid nitrogen) yielded an orange oil which crystallized upon standing to form copious amounts of diamond shaped crystals (some as large as 10 mm per side). These crystals were characterized as *cis*-diazadiphosphetidine $[Dip\text{-}N{=}P\text{-}Cl]_2$, yield: 0.936 g, 3.873 mmol, 14 % (first crop), mp. 197-202°C.

Anal. Calcd. C, 59.63; H, 7.09; N, 5.80%;
Found C, 59.54; H, 7.20; N, 5.76%;

IR ($cm^{-1}$): 3071w(sh), 3060w, 2724vw, 1945vw, 1586vw, 1383m, 1346w(sh), 1320m, 1280w, 1276m(sh), 1260m(sh), 1249m, 1198s, 1180m, 1147w, 1104m, 1056w, 1039m, 974w, 965vw(sh), 935m(sh), 923s(sh), 907s, 801s, 747vw, 600w, 537m, 529m, 496s, 452w(sh), 421s, 379w;

Raman ($cm^{-1}$) 166 mW: 85vs, 102s(sh), 132s, 173s, 245m, 290m, 339w, 419m, 447m, 496m, 537m, 573w, 632m, 886m, 955w, 981w, 1046m, 1107m, 1163w, 1180w, 1224w, 1280vs, 1314w, 1338m, 1384w, 1443m, 1461m, 1589s, 2518w, 2712w, 2756w, 2864s, 2907s(sh), 2930vs, 2949s(sh), 2963s, 3027w, 3060m, 3087w(sh), 3170w;

$^1H$ NMR (ppm, $CD_2Cl_2$): 1.33 (d, $^3J_{H\text{-}H}$ 6.72 Hz, 12H), 3.6-4.4 (broad s, 2H), 7.18-7.34 (m, 3H);

$^{13}C$ NMR (ppm, $CD_2Cl_2$): 25.6, 29.6, 124.7, 129.2, 131.0 (t, $^2J_{P\text{-}C}$ 7.15 Hz), 149.5 (br);

$^{31}P$ (ppm, $CD_2Cl_2$): 211.9 ppm;

Crystal data: monoclinic, space group: $P2_1/a$ (#14), a = 9.814(9) Å, b = 17.579(8) Å, c = 16.002(5) Å, β = 103.37(4)°; V = 2686(3) $Å^3$, $D_{calc}$ = 1.195 $g/cm^3$, $R_1$ = 0.068.

**Preparation of $[DipN=P-OTf]_2$, 6.7.**

A mixture of $[DipNPCl]_2$ (0.362g, 0.749 mmol) and AgOTf (0.402g, 1.565 mmol) were placed in a bulb and hexane (30 ml) was distilled onto this to produce a pale orange suspension. This was stirred in the dark overnight resulting in copious amounts of white precipitate and a colourless solution. The mixture was filtered through a fiberglass frit yielding a colourless solution. Slow removal of solvent by tap distillation resulted in the deposition of very large (4mm/side) diamond-shaped crystals which were characterized as $[DipNPOTf]_2$ (multinuclear NMR shows formation of both cis (75%) and trans (25%) diazadiphosphetidines), yield: 0.362g, 0.501 mmol, 68%, m.p. 127-130°C (trans isomer) and 182-184°C (cis isomer).

Anal. Calcd. C, 43.94; H, 4.82; N, 3.94%;
Found C, 44.10; H, 4.87; N, 4.39%;

IR ($cm^{-1}$): 3064vw, 2722vw, 2678vw(br), 1589vw, 1444s, 1406vs, 1386s, 1367s, 1344w, 1317m, 1294w, 1261m(sh), 1240vs, 1213vs(br), 1186vs, 1139vs, 1105m, 1056w, 1038w, 974 vw(br), 936w, 924.7s, 872s, 836vs(br), 801vs, 767s, 665m, 633.6m, 624m(sh), 613m(sh), 603s, 574vw, 548w, 525w, 512w, 466w, 428w, 401vw, 382s, 305w;

Raman ($cm^{-1}$) 166 mW: 83s, 105s, 134s, 180m, 254m, 280m, 313m, 338w, 402w,

449w, 538w, 569w, 599w, 663m, 732w, 768m, 800w, 835w, 869m, 887m, 955w, 984w, 1050m, 1105m, 1142w, 1167w, 1182w, 1221w, 1242m(sh), 1275vs, 1333m, 1405w, 1445m, 1463m, 1590s, 2520w, 2719w, 2766w, 2871s, 2913vs(sh), 2936vs, 2971s, 3031w, 3065m, 3085m(sh), 3173w;

$^{1}$H NMR (ppm, $CD_2Cl_2$): 1.26-1.43 (broad m, 12H), 3.17-3.79 (broad m, 2H), 7.23-7.46 (broad m, 3H) (the overlapping signals from the cis and trans products do not allow for proper assignment);

$^{13}$C NMR (ppm, $CD_2Cl_2$): 25.4 (Me), 29.9 (d, J 7.63 Hz, $\underline{C}HMe_2$), 118.7 (q, $^{1}J_{C-F}$ 319.96 Hz, $CF_3$), 125.2, 129.0 (t, $^{2}J_{P-C}$ 7.15 Hz), 130.2, 147.1;

$^{31}$P (ppm, $CD_2Cl_2$): 177.5 (m, 75% overall intensity, cis **6.7**), 273.9 (m, 25% overall intensity, trans **6.7**) ppm;

$^{19}$F NMR (ppm, $CD_2Cl_2$): -75.1 (broad "t", "J" 8.72 Hz, 75% overall intensity, cis **6.7**), -76.3 (broad "d", "J" 15.25 Hz, 25% overall intensity, trans **6.7**).

Crystal data (cis isomer): monoclinic, space group: $P2_1/c$ (#14), a = 10.772(2) Å, b = 29.335(3) Å, c = 11.170(2) Å, $\beta$ = 106.53(1)°; V = 3384.0(9) Å$^3$, $D_{calc}$ = 1.395 g/cm$^3$, $R_1$ = 0.048.

**Preparation of ClP($\mu$-NDip)$_2$POTf, 6.9.**

A mixture of $[DipNPCl]_2$ (0.230g, 0.48 mmol) and AgOTf (0.165g, 0.64 mmol)

were placed in a bulb and hexane (30 ml) was distilled onto this to produce a pale orange suspension. This was stirred in the dark for seven days resulting in copious amounts of white precipitate and a colourless solution. The mixture was filtered through a fiberglass frit yielding a colourless solution. Slow removal of solvent by tap distillation resulted in the deposition colourless cube-shaped crystals which were characterized as a mixture of $ClP(\mu\text{-}NDip)_2POTf$ (61% total integration), $[DipNPCl]_2$ (4%) and $[DipNPOTf]_2$ (multinuclear NMR shows formation of both cis (26%) and trans (9%) diazadiphosphetidines), yield: 0.110g, 0.18 mmol, 39%, m.p. 119-123 °C.

IR ($cm^{-1}$): 3063w, 2728w, 2671w, 1588w, 1525w, 1404M(sh), 1397m, 1366s, 1345m, 1318m, 1278s, 1251s(br), 1201s(sb), 1145s, 1106m, 1055m, 1037m, 974m, 960m, 935m(sh), 925m, 909m(sh), 849m(br), 801s, 766m, 736wm 665wm 635nm 609m, 595w(sh), 539w, 525w, 513w, 489w, 425w, 378w, 304w, 249w;

Raman ($cm^{-1}$) 166 mW: 81m, 136s, 178m, 252m(sh), 283m, 314m, 339w(sh), 448w, 539w, 647m, 768m885m, 956w, 984w, 1050m, 1106m, 1178w, 1276vs, 1337m, 1403w, 1447s, , 1590s, 2719w, 2764w, 2871s, 2933vs, 2970vs, 3027m, 3066s;

$^1H$ NMR (ppm, $CD_2Cl_2$): 1.33 (m, 12H), 3.4-4.0 (broad s, 2H), 7.24-7.46 (m, 3H);

$^{13}C$ NMR (ppm, $CD_2Cl_2$): 26.1, 39.9 (br), 118.7 (q, $^1J_{F\text{-}C}$ 320.0 Hz), 125.0, 129.7, 148.0 (br);

$^{31}P$ (ppm, $CD_2Cl_2$): 189.3 ppm (d of d, $^2J_{P\text{-}P}$ = 62.9 Hz, $^4J_{F\text{-}P}$ = 17.4 Hz, 1P), 203.2 (d, $^2J_{P\text{-}P}$ = 62.9 Hz, 1P);

$^{19}F$ NMR (ppm, $CD_2Cl_2$): -75.9 (d, $^4J_{F-P}$ = 17.4 Hz).

**Preparation of $DipN(PCl_2)_2$, 6.8.**

A degassed sample of $DipNH_2$ (5.00g, 28.2 mmol) was dissolved in hexane (30 ml), frozen and placed under vacuum. $PCl_3$ (20 ml) and $NEt_3$ (40 ml) were distilled onto the mixture which was then warmed to room temperature and mixed resulting in the formation of a yellow colour and a copious amount of white precipitate. The mixture was stirred for one week then filtered producing a darker yellow solution which yielded a yellow/orange solid upon removal of solvent. The solid was sublimed at 80°C under static vacuum resulting in the formation of pale tan crystals characterized as $DipN(PCl_2)_2$; yield 5.30 g, 14.0 mmol, 49.6%, m.p. 69.5-71.0°C.

Anal. Calcd. C, 38.03; H, 4.52; N, 3.70%;
Found C, 38.08; H, 4.52; N, 3.75%;

IR ($cm^{-1}$): 3060w(br), 2725w, 2144w, 1947w, 1871w, 1794w, 1716w, 1700w, 1639w, 1584m, 1541w, 1433s, 1362s, 1346m, 1322m, 1309m, 1259m, 1249m,, 1240m, 1197w, 1180w, 1158s, 1104m, 1095m, 1050m, 1040m, 975w, 954w, 931m, 903s, 883s(br), 799s, 744m, 717m, 633w, 611w, 544w, 533w, 515s, 490s, 481s, 451m, 437m, 431m, 417m, 310m;

Raman ($cm^{-1}$) 193 mW: 109m, 131msh, 154m, 168m(sh), 192m, 227w, 243w(sh), 283m, 313m, 355w, 419m, 437wsh, 454s, 476s, 515w, 534w, 544w, 612w, 719w, 881w, 903w, 954w, 1042w, 1102w, 1159w, 1240m, 1346w, 1443w, 1461w, 1585m, 2863m, 2909m, 2937m(sh), 2957s, 2957s, 2980m(sh), 3025w, 3061m;

$^{1}$H NMR (ppm, $CD_2Cl_2$): 1.19 (d, $^{3}J_{H-H}$ 7.00 Hz, 12H), 3.12 (sept, $^{3}J_{H-H}$ 7.00 Hz, 2H), 7.26 (m, 3H);

$^{13}$C NMR (ppm, $CD_2Cl_2$): 25.2, 30.1, 125.4, 130.6, 150.0;

$^{31}$P (ppm, $CD_2Cl_2$): 164.7 ppm.

Crystal data: monoclinic, space group: $P2_1/a$ (#14), a = 14.34(1) Å, b = 9.455(4) Å, c = 26.478(9) Å, β = 103.70(5)°; V = 3487(3) Å$^3$, $D_{calc}$ = 1.444 g/cm$^3$, $R_1$ = 0.074.

**Preparation of Mes*N(TMS)$PnCl_2$ derivatives.**

In a typical reaction, a solution of $^{n}$BuLi (1.6 M in hexane) was slowly added through a septum to a cooled (0°C) equimolar solution of Mes*NH(TMS) (*ca.* 1.0 g, 2.4 mmol) in diethyl ether (50 ml) under nitrogen in one chamber of the reactor. This was stirred and allowed to warm to room temperature then stirred for an additional 2 hours, producing a dark yellow solution. The mixture was then added over a period of 15 minutes to a stirring solution of $PnCl_3$ (excess for Pn = P, As, equimolar for Pn = Sb) in diethyl ether (30 ml) producing coloured solutions (Pn = P, intense orange solution; Pn = As, peach solution; Pn = Sb, yellow solution) and depositing a white precipitate (LiCl). The reaction mix was isolated in a bulb and the septum bulb was removed and replaced with a flame dried fritted bulb. The reaction mixture was frozen, the reactor was evacuated and the mixtures were allowed to stir for 2 days then filtered to yield clear coloured solutions. Diethyl ether was removed by the "soft liquid nitrogen method" to yield crystalline solids.

**Characterization of Mes*N(TMS)$PCl_2$, 7.13.**

Cube shaped orange crystals; yield 0.61 g, 1.39 mmol, 81 %; m.p. 65-75°C;

IR ($cm^{-1}$): 3331m, 3302w, 3097w, 3075w, 1601m, 1423m, 1392m, 1363s, 1325m, 1286w, 1263m(sh), 1258m, 1251m, 1217s, 1199m, 1189w(sh), 1168w, 1113m, 1087m, 1021w, 943s, 920m, 903m, 880m, 849s(br), 820w(sh), 807w(sh), 766w, 650w, 641w, 560w(sh), 549m(sh), 542m, 524m, 488s, 476m, 454s, 402w(br), 377w(sh);

Raman ($cm^{-1}$) 166 mW: 88m, 137m, 160m(sh), 177m(sh), 249w, 320vw(br), 376w, 458m, 488w, 542w, 569w, 641w, 822m, 922w(br), 1024w, 1062w, 1086w, 1114w, 1135w, 1147w, 1199w(br), 1244w, 1292w, 1362w, 1454s, 1600m, 2708w, 2779w, 2908s, 2963s, 3098w, 3329w;

$^1H$ NMR (ppm, $CD_2Cl_2$): 0.27 (s, 9H, TMS), 1.30 (s, 9H, p-$^t$Bu), 1.54 (s, 18H o-$^t$Bu), 7.46 (s, 2H, Ar-H);

$^{31}P$ (ppm, $CD_2Cl_2$): 175.2.

Crystal data: Orthorhombic, space group: Pbca (#61), a = 19.85(1) Å, b = 19.568(8) Å, c = 12.82(1) Å; V = 4978(4) $Å^3$, $D_{calc}$ = 1.159 $g/cm^3$, $R_1$ = 0.063.

**Note:** Most of the following reactions are characterized by spectroscopic methods only. The relative purity of samples was estimated on the basis of $^{1}H$, $^{19}F$ or $^{31}P$ NMR integration. This project is being continued by D. Walsh and she will report the complete characterization of these compounds in the future.

**Characterization of Mes*N(TMS)$AsCl_2$, 7.14.**

Cube shaped pale yellow crystals; yield 0.514 g, 1.07 mmol, 49%; m.p. 109-110°C;

Anal. Calcd. C, 52.72; H, 8.01; N, 2.93%;
Found C, 53.03; H, 8.02; N, 2.96%;

IR ($cm^{-1}$): 3409w, 1602w, 1425m, 1393m, 1363s, 1273m(sh), 1256s, 1240m(sh), 1216m, 1199m, 1171m, 1137w, 1114w, 1096m, 1025w(br), 911m, 868s, 842s(sh), 816m(sh), 769w(sh), 753m(br), 695w, 674w, 644w, 545w, 475m, 432w(sh), 368s, 326m;

Raman ($cm^{-1}$) 166 mW: 120m, 136w(sh)155m, 189w, 235w, 255w, 322m, 362s, 430w, 479w, 571w, 635w, 676w, 743w, 818w, 866w, 922w, 1027w, 1094w, 1134m, 1179w, 1197w, 1240w, 1285w, 1362w, 1444w, 1601m, 2709w, 2779w, 2905s, 2965s, 3089w;

$^{1}H$ NMR (ppm, $CD_2Cl_2$): 0.27 (s, 9H, TMS), 1.28 (s, 9H, p-$^{t}$Bu), 1.54 (s, 18H, o-$^{t}$Bu), 7.48 (s, 2H, Ar-H);

$^{1}H$ NMR (ppm, THF-D8): 0.34 (s, 9H, TMS), 1.31 (s, 9H, p-$^{t}$Bu), 1.56 (s, 18H, o-

$^{t}$Bu), 7.53 (s, 2H, Ar-H);

$^{13}$C NMR (ppm, $CD_2Cl_2$): 4.5, 31.2, 33.7, 35.4, 38.6, 122.4, 126.2, 148.5, 150.7.

Crystal data: Orthorhombic, space group: Pbca (#61), a = 19.771(2) Å, b = 19.607(2) Å, c = 12.940(2) Å; V = 5016.3(7) Å$^3$, $D_{calc}$ = 1.267 g/cm$^3$, $R_1$ = 0.042.

**Characterization of Mes*N(TMS)SbCl$_2$, 7.15.**

Yellow solid (not suitable for X- ray crystallography); yield 0.74g, 1.41 mmol, 89%, m.p. broad: 96-110°C;

IR (cm$^{-1}$): 3515w, 3448w, 1601w, 1393m, 1377m, 1269m, 1252s, 1237m, 1215m, 1198w, 1172m, 1137w, 1100s, 1024w(br), 910m, 865s(br), 813m(sh), 772w(sh), 754m, 690w, 671w, 643m, 540w, 471m, 458w(sh), 418w, 376w, 339s, 314s, 280w, 247w, 227w;

Raman (cm$^{-1}$) 166 mW: 91w, 132m(sh), 148m, 212w, 258w, 313m, 338s, 430w, 571m, 630w, 690w, 712w, 823m, 921w, 1027w, 1100w, 1137m, 1173w, 1199w, 1283w, 1447m, 1601m, 2709w, 2779w, 2904s, 2963s, 3081w;

$^1$H NMR (ppm, $CD_2Cl_2$): 0.31 (s, 9H, TMS), 1.29 (s, 9H, p-$^{t}$Bu), 1.57 (s, 18H, o-$^{t}$Bu), 7.47 (s, 2H, Ar-H).

**Preparation of Mes*N(H)AsCl$_2$, 7.17.**

A pale yellow 1.6 M solution of $^{n}$BuLi in hexane (9.6 ml, 15.4 mmol) was added

to a stirred 0°C colourless solution of Mes*$NH_2$ (3.93 g, 15.0 mmol) over a period of 15 minutes resulting in the formation of a yellow solution. This was allowed to warm to room temperature and stirred overnight. The yellow mixture was added to $AsCl_3$ (1.5 ml, 17.8 mmol) resulting in a pinkish solution with copious amounts of white precipitate. This was stirred overnight then filtered through a fiberglass frit. The resultant tan solution was concentrated by the soft liquid nitrogen method. This produced small beige crystals characterized as Mes*N(H)$AsCl_2$, yield: 5.75g, 14.2 mmol, 94%, mp. 60-65 °C.

IR ($cm^{-1}$): 3520w, 3453w, 3406m(sh), 3386s, 3095w, 2744w, 2713w, 1768w, 1620w, 1598m, 1558w, 1434s(sh), 1420s, 1393s, 1361s, 1286m, 1265m, 1240w, 1216s, 1201s(sh), 1190s(sh), 1114s, 1022w, 928w, 880s, 834s, 816m, 792m, 769w, 757m, 642m, 547w, 466m, 361s, 332s(sh), 281m;

Raman ($cm^{-1}$) 166 mW: 85w, 128m, 155m, 189m, 267m, 336m(sh), 370s, 570m, 637w, 754w, 820m, 844w, 930m, 1116w, 1146m, 1192m, 1218m(sh), 1241w, 1288mj, 1393w, 1444m, 1468m, 1599m, 2706m, 2782w, 2911vs, 2967vs, 3034m, 3099w, 3385w;

$^1H$ NMR (ppm, $CD_2Cl_2$): 1.30 (s, 9H, p-$^t$Bu), 1.51 (s, 18H, o-$^t$Bu), 5.85 (broad s, N-H), 7.38 (s, 2H, Ar-H).

Crystal data: Orthorhombic, space group: Pbca (#61), a = 16.412(3) Å, b = 25.188(2) Å, c = 10.088(3) Å; V = 4170(1) $Å^3$, $D_{calc}$ = 1.294 $g/cm^3$, $R_1$ = 0.046.

**Preparation of Mes*N=As-Cl (and decomposition products) from Mes*N(TMS)PnCl$_2$.**

**Thermolysis of solid Mes*N(TMS)PCl$_2$.**[250]

A sample of solid orange Mes*N(TMS)PCl$_2$ to 80°C under a nitrogen atmosphere resulted in the formation of an oily red solid characterized as Mes*N=P-Cl by $^{31}$P NMR (δ 136.6 ppm: 65% of total integration) (with unidentified by-products: δ 153.2 ppm: 5%, δ 220.4 ppm: 35%).

A sample of Mes*N(TMS)PCl$_2$ in a melting point capillary was heated to 130°C in a melting point apparatus resulting in the formation of a dark red melt which cooled to produce a dark red solid. Raman spectroscopy indicates a mixture of Mes*N(TMS)PCl$_2$ and Mes*N=P-Cl.

**Thermolysis of solid Mes*N(TMS)AsCl$_2$.**

Solid Mes*N(TMS)AsCl$_2$ (0.500g) was sealed *in vacuo* in a reaction tube which was placed in a 240°C oven for 3 hours. This resulted in the deposition of a metallic mirror (As metal) on the inside of the tube.

Pale yellow crystals of Mes*(TMS)AsCl$_2$ (0.050g) under an atmosphere of nitrogen were heated to 130°C in a bulb on a three-neck reactor submerged in an oil bath. This produced bubbling and resulted in the darkening of the melt. The reactor was exposed to dynamic

vacuum resulting in the deposition of pale yellow crystals on the cool sides of the reaction bulb which were dissolved in $CD_2Cl_2$. Proton and $^{13}C$ NMR indicate the presence of $Mes^*N(TMS)AsCl_2$ only.

Samples of $Mes^*N(TMS)AsCl_2$ in melting point capillaries were heated to 130°C in a melting point apparatus resulting in the formation of a purple/red melt which cooled to produce a colourless solid, shown by Raman spectroscopy to be $Mes^*N(TMS)AsCl_2$. The samples were then heated to 190°C producing a dark purple/red melt which cooled to a red/brown solid. The Raman spectrum of the solid shows the loss of the signals due to the TMS and $AsCl_2$ vibrations:

Raman ($cm^{-1}$) 166 mW: 150m(br), 254w, 303m, 343w(sh), 381m, 473w, 514w, 566m, 589w(sh), 639w, 679w, 724w, 761w(sh), 781w, 826m, 923m, 1078w, 1117w, 1144m, 1199m, 1239w, 1266w, 1293w, 1365w, 1400w, 1451m(br), 1601m, 2668w(br), 2708w, 2787w, 2904s, 2963s, 3110w, 3195w.

The Raman spectrum of the product is almost identical to that of the cyclodecomposition product **7.19** (*vide infra*).

**Thermolysis of $Mes^*N(TMS)AsCl_2$ in solution.**

A solution of $Mes^*N(TMS)AsCl_2$ in THF-$D_8$ in a sealed NMR tube was heated in an oil bath at 70°C for 4 hours resulting in the appearance of a slight pink colour. Proton NMR of the solution reveals formation of a new series of signals:

$^1H$ NMR (ppm, $CD_2Cl_2$): 0.30 (s, 9H), 1.31 (s, 9H), 1.45 (s, 18H), 7.36 (s, 2H);

Further heating for 9 hours at 100°C resulted in an increase in the intensity of these peaks relative to those of the starting material. Caution: Heating at 120°C caused the NMR tube to explode after 8 hours. Heating of a sample of Mes*N(TMS)$AsCl_2$ in $CD_2Cl_2$ resulted in no apparent change by $^1H$ NMR.

**Preparation of Mes*N=As-Cl, 7.20 derivatives from Mes*N(H)$AsCl_2$**

In a typical reaction a colourless solution of triethylamine (*ca.* 3.6 g, 36 mmol) in the selected solvent (*ca.* 30 ml) was added rapidly to a shaken yellow solution of Mes*N(H)$AsCl_2$ (*ca.* 1g, 2.5 mmol) in the solvent (*ca.* 30 ml) (some also contained an equimolar amount of triphenylphosphine or an excess of pyridine- *vide infra*). This resulted in the immediate formation of dark red solutions with an off-white precipitate. The solutions were then filtered through fiberglass filters and aliquots of the solution were isolated in NMR tubes. Volatiles were removed *in vacuo* and the solid residue was dissolved in $CD_2Cl_2$. NMR identification for the reactions are listed below:

**NMR identification of Mes*N=As-Cl 7.20 and its cyclo-decomposition product, 7.19. (toluene)**

Reaction of Mes*N(H)$AsCl_2$ with triethylamine in toluene gave a mixture with a $^1H$ NMR spectrum that shows a marked reduction in the signal for the amino proton and is indicative of the resultant formation of Mes*N=As-Cl (>90% of total signal integration is assigned to this product):

$^1H$ NMR (ppm, $CD_2Cl_2$): 1.33 (s, 9H, p-$^t$Bu), 1.54 (s, 18H, o-$^t$Bu), 7.41 (s, 2H, Ar-H);

The remaining signals are assigned to the cyclo-decomposition product **7.20** of Mes*N=As-Cl:

$^1$H NMR (ppm, $CD_2Cl_2$): 1.32 ppm (s, 9H, p-$^t$Bu), 1.46 and 1.47 (two overlapping s, 15H total, 4-$^t$Bu and 2-$CMe_2$), 2.47 (very broad m, 2H, $CH_2$-As), 5.95 (broad s, 1H, N-H), 7.28 (d, $^4J_{H-H}$ 2.14 Hz, Ar-H), 7.32 (d, $^4J_{H-H}$ 2.14 Hz, Ar-H).

The structure of the heterocycle **7.19** is confirmed by X-ray crystallographic analysis:

Crystal data: monoclinic, space group: $P2_1/a$ (#14), a = 12.088(2) Å, b = 9.614(1) Å, c = 16.7819(7) Å, $\beta$ = 107.343(6)°; V = 1861.6(3) Å$^3$, $D_{calc}$ = 1.319 g/cm$^3$, $R_1$ = 0.0399.

**NMR identification of Mes*N=As-Cl (toluene and pyridine)**

Reaction of Mes*N(H)As$Cl_2$ with an excess of both triethylamine and pyridine in toluene gave Mes*N=As-Cl (42% total signal integration):

$^1$H NMR (ppm, $CD_2Cl_2$): 1.31 (s, 9H, p-$^t$Bu), 1.51 (s, 18H, o-$^t$Bu), 7.38 (s, 2H, Ar-H);

the cyclo-decomposition product **7.19** (33% total signal integration):

$^1$H NMR (ppm, $CD_2Cl_2$): 1.32 ppm (s, 9H, p-$^t$Bu), 1.47 (broad s, 15H total, 4-$^t$Bu and 2-$CMe_2$), 2.35 (d, $^2J_{H-H}$ 13.63 Hz, 1H, $CH_2$-As), 2.63 (d, $^2J_{H-H}$ 13.63 Hz, 1H, $CH_2$-As), 5.95 (broad s, 1H, N-H), 7.28 (d, $^4J_{H-H}$ 2.45 Hz, 1H, Ar-H), 7.32 (d, $^4J_{H-H}$ 2.45 Hz, 1H) Ar-H);

and a product containing a more deshielded Mes* substituent, tentatively characterized as

Mes*N=As-Cl•pyr **7.21** (25%):

$^1$H NMR (ppm, $CD_2Cl_2$): 1.28 (s, 9H, p-$^t$Bu), 1.44 (s, 18H, o-$^t$Bu), 7.19 (s, 2H, Ar-H), and the only observed pyridine signals: 7.44 (d, $^3J_{H-H}$ 2.24 Hz, Ar-H), 7.51 (d, $^3J_{H-H}$ 2.44 Hz, Ar-H), 7.55 (d, $^3J_{H-H}$ 2.74 Hz, Ar-H).

**NMR identification of Mes*N=As-Cl•$PPh_3$, 7.22 (toluene)**

Reaction of equimolar amounts of Mes*N(H)$AsCl_2$ and triphenylphosphine with an excess of triethylamine in toluene gave Mes*N=As-Cl•$PPh_3$ (*ca.* 80% total integration):

$^1$H NMR (ppm, $CD_2Cl_2$): 1.32 (s, 9H, p-$^t$Bu), 1.54 (s, 18H, o-$^t$Bu), 7.25-7.42 (broad m, 17H, Ar-H atoms on Mes* and $PPh_3$ molecules);

$^{31}$P NMR (ppm, $CD_2Cl_2$): -5.1 (s);

and numerous small signals from unidentified products (*ca.* 20% total integration).

**NMR identification of Mes*N=As-Cl•$OEt_2$ (diethyl ether)**

Reaction of Mes*N(H)$AsCl_2$ with an excess of triethylamine in diethyl ether gave Mes*N=As-Cl•$OEt_2$:

$^1$H NMR (ppm, $CD_2Cl_2$): 0.95 (broad s, 6H, O-$CH_2C\underline{H}_3$), 1.32 (s, 9H, p-$^t$Bu), 1.49 (s, 18H, o-$^t$Bu), 2.49 (broad s, 4H, O-$C\underline{H}_2CH_3$), 7.38 (s, 2H, Ar-H).

**Preparation of Mes*N(TMS)As(Cl)OAr, 7.23**

A colourless solution of Li-O-Ar (0.111 g, 0.49 mmol) in diethyl ether (30 ml) was added to a pale yellow solution of Mes*N(TMS)$AsCl_2$ (0.233 g, 0.48 mmol) in diethyl ether (50 ml) resulting in the formation of a pale pink solution and a white precipitate. The mixture was stirred for three days then filtered, to give a clear pale pink solution. Removal of solvent by the "tap method" afforded a purple oil which was dissolved in hexane and refiltered to give a pale pink solution. Removal of solvent by the "tap method" and washing by back-distillation gave a colourless solid characterized as Mes*N(TMS)As(Cl)OAr; yield 0.095 g, 0.17 mmol, 36%, m.p. 144-147°C;

IR ($cm^{-1}$): 1437m, 1420w, 1405m, 1395m, 1386m, 1361s, 1254s, 1214w, 1168m, 1099m, 912w, 882m, 876m, 853m, 839m, 814w, 775m, 756w, 690w, 649w, 621w, 553m, 487w, 460w;

Raman ($cm^{-1}$) 166 mW: 100m, 139m, 227m, 273m, 358m, 408w, 463w, 553w(sh), 569m, 620w, 642w, 686w, 717w, 769w, 817m, 875w, 927w, 1026w, 1104w, 1140w, 1173m, 1200w(sh), 1258w, 1284w, 1379w(sh), 1408w(sh), 1449m, 1565w, 1600m, 2710w, 2781w, 2906vs, 2965s, 3056m, 3199w;

$^1H$ NMR (ppm, $CD_2Cl_2$): 0.51 (s, 9H, TMS), 1.33 (9H, p-$^t$Bu), 1.51 (18H, o-$^t$Bu), 1.66 (18H, o-$^t$Bu), 2.22 (3H, p-Me), 6.96 (2H, Ar-H), 7.55 (2H, Ar-H).

**NMR identification of Mes*N=As-OAr, 7.25**

A colourless solution of TMS-OTf (2.46 g, 11.0 mmol) in toluene (5 ml) was added to a pale pink solution of Mes*N(TMS)As(Cl)OAr (0.035 g, 0.07 mmol) in toluene (10 ml) which resulted in the immediate formation of a dark purple solution. An aliquot of this solution was decanted into an NMR tube and volatiles were removed *in vacuo*. The principal product of the reaction is characterized as Mes*N=As-OAr (*ca.* 65% total signal integration):

$^1$H NMR (ppm, $CD_2Cl_2$): 1.32 (9H, p-$^t$Bu), 1.49 (18H, o-$^t$Bu), 1.53 (18H, o-$^t$Bu), 2.29 (3H, p-Me), 7.12 (2H, Ar-H), 7.40 (2H, Ar-H);
and numerous small signals from TMS-OTf and several unidentified products (*ca.* 35% total integration).

**Preparation of Mes*N=As-OTf, 7.25 derivatives from Mes*N(TMS)$AsCl_2$**

In a typical reaction, Mes*N(TMS)$AsCl_2$ (*ca.* 0.20 g, 0.42 mmol) and AgOTf (0.12 g, 0.45 mmol) were placed in one compartment (equipped with a filter) of a 3 compartment vessel. Solvent (*vide infra*) was distilled into the compartment which gave a yellow solution. This was stirred in the dark for three days then an aliquot was filtered into an NMR tube and volatiles were removed *in vacuo*. The resultant yellow or orange residue was dissolved in $CD_2Cl_2$. In all cases the TMS moiety is absent (or a very minor component) in the $^1$H NMR spectra of the reaction mixtures.

**NMR identification of Mes*N=As-OTf (hexane)**

For a reaction done in hexane a significant component of the solution was characterized as Mes*N=As-OTf (*ca.* 50% of total signal integration):

$^1$H NMR (ppm, $CD_2Cl_2$): 1.29 (s, 9H, p-$^t$Bu), 1.51 (s, 18H, o-$^t$Bu), 7.52 (s, 2H, Ar-H);

the other component (*ca.* 50% of total signal integration) displays similar chemical shifts:

$^1$H NMR (ppm, $CD_2Cl_2$): 1.32 (s, 9H, p-$^t$Bu), 1.60 (s, 18H, o-$^t$Bu), 7.38 (s, 2H, Ar-H);

$^{19}$F NMR (ppm, $CD_2Cl_2$): -77.9 (s).

Another reaction in hexane produced Mes*N=As-OTf as a minor product (*ca.* 30% of total signal integration) and the principal component of the reaction mixture was characterized as the cyclodecomposition product **7.26** of Mes*N=As-OTf:

$^1$H NMR (ppm, $CD_2Cl_2$): 1.33 ppm (s, 9H, p-$^t$Bu), 1.48 (s, 9H, 4-$^t$Bu), 1.58 (s, 6H, 2-$CMe_2$), 2.50 (broad "s", 2H, As-$CH_2$), 6.04 (broad s, 1H, N-H), 7.29 (d, $^4J_{H-H}$ 2.13 Hz, Ar-H), 7.34 (d, $^4J_{H-H}$ 2.14 Hz, Ar-H).

$^{19}$F NMR (ppm, $CD_2Cl_2$): -77.9 (s).

**NMR identification of Mes*N=As-OTf (toluene)**

For a reaction done in toluene the principal component of the reaction mixture was characterized as Mes*N=As-OTf (*ca.* 85% of total signal integration):

$^1$H NMR (ppm, $CD_2Cl_2$): 1.28 (s, 9H, p-$^t$Bu), 1.54 (s, 18H, o-$^t$Bu), 7.48 (s, 2H, Ar-H);

$^{19}$F NMR (ppm, $CD_2Cl_2$): -77.4 (s);

the other product was characterized as [Mes*N(H)AsN(H)Mes*][OTf] (*ca.* 15%) (*vide infra*).

**NMR identification of Mes*N=As-OTf•$Et_2O$ (diethyl ether)**

For a reaction done in diethyl ether the principal component of the solution was characterized as Mes*N=As-OTf•$Et_2O$ (*ca.* 65% of total signal integration):

$^1$H NMR (ppm, $CD_2Cl_2$): 1.14 (t, $^3J_{H-H}$ 7.02 Hz, 3H, $OCH_2C\underline{H}_3$), 1.30 (s, 9H, p-$^t$Bu), 1.56 (s, 18H, o-$^t$Bu), 3.43 (q, $^3J_{H-H}$ 7.02 Hz, 3H, $OC\underline{H}_2CH_3$), 7.53 (s, 2H, Ar-H);

$^{13}$C NMR (ppm, $CD_2Cl_2$): 15.5, 31.0, 33.7, 34.1, 37.2, 66.0, 124.2, 132.2, 148.3, 151.5, (q for $CF_3$ group is not observed);

$^{19}$F NMR (ppm, $CD_2Cl_2$): -78.2 (s);

and numerous small signals from unidentified products (*ca.* 35% total integration).

**Preparation of [Mes*N(H)AsN(H)Mes*][OTf], 7.27**

A colourless mixture of triflic acid (HOTf) (0.24 g, 1.6 mmol) in hexane (20 ml) was added to a stirred dark purple solution of Mes*N=AsN(H)Mes* (0.503 g, 0.85 mmol) in hexane (60 ml) which resulted in the rapid (less than one minute) formation of a bright yellow opaque mixture. This was stirred overnight then filtered to give a clear yellow solution and an aliquot was decanted into an NMR tube then volatiles were removed *in vacuo*. The yellow residue was dissolved in $CD_2Cl_2$ and characterized as [Mes*N(H)AsN(H)Mes*][OTf]:

$^1$H NMR (ppm, $CD_2Cl_2$): 1.31 (18H, p-$^t$Bu), 1.55 (36H, o-$^t$Bu), 7.49 (4H, Ar-H), 8.55 (broad, 2H, N-H);

$^{13}$C NMR (ppm, $CD_2Cl_2$): 31.3, 31.8, 34.1, 35.4, 124.2, 143.9, 148.3, 152.3, (q from

$CF_3$ is not observed);

$^{19}F$ NMR (ppm, $CD_2Cl_2$): -78.7 (s);

*c.f.* [Mes*N(H)AsN(H)Mes*][OTf] from reaction of Mes*N(TMS)$AsCl_2$ and AgOTf in toluene:

$^1H$ NMR (ppm, $CD_2Cl_2$): 1.33 (18H, p-$^t$Bu), 1.56 (36H, o-$^t$Bu), 7.52 (4H, Ar-H), 8.50 (broad, 2H, N-H);

$^{13}C$ NMR (ppm, $CD_2Cl_2$): 31.4, 31.7, 34.1, 35.4, 124.2, 143.6, 148.3, 151.5, (q from $CF_3$ is not observed);

$^{19}F$ NMR (ppm, $CD_2Cl_2$): -78.2 (s);

IR ($cm^{-1}$): 3454w, 3418w, 3283w, 2729m, 2669m, 1599m, 1516w, 1424m, 1398m, 1377s, 1340w, 1312m(sh), 1296m, 1256s, 1231s, 1221s, 1209s, 1183m, 1175m, 1155m, 1109m, 1021s, 992w, 978w(sh), 930w(sh), 912w, 885w(sh), 879m, 855m, 799w, 783w, 756w, 746w(sh), 734m, 635s, 591w, 575w, 534w, 520w, 359w(sh), 350w;

Crystal data: monoclinic, space group: $P2_1/n$ (#14), a = 16.713(2) Å, b = 10.259(2) Å, c = 24.024(2) Å, $\beta$ = 93.41(1)°; V = 4112(1) $Å^3$, $D_{calc}$ = 1.200 $g/cm^3$, $R_1$ = 0.063.

**Endnotes (References)**


1. For an interesting historical discussion of the development of the periodic table see: Seaborg, G.T. *J. Chem. Soc., Dalton Trans.* **1996**, 3899-3907.

2. *CRC Handbook of Chemistry and Physics*, 77th ed. 1996-1997; Lide, D.R., Ed.; CRC Press: New York, 1996.

3. For a good introduction see: Norman, N.C. *Periodicity and the p-Block Elements*; Oxford University Press: New York, 1994.

4. Allen, L.C. *J. Am. Chem. Soc.* **1989**, *111*, 9003-9014.

5. Bondi, A. *J. Phys. Chem.* **1964**, *68*, 441-451.

6. Pauling, L. *The Nature of the Chemical Bond*, 3rd ed.; Cornell University Press: Ithaca, 1960.

7. Allen, F.H.; Kennard, O.; Watson, D.G.; Brammer, L.; Orpen, A.G.; Taylor, R. *J. Chem. Soc., Perkin Trans II.* **1987**, S1-S19.

8. Nagase, S. In *The chemistry of organic arsenic, antimony and bismuth compounds*; Patai, S., Ed.; John Wiley & Sons: New York, 1994; Chapter 1, and references therein.

9. Kutzelnigg, W. *Angew. Chem. Int. Ed. Engl.* **1984**, *23*, 272-295.

10. Cowley, A.H. *Polyhedron* **1984**, *3*, 389-432.

11. Cowley, A.H. *Acc. Chem. Res.* **1984**, *17*, 386392.

12. Norman, N.C. *Polyhedron* **1993**, *12*, 2431-2446.

13. Inorganic chemistry textbooks: (a) Huheey, J.E.; Keiter, E.A.; Keiter, R.L. *Inorganic Chemistry: Principles of Structure and Reactivity*, 4th ed.; Harper Collins: New York, 1993. (b) Cotton, F.A.; Wilkinson, G. *Advanced Inorganic Chemistry: A Comprehensive Text*, 4th ed.; John Wiley & Sons: New York, 1980. (c) Miessler, G.L.; Tarr, D.A. *Inorganic Chemistry*; Prentice Hall: Toronto, 1991. (d) Cotton, F.A.; Wilkinson, G.; Gaus, P.L. *Basic Inorganic Chemistry*, 3rd ed.; John Wiley & Sons: New York, 1995.

14. Driess, M.; Grützmacher, H. *Angew. Chem. Int. Ed. Engl.* **1996**, *35*, 828-856.

15. An excellent introduction to the importance of steric interactions is: Förster, H.; Vögtle, F. *Angew. Chem. Int. Ed. Engl.* **1977**, *16*, 429-441.

16. A historical perspective on the importance of steric interactions in organic chemistry is: Mosher, H.S.; Tidwell, T.T. *J. Chem. Educ.* **1990**, *67*, 9-14.

17. References for the ligands are found in the references for compounds containing them except the molecular bowl ligand: (a) Goto, K.; Holler, M.; Okazaki, R. *Tetrahedron Lett.* **1996**, *37*, 3141-3144. Crystal structures for bulky lithium aryl

reagents are also described: (b) Ruhlandt-Senge, K.; Ellison, J.J.; Wehmschulte, R.J.; Pauer, F.; Power, P.P. *J. Am. Chem. Soc.* **1993**, *115*, 11353-11357.

18. (a) Saito, S.; Yamamoto, H. *J. Chem. Soc., Chem. Commun.* **1997**, 1585-1592. (b) Ref. 10 (c) Ref. 11 (d) Ref. 12 (e) Ref. 14 (f) Eaborn, C.; Izod, K.; Smith, J.D. *J. Organomet. Chem.* **1995**, *500*, 89-99. (g) Wiberg, N.; Amelunxen, K.; Lerner, H.-W.; Schuster, H.; Nöth, H.; Krossing, I.; Schmidt-Amelunxen, M.; Seifert, T. *J. Organomet. Chem.* **1997**, *542*, 1-18.

19. *Multiple Bonds and Low Coordination in Phosphorus Chemistry*; Regitz, M., Scherer, O.J., Eds.; Georg Thieme Verlag: New York, 1990.

20. Tokitoh, N.; Arai, Y.; Sasamori, T.; Okazaki, R.; Nagase, S.; Uekusa, H.; Ohashi, Y. *J. Am. Chem. Soc.* **1998**, *120*, 433-434.

21. Tokitoh, N.; Arai, Y.; Okazaki, R.; Nagase, S. *Science* **1997**, *277*, 78-80.

22. (a) Su, J.; Li, X.-W.; Crittendon, R.C.; Robinson, G.H. *J. Am. Chem. Soc.* **1997**, *119*, 5471-5472. (b) Xie, Y.; Grev, R.S.; Gu, J.; Schaefer, H.F., III; Schleyer, P.v.R.; Su, J.; Li, X.-W.; Robinson, G.H. *J. Am. Chem. Soc.* **1998**, *120*, 3773-3780.

23. Cotton, F.A.; Cowley, A.H.; Feng, X. *J. Am. Chem. Soc.* **1998**, *120*, 1795-1799.

24. Klinkhammer, K.W. *Angew. Chem. Int. Ed. Engl.* **1997**, *36*, 2320-2322.

25. Su, J.; Li, X.-W.; Crittendon, R.C.; Campana, C.F.; Robinson, G.H. *Organometallics* **1997**, *16*, 4511-4513.

26. Cotton, F.A.; Feng, X. *Organometallics* **1998**, *17*, 128-130.

27. (a) Takeda, N.; Tokitoh, N.; Okazaki, R. *Angew. Chem. Int. Ed. Engl.* **1996**, *35*, 660-662. (b) Takeda, N.; Tokitoh, N.; Okazaki, R. *Tetrahedron* **1997**, *53*, 12167-12182.

28. (a) Kano, N.; Tokitoh, N.; Okazaki, R. *Chem. Lett.* **1997**, 277-278. (b) Tokitoh, N.; Matsumoto, T.; Okazaki, R. *J. Am. Chem. Soc.* **1997**, *119*, 2337-2338.

29. Kuchta, M.; Parkin, G. *Coord. Chem. Rev.*, in press.

30. (a) Märkl, G.; Sejpka, H. *Angew. Chem. Int. Ed. Engl.* **1986**, *25*, 264. (b) Hitchcock, P.B.; Jones, C.; Nixon, J.F. *J. Chem. Soc., Chem. Commun.* **1994**, 2061-2062.

31. (a) Robinson, G.H. *Main Group Chemistry News*, **1996**, *4*, 4-9, and references therein. (b) Olmstead, M.M.; Pu, L.; Simons, R.S.; Power, P.P. *J. Chem. Soc., Chem. Commun.* **1997**, 1595-1596.

32. Muira, Y.; Momoki, M.; Nakatsuji, M.; Teki, Y. *J. Org. Chem.* **1998**, *63*, 1555-1565.

33. (a) Tomioka, H.; Nakajima, J.; Mizuno, H.; Sone, T.; Hirai, K. *J. Am. Chem. Soc.* **1995**, *117*, 11355-11356. (b) Tomioka, H. *Acc. Chem. Res.* **1997**, *30*, 315-321.

34. Haubrich, S.T.; Power, P.P. *J. Am. Chem. Soc.* **1998**, *120*, 2202-2203.

35. Sekiguchi, A.; Tsukamoto, M.; Ichinohe, M. *Science* **1997**, *275*, 60-61.

36. (a) Li, X.-W.; Pennington, W.T.; Robinson, G.H. *J. Am. Chem. Soc.* **1995**, *117*, 7578-7579. (b) Li, X.-W.; Xie, Y.; Schreiner, P.R.; Gripper, K.D.; Crittendon, R.C.; Campana, C.F.; Schaefer, H.F., III; Robinson, G.H. *Organometallics* **1996**, *15*, 3798-3803. (c) Xie, Y.; Schreiner, P.R.; Schaefer, H.F., III; Li, X.-W.; Robinson, G.H. *J. Am. Chem. Soc.* **1996**, *118*, 10635-10639.

37. Niecke, E.; Fuchs, A.; Baumeister, F.; Nieger, M.; Schoeller, W. *Angew. Chem. Int. Ed. Engl.* **1995**, *34*, 555-557.

38. (a) Barclay, L.R.C.; Cooke, G.A.; Hall, N.D. *Chem. Abs.* **1961**, *55*, 27190h-27191a. (b) Graham, J.; Quayle, J.R. *J. Chem. Soc.* **1955**, 3814-3817. (c) Bunton, C.A.; Comyns, A.E.; Graham, J.; Quayle, J.R. *J. Chem. Soc.* **1955**, 3817-3824.

39. Burford, N.; Clyburne, J.A.C.; Chan, M. *Inorg. Chem.* **1997**, *36*, 3204-3206.

40. These studies are summarized in: du Mont, W.-W. *Main Group Chemistry News*

**1994**, *2*, 18-26.

41. Dasent, W.E. *Non-Existent Compounds: Compounds of Low Stability*; Marcel Dekker: New York, 1965.

42. Burford, N.; Clyburne, J.A.C.; Mason, S.; Richardson, J.F. *Inorg. Chem.* **1993**, *32*, 4988-4989.

43. For a compendium of transient carbenoids see: Nefedov, O.M.; Egorov, M.P.; Ioffe, A.I.; Menchikov, L.G.; Zuev, P.S.; Minikin, V.I.; Simkin, B.Y.; Glukhovtsev, M.N. *Pure & Appl. Chem.* **1992**, *64*, 265-314.

44. See, for example: (a) Herrmann, W.A.; Gooβen, L.J.; Artus, G.R.J.; Köcher, C. *Organometallics* **1997**, *16*, 2472-2477. (b) Hermann, W.A.; Goossen, L.J.; Spiegler, M. *J. Organomet. Chem.* **1997**, *547*, 357-366.

45. (a) Herrmann, W.A.; Elison, M.; Fischer, J.; Köcher, C.; Artus, G.R.J. *Angew. Chem. Int. Ed. Engl.* **1995**, *34*, 2371-2374. (b) Herrmann, W.A.; Köcher, C. *Angew. Chem. Int. Ed. Engl.* **1997**, *36*, 2162-2187.

46. Regitz, M. *Angew. Chem. Int. Ed. Engl.* **1996**, *35*, 725-728, and references therein.

47. *Houben-Weyl, Methoden der Organischen Chemie*, Regitz, M.,Ed; Thieme: Stuttgart, 1989; Teil 2, Band E19b.

48. Arduengo, A.J., III; Harlow, R.L.; Kline, M. *J. Am. Chem. Soc.* **1991**, *113*, 361-363.

49. For example: (a) Dixon, D.A.; Arduengo, A.J., III *J. Phys. Chem.* **1991**, *95*, 4180-4182. (b) Arduengo, A.J., III; Dias, H.V.R.; Harlow, R.L.; Kline, M. *J. Am. Chem. Soc.* **1992**, *114*, 5530-5534. (c) Arduengo, A.J., III, Dixon, D.A.; Kumashiro, K.K.; Lee, C.; Power, W.P.; Zilm, K.W. *J. Am. Chem. Soc.* **1994**, *116*, 6361-6367. (d) Arduengo, A.J., III; Bock, H.; Chen, H.; Denk, M.; Dixon, D.A.; Green, J.C.; Herrmann, W.A.; Jones, N.L.; Wagner, M.; West, R. *J. Am. Chem. Soc.* **1994**, *116*, 6641-6649. (e) Arduengo, A.J., III; Dias, H.V.R.; Dixon, D.A.; Harlow, R.L.; Klooster, W.T.; Koetzle, T.F. *J. Am. Chem. Soc.* **1994**, *116*, 6812-6822. (f) Arduengo, A.J., III; Goerlich, J.R.; Marshall, W.J. *J. Am. Chem. Soc.* **1995**, *117*, 11027-11028. (g) Arduengo, A.J., III; Calabrese, J.C.; Cowley, A.H.; Dias, H.V.R.; Goerlich, J.R.; Marshall, W.J.; Riegel, B. *Inorg. Chem.* **1997**, *36*, 2151-2158. (h) Arduengo, A.J., III; Davidson, F.; Dias, H.V.R.; Goerlich, J.R.; Khasnis, D.; Marshall, W.J.; Prakasha, T.K. *J. Am. Chem. Soc.* **1997**, *119*, 12742-12749. (i) Arduengo, A.J., III; Goerlich, J.R.; Marshall, W.J. *Liebigs Ann./Recueil* **1997**, 365-374.

50. Alder, R.A.; Allen, P.R.; Murray, M.; Orpen, A.G. *Angew. Chem. Int. Ed. Engl.* **1996**, *35*, 1121-1123.

51. Denk, M.K.; Thadani, A.; Hatano, K.; Lough, A.J. *Angew. Chem. Int. Ed. Engl.* **1997**, *36*, 2607-2609.

52. Tsumuraya, T.; Batcheller, S.A.; Masamune, S. *Angew. Chem. Int. Ed. Engl.* **1991**, *30*, 902-930.

53. Neumann, W.P. *Chem. Rev.* **1991**, *91*, 311-334.

54. See, for example: (a) Brooker, S.; Buijink, J.-K.; Edelmann, F.T. *Organometallics* **1991**, *10*, 25-26. (b) Gehrhus, B.; Hitchcock, P.B.; Lappert, M.F. *Angew. Chem. Int. Ed. Engl.* **1997** *36*, 2514-2516.

55. Sanchez, M.; Mazières, M.-R.; Lamandé, L.; Wolf, R. In Ref. 19; Chapter D1.

56. Cowley, A.H.; Cushner, M.C.; Lattman, M.; McKee, M.L.; Szobota; J.S.; Wilburn, J.C. *Pure & Appl. Chem.* **1980**, *52*, 789-797.

57. Cowley, A.H.; Kemp, R.A. *Chem. Rev.* **1985**, *85*, 367-382.

58. (a) Flemming, S.; Lupton, M.K.; Jekot, K. *Inorg. Chem.* **1972**, *11*, 2534-2540. (b) Maryanoff, B.E.; Hutchins, R.O. *J. Org. Chem.* **1972**, *37*, 3475-3480.

59. (a) Cowley, A.H.; Cushner, M.C.; Szobota, J.S. *J. Am. Chem. Soc.* **1978**, *100*, 7784-7786. (b) Luber, J.; Schmidpeter, A. *Angew. Chem. Int. Ed. Engl.* **1976**, *15*, 111-112. (c) Luber, J.; Schmidpeter, A. *J. Chem. Soc., Chem. Commun.* **1976**, 887-888. (d) Friedrich, P.; Huttner, G.; Luber, J.; Schmidpeter, A. *Chem. Ber.* **1978**, *111*, 1558-1563.

60. Burford, N; Losier, P.; Macdonald, C.; Kyrimis, V.; Bakshi, P.K.; Cameron,

T.S. *Inorg. Chem.* **1994**, *33*, 1434-1439.

61. For example: (a) Burford, N.; Royan, B.W.; White, P.S. *J. Am. Chem. Soc.* **1989**, *111*, 3746-3747. (b) Burford, N.; Parks, T.M.; Royan, B.W.; Richardson, J.F.; White, P.S. *Can. J. Chem.* **1992**, *70*, 703-709. (c) Veith, M.; Bertsch, B.; Huch, V. *Z. Anorg. Allg. Chem.* **1988**, *559*, 73-88. (d) Payrastre, C.; Madaule, Y.; Wolf, J.-G. *Tetrahedron Lett.* **1992**, *33*, 1273-1276. (e) Payrastre, C.; Madaule, Y.; Wolf, J.-G.; Kim, T.C.; Mazières, M.-R.; Wolf, R.; Sanchez, M. *Heteroatom Chem.* **1992**, *3*, 157-162. (f) Burford, N.; Royan, B.W. *J. Chem. Soc., Chem. Commun.* **1989**, 19-21. (g) Anderson, R.H.; Cragg, R.H. *J. Chem. Soc., Chem. Commun.* **1971**, 1414.

62. Burford, N.; Macdonald, C.L.B.; Parks, T.M.; Wu, G.; Borecka, B.; Kwiatkowski, W.; Cameron, T.S. *Can. J. Chem.* **1996**, *74*, 2209-2216.

63. Burford, N.; Parks, T.M.; Royan, B.W.; Borecka, B.; Cameron, T.S.; Richardson, J.F.; Gabe, E.J.; Hynes, R. *J. Am. Chem. Soc.* **1992**, *114*, 8147-8153.

64. Burford, N.; Parks, T.M.; Bakshi, P.K.; Cameron, T.S. *Angew. Chem. Int. Ed. Engl.* **1994**, *33*, 1267-1268.

65. (a) Coleman, A.P.; Nieuwenhuyzen, M.; Rutt, H.N.; Seddon, K.R. *J. Chem. Soc., Chem. Commun.* **1995**, 2369-2370. (b) Neuhaus, A.; Frenzen, G.; Pebler, J.; Dehnicke, K. *Z. Anorg. Allg. Chem.* **1992**, *618*, 93-97. (c) Ref. 61f. (d) Ref. 61c.

66. See, for example: (a) Frank, W.; Weber, J.; Fuchs, E. *Angew. Chem. Int. Ed. Engl.* **1987**, *26*, 74-75. (b) Alcock, N.W.; Ravindran, M.; Willey, G.R. *J. Chem. Soc. Chem. Commun.* **1989**, 1063-1065. (c) Rogers, R.D.; Bond, A.H.; Aguinaga, S.; Reyes, A. *J. Am. Chem. Soc.* **1992**, *114*, 2967-2977. (d) Clegg, W.; Farrugia, L.J.; McCamley, A.; Norman, N.C.; Orpen, A.G.; Pickett, N.L.; Stratford, S.E. *J. Chem. Soc., Dalton Trans.* **1993**, 2579-2587. (e) Allman, T.; Goel, R.G.; Prasad, H.S. *J. Organomet. Chem.* **1979**, *166*, 365-371. (f) Carmalt, C.J.; Norman, N.C.; Orpen, A.G.; Stratford, S.E. *J. Organomet. Chem.* **1993**, *460*, C22-C24. (g) Agocs, L.; Burford, N.; Cameron, T.S.; Curtis, J.M.; Richardson, J.F.; Robertson, K.N.; Yhard, G.B. *J. Am. Chem. Soc.* **1996**, *118*, 3225-3232. (h) Agocs, L.; Briand, G.G.; Burford, N.; Cameron, T.S., Kwiatkowski, W.; Robertson, K.N. *Inorg. Chem.* **1997**, *36*, 2855-2860.

67. The monomeric 6-$\pi$ unsaturated analogue of **2.5** was reported recently: Carmalt, C.J.; Lomeli, V.; McBurnett, B.G.; Cowley, A.H. *J. Chem. Soc., Chem. Commun.* **1997**, 2095-2096.

68. First reported but poorly characterized In Ref. 61e.

69. *CRC Handbook of Chemistry and Physics*, 67th ed.; Weast, R.C., Ed.; CRC: Boca Raton, Florida, 1986; D-188.

70. Ahlemann, J.-T.; Künzel, A.; Roesky, H.W.; Noltemeyer, M.; Markovskii, L.; Schmidt, H.-G. *Inorg. Chem.* **1996**, *35*, 6644-6645.

71. See, for example, (a) Ref 19d. (b) Camerman, A.; Trotter, J. *J. Chem. Soc.* **1965**, 730-738.

72. See, for example, (a) Wiess, V.J.; Eisenhuth, W. *Z. Anorg. Allg. Chem.* **1967**, *350*, 9-17. (b) Gieren, A.; Betz, H.; Hübner, T.; Lamm, V.; Herberhold, M.; Guldner, K. *Z. Anorg. Allg. Chem.* **1984**, *513*, 160-174. (c) Bohra, R.; Roesky, H.W.; Noltemeyer, M.; Sheldrick, G.M. *Acta. Crystallogr. Sect. C.* **1984**, *40*, 1150-1152. (d) Grützmacher, H.; Pritzkow, H. *Chem. Ber.* **1989**, *122*, 1417-1421.

73. Frisch, M.J.; Trucks, G.W.; Schlegel, H.B.; Gill, P.M.W.; Johnson, B.G.; Robb, M.A.; Cheeseman, J.R.; Keith, T.A.; Petersson, G.A.; Montgomery, J.A.; Raghavachari, K.; Al-Laham, M.A.; Zakrewski, V.G.; Ortiz, J.V.; Foresman, J.B.; Cioslowski, J.; Stefanow, B.B.; Nanayakkara, A.; Challacombe, M.; Peng, C.Y.; Ayala, P.Y.; Chen, W.; Wong, M.W.; Andres, J.L.; Replogle, E.S.; Gomperts, R.; Martin, R.L.; Fox, D.J.; Binkley, J.S.; DeFrees, D.J.; Baker, J.; Stewart, J.P.; Head-Gordon, M.; Gonzalez, C.; Pople, J.A. GAUSSIAN 94 (Revision B.2) (Gaussian, Inc., Pittsburgh PA, 1995).

74. Reed, A.E.; Curtiss, L.A.; Weinhold, F. *Chem. Rev.* **1988**, *88*, 899-926.

75. Heinemann, C.; Müller, T.; Apeloig, Y.; Schwarz, H. *J. Am. Chem. Soc.* **1996**, *118*, 2023-2038.

76. Boehme, C.; Frenking, G. *J. Am. Chem. Soc.* **1996**, *118*, 2039-2046.

77. Sauers, R.R. *Tetrahedron Lett.* **1996**, *37*, 149-152.

78. Harrison, J.F. *J. Am. Chem. Soc.* **1981**, *103*, 7406-7413.

79. Trinquier, G.; Marre, M.-R. *J. Phys. Chem.* **1983**, *87*, 1903-1905.

80. Cramer, C.J.; Dulles, F.J.; Storer, J.W.; Worthington, S.E. *Chem. Phys. Lett.* **1994**, *218*, 387-394.

81. MacLennan, M.T.; Darvesh, K.V. *Can. J. Chem.* **1995**, *73*, 544-549.

82. Sauers, R.R. *Tetrahedron*, **1997**, *53*, 2357-2364.

83. Latifzadeh-Masoudipour, L.; Balasubramanian, K. *J. Chem. Phys.* **1997**, *106*, 2695-2701.

84. Latifzadeh, L.; Balasubramanian, K. *Chem. Phys. Lett.* **1996**, *258*, 393-399.

85. Schoeller, W.W.; Tubbesing, U. *J. Mol. Struct.* **1995**, *343*, 49-55.

86. See, for example: (a) Ford, G.P.; Scribner, J.D. *J. Am. Chem. Soc.* **1981**, *103*, 4281-4291. (b) Falvey, D.E.; Cramer, C.J. *Tetrahedron Lett.* **1992**, *33*, 1705-1708. (c) Su, K.; Hu, X.; Li, X.; Wang, Y.; Wen, Z. *Chem. Phys. Lett.* **1996**, *258*, 431-435. (d) Cramer, C.J.; Falvey, D.E. *Tetrahedron Lett.* **1997**, *38*, 1515-1518.

87. Cramer, C.J.; Dulles, F.J.; Falvey, D.E. *J. Am. Chem. Soc.* **1994**, *116*, 9787-9788.

88. Baird, N.C.; Taylor, K.F. *J. Am. Chem. Soc.* **1978**, *100*, 1333-1338.

89. Wiberg, K.B.; Breneman, C.M.; LePage, T.J. *J. Am. Chem. Soc.* **1990**, *112*, 61-72.

90. Reed, R.W.; Xie, Z.; Reed, C.A. *Organometallics* **1995**, *14*, 5002-5004, and references therein.

91. Regitz, M. *Angew. Chem. Int. Ed. Engl.* **1991**, *30*, 674-676, and references therein.

92. See, for example: (a) Apeloig, Y. In *The chemistry of organic silicon compounds, part 1*; Patai, S.; Rappoport, Z, Eds.; John Wiley and Sons: Toronto, 1989; Chapter 2 and references therein. (b) Maxka, J.; Apeloig, Y. *J. Chem. Soc., Chem. Commun.* **1990**, 737-739. (c) Karni, M.; Apeloig, Y. *J. Am. Chem. Soc.* **1990**, *112*, 8589-8590. (d) Apeloig, Y.; Müller, T. *J. Am. Chem. Soc.*, **1995**, *117*, 5363-5364.

93. See, for example: (a) Schönherr, H.-J.; Wanzlick, H.-W. *Chem. Ber.* **1970**, *103*, 1037-1046, and references therein. (b) Veith, M. *Z. Naturforsch. B.* **1978**, *33*, 1-6. (c) Veith, M. *Z. Naturforsch. B.* **1978**, *33*, 7-13. (d) Veith, M.; Recktenwald, D.; Humpfer, E. *Z. Naturforsch. B.* **1978**, *33*, 14-19. (e) Jutzi, P.; Holtmann,

U.; Bögge, H.; Müller, A. *J. Chem. Soc., Chem. Commun.* **1988**, 305-306. (f) Sakamoto, K.; Tsutsui, S.; Sakurai, H.; Kira, M. *Bull. Chem. Soc. Jpn.* **1997**, *70*, 253-260.

94. P. v. R. Schleyer *et. al.* have determined that it is not inherently poor π-overlap, but an increasing hybridization (planarization) energy that renders heavier p-bonding unfavourable: Kapp, J.; Schade, C.; El-Nahasa, A.M.; Schleyer, P.v.R. *Angew. Chem. Int. Ed. Engl.* **1996**, *35*, 2236-2238.

95. (a) Brown, D.S.; Decken, A.; Schnee, C.A.; Cowley, A.H. *Inorg. Chem.* **1995**, *34*, 6415-6416. (b) Cowley, A.H.; Brown, D.S.; Decken, A.; Kamepalli, S. *J. Chem. Soc., Chem. Commun.* **1996**, 2425-2426.

96. Sohn, H.; Powell, D.R.; West, R.; Hong, J.-H.; Joo, W.-C. *Organometallics* **1997**, *16* , 2770-2772.

97. Ziegler, T.; Rauk, A. *Theoret. Chim. Acta.* **1977**, *46*, 1-10.

98. See, for example, Sandblom, N.; Ziegler, T.; Chivers, T. *Inorg. Chem.* **1998**, *37*, 354-359.

99. Burford, N.; Losier, P.; Bakshi, P.K.; Cameron, T.S. *J. Chem. Soc., Chem. Commun.* **1996**, 307-308.

100. Burford, N.; Parks, T.M.; Wu, G. *Phosphorus, Sulfur and Silicon* **1994**, *93-94*,

397-398.

101. For examples of other phosphenium diene cycloadducts see: (a) SooHoo, C.K.; Baxter, S.G. *J. Am. Chem. Soc.* **1983**, *105*, 7443-7444. (b) Cowley, A.H.; Kemp, R.A.; Lasch, J.G.; Norman, N.C.; Stewart, C.A. *J. Am. Chem. Soc.* **1983**, *105*, 7444-7446. (c) Cowley, A.H.; Kemp, R.A.; Lasch, J.G.; Norman, N.C.; Stewart, C.A.; Whittlesey, B.R.; Wright, T.C. *Inorg. Chem.* **1986**, *25*, 740-749.

102. Regitz, M. In Ref. 19; Chapter C2.

103. Appel, R. In Ref. 19; Chapter D4.

104. Märkl, G. In Ref. 19; Chapter D5.

105. See, for example: Fleming, I. *Molecular Orbitals in Organic Chemistry*; J. Wiley and Sons: New York, 1976.

106. Sauer, J.; Sustmann, R. *Angew. Chem. Int. Ed. Engl.* **1980**, *19*, 779-807, and references therein.

107. (a) Woodward, R.B.; Hoffmann, R. *J. Am. Chem. Soc.* **1965**, *87*, 395-397. (b) Hoffmann, R.; Woodward, R.B. *J. Am. Chem. Soc.* **1965**, *87*, 2046-2048. (c) Woodward, R.B.; Hoffmann, R. *J. Am. Chem. Soc.* **1965**, *87*, 2511-2513. (d) Hoffmann, R.; Woodward, R.B. *J. Am. Chem. Soc.* **1965**, *87*, 4388-4389. (e) Hoffmann, R.; Woodward, R.B. *J. Am. Chem. Soc.* **1965**, *87*, 4389-4390.

108. Evanseck, J.D.; Mareda, J.; Houk, K.N. *J. Am. Chem. Soc.* **1990**, *112*, 73-80, and references therein.

109. See, for example: Tokitoh, N.; Kishikawa, K.; Matsumoto, T.; Okazaki, R. *Chem. Lett.* **1995**, 827-828.

110. See, for example: Saito, M.; Tokitoh, N.; Okazaki, R. *Chem. Lett.* **1996**, 265-266.

111. Review of arsaalkene and arsaalkynes: Weber, L. *Chem. Ber.* **1996**, *129*, 367-379.

112. Diels, O.; Alder, K. *Justus Liebigs Ann. Chem.* **1928**, *460*, 98-122.

113. Houk, K.N.; González, J.; Li, Y. *Acc. Chem. Res.* **1995**, *28*, 81-90.

114. See, for example: Houk, K.N.; Li, Y.; Evanseck, J.D. *Angew. Chem. Int. Ed. Engl.* **1992**, *31*, 682-708, and references therein.

115. Mean bond enthalpies from: Elschenbroich, C.; Salzer, A. *Organometallics*, 2nd ed.; VHC: New York, 1992; p 11.

116. Niecke, E. In Ref.19; Chapter D8.

117. Phillips, C.S.G; Williams, R.J.P. *Inorganic Chemistry*; Oxford University Press:

London, 1966; Vol. 1, pp 632-638.

118. See, for example: (a) Xie, Z.; Bau, R.; Benesi, A.; Reed, C.A. *Organometallics* **1995**, *14*, 3933-3941. (b) Xie, Z.; Manning, J.; Reed, R.W.; Mathur, R.; Boyd, P.D.W.; Benesi, A.; Reed, C.A. *J. Am. Chem. Soc.* **1996**, *118*, 2922-2928.

119. Witt, M.; Roesky, H.W. *Prog. Inorg. Chem.* **1992**, *40*, 353-444.

120. Edelmann, F.T. *Comments Inorg. Chem.* **1992**, *12*, 259-284.

121. Plenio, H. *Chem. Rev.* **1997**, *97*, 3363-3384.

122. McBee, E.T.; Leech, R.E. *Ind. Eng. Chem.* **1947**, *39*, 393-394.

123. Takahashi, K.; Yoshino, A.; Hosokawa, K.; Muramatsu, H. *Bull. Chem. Soc. Jpn.* **1985**, *58*, 755-756.

124. McBee, E.T.; Sanford, R.A. *J. Am. Chem. Soc.* **1950**, *72*, 5574-5575.

125. Carr, G.E.; Chambers, R.D.; Holmes, T.F.; Parker, D.G. *J. Organomet. Chem.* **1987**, *325*, 13-23.

126. Burmakov, A.I.; Alekseeva, L.A.; Yagupol'skii, L.M. *Zh. Organ. Khim.* **1970**, *6*, 144-148.

127. Stalke, D.; Whitmire, K.H. *J. Chem. Soc., Chem. Commun.* **1990**, 833-834.

128. (a) Dmowski, W.; Porwisiak, J. *J. Fluorine Chem.* **1992**, *59*, 321-331. (b) Dmowski, W.; Porwisiak, J.; Krajewski, J.; Mishnyov, A.; Kemme, A. *J. Fluorine Chem.* **1993**, *62*, 15-23. (c) Koroniak, H.; Fiedorow, P.; Dmowski, W.; Porwisiak, J. *J. Mol. Struct.* **1995**, *351*, 187-195. (d) Kolomeitsev, A.A.; Movchun, V.N.; Yagupolskii, Y.L.; Porwisiak, J.; Dmowski, W. *Tetrahedron Lett.* **1992**, *33*, 6191-6192.

129. Schlosser, M.; Porwisiak, J.; Mongin, F. *Tetrahedron* **1998**, *54*, 895-900.

130. (a) Bertel, N.; Roesky, H.W.; Edelmann, F.T.; Noltemeyer, M.; Schmidt, H.-G. *Z. Anorg. Allg. Chem.* **1990**, *586*, 7-18. (b) Labahn, D.; Bohnen, F.M.; Herbst-Irmer, R.; Pohl, E.; Stalke, D.; Roesky, H.W. *Z. Anorg. Allg. Chem.* **1994**, *620*, 41-47. (c) Ref. 134 (d) Ref. 125 (e) Ref. 126 (f) Ref. 119, and references therein. (g) Ref. 120, and references therein.

131. Schluter, R.D.; Isom, H.S.; Cowley, A.H.; Atwood, D.A.; Jones, R.A.; Olbrich, F.; Corbelin, S.; Lagow, R.J. *Organometallics* **1994**, *13*, 4058-4063.

132. Schluter, R.D.; Cowley, A.H.; Atwood, D.A.; Jones, R.A.; Bond, M.R.; Carrano, C.J. *J. Am. Chem. Soc.* **1993**, *115*, 2070-2071.

133. Roesky, H.W.; Scholz, M.; Noltemeyer, M.; Edelmann, F.T. *Inorg. Chem.* **1989**, *28*, 3829-3830.

134. Scholz, M.; Noltemeyer, M.; Roesky, H.W. *Angew. Chem. Int. Ed. Engl.* **1989**,

*28*, 1383-1384.

135. Ahlemann, J.-T.; Roesky, H.W.; Murugavel, R.; Parisini, E.; Noltemeyer, M.; Schmidt, H.-G.; Müller, O.; Herbst-Irmer, R.; Markovskii, L.N.; Shermolovich, Y.G. *Chem. Ber./Recueil* **1997**, *130*, 1113-1121.

136. Bender, J.E., IV; Banaszak Holl, M.M.; Kampf, J.W. *Organometallics* **1997**, *16*, 2743-2745.

137. Grützmacher, H.; Pritzkow, H.; Edelmann, F.T. *Organometallics* **1991**, *10*, 23-25.

138. Brooker, S.; Buijink, J.-K.; Edelmann, F.T. *Organometallics* **1991**, *10*, 25-26.

139. Lay, U.; Pritzkow, H.; Grützmacher, H. *J. Chem. Soc., Chem. Commun.* **1992**, 260-262.

140. Masamune, S.; Sita, L.R. *J. Am. Chem. Soc.* **1985**, *107*, 6390-6391.

141. Bigwood, M.P.; Corvan, P.J.; Zuckerman, J.J. *J. Am. Chem. Soc.* **1981**, *103*, 7643-7646.

142. Weidenbruch, M.; Schlaefke, J.; Schäfer, A.; Peters, K.; von Schnering, H.G.; Marsmann, H. *Angew. Chem. Int. Ed. Engl.* **1994**, *33*, 1846-1848.

143. Scholz, M.; Roesky, H.W.; Stalke, D.; Keller, K.; Edelmann, F.T. *J. Organomet.*

*Chem.* **1989**, *366*, 73-85.

144. Whitmire, K.H.; Labahn, D.; Roesky, H.W.; Noltemeyer, M.; Sheldrick, G.M. *J. Organomet. Chem.* **1991**, *402*, 55-66.

145. Voelker, H.; Pieper, U.; Roesky, H.W.; Sheldrick, G.M. *Z. Naturforsch.* **1994**, *49b*, 255-257.

146. Lübben, T.; Roesky, H.W.; Gornitzka, H.; Steiner, A.; Stalke, D. *Eur. J. Solid State Inorg. Chem.* **1995**, *32*, 121-130.

147. Hitchcock, P.B.; Lappert, M.F.; Rai, A.K.; Williams, H.D. *J. Chem. Soc., Chem. Commun.* **1986**, 1633-1634.

148. Crutchfield, M.M.; Dungan, C.H.; Letcher, J.H.; Mark, V.; Van Wazer, J.R. In *$P^{31}$ Nuclear Magnetic Resonance*; Grayson, M.; Griffith, E.J., Eds.; John Wiley and Sons: New York, 1967; p 242.

149. There is a reference to $Fmes_2PCl$ in: Heuer, L.; Jones, P.G.; Schmutzler, R. *J. Fluorine Chem.* **1990**, *46*, 243-254.

150. Trotter, J. *Can. J. Chem.* **1962**, *40*, 1590-1593.

151. Fukuyo, M.; Nakatsu, K.; Shimada, A. *Bull. Chem. Soc. Jpn.* **1966**, *39*, 1614-1615.

152. Pennington, W.T.; Cordes, A.W.; Graham, J.C.; Jung, Y.W. *Acta. Cryst.* **1983**, *C39*, 1010-1012.

153. Sowerby, D.B. In *The chemistry of organic arsenic, antimony and bismuth compounds*; Patai, S., Ed.; John Wiley and Sons: Toronto, 1994; Chapter 2 and references therein.

154. Ref. 6; p 224.

155. There are only 9 articles and most of the structures are derivatives of one compound made by K. Akiba *et. al.* See, for example: (a) Yamamoto, Y.; Chen, X.; Kojima, S.; Ohdoi, K.; Kitano, M.; Doi, Y.; Akiba, K. *J. Am. Chem. Soc.* **1995**, *117*, 3922-3932. (b) Kojima, S.; Takagi, R.; Nakata, H.; Yamamoto, Y.; Akiba, K. *Chem. Lett.* **1995**, 857-858. (c) Yamamoto, Y.; Okazaki, M.; Wakisaka, Y.; Akiba, K. *Organometallics* **1995**, *14*, 3364-3369. (d) Akiba, K.; Nakata, H.; Yamamoto, Y.; Kojima, S. *Chem. Lett.* **1992**, 1559-1562. (e) Begley, M.J.; Sowerby, D.B.; Wesolek, D.M.; Silvestru, C.; Haiduc, I. *J. Organomet. Chem.* **1986**, *316*, 281-289. (f) Wieber, M.; Graf, N. *Z. Anorg. Allg. Chem.* **1993**, *619*, 1991-1997. (g) Breneman, G.L. *Acta. Cryst.* **1979**, *B35*, 731-733. (h) Ref. 159. (i) Ref. 160.

156. Labahn, D.; Brooker, S.; Sheldrick, G.M.; Roesky, H.W. *Z. Anorg. Allg. Chem.* **1992**, *610*, 163-168.

157. Ref. 13a; p 292.

158. Schoeller, W.W.; Schneider, R. *Chem. Ber./Receuil* **1997**, *130*, 1013-1020.

159. Bone, S.P.; Sowerby, D.B. *J. Organometal. Chem.* **1980**, *184*, 181-188.

160. Bordner, J.; Andrews, B.C.; Long, G.G. *Cryst. Struct. Comm.* **1974**, *3*, 53-56.

161. Cramer, C.J.; Truhlar, D.G.; Falvey, D.E. *J. Am. Chem. Soc.* **1997**, *119*, 12338-12342.

162. **2,6-Di-*t*-butylphenyl:** (a) Healy, M. D.; Power, M.B.; Barron, A.R. *Coord. Chem. Rev.* **1994**, *130*, 63-135. **2,6-Di-*t*-butyl-4-methylphenyl:** (b) Healy, M.D.; Leman, J.T.; Barron, A.R. *J. Am. Chem. Soc.* **1991**, *113*, 2776-2777. (c) Healy, M.D.; Barron, A.R. *Angew. Chem. Int. Ed. Engl.* **1992**, *31*, 921-922. **Adamantyl:** (d) Brook, A.G.; Nyburg, S.C.; Abdesaken, F.; Gutekunst, B.; Gutekunst, G.; Kallury, R.K.M.R.; Poon, Y.C.; Chang, Y.M.; Wong-Ng, W. *J. Am. Chem. Soc.* **1982**, *104*, 5667-5672. **1,2,3,4,5-Pentamethylcyclopentadienyl:** (e) Jutzi, P; Meyer, U.; Krebs, B.; Dartmann, M. *Angew. Chem. Int. Ed. Engl.* **1986**, *25*, 919-921. **Tris(trimethylsilyl)methyl:** (f) Cowley, A.H.; Kilduff, J.E.; Newman, T.H.; Pakulski, M.J. *J. Am. Chem. Soc.* **1982**, *104*, 5820-5821. **2,4,6-Tris[bis(trimethylsilyl)methyl]-phenyl:** (g) Tokitoh, N.; Matsumoto, T.; Manmaru, K.; Okazaki, R. *J. Am. Chem. Soc.* **1993**, *115*, 8855-8856.

163. See, for example: (a) Hitchcock, P.B.; Jasim, H.A.; Lappert, M.F.; Williams, H.D. *J. Chem. Soc., Chem. Commun.* **1984**, 662-664. (b) Atwood, D.A.;

Cowley, A.H.; Jones, R.A.; Mardones, M.A. *J. Am. Chem. Soc.* **1991**, *113*, 7050-7052. (c) Petrie, M.A.; Ruhlandt-Senge, K.; Power, P.P. *Inorg. Chem.* **1992**, *31*, 4038-4039. (d) Wehmschulte, R.J.; Ellison, J.J.; Ruhlandt-Senge, K.; Power, P.P. *Inorg. Chem.* **1994**, *33*, 6300-6306. (e) Wehmschulte, R.J.; Power, P.P. *Inorg. Chem.* **1994**, *33*, 5611-5612. (f) Brothers, P.J.; Wehmschulte, R.J.; Olmstead, M.M.; Ruhlandt-Senge, K.; Parkin, S.R.; Power, P.P. *Organometallics* **1994**, *13*, 2792-2799. (g) Cowley, A.H.; Gabbaï, F.P.; Isom, H.S.; Carrano, C.J.; Bond, M.R. *Angew. Chem. Int. Ed. Engl.* **1994**, *33*, 1253-1255. (h) Schultz, S.; Pusch, S.; Pohl, E.; Dielkus, S.; Herbst-Irmer, R.; Meller, A.; Roesky, H.W. *Inorg. Chem.* **1993**, *32*, 3343-3315. (i) Cowley, A.H.; Gabbaï, F.P.; Decken, A. *Angew. Chem. Int. Ed. Engl.* **1994**, *33*, 1370-1372.

164. See, for example: (a) Jutzi, P.; Becker, A.; Leue, C.; Stammler, H.G.; Neumann, B. *Organometallics* **1991**, *10*, 3838-3842. (b) Underiner, G.E.; Tan, R.P.; Powell, D.R.; West, R. *J. Am. Chem. Soc.* **1991**, *113*, 8437-8443.

165. See, for example: (a) Yoshifuji, M.; Shima, I.; Inamoto, N. *J. Am. Chem. Soc.* **1981**, *103*, 4587-4589. (b) Cowley, A.H.; Kilduff, J.E.; Lasch, J.G.; Mehrotra, S.K.; Norman, N.C.; Pakulski, M.; Whittlesey, B.R.; Atwood, J.A.; Hunter, W.E. *Inorg. Chem.* **1984**, *23*, 2582-2593. (c) Cowley, A.H.; Lasch, J.G.; Norman, N.C.; Pakulski, M.; Whittlessey, B.R. *J. Chem. Soc., Chem. Commun.* **1983**, 881-882. (d) Cowley, A.H.; Lasch, J.G.; Norman, N.C.; Pakulski, M. *J. Am. Chem. Soc.* **1983**, *105*, 5506-5507. (e) Märkl, G.; Sejpka, H. *Tetrahedron Lett.* **1986**, *27*, 171-174. (h) Märkl, G.; Sejpka, H. *Angew. Chem. Int. Ed. Engl.* **1986**, *25*, 264. (i) Appel, R.; Knoch, F.; Kunze, H. *Angew. Chem. Int.*

*Ed. Engl.* **1984**, *23*, 157-158. (j) Bender, H.R.G.; Niecke, E.; Nieger, M. *J. Am. Chem. Soc.* **1993**, *115*, 3314-3315. (k) Appel, R.; Paulen, W. *Angew. Chem. Int. Ed. Engl.* **1983**, *22*, 785-786. (l) Appel, R.; Fölling, P.; Josten, B.; Siray, M.; Winkhaus, V.; Knoch, F. *Angew. Chem. Int. Ed. Engl.* **1984**, *23*, 619-620. (m) Niecke, E.; Gudat, D. *Angew. Chem. Int. Ed. Engl.* **1991**, *30*, 217-237. (n) Romanenko, V.D.; Ruban, A.V.; Drapailo, A.B.; Chernega, A.N.; Rusanov, E.B. *Heteroatom Chem.* **1992**, *3*, 181-187.

166. Burford, N.; Macdonald. C.L.B.; Robertson, K.N.; Cameron, T.S. *Inorg. Chem.* **1996**, *35*, 4013-4016.

167. Syntheses of trisaminostibines are: (a) Moedritzer, K. *Inorg. Chem.* **1964**, *3*, 609-610. (b) Kiennemann, A.; Levy, G.; Schué, F.; Taniélian, C. *J. Organomet. Chem.* **1972**, *35*, 143-148.

168. Edwards, A. J.; Paver, M. A.; Raithby, P. R.; Russell, C. A.; Wright, D. S. *J. Chem. Soc., Dalton Trans.* **1993**, 2257-2258.

169. See, for example: (a) Veith, M.; Goffing, F.; Huch, V. *Z. Naturforsch.* **1988**, *43b*, 846-856. (b) Ergezinger, C.; Weller, F.; Dehnicke, K. *Z. Naturforsch.* **1988**, *43b*, 1119-1124. (c) Fitzgerald, A.; Stenkamp, R.E.; Watenpaugh, K.D.; Jensen, L.H. *Acta Crystallogr.* **1977**, *B33*, 1688-1696. (d) Stewart, C.A.; Harlow, R.L.; Arduengo, A.J., III *J. Am. Chem. Soc.* **1985**, *107*, 5543-5544. (e) Arduengo, A.J., III; Stewart, C.A.; Davidson, F.; Dixon, D.A.; Becker, J.Y.; Culley, S.A.; Mizen, M.B. *J. Am. Chem. Soc.* **1987**, *109*, 627-647. (f) Ross, B.; Belz, J.; Nieger, M. *Chem. Ber.* **1990**, *123*, 975-978. (g) Brandl, A.; Nöth,

H. *Chem. Ber.* **1988**, *121*, 1321-1327. (h) Garbe, R.; Pebler, J.; Dehnicke, K.; Fenske, D.; Goesmann, H.; Baum, G. *Z. Anorg. Allg. Chem.* **1994**, *620*, 592-598. (i) Höneise, W.; Schwarz, W.; Heckmann, G.; Schmidt, A. *Z. Anorg. Allg. Chem.* **1986**, *533*, 55-64. (j) Ref. 61c. (k) Beswick, M.A.; Wright, D.S. *Coord. Chem. Rev.*, in press.

170. (a) Clegg, W.; Compton, N.A.; Errington, R.J.; Fisher, G.A.; Green, M. F.; Hockless, D.C.R.; Norman, N.C. *Inorg. Chem.* **1991**, *30*, 4680-4682. (b) Clegg, W.; Compton, N.A.; Errington, R.J.; Norman, N.C.; Wishart, N. *Polyhedron* **1989**, *8*, 1579-1580.

171. (a) Block, E.; Ofori-Okai, G.; Kang, H.; Wu. J.; Zubieta, J. *Inorg. Chem.* **1991**, *30*, 4784-4788. (b) Herrmann, W.A.; Kiprof, P.; Scherer, W.; Pajdla, L. *Chem. Ber.* **1992**, *125*, 2657-2660. (c) Battaglia, L.P.; Bonamartini Corradi, A.; Nardelli, M.; Vidoni Tani, M.E. *J. Chem. Soc., Dalton Trans.* **1978**, 583-587. (d) Crispini, A.; Errington, R.J.; Fisher, G.A.; Funke, F.J.; Norman, N.C.; Orpen, A.G.; Stratford, S.E.; Struve, O. *J. Chem. Soc., Dalton Trans.* **1994**, 1327-1335. (e) Raston, C.L.; Rowbottom, G.L.; White, A.H. *J. Chem. Soc., Dalton Trans.* **1981**, 1389-1391. (f) Forster, G.E.; Begley, M.J.; Sowerby, D.B. *J. Chem. Soc., Dalton Trans.* **1995**, 383-387. (g) Bertazzi, N.; Alonzo, G.; Battaglia, L.P.; Bonamartini Corradi, A.; Pelosi, G. *J. Chem. Soc., Dalton Trans.* **1990**, 2403-2405. (h) Bensch, W.; Reifler, F.A.; Reller, A.; Oswald, H.R. *Z. Kristallogr.* **1989**, *189*, 169-179. (i) Galdecki, Z.; Glowka, M.L.; Golinski, B. *Acta Crystallogr.* **1976**, *B32*, 2319-2321.

172. Edwards, A.J.; Paver, M.A.; Rennie, M.-A.; Raithby, P.R.; Russell, C.A.;

Wright, D.S. *J. Chem. Soc., Dalton Trans.* **1994**, 2963-2966.

173. For other similar Sb-N-Sb-N rings see: Edwards, A.J.; Leadbeater, N.E.; Paver, M.A.; Raithby, P.R.; Russell, C.A.; Wright, D.S. *J. Chem. Soc., Dalton Trans.* **1994**, 1479-1482.

174. Bochmann, M.; Song, X.; Hursthouse, M.B.; Karaulov, A. *J. Chem. Soc., Dalton Trans.* **1995**, 1649-1652.

175. Atwood, D.A.; Cowley, A.H.; Hernandez, R.D.; Jones, R.A.; Rand, L.L.; Bott, S.G.; Atwood, J.L. *Inorg. Chem.* **1993**, *32*, 2972-2974.

176. (a) Cobbledick, R.E.; Einstein, F.W.B. *Acta Crystallogr.* **1975**, *B31*, 2731-2733. (b) Rømming, C.; Songstad, J. *Acta Chem. Scand.* **1978**, *A32*, 689-699. (c) Rømming, C.; Songstad, J. *Acta Chem. Scand.* **1980**, *A34*, 365-373.

177. Atwood, J.L.; Cowley, A.H.; Hunter, W.E.; Mehrotra, S.K. *Inorg. Chem.* **1982**, *21*, 1354-1356.

178. Nieger, M.; Niecke, E.; Gärtner-Winkhaus, C. *Acta Crystallogr.* **1990**, *C46*, 2470-2472.

179. (a) Khasnis, D.V.; Zhang, H.; Lattman, M. *Organometallics* **1992**, *11*, 3748-3753. (b) Weiss, J.; Eisenhuth, W. *Z. Anorg. Allg. Chem.* **1967**, *350*, 9-17. (c) van Bonn, K.-H.; Schreyer, P.; Paetzold, P.; Boese, R. *Chem. Ber.* **1988**, *121*, 1045-1057.

180. Wirringa, U.; Roesky, H.W.; Noltemeyer, M.; Schmidt, H.-G. *Inorg. Chem.* **1994**, *33*, 4607-4608.

181. Wirringa, U.; Roesky, H.W.; Noltemeyer, M.; Schmidt, H.-G. *Angew. Chem. Int. Ed. Engl.* **1993**, *32*, 1628-1630.

182. James, S.C.; Norman, N.C.; Orpen, A.G.; Quayle, M.J.; Weckenmann, U. *J. Chem. Soc., Dalton Trans.* **1996**, 4159-4161.

183 (a) Niecke, E.; Rüger, R.; Schoeller, W.W. *Angew. Chem. Int. Ed. Engl.* **1981**, *20*, 1034-1036. (b) Niecke, E.; Lysek, M.; Symalla, E. *Chimia* **1986**, *40*, 202-205.

184. For an extensive review on the synthesis of $RN(PX_2)_2$, diazadiphosphetidines and coordination complexes of both of these see: Balakrishna, M.S.; Reddy, V.S.; Krishnamurthy, S.S.; Nixon, J.F.; Burckett St. Laurent, J.C.T.R *Coord. Chem. Rev.* **1994**, *129*, 1-90, and references therein.

185. Scherer, O.J.; Gläβel, W. *Chem. Ber.*, **1977**, *110*, 3874-3888.

186. Scherer, O.J.; Conrad, H. *Z. Naturforsch.* **1981**, *B36*, 515-517.

187. Yoshifuji reported the observation of $[Mes^*PN(2,6\text{-di-}^tBuphenyl)]_2$ and others by

$^{31}$P NMR, however the materials could not be isolated and fully characterized: Yoshifuji, M.; Shibayama, K.; Toyota, K.; Inamoto, N.; Nagase, S. *Chem. Lett.* **1985**, 237-240.

188. Niecke, E.; Detsch, R.; Nieger, M.; Reichert, F.; Schoeller, W.W. *Bull. Soc. Chim. Fr.* **1993**, *130*, 25-31.

189. Niecke, E.; Gudat, D.; Symalla, E. *Angew. Chem. Int. Ed. Engl.* **1986**, *25*, 834-835.

190. Gudat *et. al.* have shown that low-coordinate P compounds can complex to Ag(OTf): Gudat, D.; Holderberg, A.W.; Kotila, S.; Nieger, M. *Chem. Ber.* **1996**, *129*, 465-469.

191. Henry, N.F.M.; Lipson, H.; Wooster, W.A. In *The Interpretation of X-ray Photographs*; MacMillan: London, 1951; pp 116-121.

192. Sheldrick, G.M. In *SHELX-97 Manual*; SHELX-97 Software; 1997; p 6-4.

193. Giacavazzo, C.; Monaco, H.L.; Viterbo, D.; Scordari, F.; Gilli, G.; Zanotti, G.; Catti, M. *Fundamentals of Crystallography*, Giacavazzo, C., Ed.; Oxford University Press: New York, 1992; pp 83-87, and references therein.

194. Ref. 6; p 221.

195. Dubourg, A.; Delarbre, J.-L.; Maury, L.; Declercq, J.-P. *Acta. Cryst.* **1992**, *C48*, 138-140.

196. Lübben, T.; Roesky, H.W.; Gornitzka, H.; Steiner, A.; Stalke, D. *Eur. J. Solid State Inorg. Chem.* **1995**, *32*, 121-130.

197. Allen, F.H.; Kennard, O. *Chemical Design and Automation News* **1993**, *8*, 131.

198. Scharz, W.; Hess, H. ; Zeiss, W. *Z. Naturforsch.* **1978**, *33b*, 723-727.

199. Romanenko, V.D.; Sarina, T.V.; Sanchez, M.; Chernega, A.N.; Rozhenko, A.B.; Mazières, M.-R.; Povolotski, M.I. *J. Chem. Soc., Chem. Commun.* **1993**, 963-965.

200. Kamil, W.A.; Bond, M.R.; Shreeve, J.M. *Inorg. Chem.* **1987**, *26*, 2015-2016.

201. David, G.; Niecke, E.; Nieger, M.; von der Gönna, V.; Schoeller, W.W. *Chem. Ber.* **1993**, *126*, 1513-1517.

202. Wirringa, U.; Voelker, H.; Roesky, H.W.; Shermolovich, Y.; Markovski, L.; Usón, I.; Noltemeyer, M.; Schmidt, H.-G. *J. Chem. Soc., Dalton Trans.* **1995**, 1951-1956.

203. Katti, K.V.; Reddy, V.S.; Singh, P.R. *Chem. Soc. Rev.* **1995**, 97-107.

204. King, R.B. *Acc. Chem. Res.* **1980**, *13*, 243-248.

205. Burford, N.; Clyburne, J.A.C.; Silvert, D.; Warner, S.; Whitla, W.A.; Darvesh, K.V. *Inorg. Chem.* **1997**, *36*, 482-484.

206. Curtis, R.D.; Schriver, M.J.; Wasylishen, R.E. *J. Am. Chem. Soc.* **1991**, *113*, 1493-1498.

207. Gudat, D.; Hoffbauer, W.; Niecke, E.; Schoeller, W.W.; Fleischer, U.; Kutzelnigg, W. *J. Am. Chem. Soc.* **1994**, *116*, 7325-7331.

208. For a definitive review, see Niecke, E.; Gudat, D. In *Phosphorus-31 NMR Spectra Properties in Compounds Characterization and Structural Analysis*; Quin, L.D.; Verkade, J.G., Eds.; VCH: New York, 1994, p 159.

209. Burford, N.; Cameron, T.S.; Clyburne, J.A.C.; Eichele, K.; Robertson, K.N.; Sereda, S.; Wasylishen, R.E.; Whitla, W.A. *Inorg. Chem.* **1996**, *35*, 5460-5467.

210. Rozhenko, A.B.; Povolotskii, M.I.; Polovinko, V.V. *Magn. Reson. Chem.* **1996**, *34*, 269-275, and references therein.

211. Detsch, R.; Niecke, E.; Nieger, M.; Reichert, F. *Chem. Ber.* **1992**, *125*, 321-330.

212. Hitchcock, P.B.; Lappert, M.F.; Layh, M. *J. Organomet. Chem.* **1997**, *529*, 243-255.

213. Keat, R.; Rycroft, D.S.; Niecke, E.; Schäfer, H.-G.; Zorn, H. *Z. Naturforsch.*

**1982**, *37b*, 1665-1666.

214. Wu, G.; Wasylishen, R.E. *J. Chem. Phys.* **1993**, *98*, 6138-6149.

215. (a) Ditchfield, R. *Mol. Physics*, **1974**, *27*, 789-807. (b) de Dios, A.C. *Progr. Nuc. Magn. Reson. Spectrosc.* **1996**, *29*, 229-278.

216. Jameson, C.J.; de Dios, A.; Jameson, A.K. *Chem. Phys. Lett.* **1990**, *167*, 575-582.

217. Tebby, J.C. In *Phosphorus-31 NMR Spectroscopy in Stereochemical Analysis*; Verkade, J.G.; Quin, L.D., Eds.; VCH: Florida, 1987; pp 1-60.

218. Lazzeretti, P.; Tossell, J.A. *J. Phys. Chem.* **1987**, *91*, 800-804.

219. Lappert, M.F. In *Inorganic Compounds with Unusual Properties*; King, R.B., Ed.; American Chemical Society: Washington, D.C., 1976; pp 256-265.

220. Ebbing, D.D. *General Chemistry*, 4th ed.; Houghton Mifflin: Toronto, 1993.

221. Andrew D. Phillips, Dalhousie University, unpublished preliminary result.

222. Another interesting comparison is the different crystal forms of CpIn and CpTl compounds: (a) Schumann, H.; Janiak, C.; Pickardt, J.; Börner, U. *Angew. Chem. Int. Ed. Engl.* **1987**, *26*, 789-790. (b) Schumann, H.; Janiak, C.; Khan, M.A.; Zuckerman, J.J. *J. Organomet. Chem.* **1988**, *354*, 7-13. (c) Schumann,

H.; Janiak, C.; Görlitz, F.; Loebel, J.; Dietrich, A. *J. Organomet. Chem.* **1989**, *363*, 243-251. (d) Janiak, C.; Hoffmann, R. *Angew. Chem. Int. Ed. Engl.* **1989**, *28*, 1688-1690. (e) Budzelaar, P.H.M.; Boersma, J. *Rec. Trav. Chim. Pays-Bas* **1990**, *109*, 187-189. (f) Janiak, C.; Hoffmann, R. *J. Am. Chem. Soc.* **1990**, *112*, 5924-5946. (g) Jutzi, P.; Schnittger, J.; Hursthouse, M.B. *Chem. Ber.* **1991**, *124*, 1693-1697. (h) Schwerdtfeger, P. *Inorg. Chem.* **1991**, *30*, 1660-1663.

223. *The Chemistry of Diazonium and Diazo Groups*; Patai, S. Ed.; John Wiley and Sons: Toronto, 1978.

224. (a) Zollinger, H. *Diazo Chemistry I* ; VCH: New York, 1994. (b) Zollinger, H. *Diazo Chemistry II* ; VCH: New York, 1995.

225. Glaser, R.; Horan, C.J. *J. Org. Chem.* **1995**, *60*, 7518-7528, and references therein.

226. See, for example, (a) Schank, K. In Ref. 223. (b) March, J. *Advanced Organic Chemistry*, 4th ed.; John Wiley and Sons: New York, 1992, and references therein.

227. Furniss, B.S.; Hannaford, A.J.; Smith, P.W.G.; Tatchell, A.R. *Vogel's Texbook of Practical Organic Chemistry*, 5th ed. John Wiley and Sons: New York, 1989.

228. See, for example, (a) Rømming, C. *Acta Chem. Scand.* **1959**, *13*, 1260-1261. (b) Rømming, C. *Acta Chem. Scand.* **1963**, *17*, 1444-1454. (c) Andresen, O.;

Rømming, C. *Acta Chem. Scand.* **1962**, *16*, 1882-1889. (d) Polynova, T.N.; Nesterova, J.M. *Acta Cryst.* **1966**, *21*, A149. (e) Nesterova, J.M.; Porai-Koshits, B.A.; Upadisheva, A.V.; Kazitsyna, L.A. *Zh. Strukt. Khim.* **1966**, *7*, 129. (f) Polynova, T.N.; Bokii, N.G.; Porai-Koshits, B.A. *Zh. Strukt. Khim.* **1965**, *6*, 878-887. (g) Mostad, A.; Rømming, C. *Acta Chem. Scand.* **1968**, *22*, 1259-1266. (h) Rømming, C.; Tjørnhom, T. *Acta Chem. Scand.* **1968**, *22*, 2934-2942.

229. Hegarty, A.F. In Ref. 223, and references therein.

230. Rigaudy, J.; Vernières, J.-C. *C. R. Acad. Sc. Paris* **1965**, *261*, 5516-5519.

231. (a) Barclay, L.R.C.; Briggs, A.G.; Briggs, W.E.; Dust, J.M.; Gray, J.A. *Can. J. Chem.* **1979**, *57*, 2172-2179. (b) Barclay, L.R.C.; Dust, J.M. *Can. J. Chem.* **1982**, *60*, 607-615.

232. *Houben-Weyl, Methoden Der Organischen Chemie*, 4th ed.; Thieme: New York, 1982, Teil 2, Band E16a.

233. Szele, I.; Zollinger, H. *Top. Curr. Chem.* **1983**, *112*, 1-66.

234. For R = Me: (a) Glaser, R.; Horan, C.J.; Choy, G.S.-C.; Harris, B.L. *J. Phys. Chem.* **1992**, *96*, 3689-3697. For R = H: (b) Glaser, R.; Horan, C.J.; Haney, P.E. *J. Phys. Chem.* **1993**, *97*, 1835-1844.

235. (a) Niecke, E.; Nieger, M.; Reichert, R. *Angew. Chem. Int. Ed. Engl.* **1988**, *27*, 1715-1716. (b) Niecke, E.; Nieger, M.; Reichert, R.; Schoeller, W.W.; *Angew.*

*Chem. Int. Ed. Engl.* **1988**, *27*, 1713-1714.

236. Burford, N.; Clyburne, J.A.C.; Bakshi, P.K.; Cameron, T.S. *J. Am. Chem. Soc.* **1993**, *115*, 8829-8830.

237. Clyburne, J.A.C. *New Nitrogen-Phosphorus Chemistry Dependent on the 2,4,6-tri-t-Butylphenyl Substituent*; Ph.D. Thesis, Dalhousie University, 1995.

238. Corbridge, D.E.C. *The Structural Chemistry of Phosphorus*, Elsevier: New York, 1974.

239. (a) Obase, H.; Tsuji, M.; Nishimura, Y. *Chem. Phys. Lett.* **1981**, *81*, 119-122. (b) Obase, H.; Tsuji, M.; Nishimura, Y. *Chem. Phys.* **1983**, *74*, 89-95.

240. Schmidt, H.M.; Stoll, H.; Preuss, H.; Becker, G.; Mundt, O. *J. Mol. Struct. (Theochem)* **1992**, *262*, 171-185, and references therein.

241. (a) Gudat, D.; Niecke, E.; Nieger, M. *Tetrahedron Lett.* **1992**, *33*, 2335-2338. (b) Gudat, D.; Niecke, E.; Nieger, M.; v.d. Gonna, V.; Shoeller, W.W. *Chem. Ber.* **1993**, *126*, 1513-1517. (c) Ref. 237. (d) Ref. 116.

242. Romanenko, V.D.; Rudzevich, V.L.; Rusanov, E.B.; Cherega, A.N.; Senio, A.; Sotiropoulos, J.-M.; Pfister-Guillouzo, G.; Sanchez, M. *J. Chem. Soc., Chem. Commun.* **1995**, 1383-1385.

243. Niecke, E.; Streubel, R.; Nieger, M.; Stalke, D. *Angew. Chem. Int. Ed. Engl.*

**1989**, *28*, 1673-1674.

244. See, for example, (a) Regitz, M. *J. Heterocyclic Chem.* **1994**, *31*, 663-677. (b) Regitz, M. *Chem. Rev.* **1990**, *90*, 191-213.

245. (a) Märkl, G.; Sejpka, H. *Angew. Chem. Int. Ed. Engl.* **1986**, *25*, 264. (b) Hitchcock, P.B.; Jones, C.; Nixon, J.F. *J. Chem. Soc., Chem. Commun.* **1994**, 2601-2062.

246. Laali, K.K.; Nixon, J.F.; Johnson, J.A. *Heteroatom Chem.* **1994**, *5*, 503-506.

247. Guillemin, J.-C.; Lassalle, L.; Dréan, P.; Wlodarczak, G; Demaison, J. *J. Am. Chem. Soc.* **1994**, *116*, 8930-8936.

248. Dobbs, K.D.; Boggs, J.E.; Cowley, A.H. *Chem. Phys. Lett.* **1987**, *141*, 372-375.

249. Curtis, J.M.; Burford, N.; Parks, T.M. *Org. Mass Spec.* **1994**, *29*, 414-418.

250. This reaction is referenced by E. Niecke In Ref. 19 as presented by Romanenko *et. al.* at the International Conference on Phosphorus Chemistry XI in Tallinn, July 1989.

251. Niecke, E., Institut für Anorganische Chemie der Universität Bonn, personal communication.

252. Romanenko, V.D.; Reitel, G.V.; Chernega, A.N.; Kirichenko, O.V.; Ruban, A.V.; Sanchez, M.; Wolf, R.; Mazières, M.-R. *Heteroatom Chem.* **1992**, *3*, 453-458.

253. Ito, S.; Toyota, K.; Yoshifuji, M. *J. Chem. Soc., Chem. Commun.* **1997**, 1637-1638.

254. Arif, A.M.; Cowley, A.H.; Pakulski, M. *J. Chem. Soc., Chem. Commun.* **1987**, 165-166.

255. Cowley, A.H.; Kilduff, J.E.; Norman, N.C.; Pakulski, M. *J. Am. Chem. Soc.* **1983**, *105*, 4845-4846.

256. David, G.; Niecke, E.; Nieger, M. *Tetrahedron Lett.* **1992**, *33*, 2335-2338.

257. Burford, N.; Muller, J.; Parks, T.M. *J. Chem. Educ.* **1994**, *71*, 807-809.

258. See, for example: (a) Parks, T.M. *Pnicogylidenes*; Ph.D thesis; Dalhousie University, 1994. (b) Ref. 236.

## Appendix A. *Ab Initio* Calculation Data.

This appendix contains tabulated data for the UMP2/6-311G*//6-311G* calculations reported in chapters 2 and 3. The listed values include: total energies and frequency analyses (A.1); optimized stuctural parameters for the cyclic (A.2) and acyclic (A.3) models; Mulliken and NBO charge distribution (A.4) for all structures; and calculated spin densities for doublet and triplet species (A.5).

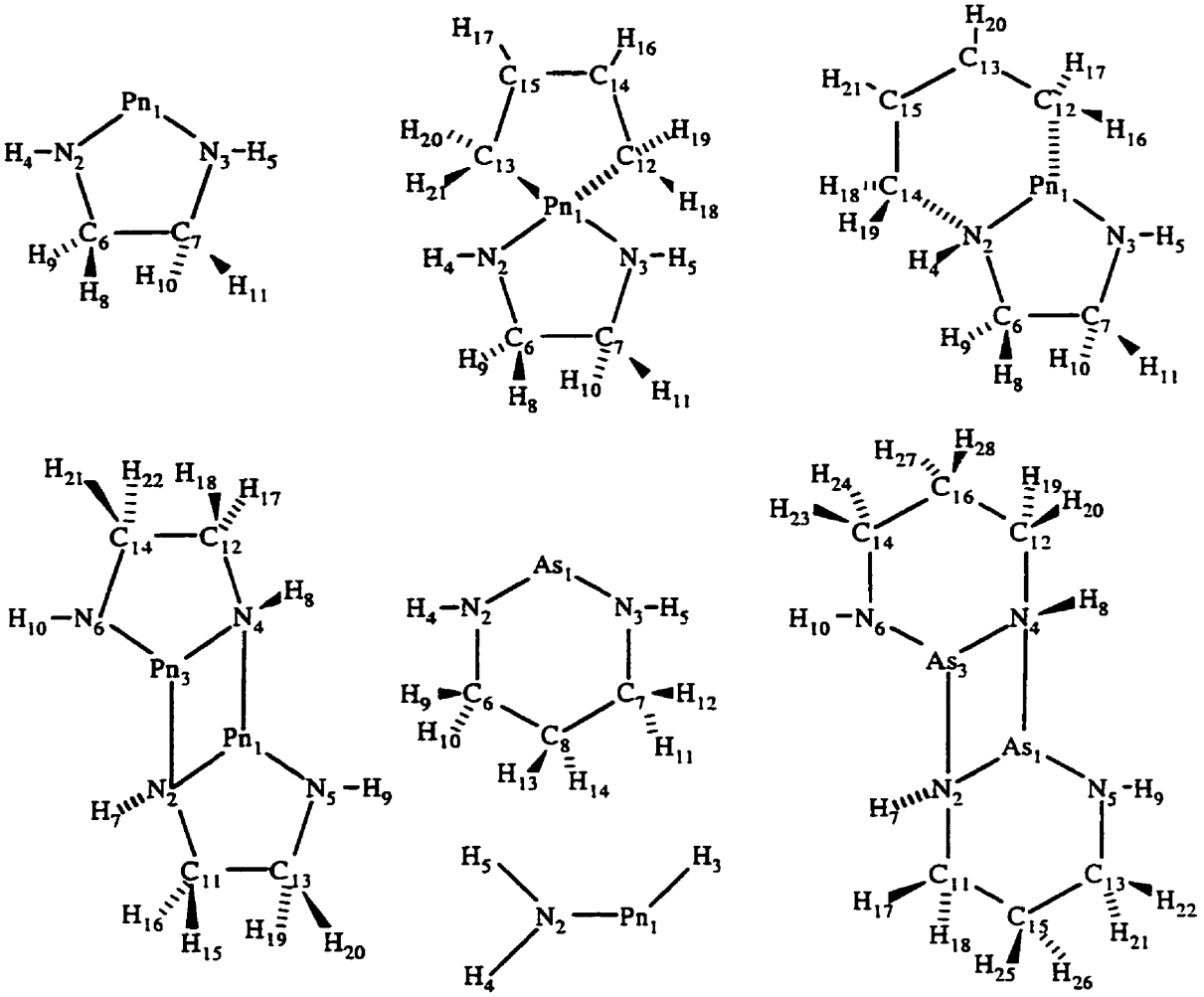

### Legend for Tables A.1-A.5.

**Note:** The symbol → indicates that the symmetry of the structure changed during the optimization.

**Table A.1.** Computed energies (HF/6-311G* and UMP2/6-311G*//HF/6-311G*) and zero point vibrational energies for all calculations. All energies in hartrees. N imag indicates the number of imaginary vibrational frequencies.

| Cyclic P cations | Symmetry | N imag | R/UHF | UMP2 | ZPVE |
|---|---|---|---|---|---|
| **2.7' (3.1')** | $C_2$ | 0 | -528.69528 | -529.40588 | 0.09915 |
| **2.7' MP2 optimization** | $C_2$ | n/a | n/a | -529.40849 | n/a |
| **2.7' t** | $C_2$ | 1 | -528.61035 | -529.29122 | 0.09364 |
| **2.7' t** | $C_1$ | 0 | -528.61721 | -529.28510 | 0.09513 |
| **2.7' t** | $C_s \rightarrow C_{2v}^*$ | 2 | -528.60995 | -529.29006 | 0.09327 |
| **3.5'** | $C_1$ | 0 | -683.70130 | -684.94874 | 0.19450 |
| **3.6'** | $C_1$ | 0 | -683.67614 | -684.93309 | 0.19893 |
| **2.21'** | $C_i$ | 0 | -1057.26550 | -1058.70949 | 0.20207 |

| Cyclic As cations | Symmetry | N imag | R/UHF | UMP2 | ZPVE |
|---|---|---|---|---|---|
| **2.5' (3.2')** | $C_2$ | 0 | -2422.08739 | -2422.80044 | 0.09742 |
| **2.5' t** | $C_2$ | 1 | -2422.02870 | -2422.70568 | 0.09273 |
| **2.5' t** | $C_1$ | 0 | -2422.03716 | -2422.70234 | 0.09385 |
| **2.5' t** | $C_s \rightarrow C_{2v}^*$ | 2 | -2422.02819 | -2422.70450 | 0.09244 |

| | | | | | |
|---|---|---|---|---|---|
| **3.7'** | $C_1$ | 0 | -2577.06294 | -2578.31324 | 0.19231 |
| **3.8'** | $C_1$ | 0 | -2577.08024 | -2578.33994 | 0.19721 |
| **2.22'** | $C_i$ | 0 | -4844.07839 | -4845.52502 | 0.19804 |
| **2.6'** | $C_s$ | 0 | -2461.13855 | -2461.99164 | 0.12873 |
| **2.23'** | $C_i$ | 0 | -4922.16511 | -4923.89126 | 0.26013 |

| Butadienes | Symmetry | N imag | R/UHF | UMP2 | ZPVE |
|---|---|---|---|---|---|
| Cis | $C_{2v}$ | 1 | -154.94271 | -155.47037 | 0.09046 |
| Trans | $C_{2h}$ | 0 | -154.94927 | -155.47636 | 0.09076 |

| Ammonia | Symmetry | N imag | R/UHF | UMP2 | ZPVE |
|---|---|---|---|---|---|
| **2.13' s** | $C_{3v}$ | 0 | -56.20097 | -56.38003 | 0.03722 |
| **2.13' s** | $D_{3h}$ | 1 | -56.19088 | -56.37079 | 0.03514 |
| **2.13' t** | $D_{3h}$ | 0 | -56.01411 | -56.17162 | 0.02205 |

| Ammonium radical cation | Symmetry | N imag | R/UHF | UMP2 | ZPVE |
|---|---|---|---|---|---|
| **2.16' d** | $C_{3v} \rightarrow D_{3h}^{*}$ | 0 | -55.88874 | -56.02726 | 0.03515 |

| | | | | | |
|---|---|---|---|---|---|
| **2.16' d** | $D_{3h}$ | 0 | -55.88874 | -56.02727 | 0.03514 |

| Acyclic P cations | Symmetry | N imag | R/UHF | UMP2 | ZPVE |
|---|---|---|---|---|---|
| **2.14' s** | $C_s$ | 0 | -396.66906 | -396.93972 | 0.03908 |
| **2.14' t** | $C_s$ #1 | 1 | -396.59385 | -396.83697 | 0.03444 |
| **2.14' t** | $C_s$ #2 | 0 | -396.61987 | -396.84550 | 0.03481 |
| **2.14' t** | $C_{2v}$ | 1 | -396.57580 | -396.82733 | 0.02803 |
| **2.14' t** | $C_1$ | 0 | -396.61408 | -396.86193 | 0.03473 |

| Acyclic P radicals | Symmetry | N imag | R/UHF | UMP2 | ZPVE |
|---|---|---|---|---|---|
| **2.17' d** | $C_s$ #1 | 1 | -396.92242 | -397.18902 | 0.03522 |
| **2.14' d** | $C_s$ #2 | 1 | -396.91302 | -397.17484 | 0.03506 |
| **2.14' d** | $C_{2v}$ | 2 | -396.85440 | -397.06781 | 0.02653 |
| **2.14' d** | $C_1$ | 0 | -396.92270 | -397.18905 | 0.03607 |

| Acyclic As cations | Symmetry | N imag | R/UHF | UMP2 | ZPVE |
|---|---|---|---|---|---|
| **2.15' s** | $C_s$ | 0 | -2290.08183 | -2290.35103 | 0.03711 |
| **2.15' t** | $C_s$ #1 | 2 | -2290.00474 | -2290.24755 | 0.03242 |

| | | | | | |
|---|---|---|---|---|---|
| **2.15' t** | $C_s$ #2 | 0 | -2290.05075 | -2290.26943 | 0.03318 |
| **2.15' t** | $C_{2v}$ | 3 | -2289.94675 | -2290.19220 | 0.03058 |
| **2.15' t** | $C_1$ | 0 | -2290.05075 | -2290.26944 | 0.03318 |

| Acyclic As radicals | Symmetry | N imag | R/UHF | UMP2 | ZPVE |
|---|---|---|---|---|---|
| **2.18' d** | $C_s$ #1 | 1 | -2290.33776 | -2290.60318 | 0.03365 |
| **2.18' d** | $C_s$ #2 | 1 | -2290.26276 | -2290.50515 | 0.03169 |
| **2.18' d** | $C_s$ #3 | 1 | -2290.33260 | -2290.59418 | 0.03386 |
| **2.18' d** | $C_{2v}$ | 2 | -2290.16059 | -2290.44008 | 0.04194 |
| **2.18' d** | $C_1$ | 0 | -2290.33903 | -2290.60427 | 0.03478 |

**Table A.2.** Selected structural parameters from HF/6-311G* optimized geometries. All lengths in Å, all angles in degrees.

| | **2.7' (3.1') s $C_2$** | **2.7' t $C_2$** | **2.7' t $C_1$** | **2.7' t $C_s \rightarrow C_{2v}$*** |
|---|---|---|---|---|
| P(1)-N(2) | 1.598 | 1.749 | 1.660 | 1.747 |
| P(1)-N(3) | 1.598 | 1.749 | 1.891 | 1.747 |
| N(2)-H(4) | 0.996 | 1.002 | 0.996 | 1.002 |
| N(2)-C(6) | 1.478 | 1.450 | 1.456 | 1.449 |
| N(3)-H(5) | 0.996 | 1.002 | 1.005 | 1.002 |
| N(3)-C(7) | 1.478 | 1.450 | 1.452 | 1.449 |
| C(6)-C(7) | 1.542 | 1.524 | 1.529 | 1.525 |
| N(2)-P(1)-N(3) | 94.1 | 83.9 | 84.1 | 83.9 |
| P(1)-N(2)-H(4) | 123.1 | 120.9 | 120.5 | 120.6 |
| P(1)-N(2)-C(6) | 117.0 | 120.8 | 120.5 | 121.8 |
| H(4)-N(2)-C(6) | 119.7 | 118.1 | 118.5 | 117.6 |
| P(1)-N(3)-H(5) | 123.1 | 120.9 | 124.8 | 120.6 |
| P(1)-N(3)-C(7) | 117.0 | 120.8 | 115.2 | 121.8 |
| H(5)-N(3)-C(7) | 119.7 | 118.1 | 119.4 | 117.6 |
| N(2)-C(6)-C(7) | 105.3 | 105.2 | 104.7 | 106.2 |

| | **2.5' (3.2') s $C_2$** | **2.5' t $C_2$** | **2.5' t $C_1$** | **2.5' t $C_s \rightarrow C_{2v}$*** |
|---|---|---|---|---|
| As(1)-N(2) | 1.725 | 1.883 | 2.046 | 1.880 |
| As(1)-N(3) | 1.725 | 1.883 | 1.783 | 1.880 |
| N(2)-H(4) | 0.996 | 1.002 | 1.005 | 1.002 |
| N(2)-C(6) | 1.476 | 1.449 | 1.452 | 1.447 |
| N(3)-H(5) | 0.996 | 1.002 | 0.996 | 1.002 |
| N(3)-C(7) | 1.476 | 1.449 | 1.455 | 1.447 |
| C(6)-C(7) | 1.536 | 1.526 | 1.530 | 1.528 |
| N(2)-As(1)-N(3) | 89.6 | 80.2 | 80.3 | 80.2 |
| As(1)-N(2)-H(4) | 123.4 | 121.9 | 127.0 | 121.5 |
| As(1)-N(2)-C(6) | 116.5 | 120.7 | 114.3 | 121.9 |
| H(4)-N(2)-C(6) | 119.2 | 117.2 | 118.1 | 116.5 |

| | | | | |
|---|---|---|---|---|
| As(1)-N(3)-H(5) | 123.4 | 121.9 | 120.9 | 121.5 |
| As(1)-N(3)-C(7) | 116.5 | 120.7 | 120.2 | 121.9 |
| H(5)-N(3)-C(7) | 119.2 | 117.2 | 118.2 | 116.5 |
| N(2)-C(6)-C(7) | 106.4 | 106.8 | 106.9 | 108.0 |

| 3.5' $C_1$ | | 3.7' $C_1$ | |
|---|---|---|---|
| P(1)-N(2) | 1.632 | As(1)-N(2) | 1.768 |
| P(1)-N(3) | 1.630 | As(1)-N(3) | 1.768 |
| P(1)-C(12) | 1.819 | As(1)-C(12) | 1.932 |
| P(1)-C(13) | 1.818 | As(1)-C(13) | 1.932 |
| N(2)-H(4) | 0.994 | N(2)-H(4) | 0.995 |
| N(2)-C(6) | 1.473 | N(2)-C(6) | 1.475 |
| N(3)-H(5) | 0.994 | N(3)-H(5) | 0.995 |
| N(3)-C(7) | 1.474 | N(3)-C(7) | 1.475 |
| C(6)-C(7) | 1.530 | C(6)-C(7) | 1.526 |
| C(12)-C(14) | 1.513 | C(12)-C(14) | 1.512 |
| C(13)-C(15) | 1.512 | C(13)-C(15) | 1.512 |
| C(14)-C(15) | 1.321 | C(14)-C(15) | 1.322 |
| N(2)-P(1)-N(3) | 94.8 | N(2)-As(1)-N(3) | 91.8 |
| N(2)-P(1)-C(12) | 113.6 | N(2)-As(1)-C(12) | 115.3 |
| N(2)-P(1)-C(13) | 117.7 | N(2)-As(1)-C(13) | 120.9 |
| N(3)-P(1)-C(12) | 120.0 | N(3)-As(1)-C(12) | 120.8 |
| N(3)-P(1)-C(13) | 115.6 | N(3)-As(1)-C(13) | 115.3 |
| C(12)-P(1)-C(13) | 96.9 | C(12)-As(1)-C(13) | 95.0 |
| P(1)-N(2)-H(4) | 123.4 | As(1)-N(2)-H(4) | 120.3 |
| P(1)-N(2)-C(6) | 112.9 | As(1)-N(2)-C(6) | 110.5 |
| H(4)-N(2)-C(6) | 119.4 | H(4)-N(2)-C(6) | 116.8 |
| P(1)-N(3)-H(5) | 123.8 | As(1)-N(3)-H(5) | 120.3 |
| P(1)-N(3)-C(7) | 113.1 | As(1)-N(3)-C(7) | 110.5 |
| H(5)-N(3)-C(7) | 119.4 | H(5)-N(3)-C(7) | 116.8 |
| N(2)-C(6)-C(7) | 104.5 | N(2)-C(6)-C(7) | 105.9 |
| N(3)-C(7)-C(6) | 104.5 | N(3)-C(7)-C(6) | 105.9 |
| P(1)-C(12)-C(14) | 102.6 | As(1)-C(12)-C(14) | 102.2 |

| | | | |
|---|---|---|---|
| C(12)-C(14)-C(15) | 117.6 | C(12)-C(14)-C(15) | 120.3 |
| C(13)-C(15)-C(14) | 117.5 | C(13)-C(15)-C(14) | 120.3 |

| 3.6' $C_1$ | | 3.8' $C_1$ | |
|---|---|---|---|
| P(1)-N(2) | 1.872 | As(1)-N(2) | 2.051 |
| P(1)-N(3) | 1.662 | As(1)-N(3) | 1.807 |
| P(1)-C(12) | 1.839 | As(1)-C(12) | 1.960 |
| N(2)-H(4) | 1.004 | N(2)-H(4) | 1.000 |
| N(2)-C(6) | 1.500 | N(2)-C(6) | 1.497 |
| N(2)-C(14) | 1.496 | N(2)-C(14) | 1.506 |
| N(3)-H(5) | 0.994 | N(3)-H(5) | 0.997 |
| N(3)-C(7) | 1.463 | N(3)-C(7) | 1.457 |
| C(6)-C(7) | 1.544 | C(6)-C(7) | 1.530 |
| C(12)-C(13) | 1.509 | C(12)-C(13) | 1.506 |
| C(13)-C(15) | 1.318 | C(13)-C(15) | 1.321 |
| C(14)-C(15) | 1.502 | C(14)-C(15) | 1.506 |
| N(2)-P(1)-N(3) | 88.7 | N(2)-As(1)-N(3) | 87.3 |
| N(2)-P(1)-C(12) | 94.4 | N(2)-As(1)-C(12) | 92.4 |
| N(3)-P(1)-C(12) | 104.1 | N(3)-As(1)-C(12) | 103.1 |
| P(1)-N(2)-H(4) | 104.8 | As(1)-N(2)-H(4) | 106.0 |
| P(1)-N(2)-C(6) | 105.9 | As(1)-N(2)-C(6) | 105.5 |
| P(1)-N(2)-C(14) | 116.0 | As(1)-N(2)-C(14) | 116.1 |
| H(4)-N(2)-C(6) | 107.5 | H(4)-N(2)-C(6) | 109.2 |
| H(4)-N(2)-C(14) | 106.9 | H(4)-N(2)-C(14) | 107.1 |
| C(6)-N(2)-C(14) | 115.1 | C(6)-N(2)-C(14) | 112.7 |
| P(1)-N(3)-H(5) | 118.0 | As(1)-N(3)-H(5) | 113.0 |
| P(1)-N(3)-C(7) | 117.3 | As(1)-N(3)-C(7) | 113.4 |
| H(5)-N(3)-C(7) | 116.4 | H(5)-N(3)-C(7) | 113.2 |
| N(2)-C(6)-C(7) | 107.7 | N(2)-C(6)-C(7) | 107.1 |
| N(3)-C(7)-C(6) | 107.5 | N(3)-C(7)-C(6) | 108.0 |
| P(1)-C(12)-C(13) | 114.0 | As(1)-C(12)-C(13) | 107.6 |
| C(12)-C(13)-C(15) | 126.4 | C(12)-C(13)-C(15) | 121.3 |
| N(2)-C(14)-C(15) | 113.2 | N(2)-C(14)-C(15) | 112.4 |
| C(13)-C(15)-C(14) | 127.0 | C(13)-C(15)-C(14) | 120.8 |

| **2.21' $C_i$** | | **2.22' $C_i$** | |
|---|---|---|---|
| P(1)-N(2) | 1.818 | As(1)-N(2) | 1.940 |
| P(1)-N(4) | 1.925 | As(1)-N(4) | 2.070 |
| P(1)-N(5) | 1.614 | As(1)-N(5) | 1.741 |
| N(2)-H(7) | 1.007 | N(2)-H(7) | 1.006 |
| N(2)-C(11) | 1.517 | N(2)-C(11) | 1.509 |
| N(5)-H(9) | 0.998 | N(5)-H(9) | 0.997 |
| N(5)-C(13) | 1.471 | N(5)-C(13) | 1.468 |
| C(11)-C(13) | 1.525 | C(11)-C(13) | 1.524 |
| C(12)-C(14) | 1.525 | C(12)-C(14) | 1.524 |
| N(2)-P(1)-N(4) | 80.6 | N(2)-As(1)-N(4) | 79.7 |
| N(2)-P(1)-N(5) | 90.6 | N(2)-As(1)-N(5) | 86.6 |
| N(4)-P(1)-N(5) | 104.7 | N(4)-As(1)-N(5) | 101.8 |
| P(1)-N(2)-P(3) | 99.4 | As(1)-N(2)-As(3) | 100.3 |
| P(1)-N(2)-H(7) | 113.2 | As(1)-N(2)-H(7) | 113.0 |
| P(1)-N(2)-C(11) | 108.8 | As(1)-N(2)-C(11) | 108.4 |
| P(3)-N(2)-H(7) | 111.6 | As(3)-N(2)-H(7) | 110.3 |
| P(3)-N(2)-C(11) | 113.8 | As(3)-N(2)-C(11) | 114.4 |
| H(7)-N(2)-C(11) | 109.9 | H(7)-N(2)-C(11) | 110.1 |
| H(8)-N(4)-C(12) | 109.9 | H(8)-N(4)-C(12) | 110.1 |
| P(1)-N(5)-H(9) | 120.9 | As(1)-N(5)-H(9) | 121.3 |
| P(1)-N(5)-C(13) | 119.2 | As(1)-N(5)-C(13) | 119.1 |
| H(9)-N(5)-C(13) | 119.5 | H(9)-N(5)-C(13) | 119.3 |
| N(2)-C(11)-C(13) | 105.5 | N(2)-C(11)-C(13) | 106.7 |
| N(4)-C(12)-C(14) | 105.5 | N(4)-C(12)-C(14) | 106.7 |
| N(5)-C(13)-C(11) | 104.0 | N(5)-C(13)-C(11) | 105.5 |
| N(6)-C(14)-C(12) | 104.1 | N(6)-C(14)-C(12) | 105.5 |

| **2.6' $C_s$** | | **2.23' $C_i$** | |
|---|---|---|---|
| As(1)-N(2) | 1.724 | As(1)-N(2) | 1.930 |
| N(2)-H(4) | 0.997 | As(1)-N(4) | 2.086 |
| N(2)-C(6) | 1.476 | As(1)-N(5) | 1.737 |

| | |
|---|---|
| C(6)-C(8) | 1.522 |
| N(2)-As(1)-N(3) | 99.8 |
| As(1)-N(2)-H(4) | 116.2 |
| As(1)-N(2)-C(6) | 128.3 |
| H(4)-N(2)-C(6) | 115.5 |
| N(2)-C(6)-C(8) | 111.3 |
| C(6)-C(8)-C(7) | 113.4 |

| | |
|---|---|
| N(2)-H(7) | 1.006 |
| N(2)-C(11) | 1.513 |
| N(5)-H(9) | 1.000 |
| N(5)-C(13) | 1.482 |
| N(6)-H(10) | 1.000 |
| N(6)-C(14) | 1.482 |
| C(11)-C(15) | 1.522 |
| C(13)-C(15) | 1.520 |
| N(2)-As(1)-N(4) | 79.5 |
| N(2)-As(1)-N(5) | 97.9 |
| N(4)-As(1)-N(5) | 104.7 |
| As(1)-N(2)-As(3) | 100.5 |
| As(1)-N(2)-H(7) | 108.7 |
| As(1)-N(2)-C(11) | 117.0 |
| As(3)-N(2)-H(7) | 108.8 |
| As(3)-N(2)-C(11) | 113.2 |
| H(7)-N(2)-C(11) | 108.2 |
| As(1)-N(5)-H(9) | 112.4 |
| As(1)-N(5)-C(13) | 133.3 |
| H(9)-N(5)-C(13) | 112.9 |
| As(3)-N(6)-H(10) | 112.4 |
| N(2)-C(11)-C(15) | 111.3 |
| N(5)-C(13)-C(15) | 112.8 |
| C(11)-C(15)-C(13) | 113.8 |

**Table A.3.** Selected structural parameters from HF/6-311G* optimized geometries. All lengths in Å, all angles in degrees.

| | **2.13' s $C_{3v}$** | **2.13' s $D_{3h}$** | **2.13' t $D_{3h}$** | **2.16' d $D_{3h}$** |
|---|---|---|---|---|
| N-H | 0.999 | 0.985 | 1.064 | 1.008 |
| H-N-H | 107.4 | 120.0 | 120.0 | 120.0 |

| | **2.14' s $C_s$** | **2.13' t $C_s$ #1** | **2.13' t $C_s$ #2** | **2.13' t $C_1$** |
|---|---|---|---|---|
| P(1)-N(2) | 1.583 | 1.617 | 1.813 | 1.640 |
| P(1)-H(3) | 1.400 | 1.389 | 1.404 | 1.403 |
| N(2)-H(4) | 1.002 | 0.998 | 1.008 | 1.003 |
| N(2)-H(5) | 1.000 | 1.000 | 1.008 | 1.003 |
| N(2)-P(1)-H(3) | 97.0 | 117.8 | 91.1 | 111.5 |
| P(1)-N(2)-H(4) | 120.7 | 122.6 | 122.8 | 120.7 |
| P(1)-N(2)-H(5) | 125.7 | 121.5 | 122.8 | 120.7 |
| H(4)-N(2)-H(5) | 113.6 | 115.9 | 113.9 | 113.5 |
| H(3)-P(1)-N(2)-H(4) | 180.0 | 180.0 | -94.1 | 103.5 |
| H(3)-P(1)-N(2)-H(5) | 0.0 | 0.0 | 94.1 | -103.5 |

| | **2.14' t $C_{2v}$** | **2.17' d $C_1$** | **2.17' d $C_s$ #1** | **2.17' d $C_s$ #2** |
|---|---|---|---|---|
| P(1)-N(2) | 1.581 | 1.694 | 1.685 | 1.719 |
| P(1)-H(3) | 3.947 | 1.408 | 1.408 | 1.425 |
| N(2)-H(4) | 1.005 | 0.993 | 0.991 | 0.998 |
| N(2)-H(5) | 1.005 | 0.993 | 0.991 | 0.998 |
| N(2)-P(1)-H(3) | 180.0 | 95.8 | 95.8 | 101.9 |
| P(1)-N(2)-H(4) | 123.4 | 117.7 | 120.4 | 115.6 |
| P(1)-N(2)-H(5) | 123.4 | 121.7 | 124.7 | 115.6 |
| H(4)-N(2)-H(5) | 113.3 | 112.8 | 114.9 | 109.1 |
| H(3)-P(1)-N(2)-H(4) | 0.0 | -170.6 | 180.0 | -64.6 |
| H(3)-P(1)-N(2)-H(5) | 0.0 | -23.5 | 0.0 | 64.6 |

| | **2.17' d $C_{2v}$** |
|---|---|
| P(1)-N(2) | 4.500 |

| | |
|---|---|
| P(1)-H(3) | 1.415 |
| N(2)-H(4) | 1.009 |
| N(2)-H(5) | 1.009 |
| N(2)-P(1)-H(3) | 180.0 |
| P(1)-N(2)-H(4) | 127.5 |
| P(1)-N(2)-H(5) | 127.5 |
| H(4)-N(2)-H(5) | 105.0 |
| H(3)-P(1)-N(2)-H(4) | 0.0 |
| H(3)-P(1)-N(2)-H(5) | 0.0 |

| | **2.15' s Cs** | **2.15' t $C_s$ #1** | **2.15' t $C_s$ #2** | **2.15' t $C_s$ #3** |
|---|---|---|---|---|
| As(1)-N(2) | 1.709 | 1.742 | 2.000 | 2.000 |
| As(1)-H(3) | 1.515 | 1.497 | 1.516 | 1.516 |
| N(2)-H(4) | 1.000 | 0.997 | 1.008 | 1.008 |
| N(2)-H(5) | 1.000 | 1.000 | 1.008 | 1.008 |
| N(2)-As(1)-H(3) | 95.3 | 117.6 | 88.5 | 88.5 |
| As(1)-N(2)-H(4) | 121.1 | 122.2 | 123.5 | 123.5 |
| As(1)-N(2)-H(5) | 124.9 | 120.8 | 123.5 | 123.5 |
| H(4)-N(2)-H(5) | 114.0 | 117.1 | 112.9 | 112.9 |
| H(3)-As(1)-N(2)-H(4) | 180.0 | 180.0 | -91.9 | 91.9 |
| H(3)-As(1)-N(2)-H(5) | 0.0 | 0.0 | 91.9 | -91.9 |

| | **2.15' t C1** | **2.15' t $C_{2v}$** | **2.18' d $C_1$** | **2.18' d $C_s$ #1** |
|---|---|---|---|---|
| As(1)-N(2) | 2.000 | 1.748 | 1.830 | 1.809 |
| As(1)-H(3) | 1.516 | 1.493 | 1.521 | 1.520 |
| N(2)-H(4) | 1.008 | 0.996 | 0.996 | 0.992 |
| N(2)-H(5) | 1.008 | 0.996 | 0.995 | 0.991 |
| N(2)-As(1)-H(3) | 88.5 | 180.0 | 94.5 | 94.4 |
| As(1)-N(2)-H(4) | 123.4 | 119.3 | 114.9 | 120.9 |
| As(1)-N(2)-H(5) | 123.5 | 119.3 | 117.6 | 124.1 |
| H(4)-N(2)-H(5) | 113.0 | 121.5 | 110.6 | 115.0 |
| H(3)-As(1)-N(2)-H(4) | 92.0 | 0.0 | -163.8 | 180.0 |
| H(3)-As(1)-N(2)-H(5) | -91.9 | 0.0 | -31.0 | 0.0 |

| | **2.18'** d $C_s$ #2 | **2.18'** d $C_s$ #3 | **2.18'** d $C_{2v}$ |
|---|---|---|---|
| As(1)-N(2) | 2.056 | 1.854 | 1.771 |
| As(1)-H(3) | 1.526 | 1.538 | 1.452 |
| N(2)-H(4) | 1.003 | 1.000 | 0.988 |
| N(2)-H(5) | 1.003 | 1.000 | 0.988 |
| N(2)-As(1)-H(3) | 86.4 | 100.1 | 180.0 |
| As(1)-N(2)-H(4) | 123.8 | 112.8 | 119.6 |
| As(1)-N(2)-H(5) | 123.8 | 112.8 | 119.6 |
| H(4)-N(2)-H(5) | 112.3 | 107.9 | 120.8 |
| H(3)-As(1)-N(2)-H(4) | -92.1 | 61.3 | 0.0 |
| H(3)-As(1)-N(2)-H(5) | 92.1 | -61.3 | 0.0 |

**Table A.4.** Mulliken and natural bond orbital (NBO) charge distributions of selected atoms.

| | **2.7'(3.1') s $C_2$** | | **2.7' t $C_1$** | |
|---|---|---|---|---|
| | Mulliken | NBO | Mulliken | NBO |
| P 1 | 1.123 | 1.552 | 0.772 | 0.968 |
| N 2 | -0.877 | -1.003 | -0.865 | -0.978 |
| N 3 | -0.877 | -1.003 | -0.505 | -0.370 |
| H 4 | 0.450 | 0.439 | 0.446 | 0.429 |
| H 5 | 0.450 | 0.439 | 0.450 | 0.397 |

| | **2.7' t $C_2$** | | **2.7' t $C_s \rightarrow C_{2v}$*** | |
|---|---|---|---|---|
| | Mulliken | NBO | Mulliken | NBO |
| P 1 | 0.627 | 0.786 | 0.620 | 0.786 |
| N 2 | -0.625 | -0.599 | -0.625 | -0.599 |
| N 3 | -0.625 | -0.599 | -0.625 | -0.599 |
| H 4 | 0.450 | 0.417 | 0.448 | 0.416 |
| H 5 | 0.450 | 0.417 | 0.448 | 0.416 |

| | **3.5' $C_1$** | | **3.6' $C_1$** | |
|---|---|---|---|---|
| | Mulliken | NBO | Mulliken | NBO |
| P 1 | 1.610 | 2.049 | 0.940 | 1.273 |
| N 2 | -0.928 | -1.036 | -0.804 | -0.699 |
| N 3 | -0.931 | -1.036 | -0.902 | -1.022 |
| H 4 | 0.425 | 0.422 | 0.447 | 0.412 |
| H 5 | 0.423 | 0.422 | 0.423 | 0.410 |
| C 12 | -0.796 | -0.705 | -0.791 | -0.718 |
| C 13 | -0.792 | -0.706 | -0.142 | -0.141 |

| | **2.21' $C_i$** | |
|---|---|---|
| | Mulliken | NBO |
| P 1 | 1.190 | 1.532 |
| N 2 | -1.033 | -1.030 |
| N 5 | -0.898 | -1.038 |

| | | |
|---|---|---|
| H 7 | 0.487 | 0.451 |
| H 9 | 0.471 | 0.454 |

| | 2.5'(3.2') s $C_2$ | | 2.5' t $C_1$ | |
|---|---|---|---|---|
| | Mulliken | NBO | Mulliken | NBO |
| As 1 | 1.161 | 1.642 | 0.824 | 1.082 |
| N 2 | -0.868 | -1.031 | -0.498 | -0.394 |
| N 3 | -0.868 | -1.031 | -0.872 | -1.028 |
| H 4 | 0.439 | 0.429 | 0.439 | 0.386 |
| H 5 | 0.439 | 0.429 | 0.434 | 0.422 |

| | 2.5' t $C_2$ | | 2.5' t $C_s \rightarrow C_{2v}$* | |
|---|---|---|---|---|
| | Mulliken | NBO | Mulliken | NBO |
| As 1 | 0.650 | 0.853 | 0.647 | 0.851 |
| N 2 | -0.618 | -0.613 | -0.621 | -0.612 |
| N 3 | -0.618 | -0.613 | -0.621 | -0.612 |
| H 4 | 0.440 | 0.407 | 0.438 | 0.407 |
| H 5 | 0.440 | 0.407 | 0.438 | 0.407 |

| | 3.7' $C_1$ | | 3.8' $C_1$ | |
|---|---|---|---|---|
| | Mulliken | NBO | Mulliken | NBO |
| As 1 | 1.571 | 2.055 | 0.997 | 1.354 |
| N 2 | -0.887 | -1.020 | -0.802 | -0.722 |
| N 3 | -0.887 | -1.020 | -0.845 | -1.018 |
| H 4 | 0.404 | 0.407 | 0.443 | 0.410 |
| H 5 | 0.404 | 0.407 | 0.395 | 0.387 |
| C 12 | -0.753 | -0.691 | -0.769 | -0.723 |
| C 13 | -0.753 | -0.691 | -0.154 | -0.126 |

| | 2.22' $C_i$ | | | 2.23' $C_i$ | |
|---|---|---|---|---|---|
| | Mulliken | NBO | | Mulliken | NBO |
| As 1 | 1.272 | 1.656 | As 1 | 1.271 | 1.652 |
| N 2 | -1.026 | -1.074 | N 2 | -1.039 | -1.077 |

| | | | | | |
|---|---|---|---|---|---|
| N 5 | -0.914 | -1.067 | N 5 | -0.950 | -1.078 |
| H 7 | 0.468 | 0.438 | H 7 | 0.459 | 0.430 |
| H 9 | 0.458 | 0.444 | H 9 | 0.440 | 0.426 |

| | **2.6' $C_s$** | |
|---|---|---|
| | Mulliken | NBO |
| As 1 | 1.155 | 1.623 |
| N 2 | -0.885 | -1.034 |
| H 4 | 0.434 | 0.420 |

| | **2.13' s $C_{3v}$** | | **2.13' s $D_{3h}$** | |
|---|---|---|---|---|
| | Mulliken | NBO | Mulliken | NBO |
| N 1 | -1.022 | -0.983 | -1.090 | -1.069 |
| H 2 | 0.341 | 0.328 | 0.363 | 0.356 |

| | **2.13' t $D_{3h}$** | | **2.16' d $D_{3h}$** | |
|---|---|---|---|---|
| | Mulliken | NBO | Mulliken | NBO |
| N 1 | -0.236 | -0.408 | -0.478 | -0.231 |
| H 2 | 0.079 | 0.136 | 0.493 | 0.410 |

| | **2.14' s $C_s$** | | **2.14' t $C_1$** | |
|---|---|---|---|---|
| | Mulliken | NBO | Mulliken | NBO |
| P 1 | 0.861 | 1.266 | 0.700 | 1.082 |
| N 2 | -0.906 | -1.066 | -0.853 | -0.977 |
| H 3 | 0.099 | -0.085 | 0.202 | 0.019 |
| H 4 | 0.473 | 0.441 | 0.476 | 0.438 |
| H 5 | 0.473 | 0.444 | 0.476 | 0.438 |

| | **2.14' t $C_s$ #1** | | **2.14' t $C_s$ #2** | |
|---|---|---|---|---|
| | Mulliken | NBO | Mulliken | NBO |
| P 1 | 0.796 | 1.238 | 0.534 | 0.758 |
| N 2 | -0.986 | -1.169 | -0.610 | -0.510 |
| H 3 | 0.233 | 0.030 | 0.122 | -0.061 |

| | | | | |
|---|---|---|---|---|
| H 4 | 0.478 | 0.450 | 0.477 | 0.407 |
| H 5 | 0.479 | 0.450 | 0.477 | 0.407 |

| | 2.14' t $C_{2v}$ | | 2.17' d $C_1$ | |
|---|---|---|---|---|
| | Mulliken | NBO | Mulliken | NBO |
| P 1 | 0.940 | 1.230 | 0.276 | 0.529 |
| N 2 | -0.902 | -1.127 | -1.025 | -1.140 |
| H 3 | 0.005 | 0.001 | -0.012 | -0.129 |
| H 4 | 0.479 | 0.448 | 0.380 | 0.369 |
| H 5 | 0.479 | 0.448 | 0.381 | 0.370 |

| | 2.17' d $C_s$ #1 | | 2.17' d $C_s$ #2 | |
|---|---|---|---|---|
| | Mulliken | NBO | Mulliken | NBO |
| P 1 | 0.276 | 0.525 | 0.341 | 0.631 |
| N 2 | -1.036 | -1.149 | -1.039 | -1.173 |
| H 3 | -0.013 | -0.128 | -0.041 | -0.176 |
| H 4 | 0.385 | 0.375 | 0.370 | 0.359 |
| H 5 | 0.387 | 0.376 | 0.370 | 0.359 |

| | 2.17' d $C_{2v}$ | |
|---|---|---|
| | Mulliken | NBO |
| P 1 | -0.006 | 0.167 |
| N 2 | -0.617 | -0.509 |
| H 3 | -0.001 | -0.168 |
| H 4 | 0.312 | 0.255 |
| H 5 | 0.312 | 0.255 |

| | 2.15' s $C_s$ | | 2.15' t $C_1$ | |
|---|---|---|---|---|
| | Mulliken | NBO | Mulliken | NBO |
| As 1 | 0.888 | 1.345 | 0.553 | 0.819 |
| N 2 | -0.945 | -1.111 | -0.614 | -0.507 |
| H 3 | 0.130 | -0.101 | 0.136 | -0.091 |
| H 4 | 0.462 | 0.432 | 0.463 | 0.390 |

| | | | | |
|---|---|---|---|---|
| H 5 | 0.465 | 0.435 | 0.463 | 0.390 |

| | **2.15' t $C_s$ #1** | | **2.15' t $C_s$ #2** | |
|---|---|---|---|---|
| | Mulliken | NBO | Mulliken | NBO |
| As 1 | 0.813 | 1.260 | 0.553 | 0.819 |
| N 2 | -1.000 | -1.178 | -0.614 | -0.507 |
| H 3 | 0.255 | 0.037 | 0.136 | -0.091 |
| H 4 | 0.467 | 0.440 | 0.463 | 0.389 |
| H 5 | 0.466 | 0.441 | 0.463 | 0.389 |

| | **2.15' t $C_s$ #3** | | **2.15' t $C_{2v}$** | |
|---|---|---|---|---|
| | Mulliken | NBO | Mulliken | NBO |
| As 1 | 0.553 | 0.819 | 0.598 | 0.962 |
| N 2 | -0.614 | -0.507 | -0.927 | -1.082 |
| H 3 | 0.136 | -0.091 | 0.383 | 0.234 |
| H 4 | 0.462 | 0.389 | 0.473 | 0.443 |
| H 5 | 0.462 | 0.389 | 0.473 | 0.443 |

| | **2.18' d $C_1$** | | **2.18' d $C_s$ #1** | |
|---|---|---|---|---|
| | Mulliken | NBO | Mulliken | NBO |
| As 1 | 0.290 | 0.586 | 0.302 | 0.587 |
| N 2 | -1.031 | -1.160 | -1.065 | -1.186 |
| H 3 | 0.006 | -0.146 | 0.003 | -0.145 |
| H 4 | 0.364 | 0.359 | 0.377 | 0.370 |
| H 5 | 0.370 | 0.362 | 0.383 | 0.373 |

| | **2.18' d $C_s$ #2** | | **2.18' d $C_s$ #3** | |
|---|---|---|---|---|
| | Mulliken | NBO | Mulliken | NBO |
| As 1 | -0.188 | -0.101 | 0.337 | 0.658 |
| N 2 | -0.616 | -0.457 | -1.032 | -1.175 |
| H 3 | 0.009 | -0.109 | -0.025 | -0.186 |
| H 4 | 0.398 | 0.334 | 0.360 | 0.352 |
| H 5 | 0.398 | 0.334 | 0.360 | 0.352 |

| | 2.18' d $C_{2v}$ | |
|---|---|---|
| | Mulliken | NBO |
| As 1 | -0.200 | 0.057 |
| N 2 | -0.935 | -1.032 |
| H 3 | 0.313 | 0.201 |
| H 4 | 0.411 | 0.387 |
| H 5 | 0.411 | 0.387 |

**Table 5.** Calculated spin densities of doublet and triplet species of selected atoms.

| | 2.7' t $C_1$ | 2.7' t $C_2$ | 2.7' t $C_s \rightarrow C_{2v}$ |
|---|---|---|---|
| P 1 | 0.787359 | 0.570222 | 0.567805 |
| N 2 | 0.2342 | 0.797118 | 0.798349 |
| N 3 | 1.111636 | 0.797118 | 0.798349 |

| | 2.5' t $C_1$ | 2.7' t $C_2$ | 2.7' t $C_s \rightarrow C_{2v}$ |
|---|---|---|---|
| As 1 | 0.77137 | 0.457429 | 0.457074 |
| N 2 | 1.13947 | 0.855826 | 0.855291 |
| N 3 | 0.215669 | 0.855826 | 0.855291 |

| | 2.14' t $C_1$ | 2.14' t $C_s$ #1 | 2.14' t $C_s$ #2 | 2.14' t $C_{2v}$ |
|---|---|---|---|---|
| P 1 | 1.45999 | 1.738679 | 1.014774 | 1.184236 |
| N 2 | 0.421357 | 0.210809 | 1.068443 | -0.25647 |
| H 3 | 0.145637 | 0.067874 | 0.020893 | 0.995796 |
| H 4 | -0.013494 | -0.023644 | -0.052055 | 0.038219 |
| H 5 | -0.01349 | 0.006282 | -0.052055 | 0.038219 |

| | 2.17' d $C_1$ | 2.17' d $C_s$ #1 | 2.17' d $C_s$ #2 | 2.17' d $C_{2v}$ |
|---|---|---|---|---|
| P 1 | 0.964238 | 0.949062 | 1.092082 | 2.092449 |

| | | | | |
|---|---|---|---|---|
| N 2 | 0.116866 | 0.141537 | -0.063631 | -1.144654 |
| H 3 | -0.054573 | -0.053942 | -0.056067 | -0.090582 |
| H 4 | -0.014537 | -0.018096 | 0.013808 | 0.071393 |
| H 5 | -0.011994 | -0.018562 | 0.013808 | 0.071393 |

| | **2.15' t $C_1$** | **2.15' t $C_s$ #1** | **2.15' t $C_s$ #2** | **2.15' t $C_s$ #3** | **2.15' t $C_{2v}$** |
|---|---|---|---|---|---|
| As 1 | 0.976501 | 1.654095 | 0.976405 | 0.976396 | 2.205972 |
| N 2 | 1.140386 | 0.241983 | 1.140418 | 1.140591 | 0.058054 |
| H 3 | -0.000567 | 0.12056 | -0.000519 | -0.00064 | -0.267776 |
| H 4 | -0.058171 | -0.024501 | -0.058152 | -0.058174 | 0.001875 |
| H 5 | -0.05815 | 0.007862 | -0.058152 | -0.058174 | 0.001875 |

| | **2.18' d $C_1$** | **2.18' d $C_s$ #1** | **2.18' d $C_s$ #2** | **2.18' d $C_s$ #3** | **2.18' d $C_{2v}$** |
|---|---|---|---|---|---|
| As 1 | 0.983212 | 0.947211 | -0.0841 | 1.095731 | 1.101254 |
| N 2 | 0.087019 | 0.137583 | 1.156323 | -0.058375 | 0.08937 |
| H 3 | -0.055764 | -0.054055 | 0.064992 | -0.05685 | -0.168619 |
| H 4 | -0.008674 | -0.015264 | -0.068607 | 0.009747 | -0.011002 |
| H 5 | -0.005794 | -0.015475 | -0.068607 | 0.009747 | -0.011002 |

| | **2.13' t $D_{3h}$** | **2.16' d $D_{3h}$** |
|---|---|---|

| | | | |
|---|---|---|---|
| N | 1 | 0.917497 | 1.202094 |
| H | 2 | 0.360834 | -0.067365 |

# IMAGE EVALUATION
# TEST TARGET (QA-3)

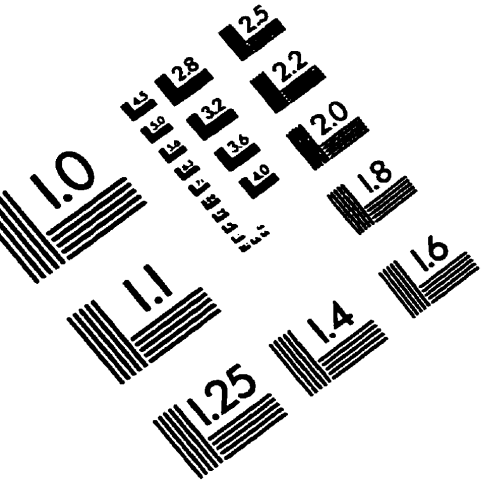


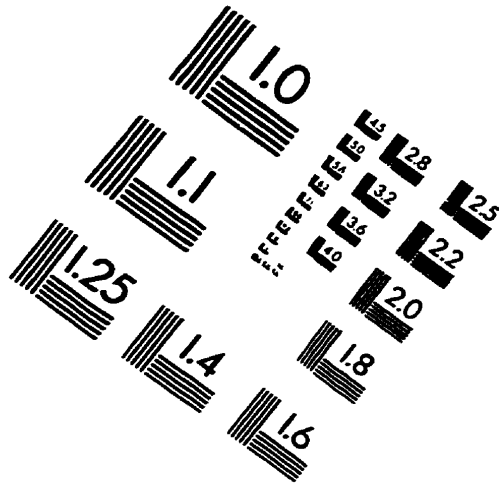


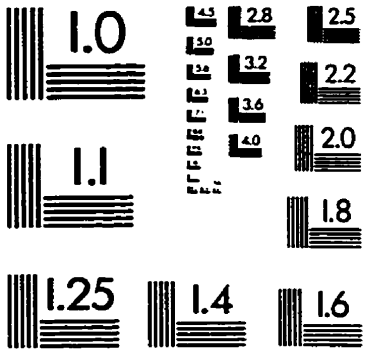


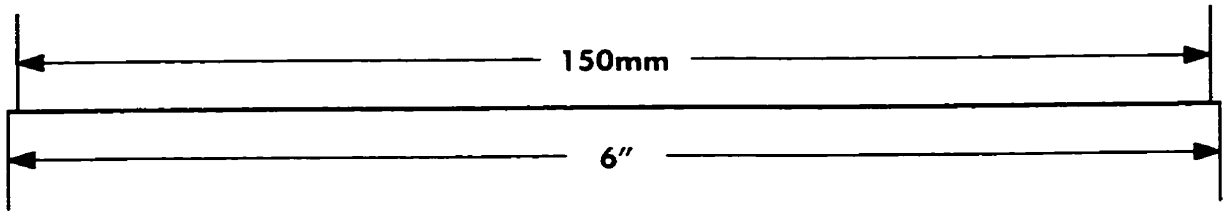


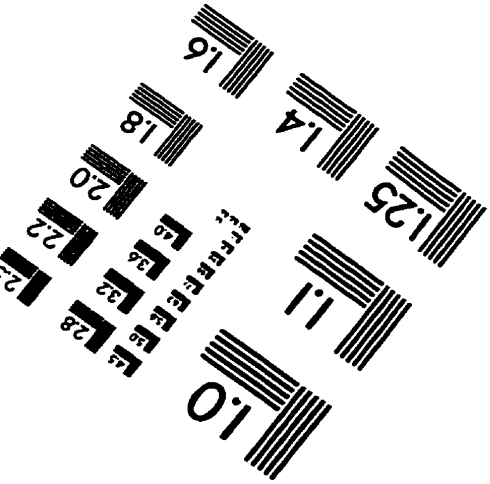


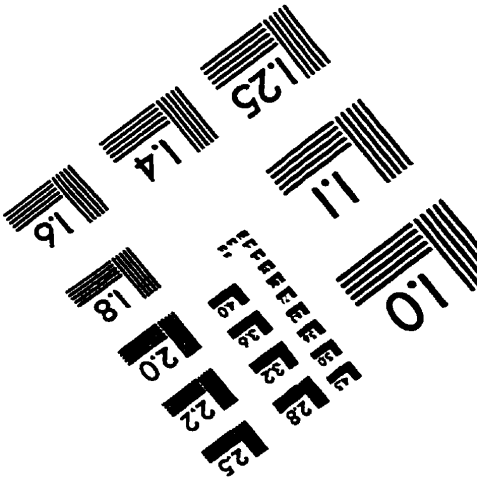


APPLIED IMAGE, Inc
1653 East Main Street
Rochester, NY 14609 USA
Phone: 716/482-0300
Fax: 716/288-5989